Evolutionary history and mechanisms for generating floral morphological diversity of *Asarum* (Aristolochiaceae) in East Asia

Daiki Takahashi

要旨

日華植物区系は温帯性植物の種多様性が世界で最も高い地域の一つであり、中新世以降の気候変動によって引き起こされた地理的隔離がその多様性形成における主な要因であると考えられてきた。一方で生物的要因、特に訪花昆虫との相互作用も植物の多様化に重要な役割を果たすが、日華植物区系では生物的要因が温帯性植物の多様化に寄与したかについては知見が少ない。ウマノスズクサ科カンアオイ属は日華植物区系に多様性の中心を持つ多年生草本であるが、分散能力が低いため地理的隔離の影響を受けやすく、また花サイズ、花色、開花期等の花形質が多様化している。本論文は、特に属内でも著しい多様性を示すカンアオイ節に着目し、地理的隔離と生物的要因が温帯性植物の多様化に与えた影響を解明することを目的とした。第一章ではカンアオイ属を対象にITS領域と*matK*領域を用いた系統解析を行い、カンアオイ節が単系統群であることを明らかにした。第二章ではカンアオイ節の多様化過程を推定するために、葉緑体ゲノムとddRAD-seq法より得られたSNPsを用いた系統解析を行った。その結果、中新世に節内の地域系統（中国大陸と日本列島・台湾）が形成され、更新世の気候変動の影響を受けて地域系統内の種分化が起きたことが示唆された。また近縁種間の隔離要因の比較から開花期や花サイズの違いも種分化に寄与したことも示唆された。次に花形質の進化要因を解明するため、分類群間で萼裂片長の地理的勾配を示すサカワサイシン列に着目した。第三章では列内の進化史を推定した。その結果、最終氷期最盛期における逃避地にて分布が重なったために、分類群間で二次的接触が起き、中間型を示す分類群が形成されたことが明らかになった。第四章では各分類群の萼裂片長の形成要因を推定した。各分類群間で萼裂片長の分化の程度は遺伝的な分化より有意に高く、各分類群の萼裂片長の派生・維持には自然選択が関与していることが示唆された。第五章では列内で最も萼裂片の長さが異なる二種の繁殖生態の比較を行い、その結果、萼裂片の長い分類群は高い双翅目昆虫の訪花頻度と他殖率を示すことが明らかになった。したがって著しく伸長した萼裂片は、その誘引メカニズムは不明であるが、双翅目昆虫を誘引し、他家受粉を増進させるために進化したと考えられる。以上より、カンアオイ節の多様化には過去の気候変動がもたらした地理的隔離と訪花昆虫との相互作用の両方が寄与したと考えられる。

Contents

Summary

The Sino Japanese Floristic Region (SJFR) harbours the world's most diverse temperate flora. Historically, this diversity has been interpreted as the outcomes of geographic isolations caused by the past climatic events, and it has been hypothesised that allopatric speciation would be major mode of speciation in this region. In contrast, biotic drivers, which can also facilitate diversifications of plants, have been rarely considered, when discussing the diversification process in this region. Section *Heterotropa* in genus *Asarum* (Aristolochiaceae) is endemic to the SJFR and comprises 85 species. This section is characterised by the limited dispersal ability and the diverse floral morphology, in terms of the shapes, sizes, and colours of calyx tubes and lobes. I considered that this section would be an ideal system to reveal relative contribution of biotic and abiotic drivers to the diversification of temperate plants in this region.

I first constructed phylogenetic trees based on ITS and *matK* sequences to confirm the monophyly of *Heterotropa* and to infer phylogenetic relationships among the sections within the genus. The results showed *Heterotropa* was a monophyletic group and sister to the clade including species distributed in North America (Chapter 1). Then, using ddRAD-seq and chloroplast genome data, I built a time-calibrated phylogenetic tree including 79 *Heterotropa* species. *Heterotropa* diverged into two clades (continental clade and insular clade) in the Miocene, and the major subclades almost corresponded to geographic entities. Several sister pairs showed floral trait divergence without geographic overlap. Thus, the diversification of *Heterotropa* would have been triggered by the geographic events during the Miocene period, and subsequent repeated floral trait evolution with and without geographic isolations in the regional lineages during the Pleistocene period (Chapter 2).

Subsequently, I focused on series *Sakawanum* in *Heterotropa*, which consists of four taxa and shows inter-taxonomic clinal variation in calyx lobe length. I considered that revealing the formation mechanisms of the clinal variation would contribute to understanding of mechanisms generating the floral diversity of *Heterotropa*. I estimated the evolutionary history within the series by using approximate Bayesian computation method based on the microsatellite and chloroplast sequence data, and ecological niche modelling. The estimated evolutionary history involved secondary contacts between previously isolated taxa triggered by the geographic range shifts to refugia during the Pleistocene period (Chapter 3). To test whether the neutral process or natural selection affects the calyx lobe length of each taxon, I conducted Q_{CT}-F_{ST} comparison. In all taxa pairs, the degrees of neutral genetic differentiation were lower than these of morphological differentiation, indicating that natural selection would shape and maintain the variation of calyx lobe length (Chapter 4). Finally, in order to infer the evolutionary insights into the calyx lobe extension, I investigated the reproductive ecology of two *Sakawanum* species; *A. costatum* and *A. minamitanianum*, which have the shortest and longest calyx lobes in the series. I conducted fine-scale spatial genetic analysis, multi-year floral visitor observations, paternity analysis of seeds, estimation of genetic diversity, and crossing experiments. The results showed that the visitation frequency of flies was higher in *A. minamitanianum*, and *A. minamitanianum* conducted predominantly outcrossing, while *A. costatum* showed a wide range of selfing rate among fruits. Thus, I considered that the extended calyx lobe of *A. minamitanianum* would have evolved for efficient outcrossing by attracting flies, while its attraction mechanisms remain unclear. In addition, both species showed common reproductive characters such as self-compatibilities, low fruiting rates due to pollen limitation, strong fine-scale spatial genetic structures caused by limited seed dispersal distances, and inbreeding depression at late-stage (Chapter 5).

Overall, my study revealed that geographic range shifts caused by the past climatic events would have caused isolations and secondary contacts of populations, and biotic drivers, especially the interactions with pollinators would have subsequently promoted the diversification of *Heterotropa*.

General Introduction

Revealing drivers of extant diversity patterns is one of the central issues in evolutionary biology (Ezard et al., 2011, Benton, 2009). Diversification of a lineage would be influenced by several mechanisms involving abiotic and/or biotic factors (Moore and Donoghue, 2007). Historically, geographic isolation has been considered to play major roles for reproductive isolation and subsequent diversification of organisms (Jordan, 1905, Barraclough and Vogler, 2000). Many studies showed that geographic barriers (i.e. mountains, seas, and rivers) would isolate populations and lead to allopatric speciation (Boucher et al., 2016, Verboom et al., 2015, Govindarajulu et al., 2011, Esselstyn et al., 2009, Pastorini et al., 2003). In addition, the evolution of phenotypic traits concerning reproductive isolation would be also one of the factors to diversification (Lagomarsino et al., 2016). Particularly, in flowering plants, floral trait evolution has been thought to promote speciation through segregation of gene flow by pollinator shifts (Armbruster, 2014, Van der Niet et al., 2014). Previous studies have shown that the evolution rates of floral traits varied among lineages, and would be highly correlated to speciation rates (Jaramillo and Manos, 2001, Givnish et al., 2015). This implied that biotic factors can play complementary roles to abiotic factors in reproductive isolation; that is, biotic factors can facilitate speciation even without geographical isolation (Rundle and Nosil, 2005). Thus, fully understanding diversification processes of a lineage requires a comprehensive study that incorporates the spatial and temporal pattern of phylogenetic relationships and morphological evolution (Barrabe et al., 2019).

The Sino-Japanese Floristic Region (SJFR) ranges from the eastern Himalayas to the Japanese Archipelago through south and central China (Wu and Wu, 1996). This region contains one of the most diverse temperate floras anywhere in the world (Ward, 1913, Wu and Wu, 1996, White, 1983, Takhtajan, 1969) with at least 33,000 vascular plants, of which 50 - 60% are endemic (Lopez-Pujol et al., 2006). Compared with North America, which has similar size and variety of habitats, this region has more diverse flora at family, genus, and taxon levels (Guo et al., 1998, Qian and Ricklefs, 1999), and at taxa within a genus disjunct between these regions (Qian and Ricklefs, 2000). It has been thought that the topographic complexity and historical environmental changes associated with the past climatic events would have formed this diversity of temperate plants (Qian and Ricklefs, 2000). Different from other regions (e.g. North America and Europa; Willis and Niklas, 2004), a large part of East Asia except for high mountain areas has never been directly impacted by extensive ice-sheets during glacial periods (Liu, 1988). As a consequence, this region served as the refugial areas of relict species, which had been widely distributed in northern hemisphere during the Miocene and the Pliocene periods (Manchester et al., 2009). In addition, past climatic events would have played a major role in formation of new lineages within this region. During glacial periods, the temperature of this region was cooler by ca. 4-6 °C and sea level was approximately 130 m lower than its present level (Lisiecki and Raymo, 2005). In this environment, temperate plants retreated to refugia at lower altitudes or southern parts (Harrison et al., 2001). In contrast, during the interglacial periods, temperate plants expanded to higher altitudes or northern parts. In the eastern island systems, sea level changes caused repeated formation and division of land-bridges in the East China Sea (Kizaki and Oshiro, 1977, Kimura, 1996). It has been hypothesised that these climatic changes triggered range shifts, vicariance, and fragmentation leading population isolations (Qiu et al., 2011), and that in temperate plants of this region, allopatric speciation was likely to be a major mode of speciation (Qian and Ricklefs, 2000). To test this hypothesis, many phylogenetic and phylogeographic studies have been conducted (reviewed in Qiu et al., 2011). Several studies reported that geographic and climatic events during the Miocene or Pliocene periods would have promoted lineage divergences (*Cardiocrinum* spp.; Lu et al., 2019, *Sagittaria* spp.; Liao et al., 2016, *Euptelea* spp.; Cao et al., 2016, *Acer mono*; Guo et al., 2014). Many studies confirmed that glacial isolation and/or geographic range shifts caused by climatic oscillations during the Pleistocene period were interpreted as primary determinants of present interspecific and intraspecific genetic structures of temperate plants (*Kirengeshoma* spp.; Qiu et al., 2009b, *Kalopanax septemlobus*; Sakaguchi et al., 2012, *Ainsliaea* spp; Mitsui et al., 2008, *Pieris* spp.; Setoguchi et al., 2008, *Platycrater arguta*; Qiu et al., 2009a). However, many studies conducted in the SJFR have only focused on the role of allopatric fragmentation due to geographic and climatic events, and few studies have considered biotic factors as drivers of the diversification of the temperate plants (but see Okuyama et al., 2008). Thus,

I considered that our knowledge of the diversification process of temperate plants in the SJFR remains incomplete, due to a lack of integrative multidimensional studies of phylogeny, biogeography, and ecology with adequate sampling of diversified groups.

Section *Heterotropa* C.Morren & Decne. in genus *Asarum* L. (Aristolochiaceae) comprises approximately 85 species of low-growing, rhizomatous herbs that grow in shady evergreen-forest understory and is endemic to the SJFR. All species in this section are myrmecochory and considered to have very limited dispersal ability (estimated to be 10 – 50 cm per year; Hiura, 1978). This section includes a number of local endemics and their distribution ranges are often confined to one island or mountain range (e.g. *Asarum majale* in a single mountain range of central Honshu; Sugawara & Taniwaki, 2007, and *Asarum mitoanum* in one island 100 km away from Kyushu island; Sugawara, 1997). Limited dispersal ability promotes genetic differentiation among populations and often leads to allopatric speciation (Petit et al., 2005). These confined distribution ranges and the limited dispersal ability led us to hypothesise that an allopatric speciation would be major mode in *Heterotropa*. In *Heterotropa*, the sepals connect beyond attachment to the ovary and form a calyx tube with calyx lobes (Sugawara, 1987). This section is also characterised by high divergence in floral traits, in terms of their shapes, sizes, and colours of calyx tubes and lobes, while their vegetative traits show almost no differences (Sugawara and Ogisu, 1992, Huang et al., 2003). Their flowers have been hypothesised to mimic fungi in order to attract fungus gnats (Sinn et al., 2015, Vogel, 1978). Several *Heterotropa* taxa are different in chemical compositions of floral scents, while their ecological roles have been unclarified (Kakishima and Okuyama, 2018, Azuma et al., 2010). In addition, *Heterotropa* species are highly divergent in phenology; most species have flowers in spring, while others have flowers in autumn or winter (Sugawara, 2006). Matsuda et al., (2017) showed that there are little evidences of introgression occurring among nine closely related *Heterotropa* species in the islands of Amami Groups even within stands composed of multiple sympatric species, which indicates their floral trait differentiation would be responsible for the species cohesion. Thus, the highly diverse floral traits of *Heterotropa* led us to consider that biotic factors would be concerned with the diversification of this section.

My primal objectives were to reveal the diversification history and to obtain implication to the mechanisms for generating the floral morphological diversity of *Heterotropa*. I firstly investigated phylogenetic relationships of five sections in genus *Asarum* using ITS and *matK* sequences (Chapter 1). This is because phylogenetic relationships between five sections within genus *Asarum* had not been unclear, and monophyly of each section had not been confirmed (Kelly, 1998). Subsequently, to infer the diversification patterns of *Heterotropa*, I constructed the time-calibrated phylogenetic tree including almost all *Heterotropa* species (79 species) using chloroplast genome sequences and genome-wide SNPs obtained from ddRAD-seq analysis. By using the results of phylogenetic analysis, I also calculated degrees of geographic and morphological isolation of sister-taxa pairs, in order to test whether geographic isolations or biotic factors were major forces for speciation in *Heterotropa* (Chapter 2).

Then, I focus on series *Sakawanum* F.Maek. in section *Heterotropa*. This series is defined by the synapomorphy of having only longitudinal ridges on inner walls of calyx tube (Maekawa, 1933), and is a monophyletic group (Chapter 1). Four taxa are included in this series; *A. minamitanianum* Hatus., *A. sakawanum* var. *stellatum* (F.Maek. ex Akasawa) T.Sugaw., *A. sakawanum* var. *sakawanum* Makino, and *A. costatum* (F.Maek.) T.Sugaw., which are allopatrically distributed in Kyushu and Shikoku islands in Japan. This series exhibits inter-taxonomic clinal variation in the calyx lobe length. *Asarum minamitanianum*, which is found in the westernmost extent of the range, has the longest calyx lobes (70–180 mm), whereas *A. costatum*, in the easternmost portion, has the shortest (10–20 mm). *Asarum sakawanum*, which is distributed between *A. minamitanianum* and *A. costatum*, has a calyx lobe length that is intermediate (var. *stellatum*; 25–50mm and var. *sakawanum*; 20–25 mm) between the other species. Clinal variation is generally considered to be the result of selection linked to micro-environmental heterogeneity (Huxley, 1938). I considered that revealing the formation mechanisms of the clinal variation would contribute to understanding of the mechanism generating the floral diversity of *Heterotropa*. In Chapter 3, I investigated evolutionary history of the four taxa by employing approximate Bayesian computation method based on both nuclear microsatellite loci and chloroplast sequences, and I also inferred the past distributions of the series by using ecological niche modelling. Although in many cases, clinal variations are interpreted as the results of local adaptations, it has been reported that neutral demographic processes (e.g. secondary contacts, range expansions, and isolation by distance) can also generate pattern of clinal variations (Vasemagi, 2006). Thus, to test whether natural selection is concerned with calyx lobe length of each taxon, I compared the

degrees of morphological differentiation and genetic differentiation between the taxa (Chapter 4). Finally, to obtain the evolutionary insight into the calyx lobe extension and to infer the ecological consequence of floral traits evolution, I estimated the reproductive ecology of *A. costatum* and *A. minamitanianum* including pollinators, pollen dispersal distances, mating systems, and seedling establishments (Chapter 5). I expected the knowledge about reproductive ecology of two species would also contribute to our understanding of the diversification mechanism of *Heterotropa*.

Chapter 1

Molecular phylogeny and taxonomic implications of *Asarum* (Aristolochiaceae) based on ITS and *matK* sequences

Abstract

The genus *Asarum* (Aristolochiaceae) encompasses approximately 120 species from five sections. Taxonomic controversies concerning the genus *Asarum* and/or its intrageneric classification remain unresolved. In particular, sect. *Heterotropa* accounts for a large percentage of the genus (85 of 120 species) and is well diverged in the Sino–Japanese Forest subkingdom. Reconstruction of *Heterotropa* phylogeny and estimation of its divergence times would provide significant insight into the process of species diversity in the Sino–Japanese floristic region. This study encompassed 106 operational taxonomic units (OTUs), and phylogenetic analyses were conducted based on internal transcribed spacer (ITS) and *matK* sequences. Although the *matK* sequences provided informative results solely for section *Geotaenium*, phylogenetic trees based on ITS regions yielded a clear result for several sections. Three sections, *Asarum*, *Geotaenium*, and *Asiasarum,* were supported as robust monophyletic groups, whereas *Heterotropa* had low support. Sect. *Hexastylis* was revealed to be polyphyletic, suggesting taxonomic reconstruction would be needed. Sect. *Heterotropa* comprises two clades, which correspond to species distribution ranges: mainland China and the island arc from Taiwan to mainland Japan via the Ryukyu Islands. It is notable that the common ancestry of the latter clade in the eastern Asian islands was highly supported, suggesting that the present species diversity of *Heterotropa* was initially caused by allopatric range fragmentation in East Asia.

Introduction

The genus *Asarum* L. (Aristolochiaceae) comprises approximately 120 species of low-growing, rhizomatous herbs that grow in shaded understories (Barringer and Whittemore, 1993, Huang et al., 2003, Ito et al., 2016). The distribution range of the genus is confined to the northern hemisphere, and most of its species diversity is in East Asia (~100 species); approximately 15 species are distributed in North America, and one species (*Asarum europaeum*) is found in Europe. *Asarum* can be distinguished from other genera of Aristolochiaceae by several morphological characteristics, including determinate seasonal growth, simple leaf blades, cataphylls, preformed flowers and leaves, and fleshy and irregularly fruits (Kelly and Gonzalez, 2003, Kelly, 1997), as well as by molecular data (Neinhuis et al., 2005, Ohi-Toma et al., 2006). Because there are many morphological differences within the genus *Asarum*, controversies have surrounded the determination of the taxonomic breadth of the genus and its intrageneric classification, including whether *Asarum* should be treated as a single genus or divided into several genera and sections. Braun (1861) recognized three sections within the genus: *Ceratasarum* (=*Hexastylis*), *Heterotropa*, and *Euasarum* (=*Asarum sensu stricto*). Duchartre (1864) later adopted Braun's intrageneric classification and added a new section, *Aschidasarum*. Araki (1953, 1937) divided the genus into two subgenera, *Choriasarum* and *Gamoasarum,* and further into nine sections. Cheng and Yang (1983) divided the genus into two subgenera, *Asarum* and *Heterotropa*, based primarily on the morphologies of the flowers and the stems, such as internode elongation, stigma position, and ovary position. On the other hand, Maekawa (1933, 1953a, 1936) divided the genus into five genera: *Asarum s.s*., *Asiasarum*, *Hexastylis*, *Geotaenium*, and *Heterotropa*. Thus, the breadth of the genus and its intrageneric subdivision have been controversial, although at least five divisions (*Heterotropa*, *Asiasarum*, *Hexastylis*, *Geotaenium*, and *Asarum s.s*.) have been consistently recognized.

Phylogenetic analyses conducted by Kelly (1998, 1997) supported the recognition of the two subgenera, *Asarum* and *Heterotropa*, and suggested that sect. *Hexastylis* should be included in sect. *Heterotropa*, since sect. *Hexastylis* was paraphyletic among the five sections. These studies were based on internal transcribed spacer (ITS) data, morphological data, and the combined

datasets of 32 species. A more recent study, however, divided the genus *Asarum* into three subgenera and six sections based on one nuclear and seven plasmid datasets: subgenus *Asarum*, subgenus *Geotaenium*, and subgenus *Heterotropa*, and sect. *Asarum*, sect. *Geotaenium*, sect. *Asiasarum*, sect. *Heterotropa*, sect. *Hexastylis*, and the new sect., *Longistylis* (Sinn et al., 2015a). Sect. *Longistylis* was distinguished from sect. *Heterotropa* by its yellow pollen and style extensions that overhang the stigmas. Sinn *et al.* (2015a) identified three species as sect. *Longistylis* (*Asarum splendens*, *Asarum delavayi*, and *Asarum maximum*) in their study that encompassed 58 operational taxonomic units (OTUs) focusing on sect. *Hexastylis*. Both studies included a limited number of taxa, for example, sections *Asiasarum* and *Geotaenium* included only one species each (*Asarum siebolii*. and *Asarum epigynum*, respectively). These studies mainly included the species distributed in North America. In phylogenetic studies, limited sampling of taxa often produces biased results and may lead to conflicting but robust topologies (Bremer et al., 1999, Rydin and Kallersjo, 2002, Wallberg et al., 2004, Hawkins et al., 2015). Moreover, in the genus *Asarum*, most of its species diversity is located in East Asia (~100 species), and with new taxa that have recently been described, the total number of species exceeds 120 (Wang et al., 2004, Yamaji et al., 2007, Lu and Wang, 2009, Sugawara, 2012). Thereby, to resolve the phylogenetic relationships in the genus *Asarum*, an inclusive molecular phylogenetic study using a wider and denser sampling of taxa, especially including species distributed in East Asia, is needed.

The greater species diversity and endemism of temperate vascular plants in the Sino–Japanese Floristic Region are well known (Qian and Ricklefs, 2000, Harrison et al., 2001, Qiu et al., 2011). In this region, the region from southwest China to Japan through Taiwan and the Ryukyu Islands is referred to as the Sino–Japanese Forest subkingdom (Wu and Wu, 1996). This subkingdom broadly includes tropical, warm temperate evergreen forest; temperate deciduous forest; and boreal forest biomes and is also characterized by rich flora and rich endemism (Qiu *et al.* 2011). The biota in this region is tightly linked to historical environmental changes associated with the Quaternary climatic oscillations. Mainland Japan was repeatedly connected to and disconnected from East China by the formation and division of a land bridge due to transgressions and regressions of sea level resulting from climatic oscillation in the Quaternary period (Kizaki and Oshiro, 1977, Ujiie, 1990, Kimura, 1996). During this period, the island arc of the Ryukyus and Taiwan, which encompasses more than 120 continental islands (Takhtajan, 1980), underwent repeated connection and division events. The Quaternary climatic changes led to repeat range fragmentation, adaptation, and extinction of plant species in this region. Many molecular phylogenetic studies have revealed the evolutionary histories of plants in the Sino–Japanese Forest subkingdom (reviewed by Qiu *et al.* 2011). However, most studies have addressed only North China, subtropical China, or China with respect Japan and Korea, whereas few studies have examined the Sino–Japanese Floristic Region that encompasses the area from China to mainland Japan *via* Taiwan and the Ryukyu islands. In particular, the Ryukyu Islands are an important region for investigating species diversity because it is well known that adaptive radiation often occurs on these islands and leads to the creation of rich species diversity (Givnish, 2010).

Sect. *Heterotropa* is endemic to the Sino–Japanese Forest subkingdom and is the most divergent section in the genus *Asarum*, including over 80 species. Moreover, in sect. *Heterotropa*, 19 species are confined to the Ryukyu Archipelago, with most recognized as insular endemics in a particular island (Hatusima and Yamahata, 1988). The seeds of *Heterotropa* species have a fleshy elaiosome, and their dispersal is ground-based and accomplished by ants and/or gravity (Beattie and Culver, 1981, Gonzalez and Rudall, 2003). The dispersion ability of *Heterotropa* species is estimated to be 10–50 cm per year (Maekawa, 1953b, Hiura, 1978). As most *Heterotropa* species have small distribution ranges, possibly due to their limited seed-dispersal ability, *Heterotropa* species may have emerged separately by local adaptation or due to various geographical effects. Reconstruction of *Heterotropa* phylogenetic relationships and estimation of divergence times in the major clades would provide better insight into the process of forming species diversity in the Sino–Japanese floristic region.

In this study, I added two DNA sequence datasets for 106 OTUs of *Asarum* molecular phylogeny: the ITS and the plastid *matK*. The ITS displays high levels of variation in the genus *Asarum* (Kelly, 1998, Yamaji et al., 2007), and the plastid *matK* region has been useful in reconstructing the phylogeny of plants within and among genera. The objectives of this study were to

1) resolve the infrageneric phylogeny of the genus *Asarum*, especially the section levels, and determine the monophyly of the five or six sections; and 2) infer the phylogeny and evolutionary history of sect. *Heterotropa* by estimating the divergence time of the crown node of this section. In addition, I discuss the evolutionary history of *Heterotropa* in East Asia based on the recognized clades.

Materials and methods

Taxon sampling

Forty-four species of *Asarum* were sampled for DNA extraction, and their ITS and *matK* regions were sequenced. In addition, 70 ITS and 33 *matK* sequence data were referenced from the GenBank database and added to analyses in this study. In total, 106 ITS and 75 *matK* sequences were included in the analyses. The ITS analysis included 64 *Heterotropa* species (including two varieties, six unknown taxa, and three species of *Longistylis*), 14 *Asarum* species (including one unknown species), nine *Hexastylis* species (including one unknown species and two varieties), three *Geotaenium* species, and 12 *Asiasarum* species (including four forms). The *matK* analysis included 10 *Asarum* species (including one unknown species), four *Hexastylis* species (including two varieties), three *Geotaenium* species, and 13 *Asiasarum* species (including four forms). *Saruma henryi*. was used as the outgroup, based on a previous study (Sinn et al., 2015a, Kelly, 1998). The taxa, GenBank accession numbers are listed in Table 1.

DNA extraction, polymerase chain reaction (PCR), and sequencing methods

For each sample, total DNA was extracted from approximately 50 mg of leaf tissue dried in silica gel from one individual using the CTAB method (Doyle and Doyle, 1987). The extracted DNA was dissolved in 100 μL of TE buffer and used for polymerase chain reaction (PCR) amplification. The entire ITS region (ITS1, 5.8S rDNA, and ITS2) was amplified using the universal primers ITS-4 and ITS-5 (White et al., 1990). The *matK* region was amplified using three primer pairs that were designed for this study (all primers are listed in Appendix Table S1). PCR was conducted in a total volume of 10 μL containing 6.75 μL of autoclaved iron-exchanged water, 0.8 μL of 0.2 mM dNTP mixture, 1 μL of 10× Ex *Taq* Buffer (Takara Ex *Taq*), 0.05 μL Takara Ex *Taq* (Takara Bio, Ohtsu, Japan), 0.2 μL of each primer (10 pmol/μL), and 1.0 μL of template DNA (approximately 50 μg/μL). PCR amprification for the primers ITS-4 and ITS-5 started with 5 min at 94°C for initial denaturation; 35 cycles of denaturation at 94°C for 1 min, primer annealing at 49.8°C for 1 min, and extension at 72°C for 1 min; and a final extension for 7 min at 72°C. For the primer pairs as-matk1f and as-matk1r, as-matk2f and as-matk2r, and as-matk3f and as-matk3r, the PCR program started with 5 min at 94°C for initial denaturation; this was followed by 32 cycles of denaturation at 94°C for 1 min, primer annealing at 60°C for 1 min, and extension at 72°C for 1 min; next, a final extension was performed for 7 min at 72°C. The PCR products were sequenced in both directions using the standard methods of the BigDye™ Deoxy Terminator ver. 3.1 Cycle Sequencing Ready Reaction Kit (Applied Biosystems, Foster City, CA, USA) using the same primers as above on an ABI 3130 Genetic Analyzer (Applied Biosystems).

Data analyses

DNA sequences were determined for 37 and 39 taxa from the ITS and *matK* regions, respectively. All sequences were deposited in DNA databases (the DNA Data Bank of Japan [DDBJ], GenBank, and the European Molecular Biology Laboratory [EMBL]). Accession numbers of the sequences used in this study are listed in Table 1. Sequence editing and assembly were performed using AutoAssembler™ (Applied Biosystems). The initial sequence alignment was performed with ClustalW (Thompson et al., 1994) with default settings. Editing and subsequent visual adjustment of the aligned sequences was performed with BioEdit 7.2.3 (Hall, 1999). In this study, I did not use the 5.8S rDNA region because some of the ITS sequences from GenBank lacked this region.

I used maximum likelihood (ML) and Bayesian inference (BI) in independent analyses of the *matK* and ITS datasets. Models of nucleotide substitution for each dataset were assessed with jModelTest v1.4.7 (Posada, 2008), with the best-fit model selected from among 24 possible models based on the Akaike information criterion (AIC) and the Bayesian information criterion (BIC). The chosen models for the different datasets were TrNef+G and GTR+G for ITS and *matK*, respectively. ML analyses were performed with PhyML v3.0 (Guindon et al., 2010) using non-parametric bootstrapping (Felsenstein, 1985), with 1000 replicates using NNI branch swapping for each dataset. BI analysis was conducted with each data-

Table 1. Materials used in the present study.

Section	Taxa	Distribution	GenBank accession NO. ITS†	*matK*
Heterotropa	*A. costatum*	Japan (Shikoku)	LC004521	LC008102
	A. sakawanum	Japan (Shikoku)	LC004516	LC008118
	A. sakawanum var. *stellatum*	Japan (Shikoku)	LC004511	LC008106
	A. minamitanianum	Japan (Kyushu)	LC004492	LC008092
	A. asperum	Mainland Japan	LC004498	LC008110
	A. asperum var. *geaster*	Mainland Japan	-	LC050648
	A. muramatsui	Mainland Japan	LC004513	LC008117
	A. tamaense	Mainland Japan	LC004490	LC008103
	A. fudsinoi	Amami Islands	FJ428638	FJ428670
	A. yaeyamense	The Ryukyu Isls. (Sakishima Isls.)	LC004501	LC008120
	A. okinawense	The Ryukyu Isls. (Okinawa Isl.)	LC004502	LC008125
	A. subglobosum	Japan (Kyushu)	LC004497	LC008101
	A. yakusimense	Yakushima Isl.	AB699853	LC008121
	A. hatsushimae	Amami Islands	AB699832	LC050649
	A. megacalyx	Mainland Japan	LC004519	LC008107
	A. nipponicum	Mainland Japan	LC004491	LC008109
	A. kumageanum	Yakushima Island	LC004505	LC008116
	A. dissitum	The Ryukyu Isls. (Sakishima Isls.)	LC004510	LC008119
	A. senkakuinsulare	The Ryukyu Isls. (Senkaku Isl.)	LC004499	LC008113
	A. monodoriflorum	The Ryukyu Isls. (Sakishima Isls.)	LC004522	LC008122
	A. crassum	Japan (Kyushu)	AF061479/AF061480	LC008090
	A. gusk	Amami Isls.	LC004506	LC008129
	A. pellucidum	Amami Isls.	LC004496	LC008114
	A. gelasinum	The Ryukyu Isls. (Sakishima Isls.)	LC004507	-
	A. simile	Amami Islands	LC004493	LC008094
	A. trinacriforme	Amami Islands	LC004489	LC008093
	A. tokarense	Japan (Kyushu)	LC004504	LC008124
	A. satsumense	Japan (Kyushu)	LC004494	LC008111
	A. unzen	Japan (Kyushu)	LC004495	LC008108
	A. asaroides	Japan (Kyushu)	LC004500	LC008112
	A. sp. "hiugana"	Japan (Kyushu)	-	LC008104
	A. magnificum	China (Guangdong, Hunan)	FJ428640	FJ428695
	A. wulingense	China (Guangdong, Guangxi, Guizhou, Hunan, Jiangxi)	FJ428636	FJ428694
	A. longerhizomatosum	China (Guangxi)	FJ428634	FJ428693
	A. campaniflorum	China (Xianning)	FJ428632	FJ428692
	A. sagittarioides	China (Guangxi)	FJ428633	FJ428690
	A. insigne	China (Guangdong. Guangxi. Jiangxi)	FJ428630	FJ428688
	A. hongkongense	China (Hong Kong)	FJ428635	FJ428687
	A. forbesii	China (Anhui, Henan, Hubei, Jiangsu, Jiangxi, Sichuan, Zhejiang)	FJ428639	FJ428686
	A. nanchuanense	China (Chongqing)	FJ428618	FJ428685
	A. bashanense	China (Sichuan)	FJ428620	FJ428684

Table 1 continued

	A. chengkouense	China (Chongqing)	FJ428616	FJ428683
	A. crispulatum	China (Sichuan)	FJ428625	FJ428682
	A. maximum‡	China (Hubei, Sichuan)	FJ428617	FJ428681
	A. ichangens	China (Anhui, Fujian, Guangxi, Hubei, Hunan, Guangdong, Jiangxi, Zhejiang)	FJ428621	FJ428680
	A. chinense	China (W Hubei, NE Sichuan)	FJ428623	FJ428679
	A. inflatum	China (Anhui, NE Sichuan)	FJ428628	FJ428675
	A. porphyronotum	China (Sichuan)	FJ428627	FJ428677
	A. delavayi‡	China (SW Sichuan, NE Yunnan)	FJ428626	FJ428676
	A. splendens‡	China (Guizhou, Hubei, Sichuan, NE Yunnan)	FJ428624	FJ428674
	A. chingchengense	China	-	DQ882196
	A. savatieri	Mainland Japan	AF061540	-
	A. savatieri subsp. *pseudosavatieri*	Mainland Japan	LC004514	LC008105
	A. leucosepalum	Amami Isls.	AB699866	-
	A. lutchuense	Amami Isls.	AB699863	-
	A. hypogynum	Taiwan	AB699861	-
	A. macranthum	Taiwan	AB699840	-
	A. blumei.	Mainland Japan	AF061483/AF061484	-
	A. celsum	Amami Isls.	AB699782	-
	A. fauriei var. *takaoi*	Mainland Japan	LC004518	LC008100
	A. crassisepalum	Taiwan	LC004508	-
	A. sp. JM114	Amami Islands	AB699859	
	A. sp. JM1043	Amami Islands	AB699862	
	A. sp. DT2607§	Mainland Japan	-	LC050647
	A. sp. DT2605§	The Ryukyu Isls.	-	LC008130
	A. sp. DT2606§	Mainland Japan	-	LC008091
	A. sp. DT2603§	Taiwan	LC006099	
	A. sp. DT2602§	The Ryukyu Isls. (Sakishma Isls.)	LC006097	LC008115
	A. sp. DT2601§	Taiwan	LC006098	LC008126
Asarum s.s.	*A. cordifolium*	SE China	LC004509	LC008127
	A. himalaicum	SE China	AF061461/AF061462	-
	A. caulenscens	China, Mainland Japan	FJ428655	FJ428668
	A. debile	China	FJ428644	FJ428667
	A. marmoratum	North America	AF061473/AF061474	-
	A. caudigerellum	China	FJ428643	FJ428666
	A. canadense	North America	FJ428645	FJ428665
	A. europaeum	Europa	FJ428646	FJ428664
	A. cardiophyllum	China	FJ428651	FJ428659
	A. caudigerum	SW China, Taiwan, The Ryukyu Isls.	FJ428652	AY952420
	A. pulchellum	SW China	JF975938	-
	A. hartwegii	North America	AF061453/AF061454	-
	A. caudatum	North America	AF061471/AF061472	DQ532034
	A. lemmonii	North America	AF061451/AF061452	-
	*A.*sp DT2604§	Vietnam	LC006100	LC008128

Table 1 continued

Hexastylis	*A. speciosum*	North America	LC004503	LC008123
	A. shuttleworthii	North America	LC004517	LC008096
	A. minus	North America	AF061494	-
	A. virginicum	North America	AF061489/AF061490	-
	A. arifolium	North America	AB699858	-
	A. arifolium var. *callifolium*	North America	LC004520	LC008098
	A. arifolium var. *ruthii*	North America	LC004512	LC008097
	A. heterophyllum	North America	KJ888524	-
	A. naniflorum	North America	KJ888521	-
	A. memmingeri	North America	KJ888536	-
	A. contractum	North America	KJ888495	-
	A. sp. BtS-2015	North America	KJ888525	-
Geotaenium	*A. yunnanense*	SW China	FJ428656	FJ428672
	A. geophilum	SW China	FJ428657	FJ428671
	A. epigynum	SW China, Taiwan	LC004515	LC008095
Asiasarum	*A. sieboldii*	China, Mainland Japan	FJ428643	FJ428669
	A. sieboldii f. *dimidiatum*	Mainland Japan	AB247087	-
	A. sieboldii f. *maculatum*	Korean peninsula	AB247015/AB247016	-
	A. sieboldii f. *misandrum*	Mainland Japan	AB247108	-
	A. patens	Korean peninsula	AB247088	-
	A. versicolor	Korean peninsula	AB247072	-
	A. tohokuense	Mainland Japan	AB247118	-
	A. maruyamae	Mainland Japan	AB246977/AB246978	-
	A. mikuniense	Mainland Japan	AB246975/AB246970	-
	A. heterotropoides	SW China, Korean peninsula, Mainland Japan	AB248267	-
	A. mandshuricum	NW China	AB247102	-
	A. mandshuricum	Korean peninsula	AB247076	-
Outgroup	*Saruma henryi*	SW China	AF207012/AF207013	FJ428696

†If ITS regions were divided into ITS1 & ITS2, the accession numbers of each regions were shown respectively.

‡These species were included in Sect. Longistylis by Sinn et al. 2015.

§Cultivated at Kyoto Botanical Garden.

-set using BEAST v.1.7.5 (Drummond and Rambaut, 2007, Drummond et al., 2012). The Markov Chain Monte Carlo (MCMC) was performed using two simultaneous independent runs with four chains each (one cold and three heated), saving one tree every 1000 generations for a total of 50,000,000 generations. Trees were summarized by using TreeAnnotator v.1.7.5 (Drummond and Rambaut 2007), and 10% were excluded as burn in. Trees were checked to ensure that all parameters were higher than 200 and to determine whether the stationary phase of likelihood was reached using Tracer v.1.5 (Rambaut and Drummond 2013). Figtree v.1.4.2 (Rambaut, 2009) was used for visualizing the tree. The posterior probability (pp) and bootstrap value (bs) of each clade were estimated in BI and ML, respectively, based on the above settings.

To estimate the approximate divergence time using ITS sequences, the BEAST method, as implemented in the program BEAST, was used. Setting values were the same as above, and an uncorrelated relaxed lognormal clock was adopted as the clock model. Because there is no known fossil record for the genus *Asarum*, I used a published ITS substitution rate: the prior probability of the clock rate was set to a truncated normal distribution with a mean of 4.13×10^{-9}, ranging from 1.72×10^{-9} to 8.34×10^{-9} substitutions per site per year. These values were set according

Table 2. Summary statistics from ITS and *matK* datasets.

	ITS (ITS1+ITS2)	*matK*
Number of sequences	106	95
Aligned length(bp)	531	1485
Invariable characters (bp)	279	1354
Variable sites (bp)	252	131
Variable sites (%)	47.4	8.8
Parsimony-informative characters (bp)	190	114
Parsimony-informative characters (%)	35.8	7.6
Most likelihood score	-3063.4	-2991.4
Model	TrNef+G	GTR+G

to a previous estimation of the ITS substitution rate in annual/perennial herbaceous plants (Kay et al., 2006).

Results

Sequence comparisons between the ITS and matK *datasets*

The ITS and *matK* sequence lengths ranged from 490 to 531 bp and from 1,474 to 1,485 bp, respectively, among the *Asarum* taxa and outgroup. All sequences obtained in this study were deposited in the DDBJ under the accession numbers listed in Table 1. The aligned ITS sequences of ca. 531 bp (excluding the 5.8S rDNA region) yielded a matrix with 190 informative sites (35.8%), whereas the *matK* sequences harbored 7.6% informative sites (114 bp of 1,485 bp) (Table 2).

Phylogenetic analysis based on the ITS dataset

The ITS tree (Figs. 1A, 1B, 2, & 3) strongly supported the monophyly of sections *Asarum*, *Asiasarum*, and *Geotaenium* (pp = 100%, bs ≥ 80%), while it supported the monophyly of *Heterotropa* with moderate or low reliability (pp = 95%, bs = 59%) and showed sect. *Hexastylis* to be polyphyletic (clade A and clade B) in both BI and ML analyses. Clade A included *Asarum arifolium*, *A. arifolium* var. *callifolium*, *A. arifolium* var. *ruthii*, and *Asarum speciosum*, whereas clade B encompassed *Asarum minus*, *Asarum shuttleworthii*, *Asarum naniflorum*, *Asarum* sp. BtS-201, *Asarum contractum*, *Asarum heterophyllum*, *Asarum memmingeri*, and *Asarum virginicum* (Figs. 2 & 3). Both clades Both clades A and B were strongly supported (pp = 100%, bs ≥ 95%). The phylogenetic position of clade A was inconsistent between the BI and ML analyses with weak support, while clade B and sect. *Heterotropa* formed a cluster with low support in both analyses (pp < 50%, bs = 59%). Sections *Asarum* and support in the BI tree (pp = 96%), and with weak support in the ML tree (bs < 50%). In both analyses, other clades above the section level were not strongly supported and there was incongruence between the two analyses (Fig. 1). The ITS data supported two major clades in sect. *Heterotropa*, which were correlated with their regional geographical distribution ranges (Figs. 2, 3, & S1). Clade D, which was supported with a pp of 100% and a bs of 55%, comprised all species distributed in mainland China. Species of section *Longistylis* (sensu Sinn et al., 2015a ; indicated with asterisks in Figs. 2 & 3) were also included in this clade. Clade E was robustly supported (pp = 100%, bs = 91%), and taxa in this clade were distributed in the island arc between Taiwan and mainland Japan through the Ryukyu Islands. Furthermore, Clade E included two monophyletic clades, F and G, and *Asarum yakusimense.* Clade F was weakly supported (pp = 62%, bs = 58%) and comprised all species distributed in mainland Japan (the islands of Honshu and Shikoku). Clade G was moderately supported (pp = 96%, bs = 68%) and comprised all species ranging from the Amami Islands to Taiwan. Species in both clades F and G were distributed in Kyushu and the neighboring islands: *Asarum unzen* and *Asarum asaroides* in the northern part of Kyushu Island were included in clade G, whereas another four species (*Asarum minamitanianum*, *Asarum subglobosum*, *Asarum satsumense* Maekawa, and *Asarum crissum*) in the Kyushu Islands were attributed to clade F. The geographic ranges of insular species in clade G were unclear. *Asarum yakushimense* nested with different clades depending on the method of analysis: clade G with Bayesian analysis and clade F with ML analysis (Figs. 2 & 3).

Phylogenetic analysis of the matK *dataset*

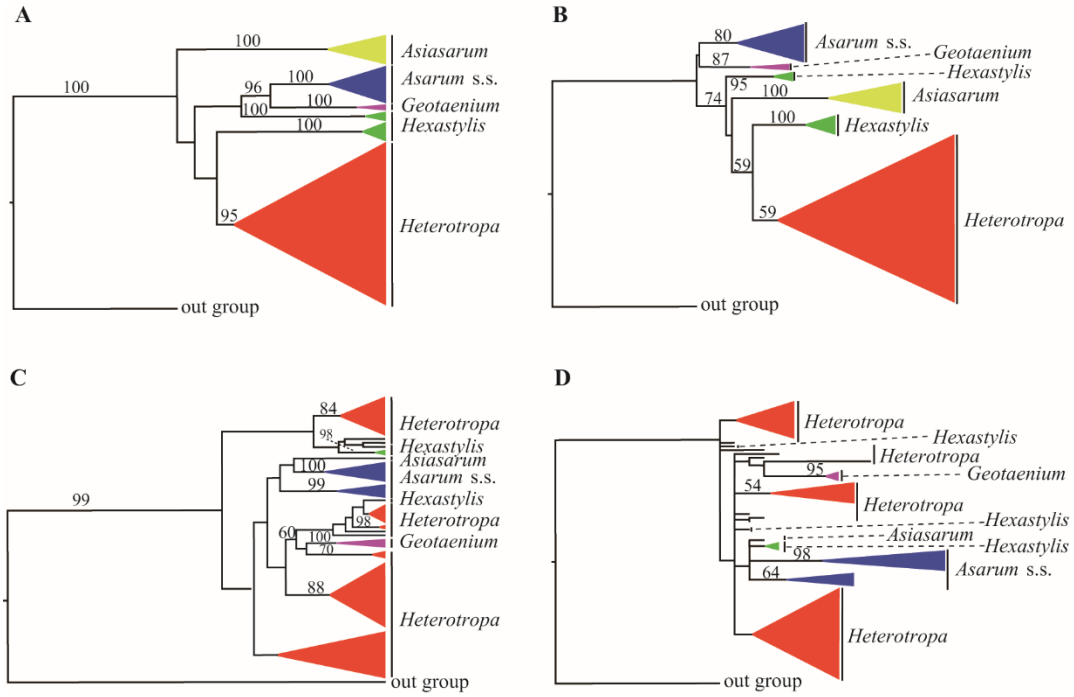

Figure 1. Phylograms at the section levels obtained from each dataset. Only bootstrap values > 50% and Bayesian posterior probabilities > 50% are shown. A) Bayesian tree obtained from ITS regions. B) ML tree obtained from ITS regions. C) Bayesian tree obtained from *matK* regions. D) ML tree obtained from *matK* regions.

Collapsed and detailed *matK* trees based on BI analysis and ML analysis are shown in Figures 1C & D, S2, & S3, respectively. In the phylogenetic trees based on *matK* sequences, only Sect. *Geotaenium* was robustly supported as a monophyly in both BI and ML analyses (pp = 100%, bs = 97%). However, Sect. *Asarum* was paraphyletic and divided into two robustly supported clades (pp = 100% and 99%, bs = 96% and 61%, respectively). Sects. *Heterotropa* and *Hexastylis* were polyphyletic with lower support. Clades found in ITS phylogenies of the six sections were polyphyletic and/or nested in polytomies with low support for each clade (pp < 50%, bs < 50%).

Dating of divergence times

I approximated divergence times using Bayesian analysis (Fig. S4). The age of the initial divergence of the genus *Asarum* clade was estimated to be 13.0 Mya (6.8–21.0 Mya, 95% highest posterior density [HPD] interval). Within the sect. *Heterotropa* clade, divergences between clades D and E were estimated at 9.3 Mya (4.8–15.2 Mya, 95% HPD interval).

Discussion

Incongruence between the* matK *and ITS phylogenies

The results of the ITS sequence analysis are mostly consistent with those of Kelly (1998), but not those of Sinn *et al*. (2015a), and not topologically with either of these studies, in that six clades (sect. *Asarum*, sect. *Asiasarum*, sect. *Geotaenium*, sect. *Heterotropa*, and two sect. *Hexastylis* clades as a paraphyletic section) were strongly supported with sect. *Longistylis* being incorporated into sect. *Heterotropa* (Figs. 1A, 1B, 2 & 3). Analyses of *matK* sequences resulted in uninformative trees in which four sections formed a polytomy with weak support (pp < 50%, bs < 50%), and only sect. *Geotaenium* formed a monophyletic group (Fig. 1C & D). This study shows that ITS sequences provided more information than *matK* sequences. In the *matK* region 7.6% of the 1485 bp were informative, whereas 35.8% of the 531 bp in the ITS region were informative. The higher interspecific variability of ITS sequences compared with cpDNA genes has been demonstrated in the Compositae and many other taxa (Bailey and Doyle, 1999, Linder et al., 2000, Mitsui et al., 2008, Nomura et al., 2010) due to the slower substitution rate in cpDNA. Thus, I concluded that the ITS region may provide much better resolution for examining infrageneric relationships of the genus *Asarum* and the evolutionary history of Sect. *Heterotropa*. In the

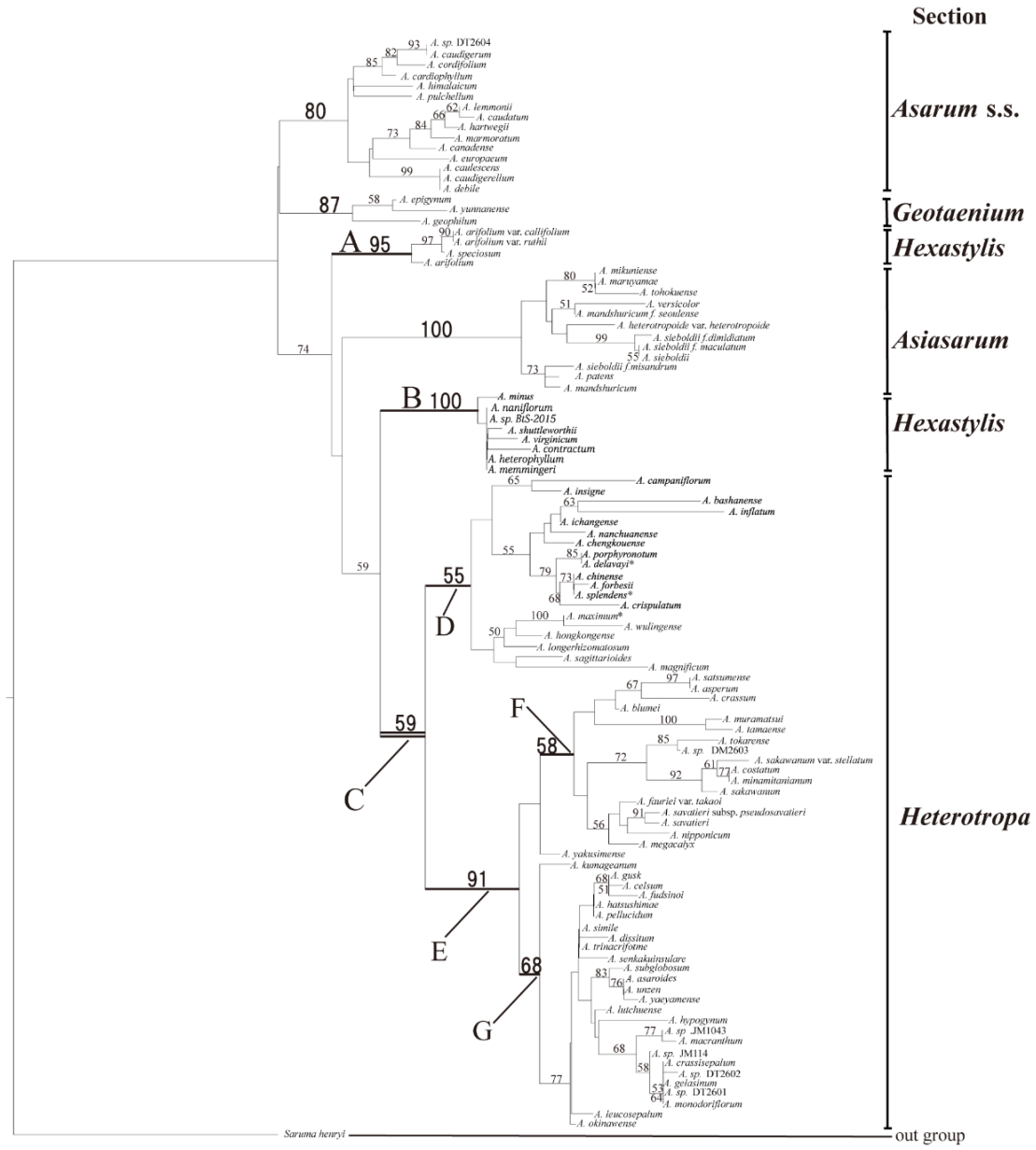

Figure 3. Majority-rule consensus tree inferred from ML analysis of ITS data. Bootstrap values are indicated above branches. Values below 50% are not shown. *These species were included in Sect. *Longistylis* by Sinn et al. 2015.

discussion below I focus primarily on the ITS phylogenetic trees.

Infrageneric classification of the genus* Asarum *sensu lato

This study contributed 106 OTUs to the ITS phylogeny of *Asarum* and clarified its intrageneric classification. The two main results were 1) Five clades in sections *Asarum*, *Asiasarum*, *Geotaenium* were strongly supported, as was a polyphyletic section made up of two sect. *Hexastylis* clades (pp = 100%, bs ≥ 80%); 2) the largest section in *Asarum*, *Heterotropa*, was also a monophyletic group, but was supported only with moderate or low support (pp = 95%, bs = 59%).

In previous phylogenetic studies (Sinn et al., 2015a, Kelly, 1998), only one species each from *Asiasarum* and *Geotaenium* (*Asarum sieboldii* and *Asarum epigynum*) was included and the monophyly of these sections was therefore unclear. In my study, inclusion of almost all species in the two sections confirmed the monophyly of the sections. Sect. *Hexastylis* was collapsed as a polyphyletic group and was divided into two

strongly supported clades (clade A & B in Fig. 2), corroborating the findings of Kelly (1998) and Sinn *et al.* (2015a). The contribution of this study includes confirming the polyphyly of sect. *Hexastylis* with strong statistical support using 106 OTUs. Morphologically, all species in clade A can be identified by a deeply cleft style with an apex that reaches the stigma and leaf blades that are triangular to ovate-sagittate or subhastate, whereas those of clade B have an undivided or shallowly cleft style with an apex that does not reach the stigma and leaf blades that are cordate to orbiculate, triangular-cordate, or subreniform (Blomquist, 1957, Gaddy, 1987). However, I could not conclude that these two clades (clades A & B) should be regarded as independent sections. Because style and leaf morphology are variable within species of *Asarum*, the relationships between the two groups remain unclear in this study. Further studies are necessary to confirm the appropriate taxonomy of sect. *Hexastylis*.

Sect. *Longistylis* species were included in the sect. *Heterotropa* clade (clade D), that is distributed in mainland China. Although sect. *Longistylis* was defined by its yellow pollen and style extensions overhanging the stigmas (Sinn et al., 2015a), some species of clade D do not share these characteristics (e.g., *Asarum chinense*, *Asarum crispulatum*, *Asarum ichangense*, and *Asarum porphyronotum*) (Huang et al., 2003), while some species within clade E share the same morphological characteristics (*Asarum nipponicum*, *Asarum asaroides*, *Asarum fauriei* var. *takaoi*, *Asarum senkakuinsulare*, *Asarum subglobosum*, and more species in Japan) (Hatusima and Yamahata, 1988). Based on these characteristics, and data from this study, I agree with Kelly (1998, 1997) that sect. *Longistylis* should be included in sect. *Heterotropa*.

Previous studies have divided the genus *Asarum s.l.* into two subgenera, subgenus *Asarum* (including sections *Asarum s.s.* and *Geotaenium*) and subgenus *Heterotropa* (including sections *Heterotropa*, *Asiasarum*, and *Hexastylis*) (Kelly, 1998, Kelly, 1997), based on morphological characteristics (e.g., ovary and stigmatic position, and internode morphology of rhizome). Sinn *et al*. (2015a) supported this subdivision, while adding a third subgenus, *Geotaenium*. The present study supports the monophyly of sections *Asarum s.s.* and *Geotaenium*, as well as the subgenus *Asarum s.s.*, in both BI and ML trees, as has been argued by Kelly (1998) (Figs. 2 & 3), however, other clades were not supported. Thereby, the intrageneric classification determined by Kelly (1998) and Sinn *et al*. (2015a) for the genus *Asarum* would be not supported by the ITS sequences used in this study.

One plausible explanation for the incongruence is attributable to taxon sampling, in particular the number of taxa included that are distributed in East Asia (in clades D or E) and in sections *Asiasarum* and *Geotaenium*. In fact, many studies have shown that limited sampling causes bias in phylogenetic trees (Bremer et al., 1999, Pirie et al., 2008, Crawley and Hilu, 2012). In my study, broader taxon sampling would contribute to a better understanding of the taxonomic status of sections *Asiasarum*, *Geotaenium*, and *Longistylis*. Another explanation for the incongruence of the phylogenetic relationships is the quality and quantity of the DNA markers. More informative datasets using single-nucleotide polymorphism (SNP) data obtained using next-generation sequencing methods with broad sampling of this genus would be needed to resolve the phylogenetic relationships among *Asarum* species and the taxonomic status of the two subgenera, sect. *Hexastylis* and sect. *Heterotropa*.

***The estimated evolutionary history of sect.* Heterotropa**

Sect. *Heterotropa* comprises two major clades, which correspond to species distribution ranges in the Sino–Japanese region: mainland China (clade D), and the East Asian island arc (including mainland Japan and Taiwan via the Ryukyu Islands: clade E) (Figs. 2, 3, & S1), with strong support in BI analysis and low or moderate support in ML analysis. The robust Clade E comprises two clades, F (species found in mainland Japan) and G (species ranging from the Ryukyu Islands to Taiwan), although the support for these two clades was relatively low in ML analysis. The divergence time between clades D and E was estimated at approximately 9 Mya, the middle Miocene.

In the Quaternary period, a land bridge was formed between mainland China and mainland Japan via Taiwan and the Ryukyu islands during glacial periods (Kizaki and Oshiro, 1977, 1980, Ujiie, 1990, Kimura, 1996). Many phylogeographic studies have noted close relationships in plant species and populations between Taiwan and mainland China due to historical gene flows between the two areas through the connected landmass that existed during the Quaternary period (Huang et al., 2002, Chiang and Schaal, 2006, Chiang et al., 2006, Mitsui et al., 2008). However, the present study suggests a

robust common ancestry of species distributed in mainland Japan and Taiwan via the Ryukyu Islands. This phylogeographic structure is relatively rare (but see Gao et al., 2007, Chou et al., 2011). One explanation for this structure would be environmental barriers between mainland China and Taiwan. In the Quaternary, the interconnected land bridge area was probably covered by steppes or semi-arid temperate woodland (Harrison et al., 2001, Ray and Adams, 2001). Most *Heterotropa* species in Taiwan are found at higher elevations, at a range of 1000 to 2000 m, and grow in moist understories (Huang et al., 2003, Lu et al., 2019a, Lu and Wang, 2014). Thus, although land bridges were formed between mainland China and Taiwan in the Quaternary, *Heterotropa* species might not have been able to migrate between these two areas. However, coalescent-based analyses and ecological niche modelling are needed to elucidate the history of divergence between the Taiwanese and continental *Heterotropa* species.

Although the origins and the past distribution of the two groups remain uncertain, it is plausible that the species of sect. *Heterotropa* first separated into two groups, those inhabiting mainland China and those in the eastern islands of the Sino–Japanese region, around the middle Miocene. I suggest that speciation within each clade would have occurred later in the Quaternary period. Several factors would have affected this diversification, including effective isolation due to the limited ability of seed dispersal in Heterotropa (Hiura, 1978). I propose that environmental complexity involving geographic barriers and this low dispersion ability would restrict the movement and crossing of *Heterotropa*, contributing to limited gene flow among populations. Population differentiation in heterogeneous environments may have accelerated genetic divergence and local adaptation to abiotic and biotic environments. My findings suggest that the current species diversity of *Heterotropa* probably resulted from allopatric speciation, mainly due to range fragmentation during the Quaternary period. Further phylogenetic studies with more informative markers are needed to confirm this hypothesis.

Appendix

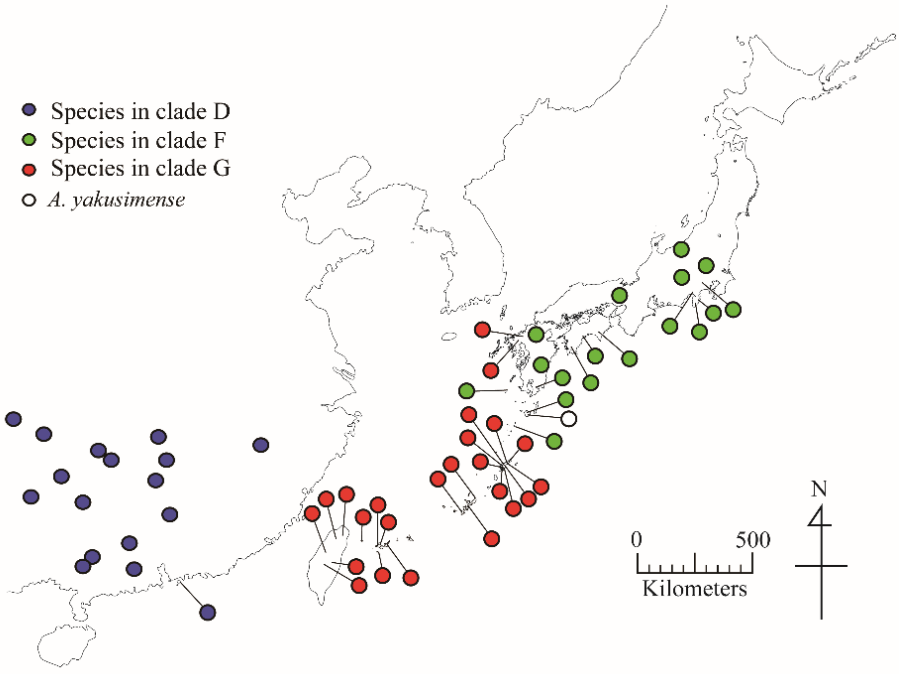

Figure S1. Geographic distributions of the species sampled in sect. *Heterotropa*. The distribution of each species follows Table 1. The centre of the range is shown for species with wide distribution ranges.

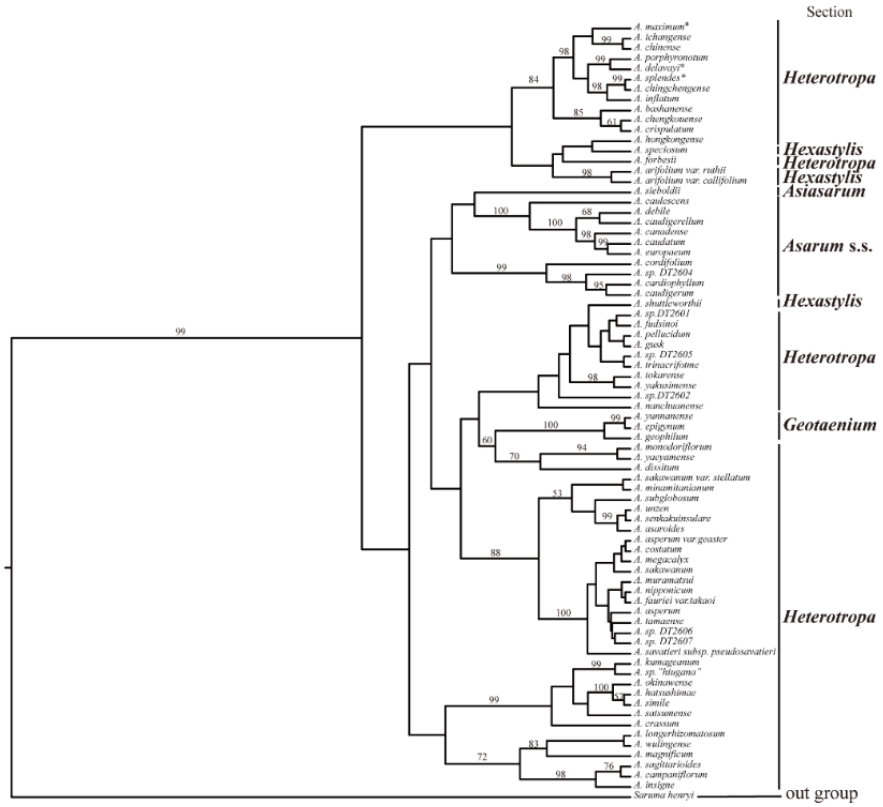

Figure S2. Majority-rule consensus tree inferred from Bayesian analysis of *matK* data. Posterior probability values are indicated above branches. Values below 50% are not shown. *These species were included in Sect. *Longistylis* by Sinn et al. 2015.

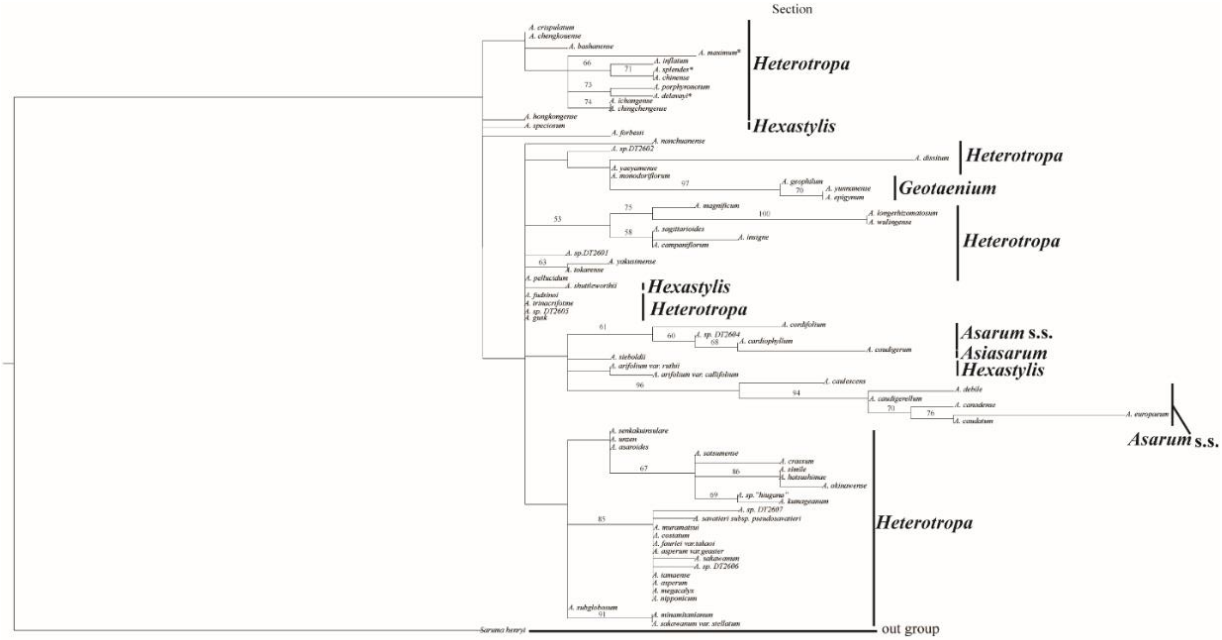

Figure S3. Majority-rule consensus tree inferred from ML analysis of *matK* data. Bootstrap values are indicated above branches. Values below 50% are not shown.

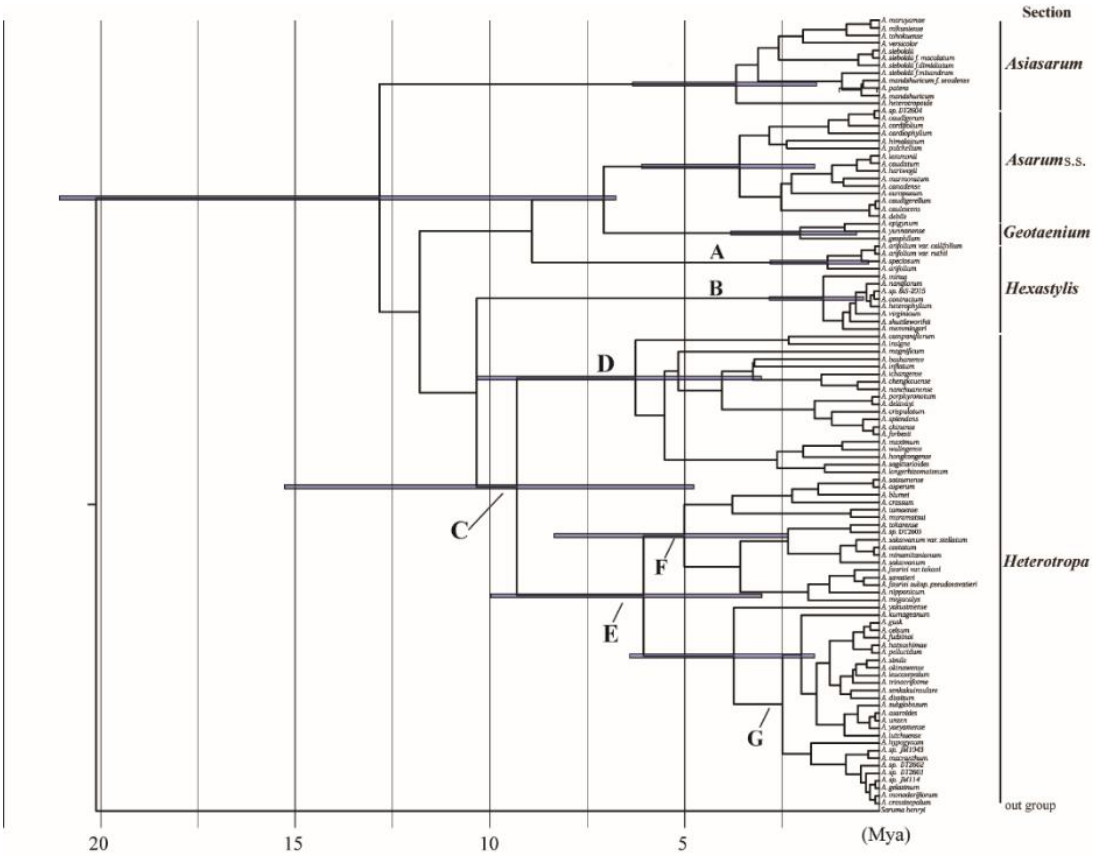

Figure S4. Majority-rule consensus tree inferred from Bayesian analysis of ITS data showing the divergence times of major nodes and 95% HPD intervals.

Table S1. Primer sequences used for PCR and cycle sequencing.

Name	Sequence
ITS-4	5'-TCCTCCGCTTATTGATATGC-3'
ITS-5	5'-GGAAGTAAAAGTCGTAACAAGG-3'
as-matk1f	5'-ACCCAAGAAATCCCCCATAC-3'
as-matk1r	5'-TCGCAATAAATGCAAAGAGG-3'
as-matk2f	5'-CCATCTGGAAATCTTGGTTCA-3'
as-matk2r	5'-TGACTCCTGACCACCAAAGG-3'
as-matk3f	5'-GGCAGGATCCAGATAAACCA-3'
as-matk3r	5'-ATTCTGCATTGGCCAGGTC-3'

Chapter 2

Geographic and subsequent biotic isolations led to a diversity anomaly of section *Heterotropa* (genus *Asarum*: Aristolochiaceae) in insular versus continental regions of the Sino-Japanese Floristic Region

Abstract

The Sino-Japanese Floristic Region is highly diverse with respect to temperate plants. However, the reasons for this diversity are poorly understood because most studies have only considered geographic isolation caused by climatic oscillations. *Heterotropa* (genus *Asarum*) is a remarkably speciose plant group here with floral diversity and shows high species diversity in insular systems (63 species) compared to continental areas (25 species). The primary purpose of this study is to reveal how abiotic and biotic factors have shaped the diversity anomaly of *Heterotropa*. Using ddRAD-seq and chloroplast genome data, I built a time-calibrated phylogenetic tree including 79 species. I estimated the patterns of floral traits (flowering time and floral size) evolution using macroevolutionary modelling. Finally, I estimated the isolation factors of all taxa pairs and sister-taxa pairs within clades based on distribution range and floral traits. Phylogenetic analysis indicated that *Heterotropa* diverged into two clades (continental clade and insular clade) in the Miocene, and the major subclades almost correspond to geographic entities. Most of the rate shifts accelerating the evolution of the floral trait occurred during the Pleistocene. A large proportion of pairs in the insular clade showed geographic isolation at various scales compared with pairs in the continental clade. Several sister pairs showed floral trait divergence without geographic overlap. The diversification of *Heterotropa* would have been triggered by the geographic and climatic events during the Miocene, and subsequent repeated floral trait evolution with and without geographic isolations in the regional lineages during the Pleistocene. My study demonstrated the importance of multidimensional studies to understand the diversification process of temperate plants in the SJFR.

Introduction

The Sino-Japanese Floristic Region (SJFR) extends from the eastern Himalayas to the Japanese Archipelago through south and central China (Wu and Wu, 1996). This region can boast one of the most diverse temperate floras anywhere in the world and has high endemism (Wu and Wu, 1996). This diversity has been thought to be linked to climatic and physiographical complexity and historical environmental changes associated with the Pleistocene (< 2.6 Mya) climatic oscillations (Qian and Ricklefs, 2000). During glacial periods, when the climate of this region was cooler by ca. 4-6 °C and sea level was approximately 130m lower than its present level, temperate plants in this region retreated to refugia at lower altitudes or southern parts (Harrison et al., 2001). During the interglacial periods, expansion to higher altitudes or northern parts would have occurred. In the eastern island systems, sea level changes due to climatic oscillations have caused repeated formation and division of land-bridges in the East China Sea (Ujiie, 1990) and these events have provided opportunities for population expansion and fragmentation (Qiu et al., 2011). Many phylogeographic studies have revealed that the present interspecific and intraspecific genetic structures of temperate plants in this region reflected the range shifts caused by climatic oscillations (reviewed in Qiu et al., 2011). It has been considered that these climatic and associated environmental changes during the Pleistocene triggered range fragmentation, vicariance, and population isolation (Qiu et al., 2011). Therefore, the allopatric speciation could be a major mode of speciation in the temperate plants of this region (Qian and Ricklefs, 2000).

Although the importance of geographic isolation as a major isolation mechanism in plants has been addressed (Boucher et al., 2016), recent studies in other regions have implied that biotic factors also promote species diversification (Lagomarsino et al., 2016). In particular, floral trait evolution has been thought to promote speciation through segregation of gene flow by pollinator shifts (Armbruster, 2014). Previous studies have shown that the tempo and pattern of floral trait evolution varies distinctively among lineages, and

floral trait evolution has been implicated in shaping patterns of species diversification (Jaramillo and Manos, 2001, Givnish et al., 2015). This implies that biotic factors can play complementary roles to abiotic factors in reproductive isolation; that is, biotic factors can facilitate reproductive isolation even without geographical isolation (Rundle and Nosil, 2005). To fully understand the diversification process of species groups, it is essential to reveal the relative contributions of biotic and abiotic factors. However, many studies conducted in the SJFR have only discussed the role of allopatric fragmentation due to geographic and climatic events, and few studies have considered other factors as drivers of the diversification of the temperate plants. In addition, most phylogeographic studies in the region have focused on individual species or only small groups, including fewer than 10 taxa (but Mitsui et al., 2011, Yoichi et al., 2017). Thus, my knowledge of the diversification process of temperate plants in the SJFR remains fragmentary, due to a lack of integrative multidimensional studies of morphology, phylogeny, biogeography, and ecology with adequate sampling of diversified groups.

In this study, I focused on the section *Heterotropa* (genus *Asarum*; Aristolochiaceae), one of the most speciose warm-temperate plant groups (comprising approximately 90 species) endemic to the SJFR (Sugawara, 2006). Taxa of *Heterotropa* are rhizomatous herbs that grow in shaded understories, and are distributed in mainland China (25 species), Taiwan (13 species), and the Japanese archipelago, including the Ryukyu islands (50 species). The species diversity of *Heterotropa* is uneven, and given the difference in areas, *Heterotropa* shows higher diversity in the eastern insular region (from Taiwan to mainland Japan; 2.7×10^{-4} species/km^2 and mainland China; 1.3×10^{-5} species/km^2, see Results). Some taxa of *Heterotropa* have very limited geographic ranges (e.g., in only one island or mountain range), and the dispersal ability of *Heterotropa* is estimated to be 10 – 50 cm per year due to its myrmecochore seeds with elaiosome (Hiura, 1978). Low dispersal ability promotes genetic differentiation among populations and often leads to allopatric speciation (Petit et al., 2005). These confined distribution ranges and the low dispersal ability led me to hypothesise an allopatric speciation process for *Heterotropa*. On the other hand, *Heterotropa* taxa are characterised by high divergence in floral traits, in terms of their shapes, sizes, and colours of calyx tubes and lobes (Figs. 4a & S5), while their vegetative traits show almost no differences (Sugawara and Ogisu, 1992). The sepals connect beyond attachment to the ovary and form a calyx tube with calyx lobes (Sugawara, 1987), and their flowers have been hypothesised to mimic fungi in order to attract fungus gnats (Sinn et al., 2015b). In addition to flower shape, *Heterotropa* taxa are highly divergent in flowering time; most taxa have flowers in spring, while others have flowers in autumn or winter (Sugawara, 2006). A genus-wide phylogenetic study of *Asarum* showed that diversification of *Heterotropa* could have been triggered by the presence of putative fungal-mimicking floral structures, loss of autonomous selfing, and loss of vegetative reproduction (Sinn et al., 2015b). Given these characteristics, I considered that *Heterotropa* would be an ideal subject for investigating the relative importance of the abiotic and biotic effects on its diversification in the SJFR. My previous phylogenetic study using the ITS region showed that *Heterotropa* was monophyletic and comprised two clades, which corresponded to geographic patterns, namely mainland China and the island arc from Taiwan to mainland Japan (Chapter 1). In order to obtain the taxonomic implications of insular *Heterotropa*, Okuyama et al., (2020) conducted phylogenetic analysis using RAD-seq datasets including 47 insular and 5 continental species, and they implied that insular *Heterotropa* comprises nine groups. However, due to the low resolution of the datasets or lack of inclusive sampling around the SJFR, the formation mechanisms of the diversity anomaly of *Heterotropa* and their diversification history in terms of temporal and spatial patterns of floral trait evolution remain unknown.

My primary purpose in this study was to reveal the diversification history of *Heterotropa* taxa in the SJFR, especially focusing on the relative contribution of abiotic and biotic drivers and the diversity anomaly. For this purpose, I first constructed a highly resolved and time-calibrated phylogenetic tree including most *Heterotropa* taxa using genome-wide single nucleotide polymorphisms (SNPs) and chloroplast genomes. Then, I estimated the patterns of floral trait evolution of clades and compared them between insular and continental lineages. In addition, to test whether geographic isolations would be major forces for speciation or whether biotic factors were more likely to facilitate speciation in *Heterotropa*, I compared degrees of geographic and morpholo-

-gical isolation of sister-taxa pairs in insular versus continental regions. The implications for the relative roles of biotic and abiotic drivers and the temporal and spatial patterns of their influences would help to understand the diversification process of temperate plants in the SJFR.

Materials and methods

Taxon sampling

Here, I present a comprehensive sample collection of section *Heterotropa*, increasing the number of species from 64 species (Chpater 1) or 52 species (Okuyama et al., 2020) to 79 species (Fig 4b, Table S2), including three undescribed but morphologically distinct taxa (*Asarum kiusianum* var. *tubulosum* nom. nud. [Maekawa, 1983], *A. tarokoense* nom. nud. [Lu et al., in prep.], and *A. titaense* nom. nud. [Setoguchi et al., in prep]) in my analysis. *A. satsumense* has been considered to be distributed in both Taiwan and Kyushu islands (Lu et al., 2010), and my preliminary examination suggested that the Taiwanese entity should be distinguished from the species (Lu and Takahashi, personal observation). Thus, in this study, I treated *A. satsumense* collected from the Taiwan and Kyushu islands as a different taxon (*A. satsumense* W; Taiwanese and *A. satsumense* K; Japanese). The sample set included 46 Japanese species (52 taxa), 13 Taiwanese species (13 taxa), and 20 mainland Chinese species (20 taxa). As an outgroup species, I used one section *Hexastylis* species (*A. shuttleworthii*) according to my previous study Chapter 1).

Sequencing and phylogenetic analysis

For phylogenetic analysis, I adopted hierarchical calibration methods using different datasets (chloroplast CDS regions and ddRAD-seq). I firstly conducted phylogenetic analysis of 59 CDS regions obtained from chloroplast genome data (Tables S3 & S4) and estimated the divergence time of *Heterotropa,* using the crown age of Magnoliidae. Then, I constructed time-calibrated phylogenetic trees of ddRAD-seq data of 85 *Heterotropa* taxa with *A. shuttleworthii* using the obtained crown age of *Heterotropa*. Details of library preparation, sequencing methods, data processing and phylogenetic analysis are described in Appendix 1.

Ancestral area reconstruction

To infer the ancestral areas and phylogeographic history of *Heterotropa* taxa, I performed statistical dispersal-vicariance analysis (S-DIVA) using RASP v3.2 (Yu et al., 2010). The maximum number of areas was constrained to 2, but I also explored the importance of changing the maximum areas (setting the number of maximum areas to 3, and 4). To accommodate phylogenetic uncertainty, the analysis was conducted using 1000 phylogenetic trees of the ddRAD-seq dataset obtained from BEAST. I divided the distribution range of *Heterotropa* into seven regions: (A) Sichuan basin and surrounding mountains, (B) other parts of mainland China, (C) Taiwan and southern Ryukyu islands, (D) central Ryukyu islands, (E) northern Ryukyu islands and Kyushu island, (F) southern part of mainland Japan including Shikoku island, and (G) northern part of mainland Japan (see Fig. 4c). The boundaries of these regions were defined with reference to biogeographic studies (e.g., C and D; Kerama gap, D and E; Tokara gap [Kimura, 1996], F and G; Itoigawa-Shizuoka tectonic line [Okamura *et al*., 2017]) and phylogeographic studies (Landrein et al., 2017). Most species used in this study are distributed in one region and only three species (*A. asperum*, *A. nipponicum* and *A. maximum*) are distributed across two regions.

Analysis of trait evolution

To test the biotic factors affecting the diversification of insular *Heterotropa*, I investigated the differences in patterns of floral trait evolution between insular and continental clades. As objected traits, I focused on flowering time, which I defined as a month when the taxon starts flowering, and calyx tube width, defined as a median value between maximum and minimum calyx tube diameters. Flowering time is related to the local environment, including pollinator fauna, and its differences play a role in the reproductive barrier among taxa. Calyx tube width would be linked to pollinator size selection and its difference could affect the difference in pollinator fauna, which leads to reproductive isolation. The trait values were obtained from field observations and literature (Huang et al., 2003, Sugawara, 2006, Lu and Wang, 2009). I first plotted each trait value on the tips of the phylogenetic tree to visualise trait-phylogeny relationships using “plotTree.wBars” function in “phytools” package (Revell, 2012) for R v. 3.5.4 (R Core Team, 2013). The flowering time of *Heterotropa* taxa ranged from October to May (Fig. S6a). In this analysis, I conveniently divided flowering time into three categories: autumn (flowering September to November), winter (flowering December to February), and spr-

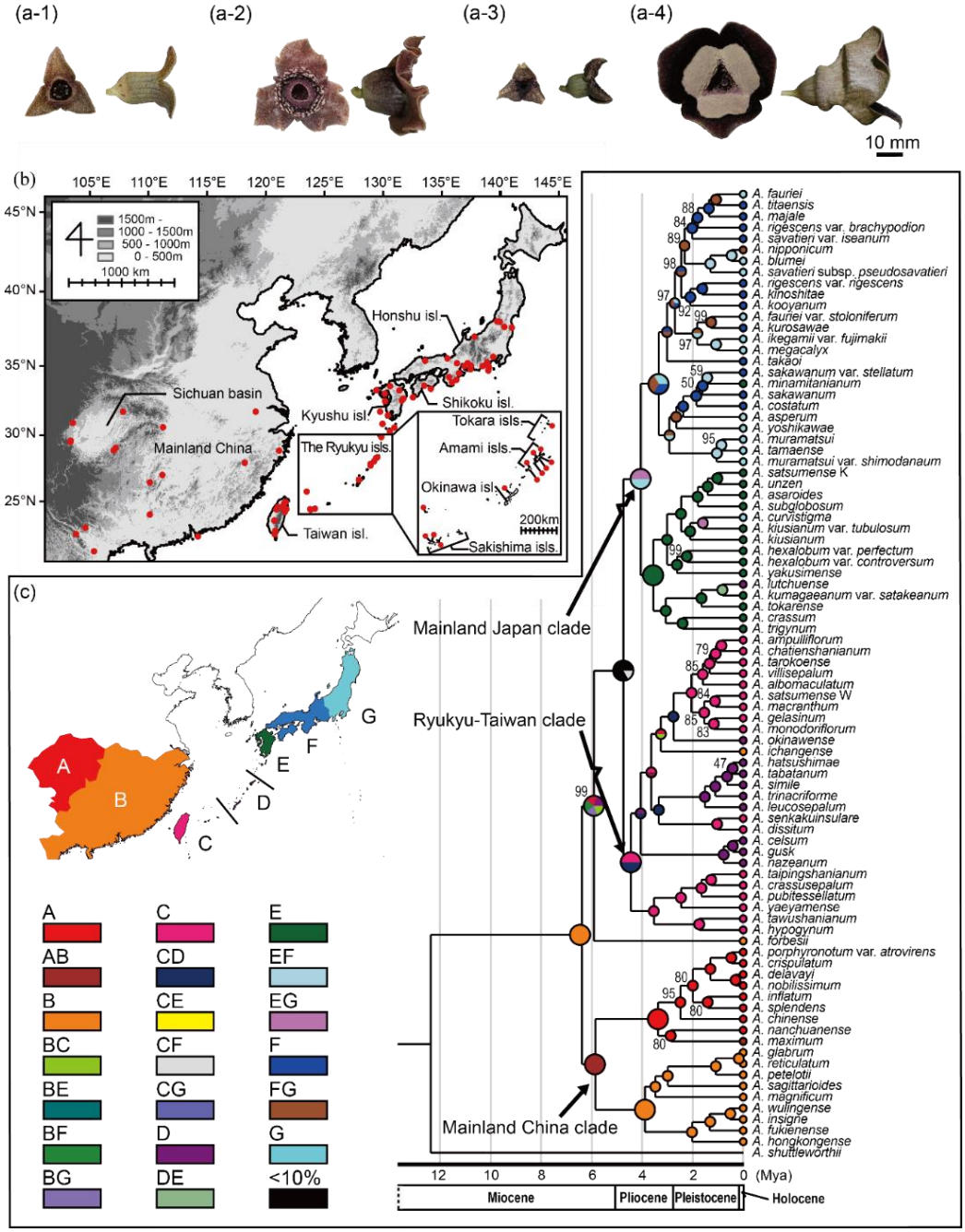

Figure 4. The diversification of *Heterotropa* in the Sino-Japanese Floristic region. (a) Photographs of the flowers of *Heterotropa* taxa (a-1; *Asarum takaoi*, a-2; *A. unzen*, a-3; *A. dissitum*, and a-4; *A. maximum*). (b) Map of the Sino-Japanese Floristic Region. Red circles indicate sampling points. (c) Time-calibrated molecular phylogenetic tree and the ancestral areas estimated from Bayesian analysis and statistical dispersal-vicariance analysis (S-DIVA). Posterior probabilities of < 100% are indicated above or below branches, and the branches without posterior probabilities are those with 100% support. The colours of pie charts reflect the estimated distribution areas according to the biogeographic delimitation as in map (A; Sichuan basin and surrounding mountains, B; other parts of mainland China, C; Taiwan and southern Ryukyu islands, D; central Ryukyu islands, E; northern Ryukyu islands and Kyushu island, F; southern part of mainland Japan including Shikoku island, and G; northern part of mainland Japan).

-ing (flowering March to June).

Then to estimate evolutionary rates and rate shifts of floral trait evolution on the phylogenetic tree of *Heterotropa*, I conducted Bayesian macroevolutionary analysis for flowering time and calyx tube width implemented in BAMM v. 2.5.2 (Rabosky, 2014). BAMM models shift in macroevolutionary regimes across a phylogenetic tree using reversible-jump Markov chain Monte Carlo (rjMCMC) sampling. Because BAMM analysis can only treat continuous characters, I transformed the flowering times to the scaled values (Fig. S6b), where October is set as 1, November as 2, December as 3, January as 4, February as 5, March as 6, April as 7 and May as 8. The prior values were set using "BAMMtools" package (Rabosky et al., 2014) for R, and the analysis was conducted using a maximum clade credibility tree obtained from BEAST. To ease model complexity, I adopted the time-invariant Brownian motion model of trait evolution. The analysis involved a rjMCMC run of 10,000,000 generations sampled every 10,000 steps, and the initial 3,000,000 generations were discarded as burn-in. The rjMCMC convergence was confirmed using BAMMtools. To infer the location of rate shifts, I calculated the marginal odds ratios on individual branches (Shi and Rabosky, 2015). Then, to infer the difference of the evolutionary rates among clades, I reported the mean scaled tree of traits from the outputs of BAMM, in which each branch length is shortened or stretched proportional to the model-averaged mean evolutionary rates of the traits. I also reported the top four most credible shift distributions for each trait. Finally, to infer the temporal change in traits' evolution rates, I plotted the evolutionary rate variation through time for each trait and clade.

Geographic overlaps within each clade

The potential geographic range of each taxon was set by creating a convex polygon from the distribution data. Distribution data for all taxa were based on the specimen records of the herbarium of Kyoto University (KYO), S-Net data portal (http://science-net.kahaku.go.jp/, accessed on 2019/1/26), and the Chinese Virtual Herbarium (http://www.cvh.org.cn/, accessed on 2019/1/26), and the results of personal observations. Because the distribution range of many *Heterotropa* taxa tends to be confined to a small area, I considered that setting any threshold values of the number of records would exclude local endemics from the dataset. Thus, I did not set any threshold values to make distribution data. In total, I collected 1396 occurrences for 84 taxa (minimum 1, maximum 197; Table S2). I was not able to find available records for *A. nobillisimum* and excluded this taxon from the analysis. A single convex polygon for each taxon was created by connecting the outline of the occurrence point(s) by placing a 1 km round buffer and masking by a costal line. Following Anacker and Strauss (2014), I calculated range overlap as the area occupied by both taxa divided by that of the smaller ranged taxa. The range overlap values ranged from 0 (no overlap) to 1 (complete overlap) and were calculated for all pairs of taxa respectively within each major clade (mainland China, Ryukyu-Taiwan, and mainland Japan clades, see Results section). All geographic analysis were conducted by using "sf" package (Pebesma, 2018) in R.

Geographic and morphological isolation

To infer speciation modes of insular and continental clades, I calculated geographic and morphological isolation values of sister taxa. I selected sister pairs with posterior probabilities of nodes higher than 80% in the phylogenetic analysis of ddRAD-seq data sets as sister taxa. The geographic isolation index was calculated by transforming the geographic overlap values into binary data (0; overlap, 1; non-overlap). I set the values of the geographic isolation index of partially overlapping pairs to 0. I also calculated the morphological isolation indices for two floral traits (flowering time and calyx tube diameter) between taxa pairs. To estimate the differentiation of the floral traits, I set the intervals of the traits using the first and last flowering months, and the maximum and minimum values of calyx tube diameters, respectively, according to the trait data. For each trait, when a pair of taxa had an overlap of the intervals, they were scored as 0 for "overlapping"; if they showed no overlaps, they were scored as 1 for "isolation". In addition, I measured the geographic and morphologic isolations between all pairs of taxa within the major clades and estimated conditional relationships among the attributes. Although present isolation would not completely link with the speciation events, this could enable me to discuss the trends and differences of isolation factors between insular and continental clades.

Results

ddRAD-seq data

After filtering low-quality reads and bases, the

number of ddRAD-seq reads of each sample ranged from 510,135 to 2,558,859 reads and the average number of reads was 1,348,526 (Table S2). My 50% genotyped matrix consisted of 469 loci, which contained 3,415 parsimony-informative SNPs. My 70% and 90% matrices included 117 and 46 loci with 710 and 266 parsimony informative SNPs, respectively.

Phylogenetic inference and ancestral area reconstruction

Phylogenetic analysis based on 59 chloroplast CDS regions supported all clades within the tree with posterior probabilities > 0.99 and showed that the *Heterotropa* was monophyletic (Fig. S7). The estimated divergence time between a mainland China taxon and the insular clade including *A. forbesii* was 9.16 Mya (95% HPD: 4.66 - 13.55 Mya).

Phylogenetic analysis with 50% genotyped ddRAD-seq matrix yielded strongly supported clades within *Heterotropa* (Fig. 4c). Within the *Heterotropa* clade, the mainland China clade diverged first, followed by a splitting off of *A. forbesii*, which is distributed in mainland China, and the clade that consisted of insular taxa with only one mainland Chinese taxa (*A. ichangense*). Within each insular and mainland Chinese clade, there were subclades that almost corresponded with the geographic entities. The mainland China clade was divided into two subclades, including the taxa distributed around the Sichuan basin and in other parts of mainland China. The insular clade consisted of two subclades, including taxa distributed in the southern parts of the Japanese island arc (from Taiwan to the Amami islands; Ryukyu-Taiwan clade) and northern parts (from Tokara islands to Honshu; mainland Japan clade). *A. ichangense* was included in the Ryukyu-Taiwan clade. Within the mainland Japan clade, almost all taxa found on Kyushu island (except for *A. minamitanianum* and *A. asperum*) formed a clade with *A. lutchuense* and *A. curvistigma*, which are found on Amami islands and Honshu island, respectively. The other taxa in mainland Japan clade split into two subclades, both of which included southern and northern Japanese taxa. All clades mentioned above showed high support (posterior probabilities > 99%) and diverged during pre-Pleistocene periods (> 2.6 Mya; Fig. S8).

My BI trees inferred from 75% and 90% genotyped ddRAD-seq matrices also supported the hypothesis that *Heterotropa* split into the insular and mainland China clades, while the nested structures were not resolved (Fig. S9). The tree obtained from the 50% genotyped matrix showed relatively high support of nodes (mean posterior probabilities = 91.0%), while other matrices showed lower supports (75% genotyped matrix; 77.7%, and 90% genotyped matrix; 63.2%). Thus, I adopted the 50% genotyped tree for further analysis.

The results of S-DIVA analysis with maximum areas set at 2 (Fig. 4c) showed that the origin of *Heterotropa* was in the mainland China region (B) and that dispersal to insular systems occurred subsequently, while the results with other settings (maximum areas = 3 or 4) failed to support this scenario (Fig. S10). From insular systems, only one back-dispersal to mainland China was estimated (*A. ichangense*). The common ancestral area of the Ryukyu-Taiwan clade is presumed to be Taiwan and the southern Ryukyu islands (C) or Taiwan with southern and central Ryukyu islands (CD). In the mainland Japan clade, several taxa colonised the northern part of Japan (G) from the southern part (E and F). These events were supported regardless of the number of maximum areas.

Analysis of trait evolution

Most *Heterotropa* taxa (55 taxa) analysed in this study start flowering in spring (March to June), whereas 11 taxa flower in autumn (September to November) and 19 taxa in winter (December to February). These autumn-flowering and winter-flowering taxa were scattered across all three major clades (Fig. 5a), implying that the flowering time of *Heterotropa* changed several times in each of the three major clades, especially in tip nodes or branches. With respect to the calyx tube width (Fig. 5b), the taxa that have more than 15 mm of calyx width represented the three major clades, and the changes would have evolved in parallel.

The results of BAMM analysis showed that for both traits, a single macroevolutionary rate was unlikely to fit my genetic data (Fig. S11), indicating that several rate shifts of trait evolution would have occurred in *Heterotropa.* The marginal odds ratios showed that for both traits, the shifts accelerating the trait's evolution were distributed across all three major clades (Fig. 5a-1 & 5b-1). Most of them were located at internal branches within the regional lineages and occurred during the Pleistocene. For both traits, the clades with relatively high evolutionary rates contained several taxa (Fig. 5a-2 & 5b-2). As an exception, the clade

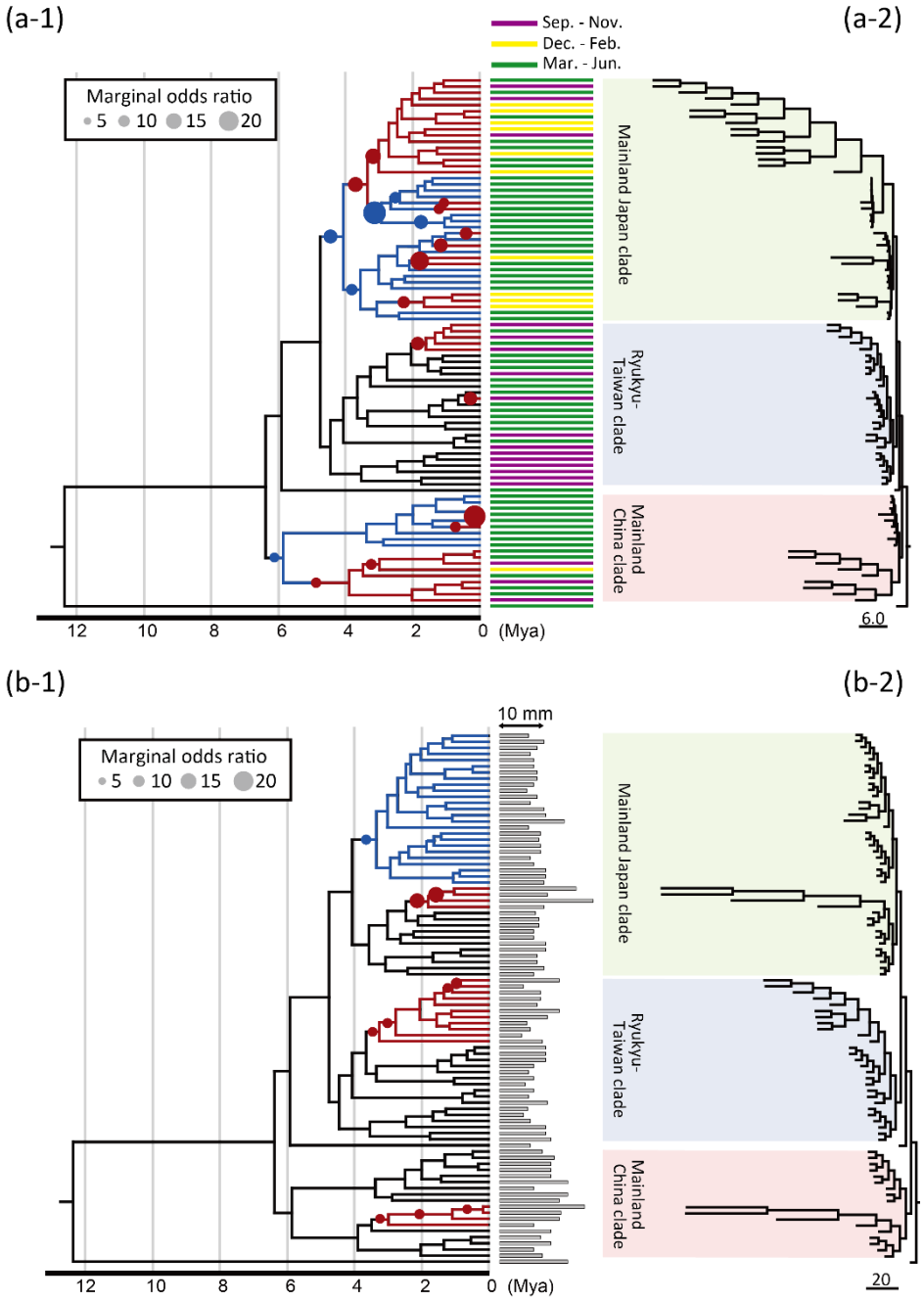

Figure 5. The results of BAMM analysis of flowering time (a), and calyx tube width (b). The circles on the left-hand trees (a-1, b-1) show the locations of rate shifts with their size proportional to the marginal odds ratio of the shift. The colours of circles and branches correspond to the fluctuation of rates before and after the shift (red; rate increase and blue; rate decrease). Shifts with marginal odds below 5 are not shown. The branch lengths of right-hand trees (a-2, b-2) are transformed to their marginal phenotypic evolution rates of each trait. The topologies of all trees are the same as in Figure 4. Colours and lengths of bars across the tips of the phylogenetic trees represent flowering time and mean calyx tube width (mm), respectively. Flowering times are classified conveniently into three types: autumn (flowering September to November; purple), winter (flowering December to February; yellow), and spring (flowering March to June; green) in this figure. BAMM analysis was conducted by using continuous variables of scaled flowering times (shown in Fig. S6).

Table 3. The proportions of taxa pairs showing geographic isolation and floral trait isolation in the three major clades (mainland Japan, Ryukyu-Taiwan, and mainland China). The values within parentheses show the number of pairs showing overlap/differentiation and number of all pairs.

	Clade		
Attribute	Mainland Japan	Ryukyu-Taiwan	Mainland China
Geographic isolations	90.36% (704/780)	88.60% (285/325)	69.85% (95/136)
Flowering time isolation	52.44% (409/780)	21.37% (75/351)	28.76% (44/153)
Calyx tube diameter isolation	36.28% (283/780)	56.13% (197/351)	68.63% (105/153)

containing 16 mainland Japanese taxa and that containing nine mainland China taxa showed high evolutionary rates of flowering time. These tendencies were supported in the top four credible shift distributions (Figs. S12 & S13). Rate variation through time plots indicated that the evolutionary rates of both traits increased in all clades through time, and although their 95% CIs overlapped, the rates of flowering time in the mainland Japan clade were higher than other clades (Fig. S14).

Geographic and floral trait isolation

The mean values of the distribution areas of the taxa within mainland China, Ryukyu-Taiwan, and mainland Japan clades were 172,168 km^2, 570 km^2, and 6,524 km^2, respectively, (Table S2, Fig S15). Within these clades, most of the taxa pairs were distributed allopatrically (Table 3, Fig. S16abc). The mainland China clade contained a relatively low proportion of geographically isolated pairs (69.85%), followed by the Ryukyu-Taiwan clade (88.60%), and mainland Japan clade (90.36%).

Eleven sister pairs out of 24 showed geographic overlaps to various degrees (17 - 100%), and seven sister pairs showed more than 80% range overlap (Table 4, Fig. S16d). In the continental clade, four sister pairs out of five, while in the insular clade, only seven sister pairs out of 18 showed range overlap. I found 14 sister pairs showing the isolation of either flowering time or calyx tube diameter. Within five pairs out of the 14 pairs, both traits were differentiated, and six sister pairs showed floral trait isolation with geographic overlap.

Within the mainland Japan clade, 52.44% of taxon pairs showed flowering time isolation, whereas the proportion of taxon pairs showing isolation in calyx tube width was lower (36.28%). Conversely, both Ryukyu-Taiwan and mainland China clades contained relatively high proportions of taxa pairs showing calyx tube diameter isolation (56.13% and 68.63%, respectively), while only 21.37% and 28.76% of taxa pairs showed flowering time isolation, respectively. All three clades included a high proportion of taxa pairs that differentiated in either flowering time or calyx tube diameter (mainland Japan: 71.02%, Ryukyu-Taiwan: 66.76%, and mainland China: 76.47%). In all three clades, most pairs showing floral trait differentiation were geographically isolated, that is, there were no conditional relationships between geographic overlaps and floral trait differentiation (Fig. 6).

Discussion

Phylogeographic history of* Heterotropa *in the SJFR

The section originated in mainland China (Fig. 4), and the divergence time between mainland China and insular clades estimated from the chloroplast phylogenetic analysis was 9.16 Mya, corresponding to the late Miocene (Fig. S7). These results were concordant with my previous study using the average substitution rate of the ITS region (9.3 Mya; Chpater 1). During the late Miocene, regressions and transgressions of the East China Sea (Haq et al., 1987) caused land-bridge formation that allowed the migration and divergence of temperate plants between the mainland China and insular systems (Yang et al., 2017, Qi et al., 2012). Furthermore, my study revealed that besides the insular clade, the mainland China clade was also composed of subclades, which corresponded to taxa geographic distribution (Fig. 4), and all subclades diverged during the late Miocene or the Pliocene (Fig. S8). During this period, the establishment of a monsoon climate caused by the uplift of the Himalayas and the Tibetan Plateau led to vegetational shifts in the SJFR, and frequent glacial-regressions and inter-/after-glacial transgressions (Kimura, 1996). I con-

Table 4. Geographic overlaps and morphological differences in the 24 sister-taxa pairs with more than 80% posterior support. For each sister-taxa pair, columns indicate the posterior probability that the two taxa are sister, proportion of range overlap, flowering time differentiation (month), calyx tube diameter differentiation (mm), and the clade name that includes two taxa.

Sister pair		Posterior probability	Geographical overlap	Flowering time differentiation	Calyx tube differentiation	Clade name
A. fauriei	*A. titaensis*	100%	0	3†	4.5	Mainland Japan
A. blumei	*A. nipponicum*	100%	1.00	6†	3.0†	Mainland Japan
A. kinoshitae	*A. rigescens* var. *rigescens*	100%	1.00	2†	2.0†	Mainland Japan
A. fauriei var. *stoloniferum*	*A. kurosawae*	100%	0	6†	4.0†	Mainland Japan
A. ikegamii var. *fujimakii*	*A. megacalyx*	100%	1.00	0	3.5	Mainland Japan
A. muramatsui	*A. tamaense*	100%	0	0	0	Mainland Japan
A. satsumense K	*A. unzen*	100%	0	1	8.5†	Mainland Japan
A. curvistigma	*A. kiusiana* var. *tubulosum*	100%	0	2†	2.0	Mainland Japan
A. hexalobum var. *controversum*	*A. hexalobum* var. *perfectum*	100%	0	0	4.0†	Mainland Japan
A. kumagaeanum var. *satakeanum*	*A. lutchuense*	100%	0	0	2.5	Mainland Japan
A. crassum	*A. trigynum*	100%	0	0	3.0	Mainland Japan
A. ampulliflorum	*A. chatienshanianum*	100%	0	3	9.8†	Ryukyu-Taiwan
A. satsumense W	*A. macranthum*	84%	0.55	2	3.5	Ryukyu-Taiwan
A. gelasinum	*A. monodoriflorum*	83%	0.99	1	1.0†	Ryukyu-Taiwan
A. senkakuinsulare	*A. dissitum*	100%	0	2†	7.5†	Ryukyu-Taiwan
A. celsum	*A. gusk*	100%	0.90	2	6.5†	Ryukyu-Taiwan
A. crassusepalum	*A. taipingshanianum*	100%	0.17	0	1.3	Ryukyu-Taiwan
A. hypogynum	*A. tawushanianum*	100%	0	0	1.5	Ryukyu-Taiwan
A. crispulatum	*A. porphyronotum* var. *atrovirens*	100%	0.63	0	3.5	Mainland China
A. nobillisimum	*A. delavayi*	100%	-‡	1	2.5	Mainland China
A. splendens	*A. inflatum*	100%	0.33	1	10.0†	Mainland China
A. maximum	*A. nanchuanense*	80%	1.00	1	2.5	Mainland China
A. glabrum	*A. reticulatum*	100%	0	2†	7.0†	Mainland China
A. wulingense	*A. insigne*	100%	0.91	4	3.0†	Mainland China

†No overlap the between the pair ‡ I could not calculate the geographic overlap because there were no available records for *A. nobillisimum.*

-sidered that geographic and climatic events would have allowed divergence between the insular and the continental lineages and formation of regional lineages of *Heterotropa,* as shown in other studies (Mitsui et al., 2008, Lu et al., 2019b).

As an exception, two Chinese species were not included in the mainland China clade: *A. forbesii* and *A. ichangense* were sister to or included in the insular clade, respectively. The phylogenetic placement of the two species is consistent with a previous phylogenetic study (Okuyama et al., 2020) and previous chromosomal studies that showed they have the same chromosome numbers (2n = 24) as the insular taxa, which is different from the other mainland China species (2n = 26) (Sugawara and Ogisu, 1992). My study using exclusive sampling of Chinese taxa demonstrated that only one back dispersal event from the insular systems to mainland China would have occurred. In addition, colonisation to other regions after formation of the regional lineages was observed only in several taxa (e.g., *A. minamitanianum* from mainland Japan to Kyushu island). This indicated that the regional lineages would have remained separated even during the Pleistocene climatic oscillations. One of the

reasons would be glacial isolation. In the SJFR, the existence of multiple refugia of temperate plants is implied by phylogeographic studies (Qiu et al., 2011). In mainland China, in addition to southern areas (< 30°N), several refugia would be located around the Sichuan basin, and this region would be isolated from other regions due to its complex topography, including high mountains and the Yangtze River (Wang et al., 2015). In mainland Japan, during the glacial periods, most parts were covered by mixed (boreal and cool temperate) forests or boreal forests (Harrison et al., 2001), and warm temperate plants would have been forced to retreat southward and survive separately in narrow glacial refugia on the southern coasts of Kyushu, Shikoku, and Honshu islands (Aoki et al., 2019). Another isolating factor would be the seaways barriers. In the Ryukyu islands, two deep-water passages (Tokara Tectonic Strait and Kerama gap, currently > 1000m in depth), were formed during the Pliocene (Kimura, 1996). These deep-water passages act as isolation barriers for plant expansion (Nakamura et al., 2009). I considered that these glacial and geographic isolations would prevent the colonisation of most *Heterotropa* taxa to other regions.

Diversity anomaly and its driving forces

Geographic isolation facilitated by the climatic oscillation has been considered to play a major role in plant speciation in the SJFR (Qian & Ricklefs, 2001). However, its effects varied among regions (Yoichi et al., 2017). The repeated exposure and submergence of the land-bridges during the Pleistocene period led to significant population isolations and declines of temperate plants, especially in insular systems (Qiu et al., 2011). Furthermore, during glacial periods, warm temperate forests were fragmented in the Japanese archipelago, while the vast areas of central to southern mainland China were covered by them (Harrison et al., 2001). In *Heterotropa*, most of speciation events would occur during the Pleistocene period (Fig. S8). Insular taxa have smaller distribution ranges than continental taxa (Fig. S15), and a large proportion of insular pairs show geographic isolation at various scales (Tables 3 & 4). These results likely reflect the repeated range fragmentations and contractions of insular taxa, and these geographic effects would have triggered the divergence of insular *Heterotropa*.

The results of trait evolutionary analyses indicated that the evolutionary rates of both traits increased through time (Fig. S14). In addition, most of the accelerating rate shifts occurred after the formation of regional lineages during the Pleistocene period (Fig. 5). A higher evolutionary rate of flowering time in the mainland Japan clade was implied (Fig. S14). The warm temperate forests of mainland Japan have been considered to have experienced significant population declines during the Pleistocene period (Aoki et al., 2019). The morphological heterogeneity would have been facilitated by geographic isolations due to Pleistocene climatic oscillations, as shown in Gao, Zhang, Gao, & Zhu (2015). The random genetic drifts in the range contractions could be one of the mechanisms of trait evolution in plants (Lande, 2000), and a simulation study also implied that a small population size would promote floral evolution, including flowering time without selective agents (Devaux and Lande, 2008). The range fragmentations during the Pleistocene period would have also led to the floral trait differentiation of *Heterotropa*.

Did biotic factors contribute to the diversification of *Heterotropa*? In general, floral morphology has been largely interpreted as the

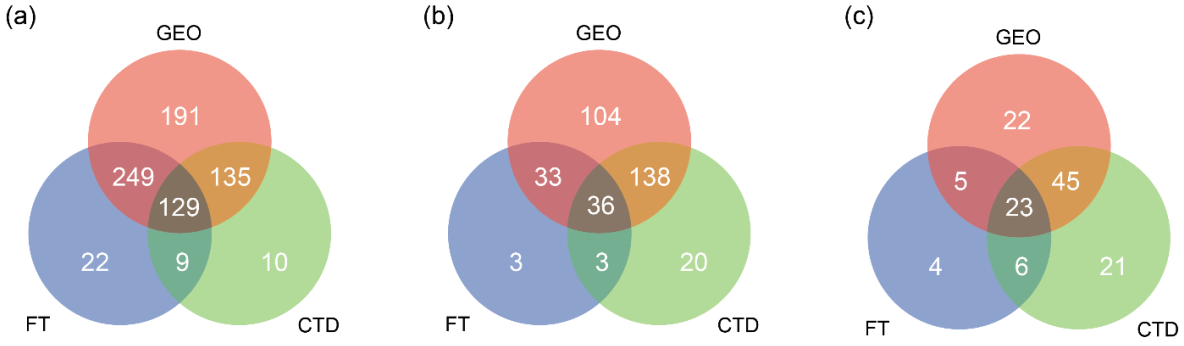

Figure 6. Venn diagrams showing the number of taxa pairs with isolation of distribution range (GEO; red), and flowering time (FT; blue) and calyx tube diameter (CTD; green) within mainland Japan clade (a), Ryukyu-Taiwan clade (b), and mainland China clade (c).

historical outcome of pollinator-mediated selection (Fenster et al., 2004). The pollinator-mediated diversification of *Heterotropa* has been hypothesised in a previous study (Sinn et al., 2015b). Empirical studies have implied that the various Diptera species are pollinators of insular *Heterotropa* taxa with specialisation (e.g., fungus gnus in *A. tamaense* [Sugawara, 1988], sciarid flies in *A. costatum* [Kakishima and Okuyama, 2018], and Calliphoridae flies in *A. fudsinoi* [Maeda, 2013]). The floral traits of *Heterotropa* would be related to attraction of Diptera species, and pollinator specialisation would lead to the formation of prezygotic isolation. However, the results of my isolation analyses using all taxa pairs showed that there were no conditional relationships between geographic isolation and floral trait isolation (Fig. 6), indicating that most pairs showing floral trait isolation were distributed allopatrically. Thus, although floral trait differentiation would act as prezygotic isolation in secondary contact zones, I considered that, among the factors investigated in this study, geographic isolation would be the major isolation mechanism and likely contribute to the formation of the diversity anomaly of *Heterotropa*.

Biotic and abiotic drivers of sister taxa divergence

I found 11 sister pairs show geographic overlaps (seven pairs in insular system, and four in continent), indicating that, besides allopatric speciation, speciation on a small spatial scale could have also occurred in both clades. Geographical overlap between close relatives requires some kind of reproductive isolation to maintain the species boundary (Weber and Strauss, 2016). Six geographically overlapping sister-taxa pairs showed floral trait isolation (Table 4). In *Heterotropa*, most taxa inhabit almost the same environments (understory of warm temperate forests) and the floral difference and/or geographic isolation would act as reproductive barriers rather than habitat differences. This insight was corroborated in a study of nine closely related *Heterotropa* taxa in the Amami islands, which are distributed in sympatry and/or close parapatry and morphologically different in floral traits (Matsuda et al., 2017). Thus, I considered that the flowering time and calyx tube diameter would have acted as one of the possible reproductive barriers in the six sister-taxa pairs, and there are possibilities that the speciation on a small spatial scale triggered by trait differentiations may have also occurred in *Heterotropa*.

Conclusion

Qian & Ricklefs (2001) hypothesised that in East Asia, climatic oscillation with topographic complexities could generate diversity of temperate plants through allopatric speciation. Although both biotic and abiotic factors have long been recognised as fundamental drivers of diversity, their relative contributions to diversification has rarely been investigated especially by using specious plant groups (Funamoto, 2019). My results showed that the repeated range fragmentations and contractions in insular systems during the Pleistocene period formed the diversity anomaly of *Heterotropa*, which basically supports Qian & Ricklefs's hypothesis. Furthermore, sister-taxa analysis implied that speciation triggered by reproductive trait differentiations without geographic isolation could have also occurred recently. Therefore, the diversification of *Heterotropa* was driven by multiple drivers, including geographic isolation and complementary floral trait evolution with different temporal scales. My study demonstrated the importance of multidimensional studies to understand the diversification process of temperate plants in the SJFR, where geographic isolation had been considered to play a dominant role in the diversification.

Appendix

Supplementary materials and methods

Chloroplast genome construction and divergence time estimation

To obtain the chloroplast genomes, I sequenced four *Heterotropa* species (*Asarum satsumense* K, *Asarum macranthum*, *Asarum wulingense*, and *Asarum forbesii*) and one *Hexastylis* species (*Asarum shuttleworthii*). I used three sequencing methods.

To *A. macranthum* and *A. wulingense*, I used the chloroplast enrichment method following Sakaguchi *et al.* (2017). To construct barcoded DNA fragment libraries, the Ion Xpress Plus Fragment library Kit (Thermo Fisher Scientific, Waltham, Massachusetts, USA) was used to process the purified DNA of *A. macranthum* and *A. wulingense*. The barcoded libraries were mixed with Ion Sphere Particle for emulsion PCR using Ion One Touch 2 system (Thermo Fisher Scientific) with Ion PGM Hi-Q OT2 Kit (Thermo Fisher Scientific). From the product of emulsion PCR, the positive particles with amplified DNA were isolated and purified by Ion OneTouch ES (Thermo Fisher Scientific) and loaded onto an Ion 318 chip (Thermo Fisher Scientific). Sequencing was performed using an Ion PGM sequencer (Thermo Fisher Scientific). Extracted DNA from *A. satsumense* K and *A. shuttleworthii* were fragmented using the Takara DNA Fragmentation Kit (Takara Bio, Ohtsu, Shiga, Japan). The library preparation was conducted using the SMARTer ThruPLEX DNA-Seq Kit (Takara Bio, USA). Barcoded libraries were sequenced with paired-end 150 bp reads on Illumina Hiseq-X (Illumina, San Diego, California, USA; sequencing was performed by Macrogen Japan, Kyoto, Japan). To *A. forbesii*, NEBNext® DNA Library Prep Kit (New England BioLabs, Ipswich, MA, USA) was used to prepare library. Nova-seq 6000 (Illumina) was used to sequence the prepared library. Library preparation and sequencing were performed by Chemical Dojin (Kumamoto, Japan).

All obtained reads were trimmed using Trimomomatic v. 0.32 software (Bolger et al., 2014) using the following commands: HEADCRAP:10, LEADING:20, TRAILING:20, SLIDINGWINDOW:4:20, AVGQUAL:20, and MINLEN:50. Because the amount of obtained reads of *A. forbesii* was too large (> 80 Gb), I reduced the data to 500,000 reads (approximately 7.5 Gb). The cleaned reads were mapped using MITObim v.1.8 (Hahn et al., 2013) to the chloroplast genome of *Asarum costatum* (AP018513; Takahashi et al., 2018) with minimum depth 4X. The obtained reads and chloroplast genomes were deposited in DDBJ (BioProject ID, PRJDB9302, Table S4).

To construct chloroplast genome phylogeny and estimate divergence time, in addition to newly obtained five sequences, I used the chloroplast genome sequences of ten Magnoliid species, including one *Heterotropa* species (*Asarum costatum*), and two Chloranthales species. The species information is shown in Table S4. As my data set included highly divergent species, to construct the chloroplast phylogeny, I used only CDS regions shared by more than 17 species out of 18 species. The CDS regions of chloroplast genomes and assemblies were identified using GeSeq with protein search identity value 85 (Tillich et al., 2017). Sequence data were manually edited and aligned using BioEdit v.7.0.5.3 (Hall, 1999). In total, 59 regions (26,786 bp) were used for the phylogenetic analysis. The phylogenetic tree construction and estimation of divergence time was conducted by using BEAST v.10.0.4 (Drummond and Rambaut, 2007) applying the GTR+I+G model inferred by JmodelTest v.1.4.7 (Posada, 2008). To estimate the divergence time of the crown age of the *Heterotropa* clade, the crown of Magnoliids was constrained using a uniform distribution with a lower bound of 169 Mya and upper bound of 180 Mya according to the study of angiosperm phylogeny using fossil calibrations (Zeng et al., 2014). The Markov Chain Monte Carlo method was performed using four independent runs with four chains of 50,000,000 generations each, saving one tree every 1000 generations. The first 10,000,000 generations were discarded as burn-in, as evaluated by TRACER v.1.5 (Rambaut and Drummond, 2013). The obtained tree was displayed using FigTree v.1.4 (Rambaut, 2009).

Double-digest restriction-associated DNA sequencing (ddRAD-seq)

Genomic DNA was extracted from silica-dried leaf tissues using the CTAB method (Doyle and Doyle, 1987). For all collected samples, a double-digest restriction-associated DNA library was prepared using Peterson's protocol with slight modifications (Peterson et al., 2012). Genomic DNA was digested with BglII and EcoRI, ligated with Y-

shaped adaptors, amplified by PCR with KAPA HiFi HS ReadyMix (KAPA BIOSYSTEMS) and size-selected with the E-Gel size select (Life Technologies, CA, USA). Approximately 350 bp of library fragments were retrieved. Further details of the library preparation method were described in a previous study (Sakaguchi et al., 2015). Sequencing was performed with paired-read 101bp + 100bp mode of HiSeq2500 (Illumina, CA, USA).

Data processing and phylogenetic analysis of ddRAD-seq data

The ddRAD-seq reads generated by Illumina sequencing were deposited in GenBank (BioProject ID: PRJDB8943). The raw reads were trimmed by Trimomomatic v. 0.32 software (Bolger et al., 2014) with the following settings: HEADCRAP:10, LEADING:30, TRAILING:30, SLIDINGWINDOW:4:30, AVGQUAL:30, and MINLEN:50. The program ipyrad (http://github.com/dereneaton/ipyrad) was used to process the ddRAD-seq reads and detect SNPs. The parameters that influenced the assembly were set as follows: the minimum depth coverage for base calling at each locus was set at 6 and the similarity threshold for clustering reads within/across samples was set at 0.85. Potential paralogous loci were filtered out based on the number of samples with shared heterozygous sites (more than 15 sites). I explored a range of thresholds for the minimum genotyped samples (30, 51, and 70 samples; equivalent to 50%, 75%, and 90% of samples were genotyped, respectively). All three data sets were examined in the phylogenetic analysis, and I selected the 50% genotyped data set as the primary data set for all other analyses (see Results section).

To construct a phylogenetic tree of ddRAD-seq data and estimate divergence times within the *Heterotropa* clade, I used Bayesian inference (BI) in BEAST v. 1.10.4 (Drummond and Rambaut, 2007). I calibrated the crown age of the *Heterotropa* clade using a uniform distribution with lower limit of 4.77 Mya and upper limit of 14.54 Mya following the results of the chloroplast genome phylogenetic analysis (see Results section). The Markov Chain Monte Carlo (MCMC) method was performed using two simultaneous independent runs with four chains each (one cold and three heated), saving one tree every 1000 generations for a total 30,000,000 generations with 10% burn-in for each run. The convergence of the chains was checked using the program Tracer v. 1.5 (Rambaut and Drummond, 2013).

Figure S5. Part of the floral diversity of *Heterotropa* taxa. The font and the side views of the flowers of *Asarum takaoi* (a), *A. savatieri* var. *iseanum* (b), *A. nipponicum* (c), *A. hexalobum* var. *perfectum* (d), *A. rigescens* (e), *A. costatum* (f), *A. trigynum* (g), *A. sakawanum* var. *stellatum* (h), *A. satsumense* K (i), *A. dissitum* (j), *A. pellucidum* (k), *A. gusk* (l), *A. senkakuinsulare* (m), *A. yaeyamense* (n), *A. tokarense* (o), *A. villisepalum* (p), *A. hypogynum* (q), *A. chatienshanianum* (r), *A. macranthum* (s), *A. forbesii* (t), *A. insigne* (u), *A. delavayi* (v), *A. petelotii* (w), *A. inflatum* (x), and *A. maximum* (y). The taxa were ordered according to their distributions: mainland Japan (a-h), the Ryukyu Islands (i-o), Taiwan (p-s), and mainland China (t-y). The colours of the alphabet indicate the flowering time of the taxa (red; autumn, blue; winter, and green; spring).

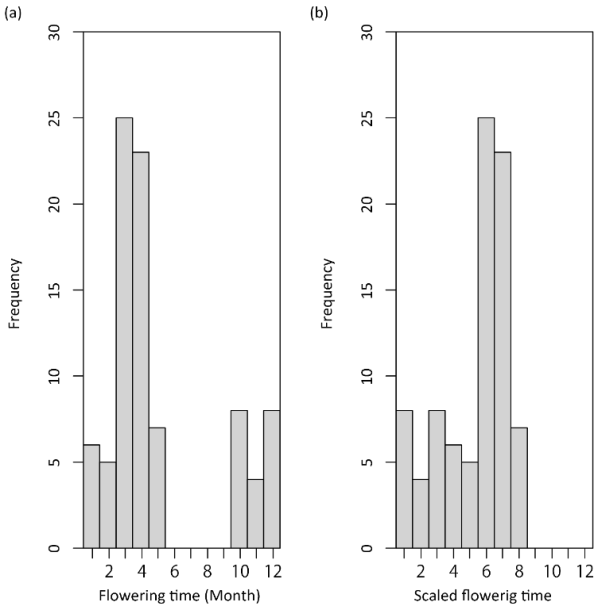

Figure S6. Histograms of Flowering time of *Heterotropa* taxa; raw data (a), and scaled data used in the BAMM analysis (b).

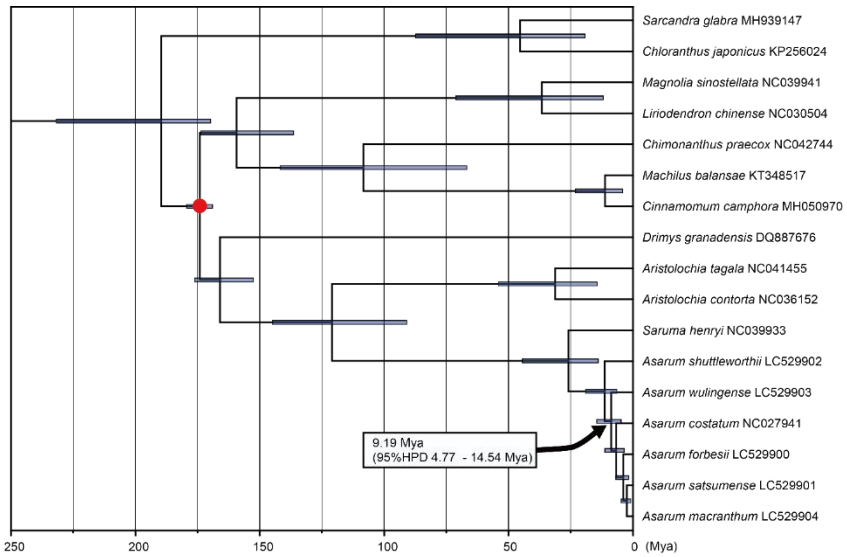

Figure S7. Phylogenetic tree based on 59 CDS regions (26,786bp) of the chloroplast genomes of the Magnoliids and Chloranthales species. The red circle indicates the calibration point (169 – 180 Mya) followed by Zeng et al. (2014). The bars indicated 95% highest posterior density (HPD) intervals of estimated divergence times of nodes. The posterior probabilities of all the blanches were > 0.999.

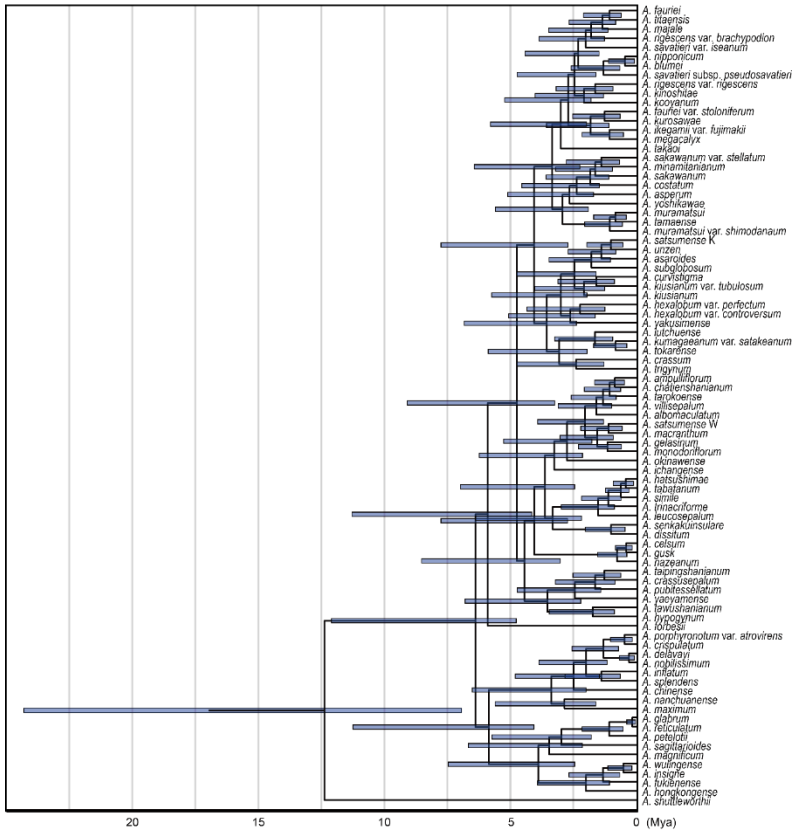

Figure S8. A majority-rule consensus tree inferred from Bayesian analysis of ddRAD-seq data (50% genotyped data) showing the divergence times of major nodes and 95% highest posterior density (HPD) intervals.

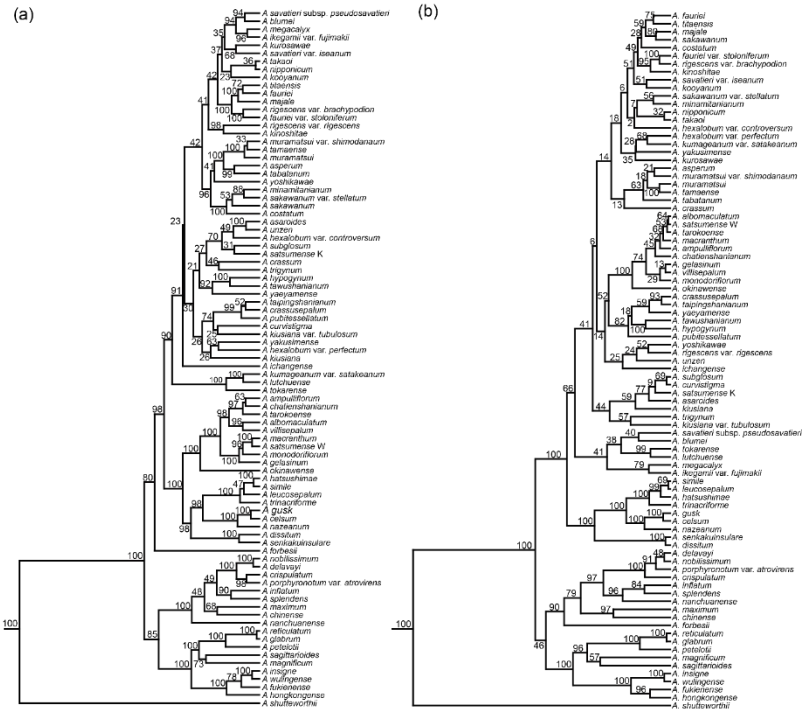

Figure S9. Molecular phylogenetic tree of Heterotropa taxa estimated from Bayesian analysis using 75% genotyped (a) and 90% genotyped (b) matrices. Values above or below branches indicate the posterior probabilities of branches.

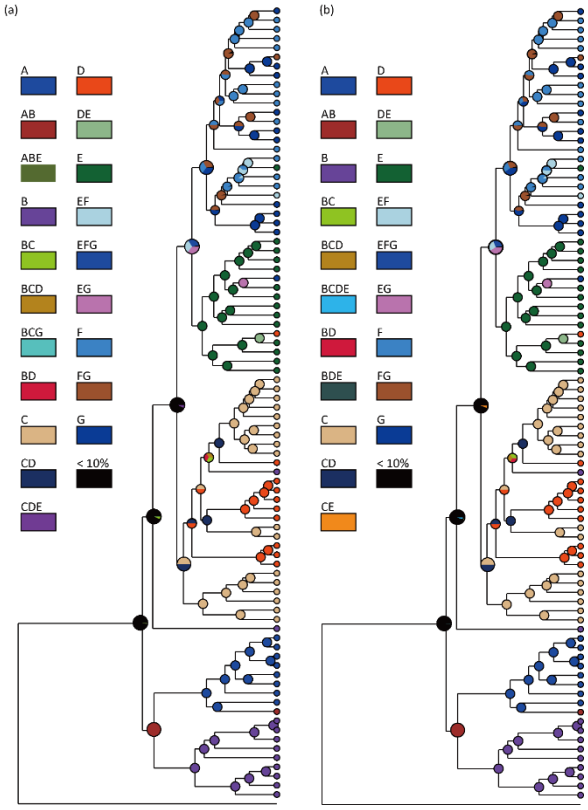

Figure S10. The results of S-DIVA with maximum number of areas to 3 (a) and 4 (b). The colours of pie charts reflect the estimated distribution areas (A; Sichuan basin and surrounding mountains, B; other parts of mainland China, C; Taiwan and southern Ryukyu islands, D; central Ryukyu islands, E; northern Ryukyu islands and Kyushu island, F; southern part of mainland Japan including Shikoku island, and G; northern part of mainland Japan).

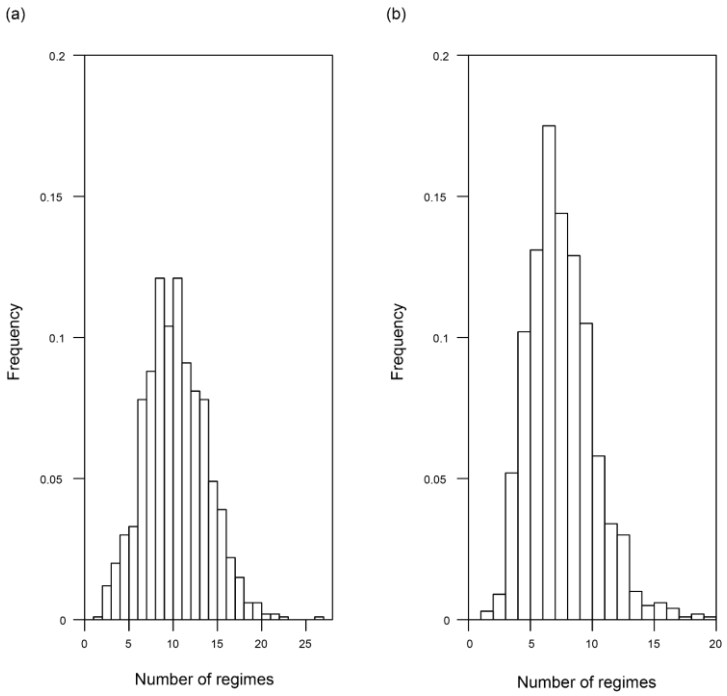

Figure S11. Histograms of supported number of macroevolutionary rate regimes for each trait evolution; (a) flowering time and (b) calyx tube width. The number of regimes = 1 indicated there were no shifts in trait evolution rate throughout the tree.

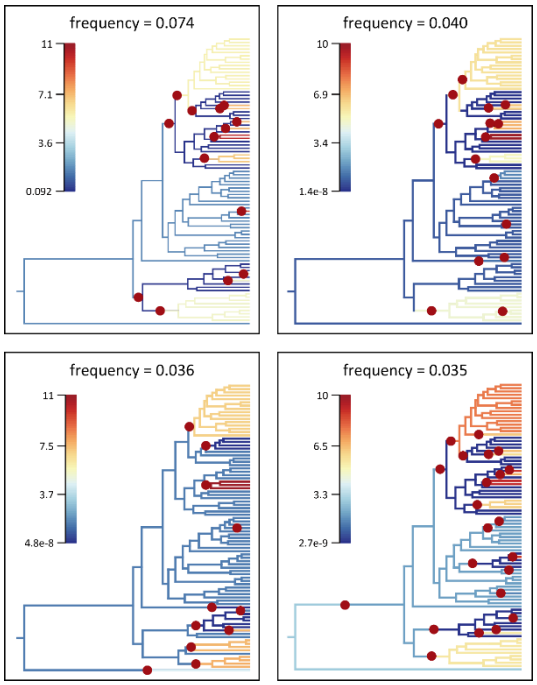

Figure S12. The top four most credible rate shift configurations estimated by BAMM analysis using flowering time. Red circles indicate the location of rate shifts and colours of blanches correspond to the evolutionary rates of traits.

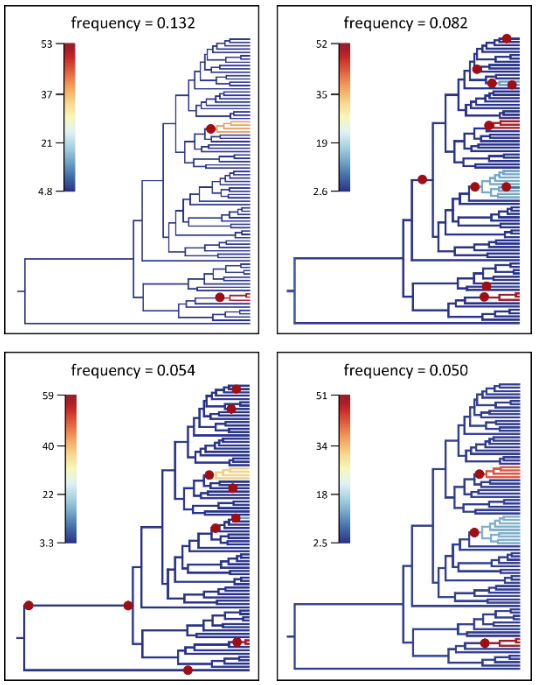

Figure S13. The top four most credible rate shift configurations estimated by BAMM analysis using calyx tube width. Red circles indicate the location of rate shifts and colours of blanches correspond to the evolutionary rates of traits.

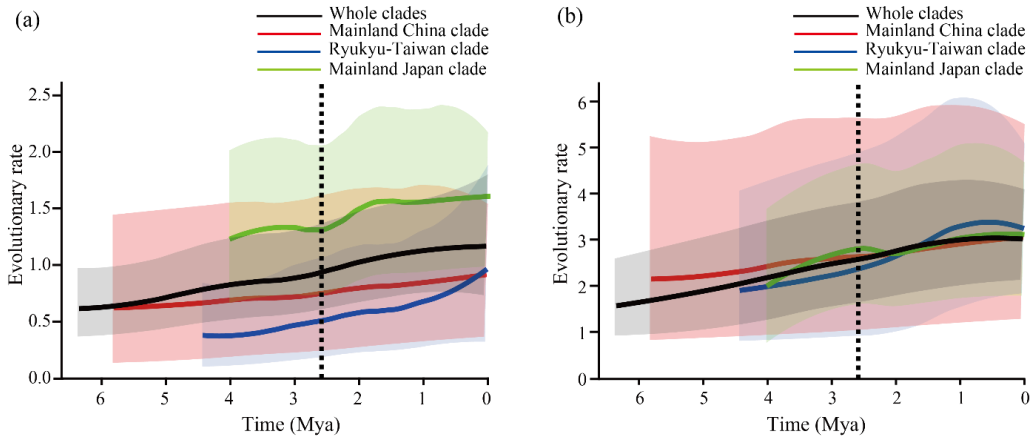

Figure S14. The median value with 95% CI of evolutionary rate of flowering time (a) and calyx tube width (b) through time in each clade (black; whole clades, red; mainland China clade, blue; Ryukyu-Taiwan clade, and light green; mainland Japan clade). Dashed vertical lines indicate the boundary between the Pliocene and the Pleistocene (2.6 Mya).

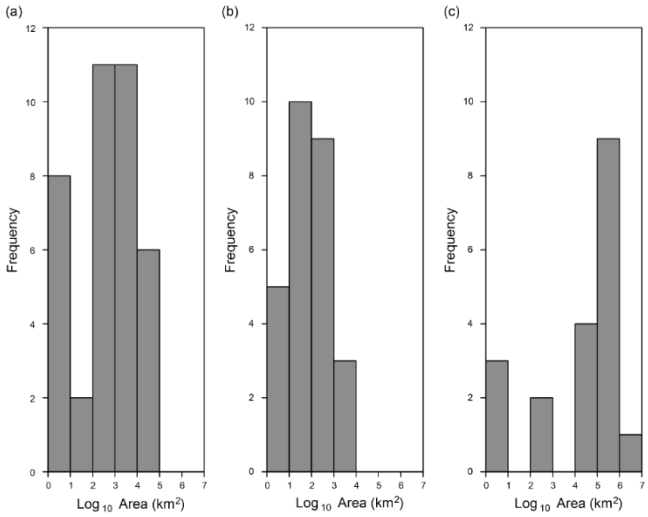

Figure S15. Histograms of distribution area of taxa within mainland Japan clade (a), Ryukyu-Taiwan clade (b), and mainland China clade (c).

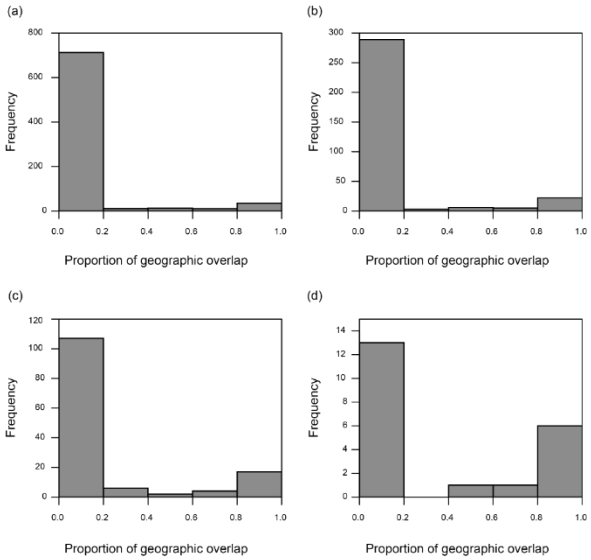

Figure S16. Histograms of proportion of geographic range overlap between taxa pairs within mainland Japan clade (a), Ryukyu-Taiwan clade (b), mainland China clade (c), and sister-taxa pairs (d).

Table S2. Sample list used in ddRAD-seq analysis. The columns indicate the distribution region used in S-DIVA, the start and end month of flowering time, median value of calyx tube diameter (mm), distribution area calculated from the polygon formed by the distribution record(s), number of records used in the geographic analysis, the number of cleaned RAD-seq reads, and the number of loci in the 50% matrices.

Taxon name	Distribution region†	Flowering time (start month)	Flowering time (end month)	Calyx tube diameter (mm) [minimum, maximum]	Distribution Area (km^2)	No. of occurrence data	No. of RAD-seq reads	No. of loci
Asarum albomaculatum	C	12	4	11 [10, 12]	4187.34	5	1,364,347	273
Asarum ampulliflorum	C	12	3	17.5 [15, 20]	215.26	4	2,558,859	369
Asarum asaroides	E	4	5	27.5 [25, 30]	7316.76	9	1,005,898	231
Asarum asperum	E,F	3	4	9 [8, 10]	64744.28	101	1,224,717	226
Asarum blumei	G	4	5	13 [12, 14]	7352.51	24	2,252,177	335
Asarum celsum	D	1	3	10 [10, 10]	216.59	15	1,900,129	318
Asarum chinense	A	4	5	10 [10, 10]	97328.52	8	1,489,480	194
Asarum chatienshanianum	C	3	4	7.75 [7, 8.5]	639.83	9	1,810,861	311
Asarum costatum	F	4	5	10.5 [8, 13]	263.60	13	1,630,505	258
Asarum crassum	E	3	4	13 [13, 13]	3.15	1	2,051,537	349
Asarum crassusepalum	C	12	2	7 [7, 7]	60.69	6	1,275,832	241
Asarum crispulatum	A	4	4	16 [12, 20]	36720.52	5	731,042	116
Asarum curvistigma	G	10	11	11.5 [10, 13]	453.86	3	2,144,205	335
Asarum delavayi	A	4	6	15 [15, 15]	218114.79	29	1,149,735	181
Asarum dissitum	C	3	3	7.5 [7, 8]	3.15	1	1,245,668	283
Asarum fauriei	G	3	4	8.5 [7, 10]	60577.40	42	989,584	217
Asarum fauriei var. *stoloniferum*	G	4	5	9 [8, 10]	6.17	2	1,454,461	253
Asarum forbesii	B	4	5	7.5 [6, 9]	1003890.28	79	835,954	169
Asarum fukienense	B	4	6	10 [10, 10]	206959.65	53	1,052,381	173
Asarum gelasinum	C	3	4	8 [8, 8]	85.24	8	801,861	198
Asarum glabrum	B	5	6	25 [25, 25]	3.15	1	1,400,872	182
Asarum gusk	D	3	4	8.5 [8, 9]	86.64	12	1,017,556	236
Asarum hatsushimae	D	3	4	13.5 [12, 15]	11.93	4	725,731	181
Asarum hexalobum var. *controversum*	E	3	3	6 [5, 7]	6.49	2	1,037,696	268
Asarum hexalobum var. *perfectum*	E	3	4	10 [10, 10]	19172.34	16	1,241,879	267
Asarum hongkongense	B	2	5	12 [12, 12]	153.31	3	915,024	159
Asarum hypogynum	C	1	3	15 [15, 15]	123.59	7	1,738,623	311
Asarum ichangense	B	4	5	10.75 [9,	686040.84	62	1,490,923	265
Asarum ikegamii var. *fujimakii*	G	3	4	13.5 [10, 17]	3.09	2	2,047,355	313
Asarum inflatum	A	5	5	15 [15, 15]	18648.29	12	983,274	154
Asarum insigne	B	4	5	15 [15, 15]	190239.57	40	978,225	137
Asarum kinoshitae	F	12	1	8 [7, 9]	5.92	2	987,677	213
Asarum kiusianum	E	3	4	11.5 [10, 13]	3993.44	6	1,400,694	292
Asarum kiusianum var. *tubulosum*	E	4	5	11.5 [10, 13]	619.41	3	1,288,659	250
Asarum kooyanum	F	5	6	11 [10, 12]	7610.56	9	2,755,598	317
Asarum kumageanum var. *satakeanum*	E	11	12	11 [10, 12]	95.81	4	889,370	209
Asarum kurosawae	F	10	11	13 [12, 14]	259.78	4	2,131,652	324
Asarum leucosepalum	D	3	3	8.5 [7, 10]	14.10	3	996,824	241

Table S2 continued

Asarum lutchuense	D	11	12	13.5 [12, 15]	423.87	23	1,512,018	272
Asarum macranthum	C	3	5	14 [12, 16]	5745.10	15	1,840,831	339
Asarum magnificum	B	4	5	15 [15, 15]	197314.94	17	1,205,629	210
Asarum majale	F	5	5	11 [9, 13]	150.22	6	963,832	189
Asarum maximum	A,B	4	5	17.5 [15, 20]	660193.87	31	1,033,092	181
Asarum megacalyx	G	3	5	17 [14, 20]	16232.02	16	2,622,210	363
Asarum minamitanianum	E	4	5	11.5 [10, 13]	181.61	6	548,610	119
Asarum monodoriflorum	C	2	4	9 [9, 9]	7.06	2	822,626	186
Asarum muramatsui	G	4	5	13.5 [12, 15]	442.44	9	530,240	132
Asarum muramatsui var. *shimodanaum*	G	4	5	13 [11, 15]	5.66	3	1,979,182	295
Asarum nanchuanense	A	5	5	20 [20, 20]	3.15	1	993,484	142
Asarum nazeanum	D	2	3	14 [12, 16]	3.15	1	1,277,878	246
Asarum nipponicum	F,G	10	11	10 [10, 10]	25797.62	197	280,645	84
Asarum nobilissimum	A	5	5	15 [15, 15]	-	0	1,107,813	171
Asarum okinawense	D	3	4	6.5 [6, 7]	3.15	1	1,735,621	315
Asarum petelotii	B	2	5	17.5 [15, 20]	57675.93	16	1,450,274	213
Asarum porphyronotum var. *atrovirens*	A	4	5	12.5 [11, 14]	173.40	3	1,144,066	173
Asarum pubitessellatum	C	1	5	9 [8, 10]	3.15	1	510,135	84
Asarum reticulatum	B	3	4	18 [18, 18]	3.15	1	1,468,132	201
Asarum rigescens var. *brachypodion*	F	1	3	9 [8, 10]	4121.65	33	2,103,002	346
Asarum rigescens var. *rigescens*	F	10	11	10 [10, 10]	8006.73	26	1,962,229	352
Asarum sagittarioides	B	11	4	9.5 [7, 12]	147658.26	40	1,261,660	219
Asarum sakawanum	F	4	5	10 [10, 10]	5180.45	22	2,622,795	369
Asarum sakawanum var. *stellatum*	F	4	5	10 [10, 10]	1115.98	7	656,868	145
Asarum satsumense K	E	4	5	22.5 [20, 25]	210.82	7	1,748,886	334
Asarum satsumense W	C	1	4	17.5 [14.8,	137.83	4	841,216	181
Asarum savatieri subsp. *pseudosavatieri*	G	10	11	11 [10, 12]	373.18	3	1,704,736	250
Asarum savatieri var. *iseanum*	F	10	11	10 [10, 10]	170.51	4	1,526,335	263
Asarum senkakuinsulare	C	5	5	15 [15, 15]	3.15	1	1,756,833	296
Asarum simile	D	3	4	13.5 [12, 15]	17.07	3	1,548,706	312
Asarum splendens	A	4	5	25 [25, 25]	262763.69	65	981,268	156
Asarum subglobosum	E	3	4	13 [12, 14]	3241.28	8	483,853	92
Asarum tabatanum	D	2	3	12.5 [10, 15]	34.53	7	596,188	158
Asarum taipingshanianum	C	12	2	8.25 [6.5, 10]	42.95	5	1,148,529	202
Asarum takaoi	F	10‡	12	9.5 [7, 12]	15158.51	35	647,715	116
Asarum tamaense	G	4	5	13.5 [12, 15]	923.82	17	2,124,523	306
Asarum tarokoense	C	10	12	12 [12, 12]	129.72	3	1,318,747	264
Asarum tawushanianum	C	1	3	13.5 [12, 15]	102.69	3	1,375,473	237
Asarum titaensis	F	12	2	13 [10, 16]	3.47	2	2,066,637	312
Asarum tokarense	E	11	12	11 [10, 12]	18.62	5	1,527,639	311
Asarum trigynum	E	3	4	10 [10, 10]	22.37	4	923,350	199
Asarum trinacriforme	D	3	4	8 [6, 10]	298.16	25	1,535,333	292

Table S2 continued

Asarum unzen	E	3	4	14 [13, 15]	4202.19	7	2,459,204	362
Asarum villisepalum	C	3	5	12.5 [11, 14]	28.61	3	904,052	185
Asarum wulingense	B	12	5	12 [12, 12]	832913.59	57	1,280,655	202
Asarum yaeyamense	C	12	3	13.5 [12, 15]	2629.23	11	1,001,880	225
Asarum yakusimense	E	3	4	13.5 [12, 15]	3.15	1	1,240,300	250
Asarum yoshikawae	G	3	4	10 [8, 12]	2528.38	30	793,701	155
Asarum shuttleworthii‡	North	5	7	27.5 [15, 40]	-	0	1,156,332	108

†A; Sichuan basin and surrounding mountains, B; other part of mainland China, C; Taiwan and southern Ryukyu islands, D; central Ryukyu islands, E; Kyushu island and northern Ryukyu islands, F; southern part of mainland Japan including Shikoku island, G; northern part of mainland Japan.
‡This value is obtained from field observation. ǂSect. *Hexastylis* taxa, used as outgroup according to Chapter 1.

Table S3. Information of newly obtained reads and chloroplast genomes of *Asarum* spp.

Taxon name	Number of raw reads	The length of chloroplast genome
Asarum macranthum	194,385	161,472
Asarum satsumense K	24,546,050	164,444
Asarum forbesii	275,687,362	164,688
Asarum wulingense	276,766	160,867
Asarum shutterwrothii	23,736,078	164,460

Table S4. The sample lists used in phylogenetic analysis of chloroplast genome.

Taxon name	Family	DDBJ accession NO.	Reference
Asarum costatum	Aristolochiaceae	AP018513	(Takahashi et al., 2018)
Asarum macranthum	Aristolochiaceae	LC529904	Newly obtained
Asarum satsumense K	Aristolochiaceae	LC529901	Newly obtained
Asarum forbesii	Aristolochiaceae	LC529900	Newly obtained
Asarum wulingense	Aristolochiaceae	LC529903	Newly obtained
Asarum shutterwrothii	Aristolochiaceae	LC529902	Newly obtained
Saruma henryi	Aristolochiaceae	NC039933	(Sinn et al., 2018)
Aristolochia tagala	Aristolochiaceae	NC041455	(Li, X et al., 2019)
Aristolochia contorta	Aristolochiaceae	NC036152	(Zhao et al., 2017)
Drimys granadensis	Winteraceae	DQ887676	(Chai et al., 2006)
Cinnamomum camphora	Laulaceae	MH050970	(Wu et al., 2019)
Chimonanthus praecox	Laulaceae	NC042744	(Zhao et al., 2019)
Machilus balansae	Laulaceae	KT348517	(Song et al., 2015)
Liriodendron chinense	Magnoliaceae	NC030504	(Li, B et al., 2016)
Magnolia sinostellata	Magnoliaceae	NC039941	(Yao et al., 2018)
Sarcandra glabra	Chloranthaceae	MH939147	(Han et al., 2018)
Chloranthus japonicus	Chloranthaceae	KP256024	(Sun et al., 2016)

Chapter 3

Genetic data reveals a complex history of multiple admixture events in presently allopatric wild gingers (*Asarum* spp.) showing intertaxonomic clinal variation in calyx lobe length

Abstract
Clinal variation is a major pattern of observed phenotypic diversity and identifying underlying demographic processes is a necessary step to understand the establishment of clinal variation. The wild ginger series *Sakawanum* (genus *Asarum*) comprises four taxa, which exhibit intertaxonomic clinal variation in calyx lobe length across two continental islands isolated by a sea strait. To test alternative hypotheses of the evolutionary history and to determine the implications for the formation of clinal variation, I conducted approximate Bayesian computation (ABC) analysis and ecological niche modelling (ENM). ABC analysis indicated that the scenario assuming multiple admixture events was strongly supported. This scenario assumed two admixture events occurred between morphologically distinct taxa, likely leading to the generation of intermediate taxa. One of the admixture events was estimated to have occurred during the last glacial maximum (LGM), during which the taxa were estimated to have formed a common refugia in southern areas by ENM analysis. Although four taxa are currently distributed allopatrically on different islands and trans-oceanic dispersal appears unlikely, the formation of a land bridge and the geographic range shift to refugia would have allowed secondary contact between previously isolated taxa. This study suggests that clinal variation can be shaped by demographic history including multiple admixtures due to climatic oscillations.

Introduction
Clinal variation is defined as gradual variation in the values of measurable traits along a geographical axis within a species or a species group (Huxley, 1938, 1939) regarded as an important phenotypic pattern in the field of evolutionary biology (Haldane, 1948, Mayr, 1956, Salomon, 2002). Deciphering the factors that drive clinal variation can aid in inferring the direction of morphological evolution and the foundation of reproductive isolation (Antoniazza et al., 2014). Selection related to environmental heterogeneity is considered a major force behind clinal variation among populations (Felsenstein, 1976, Etterson et al., 2016, Hedrick, 1986). Many studies have reported examples of clinal variation and the associated selective forces such as environmental heterogeneity across altitude, latitude, and longitude (Watt et al., 2010, Hut et al., 2013, Takahashi, 2015). Neutral demographic processes can also shape patterns of clinal variation (Endler, 1973, Vasemagi, 2006, Zink and Remsen, 1986). Demographic and selective processes are not mutually exclusive and both processes may often shape the patterns of clinal variation (Bergland et al., 2016). Thus, elucidating the underlying demographic process is crucial to resolving the mechanism by which clinal variation is established (Adams et al., 2006).

Several demographic processes have been proposed as factors driving clinal variation (Vasemagi, 2006), including admixture of previously isolated species or populations (Endler, 1973). Due to introgression of parental alleles, a hybrid species or population can show intermediate morphology, leading to allelic and phenotypic clinal variation (Endler, 1973, Barton and Hewitt, 1985). A series of founder effects during range expansion can also shape clinal variation (Excoffier et al., 2009). Range expansion with continual founder effects could lead to the formation of clinal variation in allele frequency (Klopfstein et al., 2006). If the frequency of alleles with phenotypic effects is altered in this process, clinal variation of phenotypes would be established (Antoniazza et al., 2014). Clinal variation arising from colonization history have been demonstrated, especially in invasive plants (Keller et al., 2009, Laaksonen et al., 2015). Moreover, random genetic drift among populations with spatially limited gene

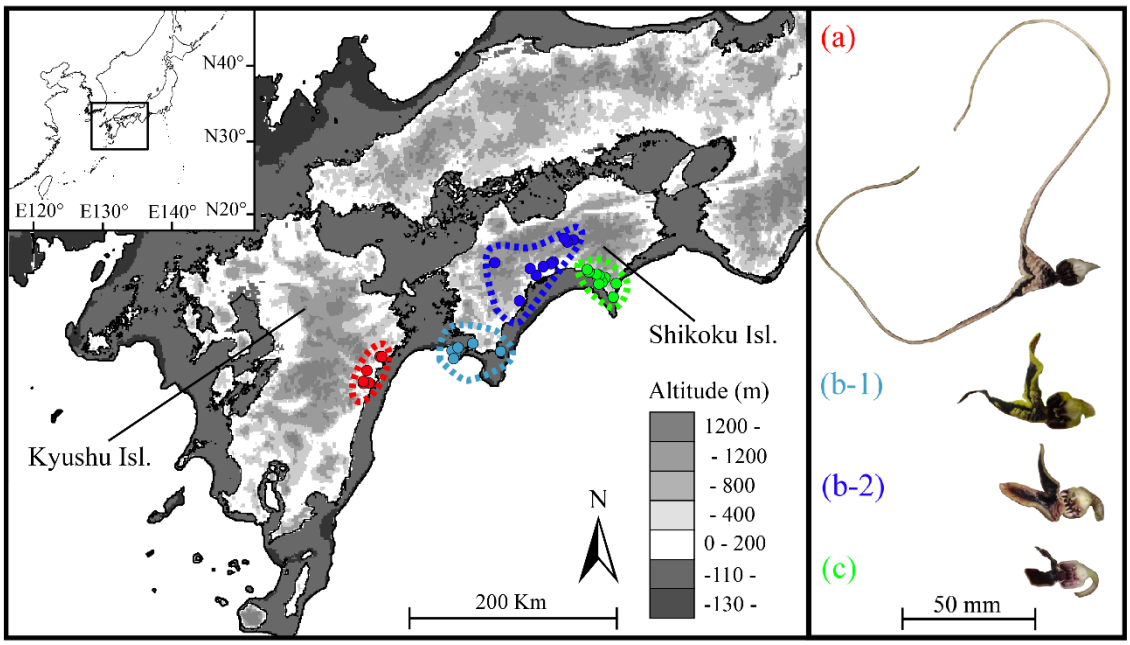

Figure 7. Map showing sampled populations of series *Sakawanum* taxa in this study, and cross-sectional views of the flowers of *Asarum minamitanianum* (a), *Asarum sakawanum* var. *stellatum* (b-1), *A. sakawanum* var. *sakawanum* (b-2), and *Asarum costatum* (c). The sampling locations are indicated by red circles (*A. minamitanianum*), light blue circles (*A. sakawanum* var. *stellatum*), dark blue circles (*A. sakawanum* var. *sakawanum*), and green circles (*A. costatum*). The distribution range of each taxon is shown with a broken line, and the paleo-coastlines during the last glacial maximum are shown assuming −110 m (light gray) and −130 m (dark gray) sea level depression, respectively.

flow (isolation by distance) would also lead to a spatially biased allele frequency distribution and clinal variation of phenotypes (Gould and Johnston, 1972). To clarify the mechanism of establishment of clinal variation, distinguishing among these alternative hypotheses and inferring the evolutionary history underlying such variation are essential (Antoniazza et al., 2014).

Series *Sakawanum* F.Maek. (genus *Asarum* L.; Aristolochiaceae), which comprises four taxa (*A. minamitanianum* Hatus., *A. sakawanum* Makino var. *stellatum* (F.Maek. ex Akasawa) T.Sugaw., *A. sakawanum* var. *sakawanum* Makino, and *A. costatum* (F.Maek.) T.Sugaw.), is monophyletic (Chpater 1) and exhibits intertaxonomic clinal variation in the length of the calyx lobe (Fig. 7), which decreases along the longitude (Akasawa and Shinma, 1984, Akasawa, 1985). *Asarum minamitanianum*, which is found in the westernmost extent of the range, has the longest calyx lobe (70–150 mm), whereas *A. costatum*, in the easternmost portion, has the shortest (8–15 mm). *Asarum sakawanum*, which is distributed between *A. minamitanianum* and *A. costatum*, has a calyx lobe length that is intermediate (var. *stellatum*; 25-50 mm and var. *sakawanum*; 20-25 mm) between the other species. My morphological measurements indicated that the calyx lobe length of each taxon was significantly differentiated, and that clinal variation was intertaxonomic (Chapter 4). These four taxa are distributed allopatrically on different islands (Kyushu and Shikoku islands) and show low mobility due to ant-mediated seed dispersal, with dispersal rates estimated as 1 m per year (Hiura, 1978). Ground prowling insects and Diptera species, which have low mobility were observed in series *Sakawanum* flowers (Kakishima and Okuyama, 2018).

All taxa in series *Sakawanum* grow in the shaded understory of warm temperate evergreen forests in southern Japan, and phylogenetic analysis indicated that the series was formed during the late Quaternary (Chpater 1). The taxon's geographical distribution and species composition in the warm temperate evergreen forests of this region are thought to be related to climatic changes during the Quaternary period, characterized by range contraction into refugia during glacial periods and range expansion during interglacial periods (Aoki et al., 2011, Liu et al., 2013b, Aoki

et al., 2019). The demographic history of warm temperate evergreen forests has been reconstructed using palynological studies (Tsukada, 1984, Matsuoka and Miyoshi, 1998) and phylogeographic studies (Aoki et al., 2004, Aoki et al., 2014). Although taxa in series *Sakawanum* are distributed allopatrically on different islands (Kyushu and Shikoku islands) and intertaxonomic dispersal is unlikely due to their low mobility, during glacial periods, these islands formed a land bridge (Ujiie, 1990) that could have provided opportunities for population isolation and secondary contact. The evolutionary history of the *Sakawanum* taxa would be influenced by these geographical range shifts and changes in climate.

The goal of the present study was to test alternative hypotheses of the evolutionary history of series *Sakawanum* taxa, which are allopatrically distributed over the sea, and to determine the implications for the formation of intertaxonomic clinal variation in the series. For these purposes, I first compared the genetic structures of nuclear microsatellite markers with that of maternally inherited DNA sequence variations. Furthermore, I statistically tested the alternative scenarios including admixture scenarios and estimated evolutionary history by employing an approximate Bayesian computation (ABC, Bertorelle et al., 2010) method using both nuclear microsatellite and plastid DNA sequence data. The ABC method can be used to compare complicated evolutionary scenarios and estimate demographic parameters such as effective population sizes and divergence or admixture times (Liu et al., 2014). Finally, I used ecological niche modeling (ENMs, Raxworthy et al., 2007) to reconstruct past species distributions and infer distribution range shifts in the series (Sakaguchi et al., 2010, Tsuda et al., 2015). A combined approach using ABC and ENM would contribute to my understanding of the evolutionary history of series *Sakawanum*, which would be impossible using traditional approaches due to the spatiotemporal dynamics of the distribution range and complicated demographic events. Although this approach cannot allow testing the role of phenotypic difference of calyx lobe length directly, this reconstructed evolutionary history would be useful for understanding the process by which clinal variation was established within the series.

Materials and methods

Plant material, microsatellite genotyping and cpDNA sequencing

Leaves of species in series *Sakawanum* were collected from 2012 to 2015 at 33 locations (six locations for *A. minamitanianum*, seven for *A. sakawanum* var. *stellatum*, 10 for *A. sakawanum* var. *sakawanum*, and 10 for *A. costatum*) throughout the distribution range (Table S5, Fig. 7). I collected eight individuals from each population, for a total of 264 individuals. After removal of polysaccharides with HEPES buffer (pH 8.0; Setoguchi and Ohba, 1995), total DNA was extracted using the CTAB method (Doyle and Doyle, 1987). The extracted DNA was dissolved in 50 μL of Tris-ethylenediaminetetraacetic acid (EDTA) buffer and used for polymerase chain reaction (PCR) analysis. For microsatellite analysis, the genotypes of individuals were determined using 17 expressed sequence tag-simple sequence repeat (EST-SSR) markers for all samples (Table S6;Takahashi et al., 2017). PCR was performed in a 10-μL multiplex reaction volume containing 10–20 ng of DNA, 3 μL of Multiplex PCR Master Mix (Qiagen, Hilden, Germany), 0.01 μM of forward primer, 0.2 μM of reverse primer, and 0.1 μM of fluorescently labeled M13 primer. PCR amplification with all primer pairs began with 15 min at 95°C for initial denaturation, followed by 35 cycles of denaturation at 95°C for 30 s, primer annealing at 60°C for 3 min, extension at 68°C for 1 min and a final extension for 20 min at 68°C. The amplified products were loaded onto an ABI 3130 autosequencer (Applied Biosystems, Foster City, CA, USA) using the GeneScan ROX-500 size standard (Applied Biosystems), POP7 polymer (Applied Biosystems), and a 36-cm capillary array, and fragment size was determined using GeneMapper software (Applied Biosystems).

Four non-coding chloroplast DNA regions (Table S7; Takahashi et al., 2018) were sequenced for 132 individuals in series *Sakawanum* (33 locations, four individuals per population). I also sequenced four individuals of *A. tokarense* Hatus. ex Hatus. & Yamahata as an outgroup, which was found to be related to series *Sakawanum* in a previous phylogenetic study (Chpater 1). PCR was performed following the procedure in Takahashi *et al*. (2018) and sequencing of PCR products was conducted with the ABI Prism BigDye Terminator Cycle Sequencing Ready Reaction kit ver. 3.1 (Applied Biosystems), followed by electrophoresis on an ABI 3130 autosequencer (Applied Biosystems). The primer characteristics for EST-SSR and chloroplast sequence markers are shown in Tables S6 and S7, respectively.

Population genetic analysis

For the EST-SSR dataset, I employed three types of population genetic analysis, Bayesian clustering analysis, principal component analysis (PCA), and distance-based phylogenetic analysis. I used the individual-based Bayesian clustering approach implemented in STRUCTURE ver. 2.3.3 (Pritchard et al., 2000). I performed a series of 15 independent runs for each value of *K*, ranging from 1 to 10. The runs were conducted using admixture and LOCPRIOR models with a burn-in of 100,000, followed by 500,000 generations after burn-in (Hubisz et al., 2009). The log posterior probability of the data L(D) and delta *K* statistics (Evanno et al., 2005) were used to determine an appropriate value of *K* using STRUCTURE HARVESTER ver. 0.6.94. (Earl and Vonholdt, 2012). Independent runs for all datasets were averaged in CLUMPP ver. 1.1.2 (Jakobsson and Rosenberg, 2007). Graphical representations of population assignments were conducted using DISTRUCT ver. 1.1 (Rosenberg, 2004). To detect genetic groupings of individuals in *Sakawanum* taxa, PCA was performed with allele frequencies calculated using the "adegenet" package (Jombart, 2008) in R ver. 3.4.4 (R Core Team, 2013). I constructed a population phylogenetic tree through the neighbor-joining method using the software POPULATIONS ver. 1.3.20 (Langella, 2002). The genetic distance was measured using Nei's *Da* (Nei et al., 1983).

Chloroplast sequence data were edited and aligned using BIOEDIT ver. 7.1.9 (Hall, 1999). DnaSP ver. 6.10.04 (Rozas et al., 2017) was used to determine the haplotypes and nucleotide diversity (π) of each locus and population. I examined hierarchical partitioning of genetic diversity among taxa, among populations within taxa, and within populations through analysis of molecular variance (AMOVA; Excoffier et al., 1992) implemented in Arlequin ver. 3.5.2.2 (Excoffier and Lischer, 2010); estimation of fixation indices was conducted using 1,000 permutations. The haplotype network was constructed through the median-joining method implemented in NETWORK ver. 5.0.0.1 (Bandelt et al., 1999).

Approximate Bayesian Computation analysis

I used population genetic datasets obtained from 17 EST-SSR markers and four chloroplast markers simultaneously to test which of 12 models best fit the datasets using the ABC approach implemented in DIYABC ver. 2.1.0 (Cornuet et al., 2008). Based on the present distributions of taxa in series *Sakawanum* and the observed genetic structures, I selected 12 alternative models. These 12 models included two branching models, three radiation models, and seven admixture models (shown in Fig. 8). All models except model C assumed that the ancestral populations of *A. minamitanianum* and *A. costatum* diverged first. Models A and B assumed that *A. sakawanum* was derived from *A. minamitanianum* or *A. costatum*, respectively, after this first divergence, and then the two varieties of *A. sakawanum* diverged. These two models corresponded to the range expansion of eastern and western species, which subsequently produced longer and shorter calyx lobes, respectively. In model C, the three species have a common ancestor from which they diverged simultaneously, and the two varieties of *A. sakawanum* diverged later. In models D and E, after the first divergence of *A. costatum* or *A. minamitanianum*, the other three taxa diverged simultaneously. Within the seven admixture models, models F–J assumed a single admixture event, whereas models K and L assumed two admixture events. All admixture models assumed hybrid origin(s) of the morphologically intermediate taxon or taxa. Models F and G were similar to model A and B respectively, but *A. sakawanum* var. *stellatum* or *A. sakawanum* var. *sakawanum* was assumed to originate from secondary contact between *A. minamitanianum* and *A. sakawanum* or between *A. costatum* and *A. sakawanum*, respectively. Model H assumed that *A. sakawanum* was derived from *A. minamitanianum*, and *A. sakawanum* var. *sakawanum* originated from secondary contact between *A. costatum* and *A. sakawanum*. On the other hand, model I assumed that *A. sakawanum* was derived from *A. costatum*, and *A. sakawanum* var. *stellatum* originated from secondary contact between *A. costatum* and *A. sakawanum*. Model J assumed that *A. sakawanum* originated from a hybrid population of *A. minamitanianum* and *A. costatum*, and the two varieties of *A. sakawanum* diverged subsequently. Models K and L also assumed hybrid origin of *A. sakawanum*, and that subsequent backcrosses with the parent taxa generated *A. sakawanum* var. *stellatum* and *A. sakawanum* var. *sakawanum*. I assumed that all admixture events had equal contributions from the parental populations. The average mutation rate across microsatellite loci was set to 1.0×10^{-5} to 1.0×10^{-3} substitutions/site/year (Marriage et al., 2009). Because I selected highly polymorphic sites when designing the chloroplast markers based on comparison of chloroplast genome sequences

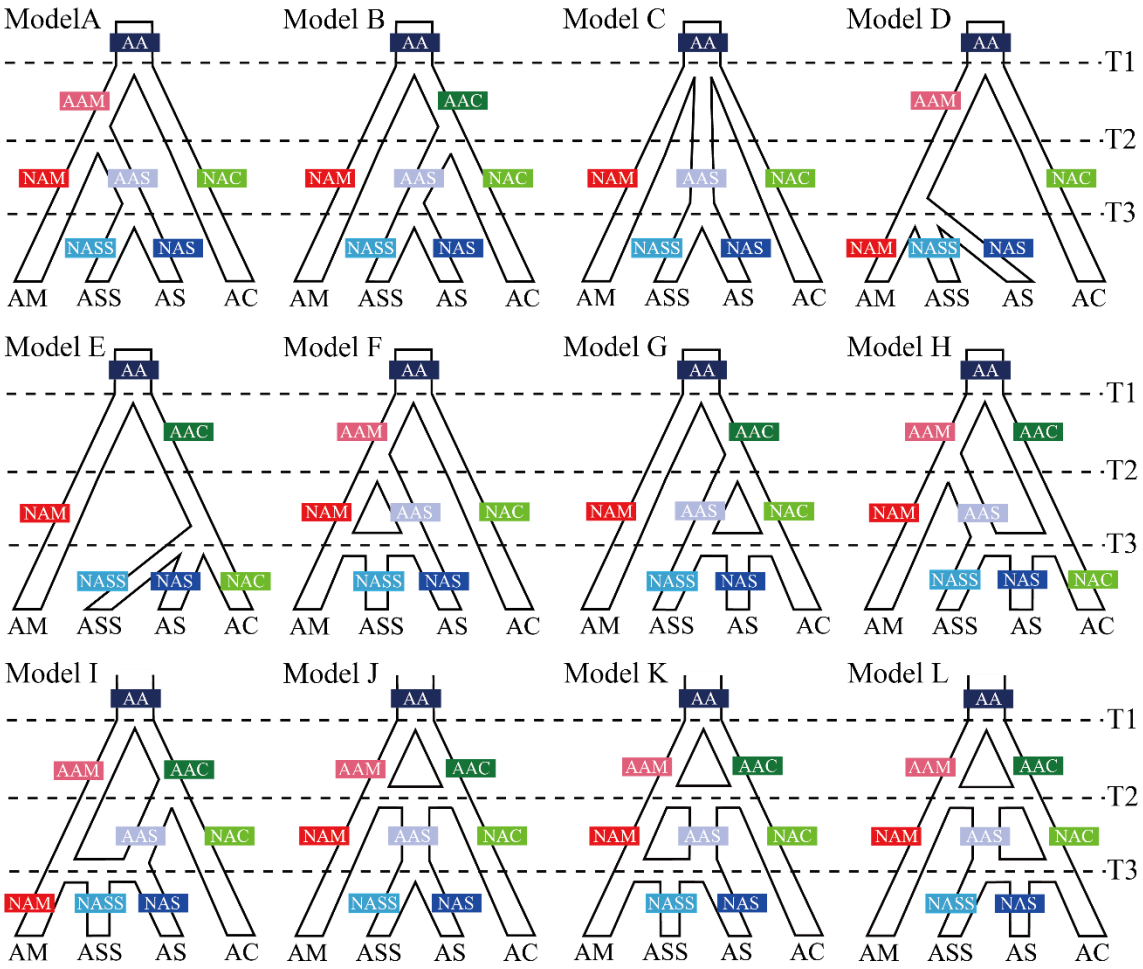

Figure 8. The 12 demographic models tested using approximate Bayesian computation (ABC) analysis. NAM, NASS, NAS, and NAC represent the current effective population sizes of *A. minamitanianum* (AM), *A. sakawanum* var. *stellatum* (ASS), *A. sakawanum* var. *sakawanum* (AS), and *A. costatum* (AC), respectively. AA, AAM, AAS, and AAC represent the ancestral effective population sizes of the common ancestor, *A. minamitanianum*, *A. sakawanum*, and *A. costatum*, respectively. T1, T2, and T3 represent the times of past events in generations.

among the species (Takahashi et al., 2018), the mutation rates of the chloroplast regions used in this study are expected to be faster than the average mutation rates of chloroplast genomes. To determine the mutation rates of the chloroplast sequences, I first calculated the rate of polymorphic sites in the whole chloroplast genome (R1: 1.4×10^{-3} SNP/bp) using the chloroplast genomes of series *Sakawanum* species (GenBank accession no. AP017908, AP018514, and AP018513) as well as that in the regions used in this study (R2: 5.9×10^{-3} SNP/bp). Subsequently, general mutation rates of the chloroplast sequence (1.1×10^{-9} to 2.9×10^{-9} mutations/site/year) estimated by Wolfe et al. (1987) were multiplied by the relative mutation rate of four regions (R2 / R1), and the values obtained were used as the mutation rates of the chloroplast sequence (4.2×10^{-9} to 1.2×10^{-8} mutations/site/year). All demographic parameters and their prior intervals (minimum and maximum ranges of values) are detailed in Table S8.

In the coalescent simulation step, I generated 1.0×10^{6} simulated datasets for each model. A total of 38 summary statistics (24 for microsatellite data and 14 for chloroplast sequence data) were used to summarize the population genetic information. For microsatellite data, I calculated the mean number of alleles, mean expected heterozygosity, and mean M index across loci (Garza and Williamson, 2001) for each taxon. I also calculated F_{ST} (Weir and Cockerham, 1984) and $(\delta\mu)^2$ distance (Goldstein et al., 1995) between all pairs of taxa. For chloroplast sequence data, I used the number of haplotypes and Tajima's *D* statistic (Tajima, 1989) within each taxon, and F_{ST} between all pairs of taxa.

To choose the best model, the relative posterior probability (with 95% confidence

intervals, CIs) of each model was estimated as the proportion of simulations accepted using the logistic regression method with a tolerance rate of 0.1%. To determine whether the support for each model varied depending on the tolerance rate, I compared the relative posterior probabilities of models at 10 different tolerance rates (0.1–1%). To estimate the performance of my method for discriminating among the 12 models, I estimated the type I and type II errors for all scenarios, comparing 100 datasets under each competing model using the logistic regression method. After the best fitting model had been chosen, I used 0.1% of simulations of the best fitting model to estimate the demographic parameter values. I report the mode, mean, and median values with 95% highest posterior density interval (HPDI) for each demographic parameter in the model. I assumed the generation time of *Asarum* species to be 10 years (Kume, 1993, Kume, 1989). To evaluate how well the posterior predictions of parameters and the model fit the data summarized by the summary statistics, I used the PCA method in DIYABC, which measures the discrepancy between the model and observed data.

Because the chloroplast and nuclear datasets showed the different genetic structures and the chloroplast dataset exhibited relatively low diversity (see result section), there were possibilities that the results of my ABC analysis were biased by the chloroplast dataset. To check validation of my results, I also performed the ABC analysis with using only EST-SSR dataset and estimated the relative posterior probabilities of 12 models. The settings and used summary statistics were same as the chloroplast and EST-SSR datasets.

Ecological niche modeling

To infer the past distribution of series *Sakawanum* taxa, I generated predictive distributions for two time periods [present and the last glacial maximum (LGM)] using the maximum entropy method implemented in Maxent ver. 3.3.3 (Phillips and Dudik, 2008). I collected occurrence data for series *Sakawanum* species from my field survey and plant specimens deposited in the herbarium of Makino Botanical Garden (Teramine, 1981). In total, 45 records were used; six occurrence data points for *A. minamitanianum*, six for *A. sakawanum* var. *stellatum*, 21 for *A. sakawanum* var. *sakawanum*, and 12 for *A. costatum* (shown in Table S9). I obtained five bioclimatic variables with 30-s resolution from the WorldClim database (Hijmans et al., 2005) as predictive variables: (1) annual mean temperature, (2) maximum temperature of the warmest month, (3) mean temperature of the warmest quarter, (4) annual precipitation, and (5) precipitation of the warmest quarter. Modeling was performed for all taxa together, because my previous study found no significant differentiation of these climate variables (including temperature and precipitation components) among *Sakawanum* taxa (Chpater 4). The default settings were used for model building. Outputs were divided with 25% for testing and the remaining 75% used for training in the model, and the output function was set as logistic. This procedure was repeated 100 times and each run included 5,000 iterations. The accuracy of the model was measured based on the area under the curve (AUC) of the receiver operating characteristic (ROC) plot (Fielding and Bell, 1997). I adopted the "maximum training sensitivity plus specificity" as the threshold value, which is considered the most accurate predictor for presence-only data (Liu et al., 2013a). The model showing the highest AIC value within 100 replicates was projected onto the climatic conditions during the LGM period simulated using the Community Climate System Model (CCSM3.0; Collins et al., 2006) and the Model for Interdisciplinary Research on Climate (MIROC3.2; Hasumi and Emori, 2004). I assumed that sea level during the LGM period was 130 m lower than at present (Yokoyama et al., 2000). I prepared the climate layers for the exposed seafloors during the LGM period with resolutions of 30 s using the method described by Sakaguchi et al. (2010).

Results

Genetic variation of SSR loci and chloroplast sequences

The summary statistics for each taxon and taxon pair calculated from DIYABC are shown in Table 5. my EST-SSR results showed that all series *Sakawanum* taxa had relatively high genetic diversity (mean expected heterozygosity: 0.731–0.781, mean number of alleles: 9.53–10.24), whereas genetic differentiation among the taxa was relatively low (pairwise F_{ST}: 0.027–0.087). Within the series, the number of alleles in the intermediate *A. sakawanum* taxa (var. *stellatum*: 10.24, var. *sakawanum*: 10.18) were higher than those of *A. minamitanianum* (9.765) and *A. costatum* (9.529), that is, there was no pattern of genetic diversity along geographical axis. Among taxon pairs, the

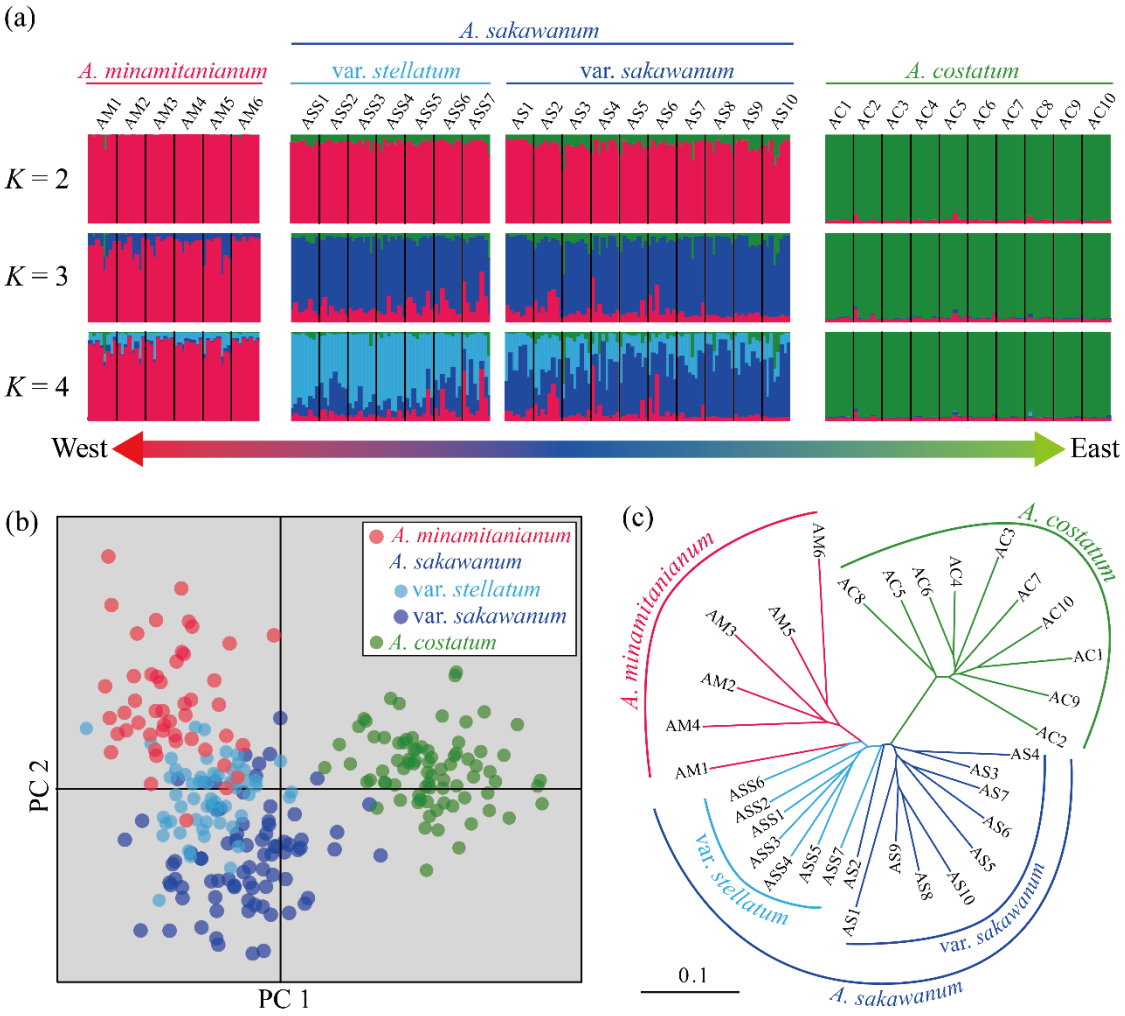

Figure 9. (a) The results of population clustering analysis using STRUCTURE (K = 2–4), (b) principal component analysis, and (c) neighbor-joining tree based on the genetic distances among populations.

level of genetic differentiation was greatest between *A. minamitanianum* and *A. costatum* (pairwise F_{ST} = 0.087) and smallest between the two varieties within *A. sakawanum* (pairwise F_{ST} = 0.027).

In STRUCTURE analysis based on 17 SSR loci, L(D) values increased gradually with increasing K; after K = 5, its variance among runs increased rapidly (Fig. S17a). Delta K had its highest value at K = 2 (Fig. S17b). At K = 2, the two clusters were quite similar to the grouping *A. minamitanianum* + *A. sakawanum* (including two varieties) vs. *A. costatum*, with *A. sakawanum* contained within the cluster of *A. costatum* (11.8%) (Fig. 9a). When K was set to 3, the clusters were consistent with three species, wherein *A. sakawanum* contained *A. minamitanianum* and *A. costatum* clusters (11.9% and 9.0%, respectively). In addition, at K = 4, *A. sakawanum* was divided into two clusters, consistent with two varieties. The results of PCA and the population neighbor-joining tree were also consistent with taxonomic units (Fig. 9b & c). Moreover, all analyses indicated the genetically intermediate position of *A. sakawanum* taxa between *A. minamitanianum* and *A. costatum*.

The combined alignment of four chloroplast regions was 1,365 bp in length. Sixteen nucleotide substitutions were found in the combined sequence, which revealed 12 haplotypes (H0-11) including the outgroup species (*A. tokarense*; haplotype H0). Among series *Sakawanum* populations, aside from five populations of *A. sakawanum* (three populations of var. *sakawanum* and two of var. *stellatum*), 28 populations represented a single haplotype. *Asarum sakawanum* var. *stellatum* had seven haplotypes and *A. sakawanum* var. *sakawanum* had five haplotypes. On the other hand, *A. minamitanianum* and *A. costatum* had smaller

numbers of haplotypes, two and three respectively. Analysis of molecular variance showed that 60.29% of the variation was distributed among taxa and 29.07% was among populations within taxa (Table S10). The chloroplast sequences obtained here were submitted to the GenBank database under accession numbers LC4146275 – LC4146292.

The distribution of 11 haplotypes among 33 sample populations of series *Sakawanum* taxa is shown in Figure 10. Within the 11 haplotypes, two haplotype groups, CP1 and CP2, were identified, which included five and six haplotypes, respectively. These two haplotype groups were differentiated by four mutation events. Two haplotype groups corresponded to geographic position (*A. minamitanianum* and *A. sakawanum* var. *stellatum* vs. *A. sakawanum* var. *sakawanum* and *A. costatum*) rather than taxonomic units. In group CP1, the most dominant haplotype (H1) was shared between *A. minamitanianum* and *A. sakawanum* var. *stellatum* in Okinoshima Island populations. The other haplotypes (H2–H5), which contained one mutation compared to H1 and which created a "star-like" relational network, were each detected in only a single population in *A. minamitanianum* or *A. sakawanum* var. *stellatum* populations. No haplotypes in group CP1 were ever found in *A. costatum* or *A. sakawanum* var. *sakawanum*. H6, the most dominant haplotype in this group CP2, was widely shared among populations distributed on Shikoku Island (five populations of *A. costatum*, four populations of *A. sakawanum* var. *sakawanum*, and two populations of *A. sakawanum* var. *stellatum*). H8 was shared between one population of *A. costatum* and one population of *A. sakawanum* var. *sakawanum*. The other haplotypes in group CP2 (H7, H9–10) were not shared among taxa.

Inconsistent genetic structures were detected between the two types of markers. EST-SSR data showed corresponding taxonomic structures (*A. minamitanianum* vs. *A. sakawanum* vs. *A. costatum*) and close relationships for the two varieties of *A. sakawanum*. On the other hand, my chloroplast analysis showed that the genetic structure of the series corresponded to geographic structure, with strong genetic differentiation between the two varieties of *A. sakawanum* (only one haplotype was shared between two taxa).

Approximate Bayesian computation analysis

My ABC analysis showed that among the 12 models, the sum of the posterior probabilities of models concerning admixture event(s) (model F–L) was 0.9998 at the tolerance rate 0.1% (Table 6). Of the 12 models, model K showed the highest support (posterior probability = 0.7773, 95% CI = 0.7098–0.8448 at tolerance rate 0.1%), followed by model I (posterior probability = 0.1263, 95% CI = 0.000–0.3853) and model L (posterior probability = 0.0735, 95% CI = 0.000–0.3017). Model K assumed that secondary contact between *A. minamitanianum* and *A. costatum* produced *A. sakawanum*, and *A. sakawanum* var. *stellatum* originated from subsequent admixture between *A. sakawanum* and *A. minamitanianum*. Model I also assumed that secondary contact of *A. minamitanianum* and *A. sakawanum* produced *A. sakawanum* var. *stellatum*, but assumed that *A. sakawanum* was derived from *A. costatum*, whereas model L assumed secondary contact between *A. minamitanianum* and *A. costatum*, but that *A. sakawanum* var. *sakawanum* originated from subsequent admixture between *A. sakawanum* and *A. costatum*. At all tolerance rates (0.1–1%), the posterior probabilities of models other than model K were less than 30% in total, and the pattern of supported models did not change (Fig. S18). The type I error for model K (the ratio for model K did not have the highest posterior

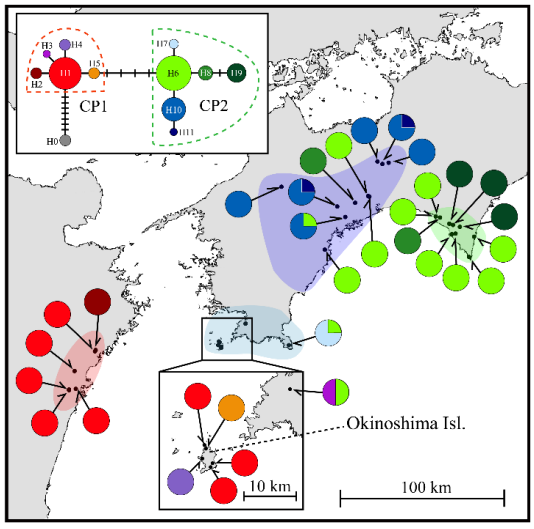

Figure 10. The haplotype network for 1365 bp combined chloroplast regions obtained from series *Sakawanum* taxa and outgroup taxa (*A. tokarense*; H0) and the geographic distribution of the 11 chloroplast haplotypes in series *Sakawanum* taxa. Two haplotype groups, CP1 and CP2 were shown with the red and green broken lines, respectively. The distribution range of each taxon is indicated by a coloured area (red: *A. minamitanianum*, light blue: *A. sakawanum* var. *stellatum*, dark blue: *A. sakawanum* var. *sakawanum*, green: *A. costatum*).

Table 5. Comparison of summary statistics for the observed dataset and *P*-values for each quantity computed using simulated datasets with parameters drawn from the posterior distributions obtained with model K. drawn from the posterior distributions obtained under the model K.

Summary statistics	Observed value	*P* value (simulated < observed)
EST-SSR data sets		
Mean number of alleles in AM	9.765	0.613
Mean number of alleles in ASS	10.235	0.505
Mean number of alleles in AS	10.177	0.434
Mean number of alleles in AC	9.529	0.606
Mean expected heterozygosity in AM	0.781	0.545
Mean expected heterozygosity in ASS	0.783	0.383
Mean expected heterozygosity in AS	0.754	0.211
Mean expected heterozygosity in AC	0.732	0.360
Mean M index across loci in AM	0.794	0.289
Mean M index across loci in ASS	0.783	0.195
Mean M index across loci in AS	0.786	0.153
Mean M index across loci in AC	0.750	0.121
F_{ST} between AM and ASS	0.030	0.529
F_{ST} between AM and AS	0.049	0.282
F_{ST} between AM and AC	0.087	0.257
F_{ST} between ASS and AS	0.027	0.432
F_{ST} between ASS and AC	0.073	0.388
F_{ST} between AS and AC	0.065	0.513
$(\delta\mu)^2$ distance between AM and ASS	1.216	0.611
$(\delta\mu)^2$ distance between AM and AS	2.478	0.574
$(\delta\mu)^2$ distance between AM and AC	4.182	0.430
$(\delta\mu)^2$ distance between ASS and AS	0.690	0.358
$(\delta\mu)^2$ distance between ASS and AC	3.265	0.525
$(\delta\mu)^2$ distance between AS and AC	2.340	0.566
Chloroplast sequence data sets		
Number of haplotypes in AM	2.000	0.206
Number of haplotypes in ASS	7.000	0.949
Number of haplotypes in AS	5.000	0.696
Number of haplotypes in AC	3.000	0.475
Tajima's *D* statistics in AM	0.139	0.610
Tajima's *D* statistics in ASS	1.950	0.978*
Tajima's *D* statistics in AS	-1.698	0.008**
Tajima's *D* statistics in AC	0.212	0.667
F_{ST} between AM and ASS	0.145	0.697
F_{ST} between AM and AS	0.901	0.993**
F_{ST} between AM and AC	0.918	0.966*
F_{ST} between ASS and AS	0.676	0.997**
F_{ST} between ASS and AC	0.715	0.914
F_{ST} between AS and AC	0.166	0.387

AM, ASS, AS, and AC indicate *A. minamitanianum*, *A. sakawanum* var. *stellatum*, *A. sakawanum* var. *sakawanum*, and *A. costatum*, respectively. **P* <0.05, ***P*<0.01

probability when it was treated as the true scenario) was 0.22, and the type II errors of other models ranged from 0 to 0.08 (Table S11). The mode, mean, and median values with 95% HPDI of the demographic parameters in model K are shown in Table S12. I adopted the mean values as the estimated parameter values. The split time of the ancestral populations of *A. costatum* and *A. minamitanianum* was 400,000 years ago (T1 [95% HPDI: 128,000–914,000]), and the first admixture event, which produced *A. sakawanum,* occurred 76,100 years ago (T2 [95% HPDI: 33,200–140,000]). The second admixture event between *A. minamitanianum* and *A. sakawanum* was estimated to take place 19,610 years ago (T3 [95% HPDI: 6,750–29,400]). The estimated current effective population sizes were 61,900, 48,200, 66,000, and52,400 for *A. minamitanianum* (NAM), *A. sakawanum* var. *stellatum* (NASS), *A. sakawanum* var. *sakawanum* (NAS), and *A. costatum* (NAC), respectively. The ancestral population size of the ancestral lineage (AA) was 56,000, and those of *A. minamitanianum* (AAM), *A. sakawanum* (AAS), and *A. costatum* (AAC) were 70,100, 56,300, and 54,500, respectively. The posterior distributions of demographic parameters with prior distributions are shown in Fig. S19. Among the 38 summary statistics, five summary statistics of chloroplast datasets (Tajima's *D* statistics in *A. sakawanum* var. *stellatum* and *A. sakawanum* var. *sakawanum*, F_{ST} between *A. minamitanianum* and *A. sakawanum* var. *sakawanum*, between *A. minamitanianum* and *A. costatum*, and between *A. sakawanum* var. *stellatum* and *A. sakawanum* var. *sakawanum*) showed significant differences between observed and simulated data based on their posterior distributions ($P < 0.05$; Table 5). However, PCA (Fig. S20) showed that the observed data point (orange circle) was in the middle of a small cluster of data from the posterior predictive distribution (closed green circle), suggesting that the observed data are generally similar to simulated data, and therefore, that model K would be fit the observed data well.

The results of model selection using only EST-SSR dataset also showed that model K was most probable model under the all tolerance rates (posterior probability = 0.7722, 95% CI = 0.7441–0.8003 at tolerance rate 0.1%), while second supported model was different. The plots of relative posterior probabilities of models were shown in Figure S21.

Ecological niche modeling

Table 6. Relative posterior probabilities of each model and 95% confidence intervals based on the logistic estimate with a tolerance rate of 0.1%.

Model	Posterior probability	95% CI (lower - upper)
A	0.0001	0.0000 - 0.2411
B	0.0000	0.0000 - 0.2411
C	0.0000	0.0000 - 0.2411
D	0.0001	0.0000 - 0.2411
E	0.0000	0.0000 - 0.2411
F	0.0022	0.0000 - 0.2425
G	0.0004	0.0000 - 0.2413
H	0.0184	0.0000 - 0.2522
I	0.1263	0.0000 - 0.3853
J	0.0018	0.0000 - 0.2423
K	0.7773	0.7098 - 0.8448
L	0.0735	0.0000 - 0.3017

The Maxent model had high predictive power (AUC = 0.944 ± 0.11 [mean ± SD]). The predicted distribution under present conditions covered most of the actual distribution of series *Sakawanum* taxa, but also predicted southern Kyushu Island as a suitable habitat (Fig. 11a). During the LGM period, when the sea level was 130 m lower than at present, Kyushu and Shikoku Islands formed a land bridge, and the coastline was south of the present coastline. Under the LGM climate conditions of the MIROC 3.2 model (Fig. 11b-1), high distribution probabilities were predicted in the southern and lowland parts (near the coastline) of Kyushu and Shikoku Islands, whereas in the CCSM 3.0 model (Fig. 11b-2), only the southern part of Kyushu was assigned high distribution
probabilities for prediction. In both models, most of the present distribution areas had low probabilities or were regarded as unsuitable.

Discussion

Inferred admixture events among series* Sakawanum *taxa

Inconsistencies in the nuclear and chloroplast data were detected in taxa of series *Sakawanum*. The results of Bayesian clustering analysis, PCA, and phylogenetic analysis based on 17 EST-SSR data showed that the genetic structures were generally consistent with morphospecies (Fig. 9). On the other hand, chloroplast sequence analysis identified two rather than three distinct lineages, which corresponded to geographic structures, and the two varieties of *A. sakawanum* did not form a monophyletic group (Fig. 10). This discordance may have resulted from historical genetic

exchanges via hybridization or incomplete lineage sorting (Chiang, 2000). It is well established that organelle genes undergo lineage sorting faster than nuclear genes due to their smaller effective population size (Hoelzer, 1997). Higher genetic diversities of the two *A. sakawanum* taxa were found in both types of markers (Table 5). These high genetic diversities implied admixture, because admixture events
usually lead to mixed genetic composition and higher genetic diversity in the hybrid population, but may have low impacts on the parental populations' genomes (Huang et al., 2011). Furthermore, my ABC analysis using EST-SSR markers and chloroplast sequences supported the models, predicting admixture events with high posterior probabilities within 12 models (the sum of posterior probabilities of Model F– L is 0.9998 at the tolerance rate 0.1%). Thus, I concluded that the inconsistency of genetic structures between nuclear and chloroplast genomes resulted from historical admixture events within series *Sakawanum* taxa rather than incomplete lineage sorting. The haplotypes of *A. sakawanum* taxa were derived from *A. minamitanianum* and/or *A. costatum* through secondary contact. Moreover, model K, which assumed that the intermediate species (*A. sakawanum*) originated through secondary contact of other species (*A. minamitanianum* and *A. costatum*) and that subsequent admixture of *A. minamitanianum* and *A. sakawanum* produced *A. sakawanum* var. *stellatum*, was supported with the highest posterior probability among 12 alternative models at all tolerance rates (Table 6, Fig. S18). Although more complicated models for series *Sakawanum* taxa are possible, I could not test such models in this study; I determined that among my 12 relatively simple models, model K best reflects the evolutionary history of taxa in series *Sakawanum*.

Implications for establishment of clinal variation

Demographic history, including admixture events, may have affected the formation of intertaxonomic clinal variation in series *Sakawanum*. Clinal variation can theoretically be affected by neutral processes (Endler, 1973, Campitelli and Stinchcombe, 2013). In addition, many studies have reported significant correlations between morphological traits and the genetic status of hybrid individuals (Minder et al., 2007, Bergland et al., 2016, Worth et al., 2016), as well as the intermediate morphology of hybrid origin species (Rieseberg, 1997, Xing et al., 2014, Yakimowski and Rieseberg, 2014). The intermediate morphology and distribution range of *A. sakawanum* taxa between *A. minamitanianum* and *A. costatum* were shown in my previous study (Chpater 4). Here, the pattern of genetic diversity of series *Sakawanum* taxa was not consistent with range expansion hypothesis of the lineage. ABC analysis inferred that two separate admixture events took place within the series: between *A. minamitanianum* and *A. costatum*, and between *A. minamitanianum* and *A. sakawanum*. I therefore speculated that the intermediate morphology of *A. sakawanum* is derived from hybridization of the two parental species, which have long and short calyx lobes and previously diverged allopatrically. Subsequently, the second admixture event between *A. minamitanianum* and *A. sakawanum* would have led to formation of the morphology of *A. sakawanum* var. *stellatum*, which has a longer calyx lobe than var. *sakawanum*. my study

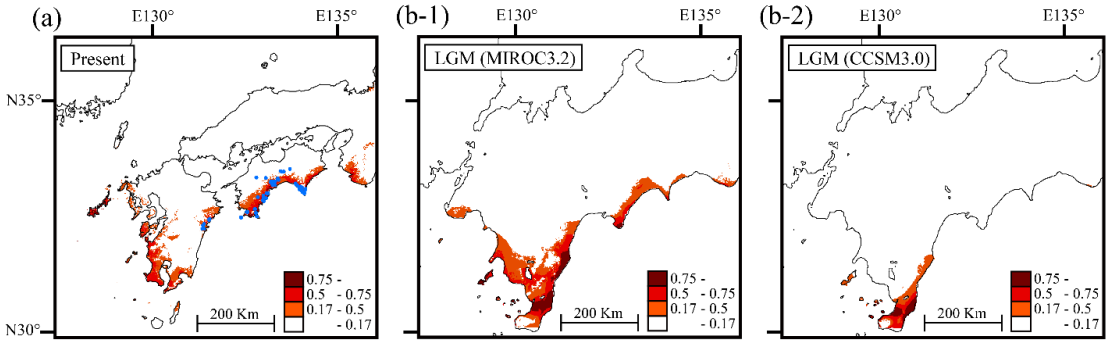

Figure 11. Predicted potential distribution of series *Sakawanum* taxa under (a) the present conditions, and (b) last glacial maximum (LGM; 21,000 years ago) conditions (1, Model for Interdisciplinary Research on Climate [MIROC] 3.2; 2, Community Climate System Model [CCSM] 3.0). Colours represent the probability of the species occurring in an area. Distribution records of series Sakawanum taxa are plotted as blue points in the map under the present condition.

indicated that complicated evolutionary history, including multiple admixture events among morphologically distinctive taxa, may have produced morphologically intermediate taxa and thus led to the establishment of clinal variation in calyx lobe length within series *Sakawanum*.

It is certain that the results of this study were derived from neutral markers, and it remains unclear whether the morphology of this series is linked to their evolutionary history. To clarify the evolution of clinal variation, further analysis is needed (e.g., developing markers linked to calyx lobe morphology and confirming the inheritance of calyx lobe length).

Biogeography of taxa in relation to the LGM period

My ABC analysis indicated that the first divergence within series *Sakawanum* from the common ancestor leading to *A. minamitanianum* and *A. costatum* occurred 400,000 years ago (T1, 95% HPDI = 128,000–914,000 years ago). The first secondary contact event within the series (between *A. minamitanianum* and *A. costatum*) occurred 76,100 years ago (T2, 95% HPDI = 33,200–140,000 years ago) and the subsequent contact (between *A. minamitanianum* and *A. sakawanum*) was 19,600 years ago (T3, 95% HPDI = 6,750–29,400 years ago). Considering the low mobility of series *Sakawanum*, these events would have been associated with geographical range shifts due to climate oscillations during the late Quaternary. The first divergence event within the series would have occurred allopatrically, as shown for other taxa of genus *Asarum* in my previous study (Chpater 1). I determined that the morphological divergence between *A. minamitanianum* and *A. costatum* occurred by the time of the initial secondary contact 76,100 years ago. The estimated time of the second admixture event was in good agreement with the LGM period (approximately 21,000 years ago). During this time, the sea level was around 130 m lower than its present level, and Shikoku and Kyushu Islands were connected as a contiguous land mass. Moreover, during this period, the warm temperate evergreen forests of southern Japan formed refugia at the southern edge of Kyushu Island and the Pacific coast of Shikoku Island (Aoki et al., 2004, Liu et al., 2013b, Aoki et al., 2019). my results of ENM indicated that these regions were suitable habitats for series *Sakawanum* taxa under LGM climate conditions using the MIROC model (Fig. 11b-1), whereas only southern and lowland parts of Kyushu Island were predicted as suitable habitat with high probabilities by the CCSM model (Fig. 11b-2). During the LGM period, taxa in series *Sakawanum* would have inhabited refugia in this region, as did other plants that grow in warm temperate evergreen forests, and this range shift would have led to secondary contact between previously isolated taxa. Several studies have indicated that range shifts and formation of refugia due to climate change could provide opportunities for secondary contact and subsequent hybridization (Eriksen and Topel, 2006, Medail and Diadema, 2009). It has been reported that pollinator fauna overlapped among series *Sakawanum* taxa, (Kakishima and Okuyama, 2018, Takahashi et al., personal observation). I found that strong limitation by climatic conditions and sharing of pollinator fauna would lead to secondary contact and the formation of intertaxonomic hybrid populations within the series. After the LGM period, the increasing temperature would have led all taxa to move to northern areas, and rising sea levels would have divided the distribution ranges. my results indicate that climatic oscillations during the Quaternary and the associated range shifts triggered the divergence and multiple admixture events within series *Sakawanum* taxa, leading to the current fragmented distribution with intertaxonomic clinal variation.

Appendix

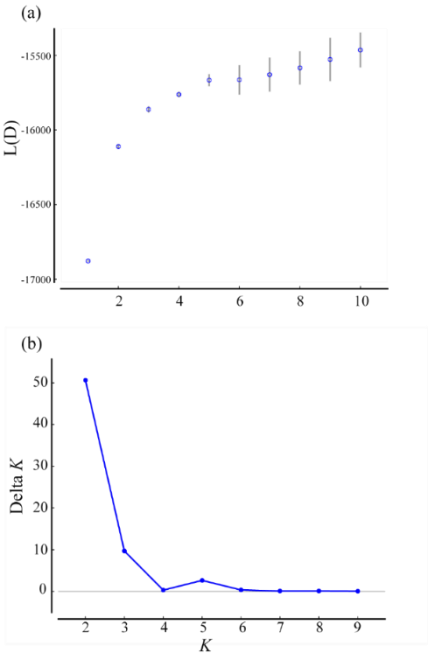

Figure S17. Graphs of L(D) values (a) and ΔK values (b) for each K obtained from STRUCTURE analysis. Error bars represent the standard deviation of each mean.

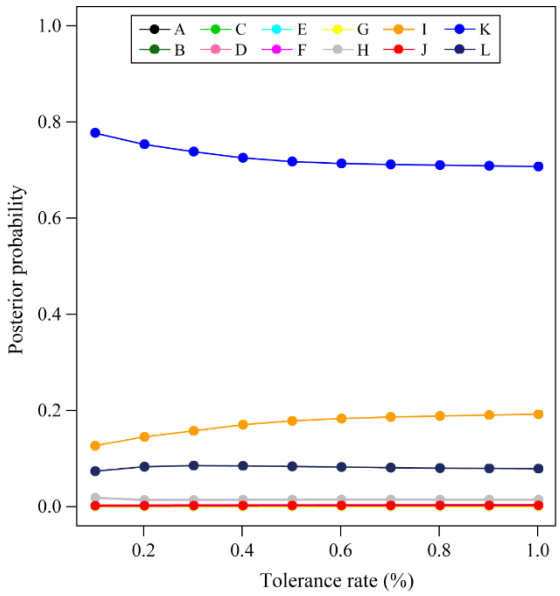

Figure S18. Plots of the relative posterior probabilities (y-axis) of 12 demographic models with 10 tolerance rates (x-axis, 0.1–1%).

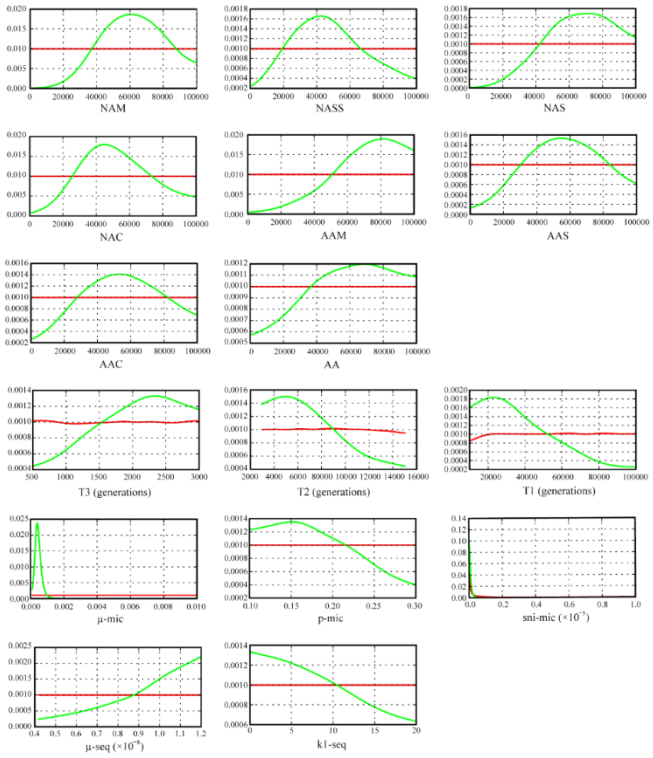

Figure S19. Posterior distributions (green lines) and prior distributions (red lines) of demographic parameters in model K. The vertical and horizontal axes of graphs indicate density values and parameter values, respectively.

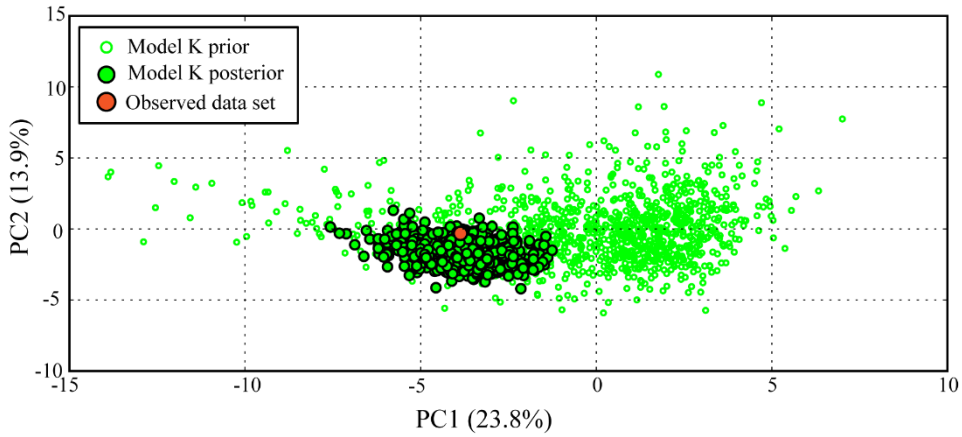

Figure S20. Principal component analysis (PCA) of summary statistics computed from simulated data with parameters drawn from the prior (open green circles) and posterior (closed green circles) distributions within model K. The observed empirical summary statistics are indicated by a closed orange circle.

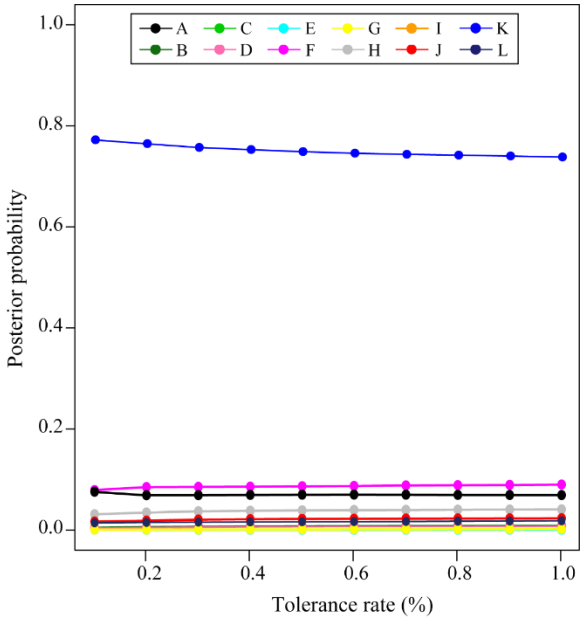

Figure S21. Plots of the relative posterior probabilities (y-axis) of 12 demographic models with 10 tolerance rates (x-axis, 0.1–1%) based on EST-SSR dataset. by a closed orange circle.

Table S5. Population information and genetic diversity indices.

Taxon name	Population name	Latitude (N°)	Longitude (E°)	EST-SSR analysis					Chloroplast sequence analysis		
				N	Na	H_O	H_E	F_{IS}	N	NH	π
A. minamitanianum	AM1	32.45	131.58	8	5.78	0.614	0.739	0.183	4	1	0
	AM2	32.45	131.58	8	5.50	0.630	0.699	0.067	4	1	0
	AM3	32.56	131.61	8	5.33	0.661	0.702	0.052	4	1	0
	AM4	32.46	131.63	8	4.61	0.546	0.644	0.143	4	1	0
	AM5	32.67	131.74	8	5.78	0.605	0.714	0.159	4	1	0
	AM6	32.68	131.74	8	4.94	0.563	0.658	0.186	4	1	0
	average				5.32	0.603	0.693	0.132		1.0	0
A. sakawanum var. *stellatum*	ASS1	32.73	132.54	8	5.50	0.718	0.733	0.015	4	1	0
	ASS2	32.75	132.55	8	5.17	0.653	0.674	0.031	4	1	0
	ASS3	32.75	132.55	8	5.50	0.620	0.700	0.096	4	1	0
	ASS4	32.71	132.56	8	5.11	0.611	0.673	0.071	4	1	0
	ASS5	32.72	132.56	8	6.00	0.707	0.746	0.057	4	1	0
	ASS6	32.85	132.72	8	5.33	0.635	0.711	0.094	4	2	0.00300
	ASS7	32.74	133.00	8	6.17	0.581	0.735	0.214	4	2	0.00037
	average				5.54	0.646	0.710	0.082		1.3	0.00048
A. sakawanum var. *sakawanum*	AS1	33.62	132.92	8	4.78	0.577	0.670	0.133	4	1	0
	AS2	33.28	133.22	8	5.83	0.590	0.709	0.172	4	1	0
	AS3	33.52	133.30	8	5.39	0.556	0.695	0.193	4	2	0.00037
	AS4	33.46	133.35	8	4.94	0.516	0.686	0.254	4	2	0.00037
	AS5	33.54	133.41	8	5.28	0.597	0.652	0.093	4	1	0
	AS6	33.58	133.50	8	5.06	0.567	0.685	0.182	4	1	0
	AS7	33.58	133.51	8	5.06	0.615	0.661	0.057	4	1	0
	AS8	33.77	133.56	8	4.39	0.583	0.641	0.061	4	1	0
	AS9	33.76	133.59	8	5.06	0.620	0.680	0.073	4	2	0.00037
	AS10	33.77	133.63	8	4.50	0.556	0.648	0.136	4	1	0
	average				5.03	0.578	0.673	0.135		1.3	0.00011

Table S5 continued

A. costatum	AC1	33.48	133.95	8	4.50	0.579	0.630	0.111	4	1	0
	AC2	33.48	133.95	8	4.67	0.506	0.658	0.223	4	1	0
	AC3	33.47	133.98	8	3.83	0.643	0.608	-0.086	4	1	0
	AC4	33.44	134.04	8	4.67	0.601	0.675	0.102	4	1	0
	AC5	33.38	134.06	8	5.06	0.547	0.652	0.144	4	1	0
	AC6	33.43	134.06	8	5.11	0.622	0.690	0.103	4	1	0
	AC7	33.38	134.08	8	4.78	0.521	0.626	0.193	4	1	0
	AC8	33.42	134.11	8	4.56	0.614	0.658	0.080	4	1	0
	AC9	33.25	134.18	8	4.67	0.551	0.652	0.150	4	1	0
	AC10	33.37	134.20	8	4.78	0.556	0.653	0.155	4	1	0
	average				4.66	0.574	0.650	0.117		1.0	0
A. tokarense	-	29.86	129.85	-	-	-	-	-	4	1	0

N, number of individuals used in each analysis; Na, number of alleles; $H_{O,}$ observed heterozygosity; $H_{E,}$ expected heterozygosity; F_{IS}, fixation index; NH, number of haplotypes; π, nucleotide diversity.

Table S6. Characteristics of the 17 expressed sequence tag-simple sequence repeat (EST-SSR) markers analysed in this study.

Locus name	Primer sequence	Na	H_O	H_E	F_{IS}
As_2526	F: TGTGGAATTGTGAGCGGAACCGCACACAGCCTTTAC	13.7	0.641	0.856	0.247
	R: GTTTCTTCACACCGCCACGAAATGAG				
As_7180	F: CTATAGGGCACGCGTGGTGAAAGTCCAGCCAAGGAGC	14.0	0.718	0.760	0.061
	R: GTTTCTTGTTGTGGAACCTGTCTCGG				
As_59081	F: CTATAGGGCACGCGTGGTTGTTGGGATTAGCTGATGGG	13.0	0.802	0.820	0.022
	R: GTTTCTTAGAGAAACAGGGCATCAGAAC				
As_12707	F: TGTGGAATTGTGAGCGGTTTCCCTAAGATGCTCCCAC	10.7	0.342	0.791	0.559
	R: GTTTCTTGTCCTCGGCAAAGCCATTC				
As_537	F: TGTGGAATTGTGAGCGGCTGAGAAGGACAATCCACAAGC	9.0	0.840	0.828	-0.016
	R: GTTTCTTTACCGTCGTCACCGAATCC				
As_3572	F: CTATAGGGCACGCGTGGTAGGCCAAGCAATGTGGAAAC	9.7	0.595	0.758	0.217
	R: GTTTCTTAGAGGAGGAGAATCTTAAAGGAATG				
As_14593	F: TGTGGAATTGTGAGCGGAGCCCTAATTCCCGCAGAC	7.7	0.503	0.712	0.284
	R: GTTTCTTCTGCATTGTGGAGGCGTTC				
As_9592	F: CTATAGGGCACGCGTGGTATCACCGAGCAAGCATTCG	10.0	0.523	0.766	0.321
	R: GTTTCTTAACCGGATCTGAAGGGCTC				
As_24077	F: CACGACGTTGTAAAACGACCCGAGGGTGTCGGAAACAG	9.0	0.771	0.789	0.023
	R: GTTTCTTTGTGAATGGGAAACGAAACCC				
As_18424	F: TGTGGAATTGTGAGCGGGAAGGCTGTTTCCTCACCG	7.0	0.512	0.666	0.230
	R: GTTTCTTCCGAAGTTTGGCGCTCTAC				
As_9117	F: CACGACGTTGTAAAACGACCTCGCAATGACATCGGTGG	9.0	0.698	0.740	0.061
	R: GTTTCTTGAGAGTGCCTACCGTCGAG				
As_29176	F: CTATAGGGCACGCGTGGTTGGTTGATGAATCTTCCTCTATTACG	17.0	0.552	0.898	0.386
	R: GTTTCTTTCACCCAATTCGTCTCTGG				
As_42062	F: CACGACGTTGTAAAACGACTGAGGGTGATGAGGTACCAAC	10.0	0.489	0.797	0.386
	R: GTTTCTTTGGCACTACTGCTTCAGGG				
As_20984	F: CTATAGGGCACGCGTGGTAAGGGACCGCCAGAATCG	7.3	0.393	0.544	0.279
	R: GTTTCTTACGACTCTCCAGATCTCCAAC				
As_21539	F: CACGACGTTGTAAAACGACCGGATCCCGAATGCGAAAC	9.3	0.578	0.623	0.072
	R: GTTTCTTTCAGTTCCAATCACCTCTGC				
As_11633	F: CTATAGGGCACGCGTGGTTTTCGGGTTCCCTTCATCC	11.7	0.488	0.751	0.322
	R: GTTTCTTGGTGCACATCGAGTTTCCG				
As_74749	F: TGTGGAATTGTGAGCGGGAGCGAGGTCCATTTACCG	8.3	0.646	0.792	0.183
	R: GTTTCTTCAGTAGGCTTACCCGGTGG				

Na, number of alleles; H_O, observed heterozygosity; H_E, expected heterozygosity; F_{IS}, fixation index.

Table S7. Characteristics of the four chloroplast sequence markers analyzed in this study.

Locus name	Primer sequence	Length	NH	π
AC_cpSNP_1	F: CCAATGGTATGGACGAATCC	310	6	0.00356
	R: CCCTGCGACGAAAGAAGTAT			
AC_cpSNP_7	F: ACATGGCCAGATGAGTGGAT	313	4	0.00215
	R: GACCAACCATCAGAGGAAGC			
AC_cpSNP_8	F: GATTCATCCTACCGGTTCCA	370	5	0.00214
	R: TGGATCAACCCGAAGAGGTA			
AC_cpSNP_15	F: TCCAATCAAACAGTTCCACAA	342	3	0.00286
	R: CGATTCGCCAGCTCTTATCT			

NH, number of haplotypes; π, nucleotide diversity.

Table S8. Prior distributions of the parameters used in DIYABC.

Parameter	Distribution	Minimum	Maximum
Effective population size	Uniform		
NAM	Uniform	1000	100000
NASS	Uniform	1000	100000
NAS	Uniform	1000	100000
NAC	Uniform	1000	100000
AAM	Uniform	1000	100000
AAS	Uniform	1000	100000
AAC	Uniform	1000	100000
AA	Uniform	1000	100000
Time scale in generations			
T1	Uniform	10000	100000
T2	Uniform	3000	15000
T3	Uniform	500	3000
Mutation model in EST-SSR data sets			
Mean mutation rate (μ-mic)	Uniform	1.0E-05	1.0E-03
Individual locus mutation rate	Gamma	1.0E-06	1.0E-02
Mean coefficient P (p-mic)	Uniform	1.0E-01	3.0E-01
Individual locus coefficient P	Gamma	2.0E-02	9.0E-01
Mean SNI rate (sni-mic)	Log-uniform	1.0E-08	1.0E-04
Individual locus SNI rate	Gamma	1.0E-09	1.0E-03
Mutation model in chloroplast sequence data sets			
Mean mutation rate (μ-seq)	Uniform	4.2E-09	1.2E-08
Individual locus mutation rate	Gamma	1.0E-09	1.0E-07
Mean coefficient k_C/T (k-seq)	Uniform	5.0E-02	1.0E+01
Individual locus coefficient k_C/T	Gamma	5.0E-02	2.0E+01

NAM, the current effective population size of *A. minamitanianum*; NASS, that of *A. sakawanum* var. *stellatum*; NAS, that of *A. sakawanum* var. *sakawanum*; NAC, that of *A. costatum*; AA, the ancestral effective population size of the common ancestor; AAM, that of *A. minamitanianum*; AAS, that of *A. sakawanum*; AAC, that of *A. costatum*.

Table S9. Occurrence data of series *Sakawanum* taxa and the values of five environmental variables used in ecological niche modeling (ENM).

Taxon	Latitude	Longitude	Bio1	Bio5	Bio10	Bio12	Bio18
A. minamitanianum	32.54	131.59	148	309	254	2390	924
A. minamitanianum	32.45	131.58	150	311	256	2471	962
A. minamitanianum	32.56	131.61	151	313	258	2321	871
A. minamitanianum	32.46	131.63	155	315	261	2375	885
A. minamitanianum	32.65	131.74	155	316	260	2146	761
A. minamitanianum	32.68	131.74	146	307	253	2216	819
A. sakawanum var. *stellatum*	33.28	133.21	161	316	266	2116	610
A. sakawanum var. *stellatum*	33.19	133.14	146	299	251	2147	620
A. sakawanum var. *stellatum*	33.18	132.98	147	301	253	2007	630
A. sakawanum var. *stellatum*	32.92	132.92	156	303	258	2095	679
A. sakawanum var. *stellatum*	32.85	132.94	160	303	260	2145	687
A. sakawanum var. *stellatum*	32.84	132.70	157	306	259	1989	703
A. sakawanum var. *sakawanum*	33.22	133.12	148	302	253	2107	603
A. sakawanum var. *sakawanum*	33.10	133.14	164	314	267	2094	620
A. sakawanum var. *sakawanum*	33.17	133.20	163	315	267	2118	618
A. sakawanum var. *sakawanum*	33.12	133.11	158	309	261	2098	630
A. sakawanum var. *sakawanum*	33.61	133.16	147	313	258	1827	530
A. sakawanum var. *sakawanum*	33.54	133.36	152	315	261	2120	637
A. sakawanum var. *sakawanum*	33.82	133.79	129	293	241	1852	609
A. sakawanum var. *sakawanum*	33.46	133.41	148	307	256	2216	676
A. sakawanum var. *sakawanum*	32.73	132.56	158	307	259	2049	743
A. sakawanum var. *sakawanum*	32.85	132.72	155	304	257	2015	709
A. sakawanum var. *sakawanum*	32.76	132.97	158	298	257	2251	719
A. sakawanum var. *sakawanum*	33.62	132.92	123	289	236	1822	583
A. sakawanum var. *sakawanum*	33.28	133.22	160	316	265	2133	569
A. sakawanum var. *sakawanum*	33.52	133.30	154	317	263	2065	596
A. sakawanum var. *sakawanum*	33.46	133.35	160	321	267	2157	613
A. sakawanum var. *sakawanum*	33.54	133.41	159	321	267	2189	671
A. sakawanum var. *sakawanum*	33.60	133.48	144	307	253	2126	682
A. sakawanum var. *sakawanum*	33.58	133.51	156	321	265	2290	759
A. sakawanum var. *sakawanum*	33.77	133.56	130	296	243	1906	626
A. sakawanum var. *sakawanum*	33.76	133.59	138	304	250	1918	629
A. sakawanum var. *sakawanum*	33.77	133.63	139	305	250	1909	627
A. costatum	33.51	133.94	154	307	258	2084	743
A. costatum	33.47	133.98	145	296	249	2136	743
A. costatum	33.44	134.04	152	300	254	2112	729
A. costatum	33.38	134.06	156	303	258	2120	722
A. costatum	33.43	134.06	142	291	245	2157	738
A. costatum	33.35	134.11	140	286	243	2202	742
A. costatum	33.42	134.11	147	294	249	2134	727
A. costatum	33.29	134.19	165	308	265	2136	704
Table S9 continued							
A. costatum	33.37	134.20	164	309	264	2118	711

A. costatum	33.39	134.12	143	289	245	2168	733
A. costatum	33.39	134.20	163	309	264	2115	715
A. costatum	33.33	134.13	154	297	254	2133	704

Bio 1, annual mean temperature; Bio 5, maximum temperature in the warmest month; Bio 10, mean temperature in the warmest quarter; Bio12, annual precipitation; Bio18, precipitation in the warmest quarter.

Table S10. Analysis of molecular variance (AMOVA) of chloroplast DNA variation in four series *Sakawanum* taxa.

Source of variance	d.f.	SS	VC	Variation (%)	Fixation index
Among four taxa	3	126.10	1.2152	60.29	0.7319*
Among populations within taxa	29	74.19	0.5858	29.07	0.8936*
Within populations	99	21.24	0.2145	10.65	0.6029*
Total	131	221.53	2.0157		

d.f., degrees of freedom; SS, sum of squares; VC, variance components. * $P < 0.001$, 1000 permutations.

Table S11. Values of type I error for each model and type II

model	Type I error	Type II error
A	0.25	0.01
B	0.36	0
C	0.27	0
D	0.31	0.01
E	0.23	0
F	0.31	0.08
G	0.29	0
H	0.13	0
I	0.17	0
J	0.27	0.04
K	0.22	-
L	0.25	0.01

Table S12. Posterior mean, median, and mode estimates and 95% highest posterior density intervals for demographic parameters in model K.

Parameter	NAM	NASS	NAS	NAC	AAM	AAS	AAC	AA	T3	T2	T1	μ-mic	p-mic	sni-mic	μ-seq	k-seq
Mean	61,900	48,200	66,000	52,400	70,100	56,300	54,500	56,000	1,960	7,610	40,000	4.7E-05	0.181	7.4E-08	9.6E-09	8.540
Median	61,500	45,800	66,900	49,800	72,800	56,400	54,100	57,800	2,030	7,040	34,600	4.3E-05	0.174	3.9E-08	1.0E-08	8.020
Mode	60,500	45,100	70,900	42,200	83,800	57,800	56,200	66,300	2,260	4,970	21,900	3.2E-05	0.158	1.1E-08	1.2E-08	0.825
Upper	28,900	14,700	28,600	20,100	25,900	17,000	13,800	5,600	675	3,320	12,800	2.2E-05	0.105	1.1E-08	1.2E-08	0.378
Lower	95,400	90,600	96,700	93,900	97,700	94,800	95,100	97,600	2,940	14,000	91,400	9.5E-05	0.281	3.3E-07	5.1E-09	18.900

NAM, the current effective population size of *A. minamitanianum*; NASS, that of *A. sakawanum* var. *stellatum*; NAS, that of *A. sakawanum* var. *sakawanum*; NAC, that of *A. costatum*; AA, the ancestral effective population size of the common ancestor; AAM, that of *A. minamitanianum*; AAS, that of *A. sakawanum*; AAC, that of *A. costatum*; T1, time of the first divergence, in generations; T2, that of the first admixture event; T3, that of the second admixture event; μ-mic, mean mutation rate of EST-SSR loci; p-mic, mean coefficient P of EST-SSR loci; μ-mic, mean mutation rate of the chloroplast sequence; k-seq, mean coefficient k_C/T of the chloroplast sequence.

Chapter 4

Relative contributions of neutral and non-neutral processes to clinal variation in calyx lobe length in the series *Sakawanum* (*Asarum*: Aristolochiaceae)

Abstract

Clines, the gradual variation in measurable traits along a geographic axis, play major roles in evolution and are considered to be good subject to investigate the relative roles of selective and neutral process on the traits. Using genetic and morphological analyses, I explored the relative contributions of neutral and non-neutral processes to infer the evolutionary history of species of the series *Sakawanum* (genus *Asarum*), which shows significant clinal variation in calyx lobe length. I sampled a total of 27 populations covering the natural geographic distribution of the series *Sakawanum*. Six nuclear microsatellite markers were used to investigate genetic structure and genetic diversity. I also measured the lengths of calyx lobes of multiple populations to quantify their geographic and taxonomic differentiation. To detect the potential impact of selective pressure, morphological differentiation values were compared with genetic differentiation (Q_{CT}-F_{ST} comparison). Average calyx lobe lengths of the longest species, *A. minamitanianum* is 124.11 mm, while that of the shortest species, *A. costatum* is 13.80 mm. Though gradually changed along geographical axis within series, calyx lobe lengths were significantly differentiated between the taxa. Genetic differentiation between taxa was low (F_{ST} = 0.099), but a significant geographic structure along the morphological cline was detected. Except for one taxon pair, pair-wise Q_{CT} values were significantly higher than neutral genetic measures of F_{ST} and G'_{ST}. Divergent selection would be concerned with forming the calyx lobe length variation in series *Sakawanum* taxa, while underlying mechanism was not clear. The low genetic differentiation with geographic structure indicated the recent divergence and/or gene flows between geographically close taxa. These neutral processes would also affect the clinal variation in the calyx lobe lengths. Overall, this study implies the roles of population history and divergent selection in shaping the current cline of a flower trait in the series *Sakawanum*.

Introduction

It has long been considered that evolutionary changes occurred by selective and neutral effects (Gould and Lewontin, 1979). Investigating the relative roles of selective and neutral process on the phenotypic traits has represented on a central issue to the understanding of evolution of local adaptation and phenotypic diversity (Bridle and Vines, 2007).

Species and/or populations showing clinal variation can be a good example in this context (Antoniazza et al., 2010). Clinal variation, the gradual variation in measurable traits along a geographic axis, is generally considered to be formed by selection linked to micro-environmental heterogeneity (Huxley, 1939, Huxley, 1938, Haldane, 1948, Salomon, 2002, Y. Takahashi, 2015, Etterson et al., 2016). Many examples of clinal variation of phenotypic traits linked to gradient environments across altitudes, latitudes, and longitudes have been reported (Watt et al., 2010, Hut et al., 2013, Y. Takahashi, 2015). Moreover, several neutral demographic processes can also generate clines (Vasemagi, 2006, Endler, 1973, Zink and Remsen, 1986). For example, spatial range expansion can form clines within a species along a geographic axis (Currat, 2012). Random genetic drift among populations with spatially limited gene exchange (isolation by distance) and genetic admixture of previously isolated populations (secondary contact) can also create clinal variations among populations and/or species (Endler, 1973, Slatkin, 1973, Barton and Hewitt, 1985, Campitelli and Stinchcombe, 2013). Thus, species showing interspecific and/or intraspecific clinal variations would be expected as a good subject to investigate the relative roles of selective and neutral processes.

The series *Sakawanum* in the genus *Asarum* (Aristolochiaceae) shows a typical cline in flower

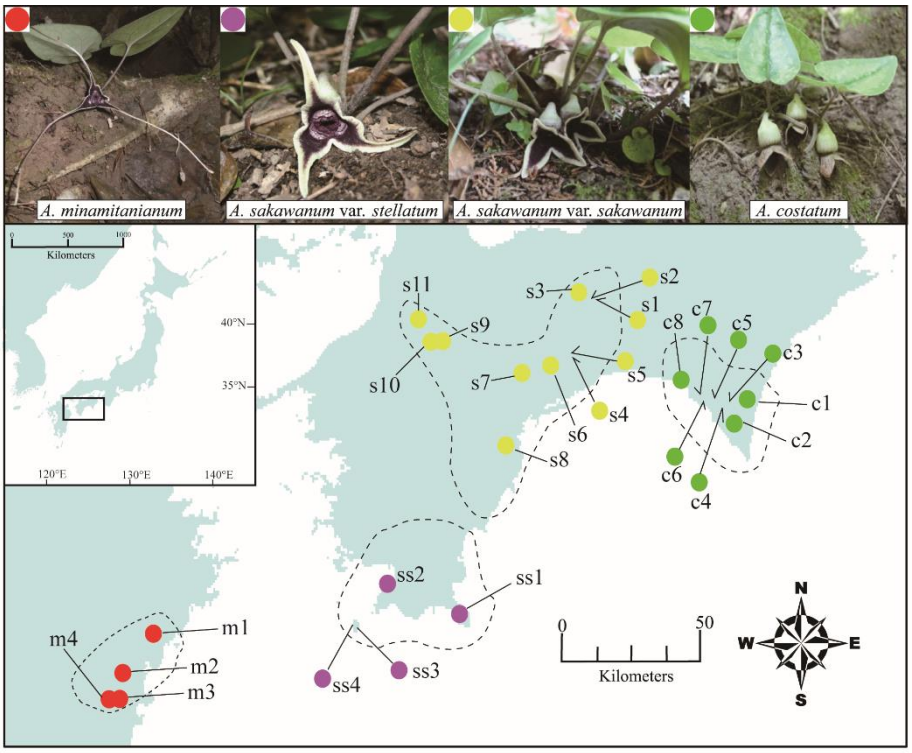

Figure 12. Photographs of *A. costatum*, *A. sakawanum* var. *sakawanum*, *A. sakawanum* var. *stellatum*, and *A. minamitanianum* and a map with sampling populations of the series *Sakawanum* in this study. Green circle, *A. costatum*; yellow circle, *A. sakawanum* var. *sakawanum*; purple circle, *A. sakawanum* var. *stellatum*; red circle, *A. minamitanianum*. The distributions of each taxon are shown by broken lines.

morphology among taxa, including three species and two varieties (*A. minamitanianum*, *A. sakawanum* var. *stellatum*, *A. sakawanum* var. *sakawanum*, and *A. costatum*). Species of the series *Sakawanum* are diploid ($2n = 24$) and have a synapomorphic character, with longitudinal ridges on the adaxial surface of the calyx tube (Sugawara, 2006); molecular phylogenetic analysis has also shown them to be a monophyletic group (Chpater 1). Within the series, the length of the calyx lobes increases gradually among the taxa inhabiting regions from east to west in southern Japan (Akasawa and Shinma, 1984, Akasawa, 1985) (Fig. 12). The calyx lobe length of the western-most species, *A. minamitanianum*, is 50–150 mm, followed by those of the central *A. sakawanum* (20–40 mm), and then by *A. costatum* (8–20 mm) at the eastern-most extent of the range (Akasawa and Shinma, 1984, Sugawara, 2006, Akasawa, 1985). The calyx lobes lengths are regarded as only one taxonomically significant characteristics that can separate all the species and varieties in the series *Sakawanum*, while form of calyx tube of *A. costatum* is tubular and forms of other taxa are depressed globose (Ohba, 2001, Sugawara, 2006, Akasawa and Shinma, 1984).

It is known that floral display (including flower size) is one of the most important aspects in attracting pollinators (Willmer, 2011). Many studies have shown that floral size is associated with efficiency of pollinator selection (Harder and Johnson, 2009), while floral size is also influenced by other biotic and/or abiotic factors (e.g. cost of reproduction, defence against other organisms, and micro environments) and the interactions of several pressures can lead to trade-offs in phenotypes (Gadgil and Bossert, 1970, Strauss and Irwin, 2004, Strauss and Whittall, 2006). Flowers of *Asarum* are pollinated by mushroom-visiting flies and/or ground-prowling insects (Mesler and Lu, 1993, Lu, 1982, Kaiser, 2006, Sugawara, 2006, Sugawara, 1988). I can consider in the series *Sakawanum*, their calyx lobes may play a role in pollinator visitation, and selective forces would be involved in their morphological differentiation.

To investigate whether selection was involved in the evolution of the length of calyx lobes in the series, I adopted a Q_{ST}-F_{ST} comparison approach. Q_{ST} is an index measuring hierarchical differentiation of a quantitative trait (Whitlock,

2008, Spitze, 1993) and F_{ST} (and related statistics) measures the extent of neutral genetic differentiation. The results of a Q_{ST}-F_{ST} comparison can be interpreted as follows: when $Q_{ST} > F_{ST}$, divergent selection would operate on the trait, and drift migration would not explain the trait variation, when $Q_{ST} < F_{ST}$, stabilising selection may affect the trait, whereas if $Q_{ST} = F_{ST}$, there is no evidence of geographic variation in natural selection (Latta, 1998, Merila and Crnokrak, 2001, Whitlock, 2008).

Additionally, to infer the evolutionary history of a species group, it would be important to define the evolutionary units (Rieseberg et al., 2006). However, in the series *Sakawanum*, whether each taxon is morphologically differentiated has remained unclear, and no extensive study on the morphometry or genetic structure of the series has been reported. Investigating the evolution of a species with clinal variation may involve taxonomic difficulties. Extensive morphological measurements and statistical analyses can contribute to the detection of evolutionary units (Sokal and Sneath, 1963, Rieseberg et al., 2006). Genetic approaches using neutral molecular markers are also effective in uncovering evolutionary units (Craft et al., 2002, Selkoe and Toonen, 2006, Caddah et al., 2012), but these may not be consistent with morphological variations influenced by non-neutral evolutionary forces.

The specific aims of this study were to (1) clarify whether the evolution of calyx lobe length in the series *Sakawanum* can be explained by neutral processes using the Q_{ST}-F_{ST} approach, (2) delineate the genetic structure of the series by molecular analyses using nuclear microsatellite (simple sequence repeat, SSR) markers, and (3) test whether the taxonomic entity is significant in terms of the calyx lobe length or whether a continuous cline is seen across the geographic range. These comprehensive analyses of the series *Sakawanum* will be an important step towards understanding the complex evolution of the morphological cline.

Material and Methods

Plant materials

For molecular analyses, I collected leaf materials from 322 individuals from 16 populations of the series *Sakawanum* (*A. minamitanianum*, 83 individuals from four populations; *A. sakawanum* var. *stellatum*, 62 individuals from three populations; *A. sakawanum* var. *sakawanum*, 89 individuals from five populations; and *A. costatum*, 88 individuals from four populations), with more than 16 individuals from each population. I also collected 433 flower materials to investigate morphological variation. In total, 94 flowers of *A. minamitanianum* (four populations), 80 flowers of *A. sakawanum* var. *stellatum* (five populations), 126 flowers of *A. sakawanum* var. *sakawanum* (nine populations), and 133 flowers of *A. costatum* (six populations) were included in these morphological measurements. In populations where both morphological measurements and genotyping were conducted, the measured individuals were also used for genotyping. For each individual, one flower was selected randomly, and measurements were taken. Leaf samplings and morphological measurements were conducted during May 2012, 2014, and 2015, when the flowers of each taxon were fully open and the calyx lobes had been extended. Details of sample locations and the number of samples are shown in Figure 12 and Table 7.

DNA extraction and genotyping

Leaf samples were dried in silica gel and subsequently pulverised to a fine powder (~20 mg) with a TissueLyser (Qiagen, Hilden, Germany) according to the manufacturer's protocol. After removal of the polysaccharides with HEPES buffer (Setoguchi and Ohba, 1995), total DNA was extracted from these powders using the cetyltrimethylammonium bromide method (Doyle and Doyle, 1987). Extracted DNA was dissolved in 150 μL of Tris-ethylenediamine tetraacetic acid buffer and used for polymerase chain reaction (PCR) analysis. The genotypes of 322 individuals were determined using six SSR markers, five of which were developed for this study, as in (Kameoka et al., 2015)), and one (Af-20) of which was adopted from the work of Matsuda and Setoguchi (Matsuda and Setoguchi, 2012). A compound SSR primer $[(AC)_6(AG)_5]$ was labelled with the fluorochrome 6-carboxyfluorescein (Applied Biosystems, Foster City, CA, USA). The primers used are listed in Supplementary Table S13. PCR was performed in a 6-μL singleplex reaction volume containing 40–60 ng of DNA, 2.5 μL of Multiplex PCR Master Mix (Qiagen), and 0.5 μM of each primer. PCR amplification for all primer pairs started with 15 min at 94°C for initial denaturation, followed by 35 cycles of denaturation at 94°C for 30 s, primer annealing at 55°C for 1.5 min, extension at 72°C for 1 min, and a final extension for 10 min at 72°C. Amplified products were loaded onto an ABI 3130

Table 7. Sample information for molecular and morphological analyses

Taxon name	Population name	No. flower samples for morphological analysis	No. leaf materials for genetic analysis	Latitude	Longitude	Mean value of calyx lobe's length (mm, ± SD)	Three months* mean temperature (°C)	Three months* precipitation (mm)
A. minamitanianum	m1	10	22	32°27'	131°34'	124.78 (± 36.47)	13.7	633
	m2	22	19	32°26'	131°34'	120.01 (± 30.52)	13.9	634
	m3	40	19	32°33'	131°36'	137.69 (± 28.36)	14.4	603
	m4	22	23	32°40'	131°44'	118.75 (± 31.74)	13.7	561
A. sakawanum var. *stellatum*	ss1	10	22	32°45'	132°32'	27.30 (± 5.18)	14.2	558
	ss2	17	-	32°44'	132°32'	35.56 (± 7.32)	14.2	558
	ss3	18	21	32°51'	132°43'	25.74 (± 6.42)	14.7	540
	ss4	24	19	32°44'	133°00'	25.60 (± 3.27)	13.6	681
A. sakawanum var. *sakawanum*	s1	20	-	33°41'	132°52'	22.65 (± 4.04)	10.8	522
	s2	16	-	33°37'	132°55'	17.97 (± 4.30)	11.8	519
	s3	11	-	33°37'	132°58'	20.38 (± 4.50)	11.6	535
	s4	16	19	33°16'	133°13'	19.33 (± 3.99)	14.4	677
	s5	11	17	33°31'	133°17'	21.48 (± 2.44)	14.3	646
	s6	-	19	33°32'	133°24'	-	14.9	670
	s7	10	-	33°34'	133°29'	22.83 (± 2.89)	13.7	652
	s8	13	17	33°34'	133°30'	17.98 (± 3.29)	14.3	669
	s9	19	-	33°46'	133°33'	21.17 (± 3.69)	12.4	554
	s10	10	-	33°45'	133°35'	18.14 (± 4.99)	12.9	560
	s11	-	17	33°46'	133°37'	-	13.1	555
A. costatum	c1	14	24	33°28'	133°56'	14.71 (± 1.82)	14.5	595
	c2	26	-	33°26	134°02'	12.78 (± 2.26)	14.4	605
	c3	-	22	33°22'	134°03'	-	14.8	614
	c4	39	-	33°25'	134°03'	14.87 (± 2.84)	13.0	629
	c5	13	-	33°22'	134°05'	14.98 (± 3.13)	14.1	624
	c6	16	-	33°25'	134°06'	11.84 (± 1.97)	13.6	622
	c7	-	19	33°15'	134°10'	-	15.4	632
	c8	25	23	33°22'	134°12'	13.35 (± 3.06)	15.3	615

* Flowering season of series *Sakawanum* species (March, April, and May)

autosequencer (Applied Biosystems) using the GeneScan ROX-350 size standard (Applied Biosystems), POP7 polymer (Applied Biosystems), and a 36-cm capillary array; fragment size was determined using GeneMapper software (Applied Biosystems). About 5% of all samples were amplified and genotyped at least twice to confirm reproducibility.

Genetic analysis

For each SSR marker, each population, and each taxon, I calculated allelic richness, private allelic richness, observed heterozygosity (H_O), expected heterozygosity (H_E), and fixation index ($F_{IS} = 1 - H_O/H_E$) using GENALEX software ver. 6.5.2; (Peakall and Smouse, 2012). Deviation from Hardy-Weinberg equilibrium was assessed using GENEPOP software (Raymond and Rousset, 1995). To check for the presence of null alleles, a maximum-likelihood estimate of the frequency of null alleles was calculated for each locus and population using the program FreeNA (Chapuis and Estoup, 2007). The coefficients of genetic differentiation within each population and each taxon were estimated in terms of F_{ST} (Weir and Cockerham, 1984) using the 'diveRsity' package (Keenan *et al.*, 2013) in R ver. 2.6.2; (R Core Team, 2013). The pattern of spatial genetic structure described as the isolation-by-distance model (Wright, 1943) was evaluated using a Mantel test

with 999 random permutations among the matrix of pair-wise population differentiation (F_{ST} / 1 – F_{ST}) and the matrix of the geographic distance using GenAlEx software. To investigate relationships among populations, I constructed a phylogenetic tree by the neighbour-joining method, based on Nei's *Da* distance using Populations software ver. 1.3.20 (Nei et al., 1983). To further assess the population structure, I used a model-based Bayesian clustering approach implemented in InStruct software (Gao et al., 2007). InStruct clusters individuals into subpopulations in cases where partial self-fertilisation or inbreeding occurs, and can estimate inbreeding coefficients simultaneously at the population level without assuming Hardy-Weinberg equilibrium within a locus. As genus *Asarum* species have self-compatibility (Wildman, 1950), I used InStruct to infer clusters of similar genotypes. To quantify the amount of variation in the likelihood for each cluster number (K), I performed a series of 15 independent runs for each value of K, ranging from 1 to 15, with a burn-in of 100,000, followed by 500,000 generations after burn-in. The log posterior probability of the data L(D) and Delta K statistics (Evanno et al., 2005, Lu, 1982) were used to determine an appropriate number for K. Graphical representations of population assignments from InStruct were produced using the program Distruct ver. 1.1 (Rosenberg, 2004).

Morphological measurements and statistical analyses

I measured the lengths of the calyx lobes of 433 flowers. Calyx lobe length was defined as the average distance from the orifice ring to three apices of calyx lobes (explained in Fig. S22) measured using digital callipers (at a resolution of 0.01 mm). To test morphological differentiation between taxa, a linear mixed-effects model (LME model) was used with a random term of intraspecific population. The LME model was used here because the data set included multiple individuals per population and multiple populations per taxon, and such nested data structures can be accommodated readily as mixed effects. To investigate whether the calyx lobe length differed between all pairs of taxa, Tukey's multiple comparison test was performed subsequently. LME models using the maximum likelihood method were fitted using the 'lme4' package (Bates *et al.*, 2015), and Tukey's multiple comparison test was applied using the 'multcomp' package (Hothorn *et al.*, 2008) in R.

Q_{CT}-F_{ST} *analysis*

To confirm the environmental uniformity of the distribution range within the series *Sakawanum*, I first conducted a statistical analysis of environmental differentiation. I used mean temperature and summed precipitation in the quarter preceding the flowering season of the series *Sakawanum* in each population (i.e. March to May) as environmental indices. Each value was extracted from the WorldClim data set (Hijmans *et al.*, 2005) and is shown in Table 7. The significance of differences in environmental indices among taxa was tested using one-way ANOVA. The degree of pair-wise taxon differentiation of calyx lobe lengths in wild populations was estimated using the modified Q_{ST} parameter. The Q_{ST} parameter is used to estimate the divergence of populations at a single spatial level (Whitlock, 2008, Spitze, 1993, Xu et al., 2010). In this study, I focused primarily on divergence between taxa, not populations, and I used the Q_{CT} parameter where populations were nested within taxa (Whitlock, 2008). Q_{CT} values were calculated as follows:

$$Q_{CT} = V_b / (V_b + V_p + 2V_w),$$

where V_b is the between-taxon variance component, V_p is the between-population (within taxon) variance component, and V_w is the within-taxon variance component. The variance components were calculated from hierarchical LME models for each taxon pair. Q_{CT} values and their confidence intervals (CI) were calculated using 200 hierarchical bootstrap samplings and the 'ape' package (Paradis et al., 2004) in R. As a comparison with Q_{CT}, a genetic differentiation measurement, both the F_{ST} value and G'_{ST} value, which are G_{ST} values standardised by expected heterozygosity, total gene diversity, and within-gene diversity, were used. This is because F_{ST} value can often underestimate differentiation, while G'_{ST} value can overestimate genetic differentiation, particularly when using high mutation rate markers (Hedrick, 2005). Pair-wise F_{ST} and G'_{ST} values with 95% CIs were calculated using the 'diveRsity' package (Keenan *et al.*, 2013) in R. I used χ^2 tests to investigate whether each Q_{CT} value was significantly different from the F_{ST} and G'_{ST} values.

Results

Molecular diversity and genetic structure

The genetic diversity parameters for SSR markers are shown in Table 8. The genetic diversity of each population (H_E) was high, ranging from 0.675 to 0.823, while the observed heterozygosity (H_O) was

Table 8. Estimation of genetic diversity in the series *Sakawanum*

Taxon name	Population	AR	PA	H_O	H_E	F_{IS}
A. minamitanianum	m1	8.833	0.667	0.365	0.814	0.549*
	m2	7.333	0.333	0.255	0.787	0.661*
	m3	8.167	0.333	0.347	0.801	0.566*
	m4	9.000	0.667	0.406	0.823	0.506*
	all	16.000	3.000	0.346	0.869	0.599*
A. sakawanum var. *stellatum*	ss1	8.500	0.500	0.442	0.792	0.426*
	ss2	9.883	0.667	0.390	0.815	0.508*
	ss3	8.000	0.333	0.355	0.761	0.525*
	all	15.000	1.833	0.396	0.828	0.505*
A. sakawanum var. *sakawanum*	s4	8.000	0.000	0.212	0.794	0.740*
	s5	6.667	0.167	0.269	0.738	0.621*
	s6	8.833	0.000	0.411	0.818	0.464*
	s8	6.667	0.333	0.424	0.778	0.459*
	s11	6.667	0.333	0.257	0.730	0.650*
	all	14.500	1.000	0.319	0.849	0.621*
A. costatum	c1	7.833	0.167	0.413	0.733	0.441*
	c3	7.333	0.500	0.417	0.681	0.390*
	c7	6.833	0.000	0.392	0.675	0.427*
	c8	7.500	0.000	0.383	0.717	0.447*
	all	12.167	0.833	0.403	0.754	0.461*

AR: allelic richness, PA: private allelic richness, H_O: observed heterozygosity, H_E: expected heterozygosity, F_{IS}: inbreeding coefficient, * significant deviation from Hardy-Weinberg equilibrium ($p < 0.01$)

relatively low, ranging from 0.212 to 0.442. Consequently, inbreeding coefficients (F_{IS}) calculated with GENALEX ranged from 0.390 to 0.661. Generally, genetic diversity was high in each taxon [H_E = 0.869 (*A. minamitanianum*) to 0.754 (*A. costatum*)]. Hardy-Weinberg equilibrium exact tests indicated that no population or locus was in equilibrium (Table S13 and Table 8). Each locus showed the presence of null alleles and the estimated frequency per locus per population ranged from 0.042 to 0.384, depending on the population (see Table S14 for more detail). The mean null allele frequency over all populations and loci was 0.186. Pair-wise F_{ST} values between populations were generally low, ranging from 0.007 to 0.156 (Table S15). Pair-wise F_{ST} values between each pair of taxa are shown in Table 9. Genetic differentiation was highest between *A. minamitaniaum* and *A. costatum* (F_{ST} = 0.096) and lowest between *A. sakawanum* var. *sakawanum* and *A. sakawanum* var. *stellatum* (F_{ST} = 0.029); global F_{ST} was also low (F_{ST} = 0.099). In the Mantel test, significant isolation by distance was detected among populations ($p < 0.0001$, R^2 = 0.234, Fig. 13). A neighbour-joining phylogenetic tree is shown in Supplementary Figure S23. In this tree, *A. costatum* and *A. minamitanianum* consisted of monophyletic clades, while *A. sakawanum* var. *sakawanum* and *A. sakawanum* var. *stellatum* were paraphyletic. Furthermore, *A. sakawanum* (including var. *stellatum* and var. *sakawanum*) was not monophyletic. The bootstrap value of each clade was low (< 60). In the clustering analysis using InStruct, L(D) increased progressively up to K = 10, at which point it started to plateau, and variance across runs was very low (Fig. 14a). Delta K peaked at K = 2, slightly higher than at K = 3 (Fig. 14b). Thus, clustering with two or three clusters was considered to most accurately reflect the genetic structure represented in the data. At K = 2, individuals of *A. minamitanianum* and *A. costatum* were assigned to different clusters (green and red; the inbreeding coefficients were 0.582 and 0.527, respectively), while individuals of *A. sakawanum* var. *sakawanum* and var. *stellatum* showed no distinct structure, with most individuals being intermediate between the two clusters. At K = 3, each cluster corresponded well with the three

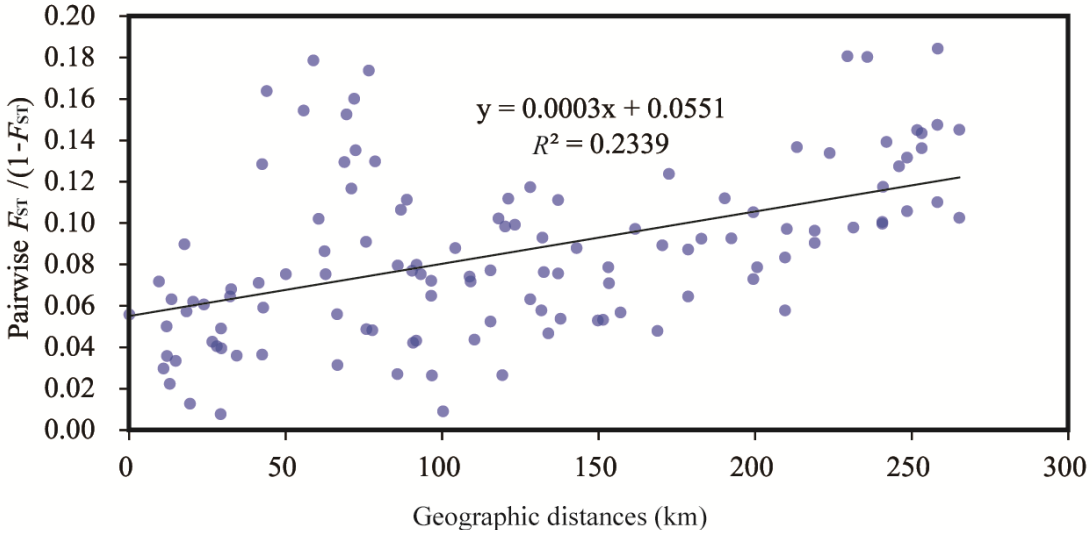

Figure 13. Correlation between geographic distance (km) and pair-wise genetic distance [F_{ST} / (1 − F_{ST})] across populations of the series *Sakawanum*.

Table 9. Pair-wise F_{ST} comparison between taxa

	A. minamitanianum	*A. sakawanum* var. *stellatum*	*A. sakawanum* var. *sakawanum*
A. sakawanum var. *stellatum*	0.058		
A. sakawanum var. *sakawanum*	0.055	0.029	
A. costatum	0.096	0.046	0.070

morphospecies (*A. minamitanianum*, *A. sakawanum*, and *A. costatum*; the inbreeding coefficients were 0.571, 0.561 and 0.519, respectively), although there was a sign of admixture of the clusters among the morphospecies. However, at $K = 4$, two varieties of *A. sakawanum* (*A. sakawanum* var. *sakawanum* and *A. sakawanum* var. *stellatum*) did not consist of single clusters.

Morphological differentiation

The calyx lobe lengths of measured individuals and population summaries are shown in Figure 15a and Table 7, respectively. The average calyx lobe lengths were 125.87 mm (standard deviation, SD = 31.12) in *A. minamitanianum*, 27.56 mm (SD = 7.09) in *A. sakawanum* var. *stellatum*, 20.15 mm (SD = 4.35) in *A. sakawanum* var. *sakawanum*, and 13.80 mm (SD = 2.86) in *A. costatum*. The LME analysis of the data showed that taxa, a fixed term, exerted a significant effect on calyx lobe length ($p < 0.01$), and subsequent Tukey's multiple comparisons supported a model with each taxon having a different length ($p < 0.05$; Fig. 15b, Table S16).

Q_{CT}-F_{ST} *comparison*

In the ANOVA analysis, no significant differentiation was detected for either environmental index among the taxa ($p > 0.05$, shown in Table S17). Pair-wise Q_{CT}, F_{ST}, and G'_{ST} values with 95% bootstrap CI are shown in Figure 16 and Supplementary Table S18. In all pairs, Q_{CT} values were significantly higher than F_{ST} values ($p < 0.05$ in χ^2 tests). Except for one G'_{ST} value between *A. sakawanum* var. *sakawanum* and *A. costatum*, Q_{CT} values were also significantly higher than G'_{ST} values ($p < 0.05$).

Discussion

Evolutionary hypothesis for calyx lobe length variation

Based on the interspecific differentiation of calyx lobe lengths and neutral genetic differentiation, I showed that strong divergent selection would have affect the calyx lobe lengths in series *Sakawanum* taxa. My analysis should be considered with caution because Q_{CT}-F_{ST} (G'_{ST}) comparisons should ideally be conducted using plants cultivated under controlled greenhouse conditions to eliminate under controlled greenhouse conditions

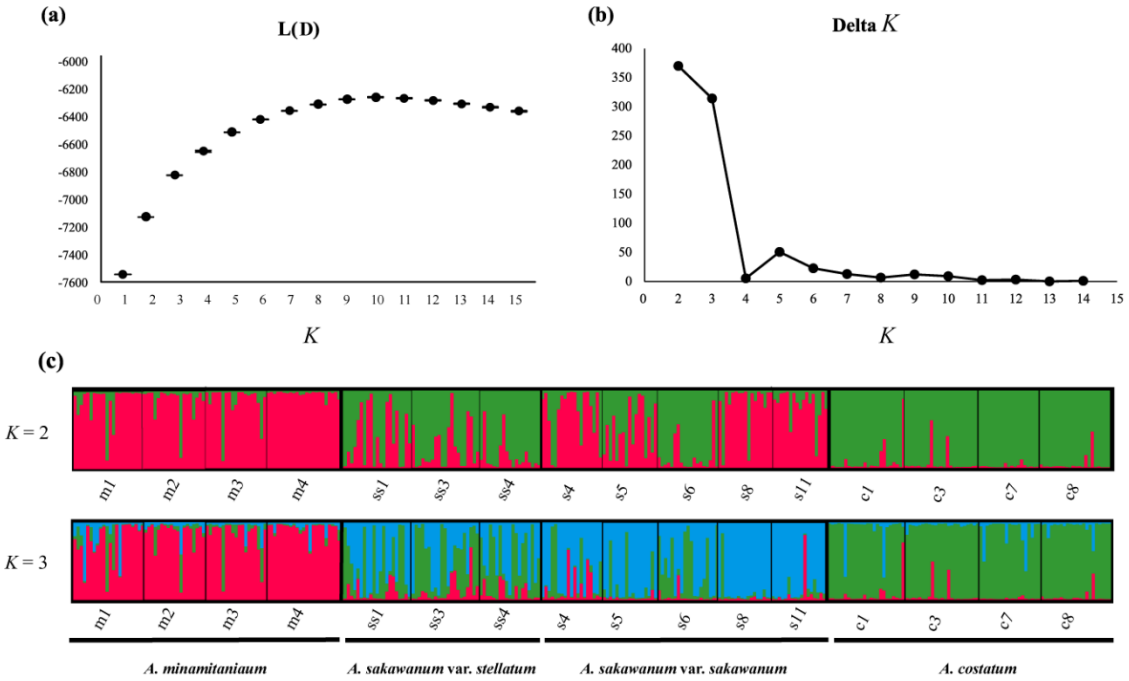

Figure 14. Clustering results for 16 populations of the series *Sakawanum* using InStruct. (a) L(D) values for each *K*. Error bars represent the standard deviation of each mean. (b) Delta *K* values for subsequent *K*s. (c) Graphical results of the most strongly supported *K* values (*K* = 2 and 3). Individuals are represented as thin vertical lines partitioned into segments, corresponding to the clusters indicated by the different colours. Population names are shown under the bar.

to eliminate any effect of the environment on traits. In my case, the measurement of a floral characteristic was performed using samples collected from natural populations, and I thus accept that my Q_{CT} estimate may be an overestimate due to environmental variance. Nevertheless, the major climatic variables for these populations only fluctuate across small ranges (Table 7), and they showed no significant differentiation among taxa (Table S17). As these species are popularly cultivated ornamental plants in Japan, the length and shape of the calyx lobes are not known to vary greatly depending on cultivation conditions (Kishi and Irizawa, 2008). Thus, I expected that although there is plasticity in series *Sakawanum* taxa caused by environmental differences, the effect would be small.

In the genus *Asarum*, no species has as long calyx lobes as *A. minamitanianum*. Assuming that ancestral state of calyx lobe length in the series *Sakawanum* would have been shorter than that of *A. minamitanianum*, it is plausible that a morphological change to longer calyx lobes would have occurred within the series *Sakawanum*. Some plants have significantly extended sepals, petals, or appendages (e.g. Dracula lafleurii, Corybas iridescens: Orchidaceae; Tolmiea megarrhina: Saxifragaceae; Fuller, 1994, Goldblatt et al., 2004, Endara et al., 2010, Policha et al., 2016). Considering these flowers and divergent selection is detected in calyx lobe lengths in series *Sakawanum*, these extended flower organs would have some important roles (e.g. visual attraction, landing foothold for pollinators, and emitting olfactory attractants), as are suggested for the other flowers with elongated organs. I could hypothesize that the variation of calyx lobes in series *Sakawanum* is concerned with pollinator attractions, while other biotic and abiotic factors may have affected the calyx lobe length. Based on the current data, I cannot conclude that pollinators are responsible for the variation of calyx lobe length in series *Sakawanum*. Pollination research and identification of chemicals included in floral scents for the series *Sakawanum* would be important to investigate the role and evolution of calyx lobe length in the series *Sakawanum*, and in addition, manipulation experiments (e.g. cutting the calyx lobes or using artificial flowers) could be performed to confirm this.

Population genetic variation in* Asarum *populations

An interesting characteristic of the genetic

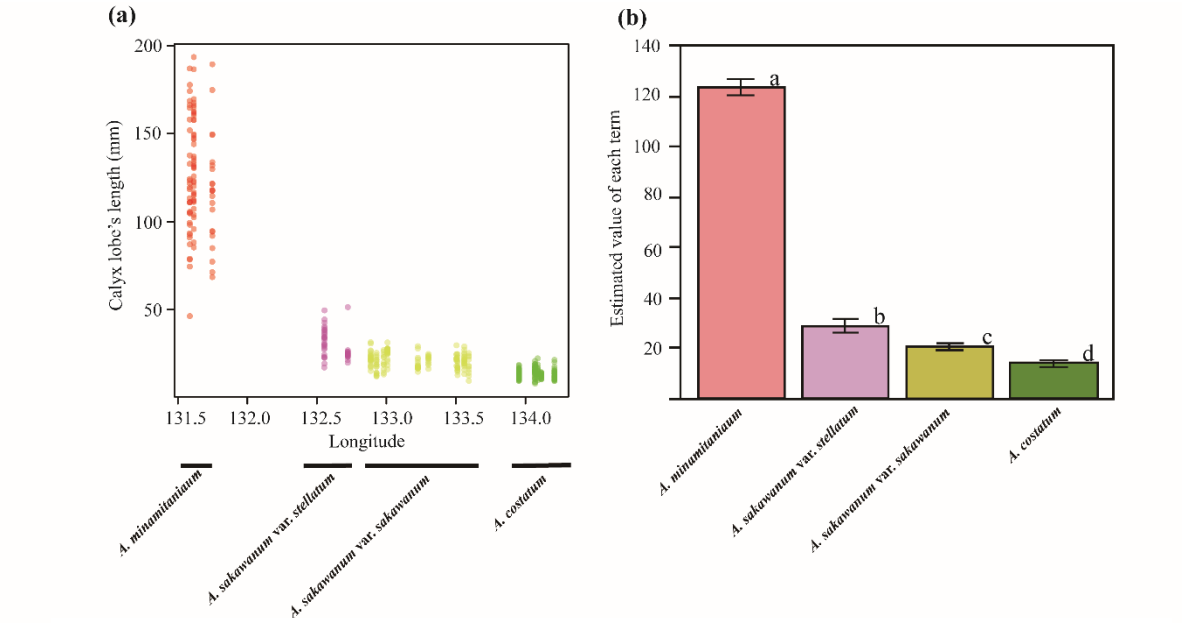

Figure 15. (a) Plot of calyx lobe length of individuals against longitude. (b) Bar plots of lmer-estimate value (± standard error) of each fixed effect term for calyx lobe length in the linear mixed effects model. Colours indicate taxa (see Fig. 12), and different lowercase letters indicate a significant difference ($p < 0.05$), based on Tukey's multiple comparison tests.

variation in *Asarum* populations was the remarkably high genetic diversity (species mean, $H_E = 0.825$) and the high inbreeding coefficients (species mean, $F_{IS} = 0.547$). The significantly high F_{IS} within populations may be attributable to the presence of null alleles, inbreeding, and a small effective size. In each locus, the presence of null alleles was shown (mean value of locus = 0.186). Null alleles are relatively common in genomic microsatellite markers and are considered to be one reason for high F_{IS} values (Dakin and Avise, 2004). Although automatic self-pollination does not occur in series *Sakawanum* species, *Asarum* species have self-compatibility. This would be one reason for high F_{IS} values in the series *Sakawanum*. In *Asarum* species, pollinators, including fungus gnats and ground-prowling insects, were observed visiting flowers at low frequencies (Wildman, 1950, Mesler and Lu, 1993, Lu, 1982, Sugawara, 1988). Seeds of *Asarum* species are dispersed by ants (Gorb and Gorb, 1995), and the dispersal ability of *Asarum* seeds has been estimated as 10–50 cm per year (Maekawa, 1953a, Hiura, 1978). These inefficient pollinators and the low seed dispersal ability can result in the formation of reproductively isolated units within a population (Hamrick et al., 1993, Gevaert et al., 2013, Sant'Anna et al., 2013). The substructuring of populations causes a reduction in heterozygosity in a population because of treating multiple subpopulations as a single large population (known as the Wahland effects; Wahlund, 1928). Accordingly, the deficiency in heterozygotes in the series *Sakawanum* in my study would be shaped by a combination of the presence of null alleles, inbreeding, and/or the Wahlund effect. Further research on the mating system and seed dispersal in *Asarum* species is needed to determine the

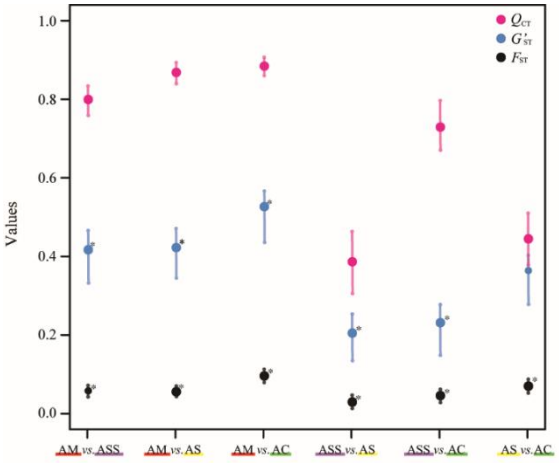

Figure 16. Pair-wise Q_{CT}, G'_{ST}, and F_{ST} values for each taxon pair. Each bar shows the 95% confidence interval. The abbreviations indicate taxon names (AM, *A. minamitanianum*; ASS, *A. sakawanum* var. *stellatum*; AS, *A. sakawanum* var. *sakawanum*; AC, *A. costatum*). *, significantly ($p < 0.05$) different from the Q_{CT} value by χ^2 test.

precise mechanism by which high genetic variation is maintained despite the deficiency in heterozygotes.

Implications for evolutionary history and the establishment of clinal variation

My morphological and genetic analyses showed that all species (*A. costatum*, *A. sakawanum*, and *A. minamitanianum*) in the series *Sakawanum* had differentiated significantly from one another. However, genetic differentiation levels were generally low (global F_{ST} = 0.099). A sign of admixture of the clusters among the morphospecies was detected by the clustering analysis, though basically each cluster was corresponded with the morphpspecies. There are two possible explanations for this low genetic divergence and genetic structure: recent species divergence and gene flow (Petit and Excoffier, 2009). Recent species divergence shows low genetic differentiation due to shared ancestral polymorphism and alleles not fixing within a population and/or a species (Pillon et al., 2013, Krak et al., 2013, Muir and Schlotterer, 2005, Linder and Rieseberg, 2004). In Japan, *Asarum* species seem to have diversified allopatrically in the Quaternary due to geographic fragmentation caused by climatic changes (Chpater 1). *Asarum* species take more than 7 years from sowing to first flowering and can live more than 20 years in wild populations (Kume, 1993, Kume, 1989). The recent origin and long lifetimes of Japanese *Asarum* species (Maekawa, 1933) suggest that each taxon in the series *Sakawanum* could have been formed in a recent timeframe, which would have resulted in low genetic differentiation, as estimated in this study.

Considering the isolation by distance within the series, interspecific gene flow was also plausible. It is known that clinal variations can involve neutral processes (Endler, 1973, Slatkin, 1973, Vasemagi, 2006, Antoniazza et al., 2010, Campitelli and Stinchcombe, 2013), and the distribution range and morphology of *A. sakawanum* are intermediate between the other two species, I can speculate that the interspecific gene flow would have contributed to forming the clinal variation of series *Sakawanum*. However, based on the genetic data currently available, it is difficult to draw definitive conclusion on whether recent species diversification or gene flow between taxa occurred in this series. In future studies, I need to test alternative population models that consider ancient gene flow, a recent population split, and population admixture using more informative data sets (e.g. SNPs) subjected to statistical population analyses (e.g. Bayesian inference, approximately Bayesian competition; Beaumont et al., 2002, Hey, 2010).

Appendix

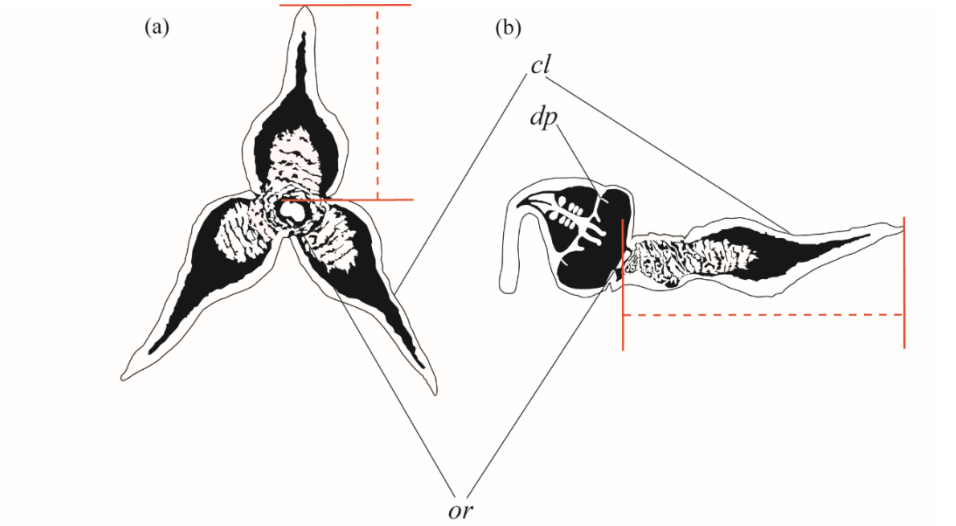

Figure S22. Morphological characteristics measured in flowers of the series Sakawanum [front view (a) and cross-sectional view (b)]. The broken lines indicate measured length of the calyx lobe. Abbreviations: cl = calyx lobe, or = orifice ring, dp = degeneration petal. on EST-SSR dataset. by a closed orange circle.

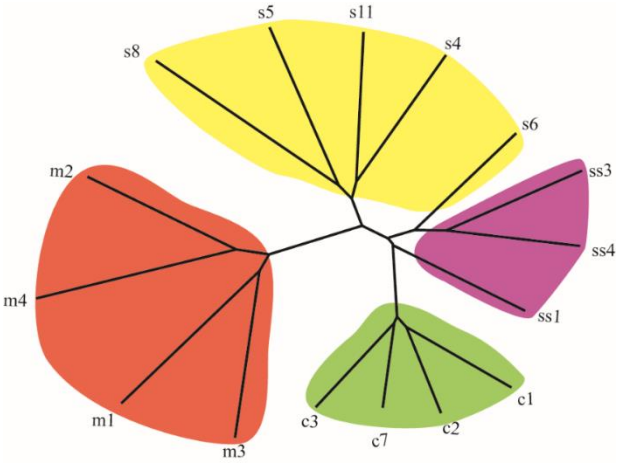

Figure S23. Neighbour-joining population phylogenetic tree of the series *Sakawanum* (*A. minamitanianum*; red, *A. sakawanum* var. *stellatum*; purple, *A. sakawanum* var. *sakawanum*; yellow, and *A. costatum*; green).

Table S13. Characteristics of six SSR markers analysed in this study

Name	Accession no.	Primer	Size range (bp)	AR	H_O	H_E	F_{IS}
Ac-11	LC101436	GGTTTGTATGATGTGGGTTC	162-197	5.875	0.418	0.731	0.423*
Af-2	LC101437	ATCTTCCTCACACCATAAACTA	111-147	6.125	0.436	0.668	0.328*
Ac-2	AB687536**	TTTACACGCACATAAAGCAC	143-197	7.750	0.219	0.809	0.729*
Ac-4	LC101438	TCATCTCCTTCCTTCTTGTC	234-280	9.875	0.364	0.838	0.570*
Ac-18	LC101439	GATGTAAAAGGGGACCTGA	78-134	10.438	0.435	0.856	0.490*
Ac-22	LC101440	GCGGGTTAAAGTTGTTAGAA	112-152	7.188	0.290	0.695	0.604*

AR; Allelic richness, H_O; Observed heterozygosity, H_E; Expected heterozygosity, F_{IS}; Inbreeding coefficient, *; Significant deviation from Hardy-Weinberg equilibrium ($p < 0.01$), **; from Matsuda and Setoguchi 2012

Table S14. Frequencies of null alleles per population per loci estimated by freeNA.

	Locus name					
Population name	Ac-11	Af-2	Ac-2	Ac-4	Ac-18	Ac-22
m1	0.121	0.186	0.314	0.301	0.211	0.141
m2	0.211	0.340	0.159	0.200	0.093	0.199
m3	0.212	0.165	0.323	0.105	0.252	0.243
m4	0.066	0.331	0.282	0.237	0.217	0.227
ss1	0.129	0.000	0.136	0.297	0.216	0.114
ss3	0.176	0.110	0.151	0.158	0.259	0.202
ss4	0.136	0.097	0.258	0.220	0.265	0.166
s4	0.236	0.102	0.053	0.193	0.176	0.213
s5	0.190	0.084	0.168	0.280	0.096	0.176
s6	0.384	0.251	0.202	0.210	0.264	0.242
s8	0.134	0.156	0.154	0.343	0.255	0.234
s11	0.218	0.178	0.261	0.341	0.033	0.114
c1	0.194	0.118	0.115	0.104	0.227	0.230
c3	0.130	0.042	0.137	0.223	0.137	0.188
c7	0.216	0.059	0.235	0.161	0.127	0.107
c8	0.137	0.030	0.308	0.159	0.132	0.221
mean	0.181	0.141	0.203	0.221	0.185	0.189

Table S15. Pairwise F_{ST} values among populations

	A. minamitanianum				*A. sakawanum* var. *stellatum*			*A. sakawanum* var. *sakawanum*					*A. costatum*		
	m1	m2	m3	m4	ss1	ss3	ss4	s4	s5	s6	s8	s11	c1	c3	c7
m2	0.0529														
m3	0.0477	0.0345													
m4	0.0468	0.0379	0.0542												
ss1	0.0672	0.0609	0.0715	0.0834											
ss3	0.0716	0.0498	0.0690	0.0701	0.0125										
ss4	0.1000	0.0703	0.0850	0.0927	0.0351	0.0076									
s4	0.0607	0.0802	0.0819	0.0730	0.0263	0.0530	0.0701								
s5	0.0953	0.0680	0.1007	0.1101	0.0418	0.0414	0.0405	0.0389							
s6	0.0770	0.0546	0.0729	0.0846	0.0258	0.0089	0.0257	0.0347	0.0288						
s8	0.0879	0.0830	0.0886	0.0848	0.0595	0.0669	0.0808	0.0558	0.0584	0.0669					
s11	0.0914	0.0906	0.0891	0.1203	0.0506	0.0709	0.1050	0.0305	0.0664	0.0607	0.0572				
c1	0.1164	0.0957	0.1052	0.1180	0.0662	0.0446	0.0896	0.1045	0.0926	0.0700	0.1138	0.1407			
c3	0.1267	0.0930	0.0992	0.1222	0.0457	0.0503	0.0547	0.0740	0.0736	0.0464	0.1146	0.1323	0.0410		
c7	0.1556	0.1285	0.1266	0.1528	0.0886	0.0808	0.0902	0.1002	0.0962	0.0460	0.1380	0.1480	0.0637	0.0218	
c8	0.1254	0.1199	0.1131	0.1530	0.0538	0.0511	0.1006	0.1149	0.1191	0.0796	0.1337	0.1515	0.0323	0.0595	0.0824

Table S16. The results of Tukey's multiple comparison test for estimated values of each taxon from LME model.

Linear Hypotheses	Estimate value (± SE)	z value
A. minamitanianum - *A. sakawanum* var. *stellatum* = 0	94.84 (± 4.311)	21.998***
A. minamitanianum - *A. sakawanum var. sakawanum* = 0	103.245 (± 3.644)	28.332***
A. minamitanianum - *A. costatum* = 0	109.616 (±3.594)	30.5***
A. sakawanum var. *stellatum* - *A. sakawanum* var. *sakawanum* = 0	8.405 (± 3.121)	2.693*
A. sakawanum var. *stellatum* - *A. costatum* = 0	14.776 (±3.063)	4.825***
A. sakawanum var. *sakawanum* - *A. costatum* = 0	6.371 (±2.018)	3.157**

*, $p < 0.05$; **, $p < 0.01$; ***, $p < 0.001$

Table S17. The results of ANOVA for two environmental indices.

Index	Sum Sq	Mean Sq	*F* value	*p* value
Three months mean temperature	860.7	286.9	2.804	0.062
Three months precipitation	3550.0	1183.4	0.452	0.718

Table S18. Q_{CT}, F_{ST} and G'_{ST} values with 95% CI between each taxon pair.

Taxon pairs	F_{ST} (95% CI)	G'_{ST} (95% CI)	Q_{CT} (95% CI)
A. minamitanianum vs. A. sakawanum var. *stellatum*	0.0577 (0.0456, 0.0707)	0.4166 (0.3331, 0.4661)	0.7990 (0.7581, 0.8328)
A. minamitanianum vs. A. sakawanum var. *sakawanum*	0.0553 (0.0443, 0.0684)	0.4220 (0.3434, 0.4691)	0.8681 (0.8393, 0.8931)
A. minamitanianum vs. A. costatum	0.0957 (0.0807, 0.1119)	0.5263 (0.4361, 0.5659)	0.8840 (0.8602, 0.9067)
A. sakawanum var. *stellatum* vs. *A. sakawanum* var. *sakawanum*	0.0293 (0.0188, 0.0415)	0.2047 (0.1339, 0.2528)	0.3862 (0.3055, 0.4634)
A. sakawanum var. *stellatum* vs. *A. costatum*	0.0456 (0.3018, 0.0605)	0.2311 (0.1493, 0.2764)	0.7289 (0.6700, 0.7957)
A. sakawanum var. *sakawanum* vs. *A. costatum*	0.0697 (0.0559, 0.0843)	0.3637 (0.2778, 0.4025)	0.4445 (0.3787, 0.5102)

Chapter 5

Comparative reproductive ecology of two sister *Asarum* species (Aristolochiaceae) in relation to the evolution of elongated floral appendage

abstract

Attractive floral structures (e.g. elongated filiform appendages) are expected to bring the fitness advantages that accrue from cross-pollination considering their energetic and ecological costs. However, this assumption has rarely been tested by using closely related species. I investigated the reproductive ecology of sister perennial herbs in genus *Asarum* (Aristolochiaceae); *Asarum costatum* has a short calyx lobe (17.3 mm), which would be ancestral, whereas *A. minamitanianum* has a remarkably elongated one (109.3 mm). I adopted combined approaches, including field observations, molecular analyses, and cultivation experiments such as fine-scale spatial genetic analysis, three-year pollinator observation, paternity analysis over four years, and crossing experiments. Pollinator observations showed the visitation rate of flies was more than three times higher in *A. minamitanianum*. Paternity analysis revealed *A. minamitanianum* conducted predominantly outcrossing, while *A. costatum* showed a wide range of selfing rates among fruits. Further, both species showed strong fine-scale spatial genetic structures implying confined seed dispersal, and showed self-compatibility, probably with late-stage inbreeding depression. These characters suggested that crossing with more distant and unrelated individuals by attracting flies would be advantageous. Overall, this study demonstrated the elongated floral appendage could have evolved for effective pollen dispersal by attracting flies, which can compensate for the costs.

Introduction

Plants exhibit a remarkable diversity in floral traits, and revealing mechanisms generating floral diversity is a major goal of plant evolutionary ecology (Ghazoul, 2006). Floral diversity has been largely interpreted as the historical outcome of pollinator-mediated selection since the age of Darwin (Harder & Johnson, 2009). The floral traits are considered to be associated with multiple aspects of reproductive ecology, such as mating systems, pollination efficiency, and pollen dispersal distances (Stebbins, 1970; Galen & Stanton, 1989; Hansen *et al.*, 2007; Sapir & Armbruster, 2010; Anton *et al.*, 2013). These reproductive characters could change in a related manner (Waser, 1983), and would jointly influence plant fitness (Gaudeul & Till-Bottraud, 2004). Theoretical studies have shown that pollinator-mediated selection should produce floral morphology, which consequently changes the ecological and reproductive characters (Morgan, 1992). However, although there have been studies reporting relationships between pollinators and floral traits (Fenster *et al.*, 2004), relatively limited studies have investigated how floral traits change the reproductive ecology of plants from evolutionary aspects, especially by using closely related species (but see Chen, 2009; Zhang *et al.*, 2011). Thus, our understanding of the evolutionary consequences of floral trait changes remains incomplete (Fenster & Marten-Rodriguez, 2007).

Flowers with elongated filiform appendages or bracts with dark colours are observed in many plant families (e.g., Annonaceae, Aristolochiaceae, Asparagaceae, Dioscoreaceae, Orchidaceae, and Saxifragaceae), and their curious appearances have attracted the interest of biologists (Proctor *et al.*, 1996). Plants with these appendages or bracts can be often seen in shady and moist forest understorey (Endara *et al.*, 2010; Lim & Raguso, 2017), and

these floral characters are frequently observed with pod-like floral structures hiding sexual organs, motile hairs, decaying odour, and absence of nectar; these characters have been hypothesised to be the syndrome of fly pollination (Faegri & Van Der Pijl, 2013). Empirical studies have reported that flowers with elongated filiform appendages or bracts are often pollinated by Diptera species (Endara *et al.*, 2010; Lim & Raguso, 2017; Guo *et al.*, 2019). Elongated filiform appendages are considered to be associated with the visual attraction of pollinators by increasing the display size and acting as their landing platforms (Policha *et al.*, 2016; Katsuhara *et al.*, 2017). In general, floral size is positively associated with the outcrossing rate (Harder & Barrett, 1995), and investment in attractive structures represents an allocation cost that plants pay to secure the fitness advantages that accrue from cross-pollination (Goodwillie *et al.*, 2010). These considerations lead to the expectation that elongated filiform appendages bring some fitness advantages by attracting pollinators, including Diptera species, which could drive the evolution of elongated floral appendages.

Here, I focused on two closely related perennial herb species from the genus *Asarum* (Aristolochiaceae), *A. costatum* and *A. minamitanianum* (Fig. 17a). Both species grow in shady evergreen forest understorey, and have flowers inconspicuously on the ground. Although there are no significant differences in vegetative traits, two species show a considerable difference in calyx lobe lengths (Maekawa, 1933); *Asarum costatum* has a short calyx lobe (10–20 mm), which is considered to be ancestral, whereas *A. minamitanianum* has a remarkably elongated calyx lobe (70–180 mm) (Chapter 4). The sepals of the two species connect beyond attachment to the ovary and form a calyx tube with calyx lobes. Previous studies implied that the genetic differentiation between the two species was relatively low (F_{ST} = 0.087 in EST-SSR data; Takahashi, Teramine, Sakaguchi, & Setoguchi, 2019) and Q_{CT} - F_{CT} comparison analysis, which can test whether selection is involved in the evolution of quantitative traits (Whitlock, 2008), showed that divergent selection was related to their calyx lobe length differentiation (Chapter 4). Thus, these two species would be ideal candidates for conducting sister-species comparison in order to obtain evolutionary insights into floral organ elongations in relation to reproductive ecology. In *Asarum*, Diptera species were observed on the flowers of several species (e.g., fungus gnats and Drosophilidae flies in *A. tamaense* [Kakishima & Okuyama, 2020; Sugawara, 1988], and Calliphoridae flies in *A. fudsinoi* [Maeda, 2013]), while only ground-dwelling insects (e.g. amphipods and springtails) were observed in other species (A. takaoi; Okamoto & Kanoh, 1977). In *A. asperum*, a related species with flowers similar to *A. costatum*, ground-dwelling insects were observed on its flowers (Okamoto & Kanoh, 1977). Kakishima and Okuyama (2018) observed diverse ground-dwelling insects (ants, isopods, myriapods, among others) on the calyx lobes of *A. costatum* and *A. minamitanianum*. However, since whether these visitors entered the calyx tubes was not confirmed and their observations were conducted in the short term, the pollinator fauna of the two species remain unknown. Moreover, most aspects of the reproductive ecology of the two species, including mating systems, fruiting rates, seed dispersal distance, and seedling establishment, have not yet been clarified.

The primary objectives of this study were to obtain evolutionary insights into the floral organ elongation, and reveal how evolutionary changes in floral traits have influenced the reproductive ecology of the two species. To test the evolutionary hypothesis, I tested whether species differences can be observed in a series of reproductive characters (pollinator visitation rates, pollen dispersal distances, mating systems [selfing rates], fruiting rates, and seedling establishments), which directly or indirectly affect plant fitness (Bertin, 1988). To investigate these reproductive characters, studies should ideally observe the behaviours of pollinators within the flowers, track their movements, measure the dispersal distance of seeds, and track the fate of produced seeds. However, due to the pod-like floral structures, extremely low frequency of pollinator visitation, and long life cycles of *Asarum*, it is challenging to directly observe these events. To overcome this difficulty, I adopted combined approaches, including field observations, molecular analyses, and crossing experiments. Firstly, I estimated the fine-scale genetic structures (SGS) of the two species. This method is advantageous for estimating the historical movements of pollen and seeds, especially for plants with long life-span (Vekemans & Hardy, 2004). In addition, I observed floral visitors over three years and conducted paternity inference of seeds using microsatellite markers over four years, which allowed us to infer effective pollinators and to estimate the movement

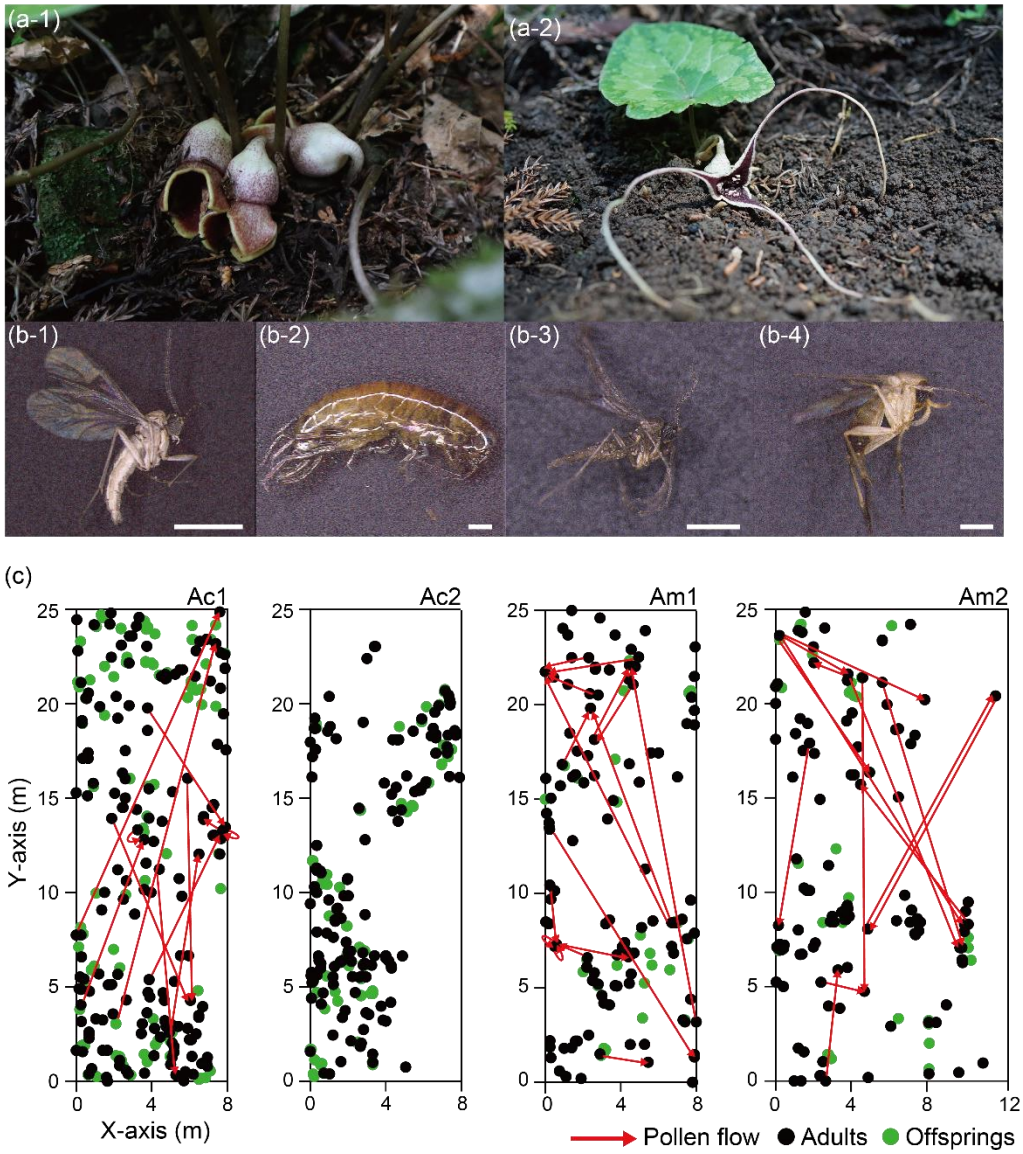

Figure 17. (a) Photographs of *Asarum costatum* (a-1) and *A. minamitanianum* (a-2). (b) Collected floral visitors; Sciaridae sp. (b-1) and amphipod (b-2) which visited *A. costatum* flowers and Sciaridae sp. (b-3) and Chironomidae sp. (b-4) which visited *A. minamitanianum* flowers. (c) The spatial distributions and estimated pollen flow of *A. costatum* (Ac1 and Ac2), and *A. minamitanianum* (Am1 and Am2) within the four plots. The colours of circles represent different cohorts (adults, black and offspring, green) and red arrows represent pollen flow (excluding selfing) estimated from paternity analysis of the four years. In Ac2 plot, there was no pollen flow detected within the plot.

of pollen (Yamagishi *et al.*, 2007; Buehler *et al.*, 2012). I also calculated genetic diversity and fixation coefficients at each life stage (seedlings, juveniles, and reproductive), which can be used to estimate the degrees and stages of inbreeding depressions (Tamaki *et al.*, 2009). Lastly, I conducted crossing experiments to check the self-compatibility of the two species. Through these combined approaches, I will discuss the evolutionary drivers of the remarkably elongated calyx lobe in *A. minamitanianum*, and the ecological consequences of the floral trait changes.

Materials and Methods

Study species

Asarum costatum and *A. minamitanianum* are diploid, low-growing perennials, and distributed in shady forest understory of western parts of Kyushu and Shikoku islands in Japan, respectively (Chapter 4) Both species form a clump and do not

-

Table 10. Parameters of genetic diversity and spatial genetic structure across 13 microsatellite loci for adult and offspring cohorts of *Asarum costatum* and *A. minamitanianum* in four plots.

Species	Plot	Cohort	N	*NA*	H_O	H_E	F_{IS}	*b*	*Sp*
Asarum costatum	Ac1	Adults	167	9.8	0.532	0.654	0.178	-0.0150*	0.0159
		Offspring	102	9.2	0.522	0.645	0.162	-0.0220*	0.0241
	Ac2	Adults	140	11.2	0.570	0.680	0.155	-0.0211*	0.0232
		Offspring	73	9.0	0.566	0.671	0.163	-0.0349*	0.0396
Asarum minamitanianum	Am1	Adults	114	10.5	0.605	0.739	0.174	-0.0131*	0.0140
		Offspring	34	8.3	0.534	0.690	0.194	-0.0238*	0.0273
	Am2	Adults	118	11.5	0.548	0.731	0.233	-0.0218*	0.0237
		Offspring	47	8.7	0.527	0.728	0.255	-0.0178*	0.0195

N, number of individuals; *NA*, number of alleles; H_O, observed heterozygosity; H_E, expected heterozygosity; F_{IS}, fixation index; *b*, lope of the regression of pairwise kinship coefficients on the logarithm of geographical distance; *Sp*, extent of spatial genetic structure. *, $p < 0.01$

reproduce clonally with stolons. Usually, one pod-like flower (occasionally, 2-5 flowers) per year is produced in April and May. *Asarum costatum* has flowers downward, and its calyx lobes are often buried underground, while the flowers of *A. minamitanianum* bloom horizontally and are rarely buried. The flowers lack nectar and show partial protogyny; stigmas become receptive one or two days before dehiscence of anthers, but in large part (about two weeks), both stages overlap (Takahashi et al., personal observations). The fruit matures in July and contains one to 30 myrmecochorous seeds with elaiosomes, which germinate in next April. Both species can take more than six years for first flowering and live more than 30 years in the wild based on the number of nodes of rhizomes (Takahashi et al., personal observation).

Study sites

I selected two populations for each species and selected one plot per population. For *A. costatum*, plot 1 (Ac1 8 × 25 m) was located in Hane-cho, Muroto city, (33.41°N, 134.11°E), and plot 2 (Ac2, 8 × 25 m) was located in Kitagawa village, Aki-gun, Kochi prefecture, Japan (33.44°N, 134.04°E). *Asarum minamitanianum*, plot 3 (Am1, 8 × 25 m in area) was located in Nakamiwa-cho (32.54°N, 131.59°E), and plot 4 (Am2, 12 × 25 m) in Kamiigata-cho, Nobeoka City, Miyazaki Prefecture, Japan (32.52°N, 131.62°E). These four plots were the natural habitats of the two species and topographically flat in the understorey of evergreen forests. All individuals within the plots were mapped, and their leaf tissues were collected in 2016. The sampled materials were used for SGS analysis and paternity analysis. I classified the collected individuals into two categories; "offspring", which included seedlings, 1–3 years old, and "adults", which included all other individuals. Discrimination between the two categories was based on the size and number of leaves; individuals with only one leaf less than 5 cm in length were classified as offspring. In total, I collected 795 individuals from the four plots (Fig. 17c). Within 795 individuals, 256 individuals were categorised as offspring, and the proportions of current-year seedlings were low (none in Ac1, one individual in Ac2, six in Am1, and 12 in Am2; data not shown).

For all four plots, I recorded flowering and fruiting individuals every year from 2016 to 2019. I calculated the flowering rate and the fruiting rate, which are defined as the number of flowering individuals divided by the number of individuals within the plot and as the number of fruiting individuals divided by the number of flowering individuals, respectively. All fruits within the plots were sampled in July, and the collected seeds were sown in a greenhouse at Kyoto University (35.0°N, 135.7°E). I collected all seedlings that germinated until the next July. The seedlings were dried in silica gel and used for paternity analysis. For observation of floral visitors and morphological measurements, I used individuals more than 15 m apart from the plots.

Morphological measurements

To quantitatively measure the differences in floral traits, I measured six characters of the two species: calyx lobe length, calyx tube width, calyx tube height, floral entrance diameter, and distance between stigma and anthers (Fig. S24). These five traits are related to the attraction or limitation of pollinators and to mating systems. The

measurements were undertaken using digital callipers. For each population, more than 20 flowers were randomly collected in 2018.

To estimate the interspecific differentiation of each floral trait, I built linear mixed models (LMM) using the lmerTest package (Kuznetsova *et al.*, 2017) in R v3.5.4 (R Core Team, 2013). Within the models, species was treated as the explanatory variable and populations were treated as the random effect. I calculated AIC scores of the models and null models, and the significance of the species term in the full model was tested with a t-test.

Molecular experiments

Total DNA was extracted following the procedure described by Takahashi et al. (2019). For SGS analysis, I used 13 expressed sequence tag-simple sequence repeat (EST-SSR) markers (Takahashi *et al.*, 2017) with tagged sequences. For paternity analysis, I used nine EST-SSR markers whose forward primers were labelled individually with each of four fluorescent dyes (JOE, CY3.5, FAM, or CY3) to reduce genotyping uncertainty in multiplexed polymerase chain reaction (PCR). Primer information is shown in Table S19. PCR was performed in a 10-μL multiplex reaction mix containing 10–20 ng of DNA and 3 μL of Multiplex PCR Master Mix (Qiagen, Hilden, Germany). For SGS analysis, 0.01 μM of forward primer, 0.2 μM of reverse primer, and 0.1 μM of fluorescently labelled M13 primer were used. For paternity analysis, 0.1 μM of forward and reverse primers were added. PCR amplification with all primer pairs began with initial denaturation for 30 min at 95 °C for, followed by 35 cycles of denaturation at 95 °C for 30 s, primer annealing at 60 °C for 3 min, extension at 68 °C for 1 min, and a final extension for 20 min at 68 °C. The amplified products were loaded onto an ABI 3130 autosequencer (Applied Biosystems, Foster City, CA, USA) using the GeneScan LIZ-600 size standard (Applied Biosystems), POP7 polymer (Applied Biosystems), and a 36-cm capillary array, and fragment size was determined using GeneMapper software (Applied Biosystems).

Spatial genetic structure

I first calculated the number of alleles (*NA*), observed heterozygosity (H_O), expected heterozygosity (H_E), and inbreeding coefficient ($F_{IS} = 1 - H_O / H_E$) using GenAlEx v6.503 (Peakall & Smouse, 2012) for each cohort within the plots. Deviation from Hardy–Weinberg equilibrium was assessed using GENEPOP v1.2 (Raymond & Rousset, 1995). To estimate SGS, I undertook spatial autocorrelation analysis using SPAGeDi v1.5a (Hardy & Vekemans, 2002). I calculated pairwise kinship coefficient (F_{ij}) between individuals, which indicates the extent of genetic similarity between individuals *i* and *j* relative to the mean genetic similarity between random individuals in the samples (Loiselle *et al.*, 1995). I divided individual pairs into six distance classes (1, 2.5, 5, 10, 15, and 25 m). F_{ij} values were averaged over each distance class (*d*), to estimate $F(d)$. Standard errors of $F(d)$ were estimated using a Jack-knife procedure over the loci. For graphical representation of SGS, I plotted the $F(d)$ values against the maximum distance of the class. I also estimated the regression slopes (b) of the estimated F_{ij} on the natural logarithm of individual distances for all pairs of individuals. I tested the significance of the kinship coefficients and the regression slopes by comparing the observed values with those obtained after 2000 random permutations of the individuals among positions. The extent of genetic structure was evaluated using the *Sp* statistics defined by Vekemans & Hardy (2004). The *Sp* values were computed using the formula $-b / (1 - F_1)$, where F_1 is the mean kinship coefficient for the shortest distance class.

Paternity analysis

For paternity analysis, I used 10 randomly chosen germinated seeds per fruit, or all seeds, when less than 10 seeds germinated from one fruit. I calculated the indices of genetic diversity (*NA*, H_O, H_E, and F_{IS}) of seeds and flowering individuals in each plot and year. Paternity analysis of known maternal broods was performed using a maximum likelihood framework implemented in CERVUS v3.0 (Kalinowski *et al.*, 2007). The confidence interval was calculated for each population by running 20000 simulations with the following parameters: 0.70 as the sampled proportion of candidate parents, 0.001 as the mistyped rate, 7 as the minimum typed locus, and 0.30 as the proportion of selfing individuals. I reported fathers assigned with 95% confidence. In addition, assignments below 95% confidence, but not mismatching at any loci, were included as likely assignments. I calculated selfing rates and pollen transfer distances using the results of the paternity analysis. Pollen transfer distances were calculated as the Euclidean distance between the mother and most likely father. Considering the low visitation frequency of insects and floral structures of the two

Table 11. The summary of flowering, fruiting, and the number of seeds in each year of four plots.

Species	Plot	Year	Number of flowering individuals	Flowering rate†	Number of fruiting individuals	Fruiting rate‡	Number of seeds		
							Collected	Germinated	Analysed
Asarum costatum	Ac1	2016	23	0.086	4	0.174	29	28	22
		2017	28	0.104	§	-	-	-	-
		2018	31	0.115	7	0.226	90	63	47
		2019	112	0.416	16	0.143	206	92	81
		Total	194	-	27	0.139	325	183	150
	Ac2	2016	21	0.099	1	0.048	2	0	-
		2017	2	0.009	0	0.000	-	-	-
		2018	31	0.146	7	0.226	82	70	24
		2019	29	0.136	3	0.103	17	3	3
		Total	83	-	11	0.133	101	73	27
Asarum minamitanianum	Am1	2016	48	0.324	11	0.229	121	103	71
		2017	35	0.236	6	0.171	82	50	31
		2018	20	0.135	5	0.250	75	64	48
		2019	23	0.155	1	0.043	5	4	3
		Total	126	-	23	0.183	283	221	153
	Am2	2016	36	0.218	8	0.222	74	62	47
		2017	31	0.188	10	0.323	101	89	67
		2018	37	0.224	12	0.324	139	116	94
		2019	19	0.115	6	0.316	118	50	28
		Total	123	-	35	0.285	432	317	236

†The number of flowering individuals divided by the total number of individuals within the plot. ‡The number of fruiting individuals divided by the number of flowering individuals within the plot. §Due to grooming of deer, I cannot collect the fruits

species, I considered that seeds within a fruit derived from the same father would be derived from one pollination event. Thus, I estimated pollen transfer distances based on the estimated father-mother pairs.

Comparison of fruiting and selfing rates

To compare fruiting and selfing rates between the two species, I conducted a generalised linear mixed model (GLMM) analysis and adopted a model selection approach. I used Bayesian methods to estimate parameters, which can treat complicated random structures, and implemented these in the brms package (Burkner, 2017) in R. As the response variable, I set the fruiting rate (binomial variable 0/1 for each flower) or selfing rate (binomial variable 0/1 for each seed) with Bernoulli error distribution. In order to test whether floral densities affect the fruiting and selfing rates, besides species, I set a floral density term (number of flowers of each individual or total number of flowers within surrounding area) as a fixed effect. I constructed buffers of 1 m, 2 m, and 3 m radii around each individual and counted the total number of flowers within the buffer, including themselves. The formation of the buffers and counting of flowers were conducted using the sf package (Pebesma, 2018) in R. For each reproductive character, I constructed the models including only species effect, only each floral density effect (number of flowers of the individual, total number of flowers within 1 m buffer, those within 2 m buffer, and those within 3 m buffer), or combinations of these two effects. For fruiting rate, populations, years, and individual ID nested within the years were used as the random effects. For selfing rate, populations, years nested within populations, and fruit ID nested within years were used as the random effects. Almost all individuals produced only one fruit each year (only three individuals produced two fruits). This made it difficult to estimate the coefficients of individual random effects within selfing rate models. Thus, I treated fruits produced by the same individual within a year as independent and did not include individual ID as a random effect in all selfing rate

models. All model formulae are shown in Table S20. Each model was updated for 5000 iterations, discarding the first 1000 iterations as the warm-up, and sampling every tenth position of the Markov chain (i.e., the thin rate). I ran four chains and used diagnostic plots to assess problems with convergence of parameter estimates. The convergences of the parameters and MCMC were also checked by using the values of Rhat (< 1.05) and neff ratio (> 0.1). The relative fit of the set of candidate models was assessed using the widely applicable information criterion (WAIC: Watanabe, 2010). I adopted the model showing minimum WAIC values as the best model, and the models with less than 2.0 delta WAIC were also considered as competitive models. For each best-fitting model, I estimated the coefficients of fixed effects (mean and 95% credible intervals [CIs]) from posterior distributions of parameters. I also reported the marginal effect plots of fixed effects in the best models.

Floral visitor observation

Floral visitors were observed at Ac1 from 2017 to 2019 for *A. costatum* and at Am2 in 2017 and 2018, and at Am1 in 2019 for *A. minamitanianum*. All surveys were conducted during the day and night in April or May (Table S21). I walked around the flowers once every 1.5 h and collected floral visitors within the calyx tube using an aspirator. Because floral visitors were invisible from outside due to the pod-like floral structures of both species, I placed the inlet tube of the aspirator at the entrance of a flower and sucked the air within the calyx tube. I performed this procedure for all observed flowers at each interval. I set 1.5 h as an observation interval and counted the number of observed flowers and collected visitors at each interval. The collected visitors were categorised into eight taxonomic groups (flies, isopods, amphipods, springtails, spiders, mites, ants, and beetles). Visitors with very low frequencies (less than five individuals observed across all years in both species) were categorised as "others". Diptera individuals were identified at the family level. I calculated the visitation frequency of each group in each *Asarum* species (visitor/flower/1.5 h). To visualise the difference in compositions of floral visitors between the species, I performed a nonmetric multidimensional scaling (NMDS) ordination analysis. The differences in the compositions of floral visitors between the species and the years were tested using permutational multivariate analysis of variance (PERMANOVA) with 1000 permutations. For both analyses, I used the visitation frequency of each group (excluding "others" column) in each observation interval, but removed the data when no visitors were observed. In total, 41 observation intervals for *A. minamitanianum* and 31 observation intervals for *A. costatum* were used for NMDS analysis and PERMANOVA. The distances between the visitation frequencies were measured using the Bray–Curtis dissimilarity matrix, and both analyses were performed with the vegan package (Oksanen *et al.*, 2007) in R.

To test whether the visitation frequency of each group and all visitors was different between the species, I used GLMM with counts of each visitor in each observation interval fitted as the response variable with Poisson error distribution and species as the explanatory variable. I employed maximum likelihood methods to estimate parameters implemented in the glmmADMB package (Bolker *et al.*, 2012) in R. Years, dates nested within years, and time periods were treated as the random effects because I considered that the visitation frequency of insects would vary depending on the conditions of each year, date, and time period (morning, noon, evening, and night). I classified each observation data into four categories of time periods (morning: 6:01–10:00, noon: 10:01–15:00, evening: 15:01–19:00, and night: 19:00–6:00). The number of flowers observed at each interval was set as the offset term. I compared the AIC values of full models with null models including only the random effects. Because isopods and amphipods were observed only in *A. costatum* over the three years (see Results section), I conducted GLMM analyses for the other six groups.

Crossing experiment

I assessed the levels of self-compatibility of the two species by comparing the number of seed sets arising from artificial selfing, artificial outcrossing, and no treatment with bagging. I used five flowers of species for each treatment, and the experiments were conducted in the greenhouse at Kyoto University. I compared the mean number of seeds in each treatment and species using Tukey-Kramer's multiple tests implemented in R.

Results

Floral morphology

The average length of calyx lobe of *A. costatum* was significantly lower (17.33 mm) than that of *A. minamitanianum* (109.31 mm). In addition, *A.*

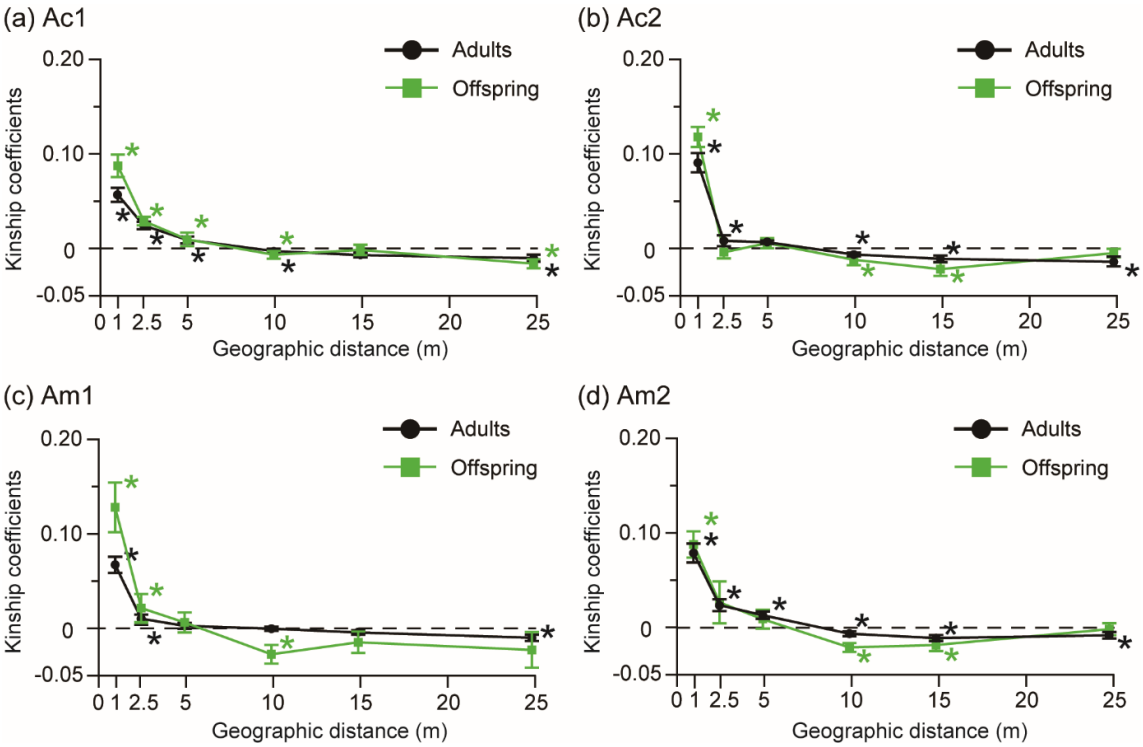

Figure 18. Correlograms of mean kinship coefficients (F_{ij}) of two cohorts (adults, black and offspring, green) for six distance classes (1, 2.5, 5, 10, 15, and 25 m) in plots Ac1 (a), Ac2 (b), Am1 (c), and Am2 (d). Error bars represent standard errors. * $p < 0.05$ indicates statistically significant deviation from null hypothesis of $F_{ij} = 0$.

costatum had significantly larger calyx tube (6.00 mm in height and 11.62 mm in width in *A. costatum*, and 4.72 mm in height and 9.12 mm in width in *A. minamitanianum*), and wider entrance of flower (2.97 mm in *A. costatum* and 1.83 mm in *A. minamitanianum*). The stigma of *A. costatum* was closer to the anthers (1.03 mm in *A. costatum* and 1.84 mm in *A. minamitanianum*). The details of the morphological measurements are shown in Table S22. The AIC values of all models were lower than those of the null models (delta AIC > 2.0; Table S23). LMM analysis showed that all five traits showed significant differences between the species ($p < 0.05$).

Genetic diversity and spatial genetic structure

The genetic diversity estimates are shown in Table 10. Both cohorts in all four plots showed relatively high genetic diversity (NA = 8.3–11.5, H_E = 0.645–0.739) and significantly positive F_{IS} values (F_{IS} = 0.155–0.255, $p < 0.05$ in Hardy–Weinberg Exact test). In all plots, the values of NA and H_E of adults were slightly higher than those of offspring. The F_{IS} values were slightly lower in adults except for the Ac1 plot. The slopes (b) of the regression were significantly lower than zero, and Sp values were relatively high in both cohorts in all four plots. In both cohorts of the four plots, pairwise kinship coefficients decreased significantly with geographic distances (Fig. 18). At the shortest distance class (< 1 m), both cohorts of the four plots showed significant deviation of the F_{ij} values from the null hypothesis of no spatial genetic structure ($F_{ij} = 0$).

Results of paternity analysis

The flowering rate showed among-year fluctuations, with varying rates of 0.9–41.6% in *A. costatum* (mean = 13.9%) and 11.5–32.4% in *A. minamitanianum* (20.0%) (Table 11). Average fruiting rates were 13.1% in *A. costatum* and 23.5% in *A. minamitanianum*, and the rates also fluctuated among years (0–22.6% in *A. costatum* and 17.1–32.4% in *A. minamitanianum*).

In four years, I collected 1141 seeds, 794 of which germinated. In total, 566 seedlings from 88 fruits were analysed. In all four plots, the genetic diversities (NA and H_E) of seedlings in each year were lower than those of the candidate parents, and in most years, the F_{IS} values were higher in seedlings (Table S24). The multi-locus exclusion probabilities over the loci for the second parent were more than 0.995 in all plots, and there were no individuals showing identical genotypes. For

Table 12. The estimated selfing and outcrossing rates of each plot at seed and fruit levels.

Species	Plot	Seed level		Fruit level		
		Selfing rate	Outcrossing rate	Selfing only	Selfing and outcrossing	Outcrossing only
Asarum costatum	Ac1	0.327 (49/150)	0.673 (101/150)	0.240 (6/25)	0.400 (15/25)	0.360 (9/25)
	Ac2	0.333 (9/27)	0.667 (18/27)	0.571 (4/7)	0.290 (2/7)	0.143 (1/7)
Asarum minamitanianum	Am1	0.105 (16/153)	0.895 (137/153)	0.095 (2/21)	0.238 (5/21)	0.714 (15/21)
	Am2	0.157 (37/236)	0.843 (199/237)	0.125 (4/32)	0.031 (1/32)	0.844 (27/32)

each plot, 33–55% of seeds were assigned with 95% confidence or matching at all loci. As my data showed little mismatches between mother and offspring genotypes, I considered that the low proportions of assigned seeds were due to unsampled fathers outside of plots rather than genotyping errors. Thus, I treated the unassigned seeds as outcrossing seeds. More than 30% of the seeds of *A. costatum* (32.7% in Ac1 and 33.3% in Ac2) were estimated to be derived from selfing, while only 10.5% in Am1 and 15.7% in Am2 of seeds were derived from selfing (Tables 12 and S25). Regarding the fruits, in *A. minamitanianum*, most fruits contained only outcrossing seeds (71.4% in Am1 and 84.4% in Am2), whereas in *A. costatum*, such fruits were minor (36.0% in Ac1 and 14.3% in Ac2). Excluding selfing seeds, fathers of 141 seeds were assigned within the plots, and 43 father-mother pairs were detected in three plots (in Ac2 plots, no pairs were detected within the plot). Mean pollen transfer distances were 5.57 m in Am1, 10.29 m in Am2, and 9.12 m in Ac1. More than 15 m of pollen transfers were detected in all three plots (Fig. S25).

Interspecific difference of reproductive characters

My GLMM analysis showed that for fruiting rate, the WAIC score was lowest in the model including only the effect of the total number of flowers within 2 m buffer (WAIC = 512.5), followed by the model including the effects of species and total number of flowers within 2 m buffer (delta WAIC = 0.4). In the best model, all values within 95% CIs of the coefficient of total number of flowers within 2 m buffer were positive (mean: 0.09, 95% CIs: 0.01–0.17). In the second model, 95% CIs of the coefficient of species effect (*A. minamitanianum*) overlapped with zero (mean: 0.83, 95% CIs: -0.75–2.76), implying that the fruiting rate would not be different between the species.

For selfing rate, the model with species and total number of flowers within 2 m buffer showed the lowest WAIC value (WAIC = 218.5), but other models including the species effect also showed relatively lower WAIC values (delta WAIC < 2.0). In the best model, 95% CIs of the coefficient of species effect (*A. minamitanianum*) slightly overlapped with zero (mean: -6.32, 95% CIs; -12.80–0.34), and the hypothesis testing function implemented in brms showed that there was sufficient evidence of a lower selfing rate in *A. minamitanianum* than in *A. costatum* (evidence ratio = 37.1 and posterior probability = 0.97). The estimated coefficient of the total number of flowers within 2 m buffer was nearly zero (mean: -0.01, 95% CIs; -0.44–0.47). The results of model selection are shown in Table 13. The estimated parameters of the best and competitive models are shown in Table S26, and the marginal effects plots are shown in Figure 19. The posterior probabilities and trace plots of the parameters of interest in the best models are shown in Figures S26 and S27.

Floral visitors in the calyx tubes

In total, 194 floral visitors were collected during 51 observation intervals (76.5 h) for *A. costatum*, and 107 during 64 observation intervals (96 h) for *A. minamitanianum*. Part of the collected visitors are shown in Figures 17b and S28. The estimated frequencies of all visitors were extremely low in both species: 0.0473 individual/flower/1.5 h in *A. costatum*, and 0.0634 in *A. minamitanianum* (Table 14). Isopods and amphipods were observed only in *A. costatum*, and six other groups, including flies, were observed in both species. All collected Diptera species belonged to Muscomorpha and included a wide range of families (Table S27). In *A. costatum*, 41.6 % (5/12) were Sciaridae and 25.0 % (3/12) were Chironomidae. In *A. minamitanianum*, 28.6 % (6/21) of the flies collected were Cecidomyiidae, 23.8 % (5/21) were Chironomidae, and 19.0 % (4/21) were Sciaridae. The estimated visitation frequencies of flies were 0.0030 individual/flower/1.5 h in *A. costatum* and 0.0102 in *A. minamitanianum*. The NMDS showed that the visitation frequencies of springtails, spiders, isopods, flies and amphipods would

contribute to the difference in the compositions between the two species (Fig. S29). The PERMANOVA showed that the compositions of floral visitors were significantly different between the species (R^2 = 0.137, p < 0.05) and among the years (R^2 = 0.030, p < 0.05) (Table S28). GLMM analysis showed that between the species, the visitation frequency of spiders was significantly higher in *A. costatum* and the visitation frequencies of flies, springtails, and beetles were significantly higher in *A. minamitanianum* (p < 0.05; Table S29). The AIC values of these models were lower than those of the null models (delta AIC > 2.0). Other groups and total visitors did not show a significant difference between the species.

Self-compatibility of two species

The flowers of the two species with bagging only treatment yielded no seeds (Table S30), indicating that both species are incapable of automatic self-pollination. In both species, all flowers with artificial selfing or outcrossing treatments became fruits, with a varying number of seeds among them (8–27). There were no significant differences in the mean number of seeds between the treatments (selfing or outcrossing) and species (p > 0.05).

Table 13. The results of model selection for Bayesian GLMM analysis based on WAIC values. The best and competitive models were written in bold letters (⊿WAIC < 2.0).

Objectives	Explanatory variables	WAIC	⊿WAIC
Fruiting	**N_flower2**	**512.5**	**0.0**
	Species + N_flower2	**512.8**	**0.4**
	N_flower1	514.9	2.5
	Species + N_flower1	515.1	2.6
	Species	515.4	2.9
	N_flower3	515.9	3.5
	Species + N_flower3	516.1	3.6
	NULL	516.3	3.8
	Species + N_flower	517.4	5.0
	N_flower	517.6	5.1
Selfing	**Species + N_flower2**	**218.5**	**0.0**
	Species + N_flower	**219.0**	**0.5**
	Species + N_flower1	**219.1**	**0.6**
	Species + N_flower3	**219.2**	**0.7**
	Species	**219.6**	**1.1**
	N_flower1	220.5	2.0
	N_flower	220.8	2.3
	N_flower2	221.1	2.6
	N_flower3	221.7	3.3
	NULL	222.0	3.5

Discussion

Evolutionary insights into calyx lobe elongation

Generally, floral morphology was interpreted as results of pollinator-mediated selection (Fenster *et al.*, 2004). The two *Asarum* species showed a remarkable difference in the calyx lobe length (on average, 17.33 mm in *A. costatum* and 109.31 mm in *A. minamitanianum*; Table S22). I expected that the elongated calyx lobe in *A. minamitanianum* would be related to the attraction of flies similar to other flowers with elongated filiform appendages, which could increase the display size (Policha *et al.*, 2016) and/or act as landing platforms (Katsuhara *et al.*, 2017). My multi-year floral visitor observations detected differences in the composition of visitors between the two species (Fig. S29 and Table S28). Although flies were observed in both species, their visitation frequency was more than three times higher in *A. minamitanianum* (Tables 14 and S29). This result supports my fly attraction hypothesis. Furthermore, empirical studies have reported that large floral sizes are maintained by natural selection, especially by pollinator-mediated selection (Parachnowitsch & Kessler, 2010; Lavi & Sapir, 2015). The previous study also indicated that the length of the calyx lobe of *A. minamitanianum* was stable among and within populations, and divergent selection would have been involved in the evolution and maintenance of the calyx lobe variation (Chapter 4). Thus, I considered that the elongated calyx lobe of *A. minamitanianum* was likely maintained by natural selection and may have evolved possibly to facilitate the attraction of flies.

I should caution that my data of floral visitors were based on only one or two populations per species, and there is the possibility that the fauna of flies and other insects are different among other populations. Furthermore, most other plants with elongated floral organs are often pollinated by specific families of flies (Lim & Raguso, 2017; Guo *et al.*, 2019), but my results showed that various kinds of flies visited flowers of both species. It has been reported that both fungus gnats and *Drosophila* species were simultaneously observed in other *Asarum* species (*A. tamaense*) in one population (Kakishima & Okuyama, 2020). This implies that in *Asarum* species, pollination could be achieved by several families of flies, whereas I cannot deny the possibility that I may have missed any specialised pollinators. Thus, further pollinator observations and manipulation

Table 14. Frequencies (/flower/1.5 h) of floral visitors of two species. The visitors are categorised into the nine groups and collected numbers are shown within the parenthesis.

	Asarum costatum				*Asarum minamitanianum*			
Groups	2017	2018	2019	Total	2017	2018	2019	Total
Fries (Diptera)	0.0009 (1)	0.0070 (10)	0.0009 (1)	0.0030 (12)	0.0101 (9)	0.0132 (10)	0.0063 (2)	0.0102 (21)
Isopods (Isopoda)	0 (0)	0.0046 (8)	0.0260 (26)	0.0072 (39)	0 (0)	0 (0)	0 (0)	0 (0)
Amphipods (Amphipoda)	0.0009 (1)	0 (0)	0.0041 (5)	0.0013 (6)	0 (0)	0 (0)	0 (0)	0 (0)
Springtails (Collembola)	0.0061 (7)	0.0056 (8)	0.014 (16)	0.0076 (31)	0.0101 (9)	0.0344 (26)	0.0418 (9)	0.0260 (44)
Ticks (Acari)	0.0061 (7)	0.0063 (8)	0.0034 (4)	0.0056 (19)	0.0049 (4)	0.0053 (4)	0.0150 (5)	0.0074 (13)
Spiders (Araneae)	0.0079 (9)	0.0192 (24)	0.0155 (18)	0.0135 (51)	0 (0)	0.0093 (7)	0.0087 (3)	0.0055 (10)
Ants (Hymenoptera)	0.0035 (4)	0.0063 (8)	0.0032 (4)	0.0044 (16)	0 (0)	0.004 (3)	0.0228 (7)	0.0070 (10)
Beetles (Coleoptera)	0 (0)	0.0014 (2)	0 (0)	0.0005 (2)	0.0011 (1)	0.0026 (2)	0.0251 (6)	0.0076 (9)
Others	0.0017 (2)	0.0045 (6)	0.0083 (10)	0.0041 (18)	0 (0)	0 (0)	0 (0)	0 (0)
All visitors	0.0271 (31)	0.0549 (74)	0.0753 (89)	0.0473 (194)	0.0258 (23)	0.0688 (52)	0.1198 (32)	0.0634 (107)

experiments (e.g., checking the fruiting rates and observation of floral visitors using flowers with the calyx lobes cut) would provide us with a more robust inference concerning the ecological roles of the elongated calyx lobe of *A. minamitanianum*.

Ecological consequence of changes in floral traits

My Bayesian GLMM analysis showed that selfing rates were significantly different between the species (Tables 13 and S26). In *A. minamitanianum*, fruits including only seeds derived from outcrossing were dominant (on average, 79.3%), whereas in *A. costatum*, such fruits were fewer (31.3%), and the selfing rates varied considerably among fruits within a population (Table 12 and Fig. 19). These results implied that in comparison with *A. costatum*, *A. minamitanianum* can be pollinated more efficiently. Considering the high mobility of flies, one reason for this could be the difference in visitation frequency of flies (Tables 13 and S29), possibly caused by the elongated calyx lobe. I considered that the other two factors are also concerned with the difference in mating system; differences in the anther-stigma distance and visitation of large ground dwelling insects. *Asarum minamitanianum* showed spatial separation between stigmas and anthers (herkogamy) (Tables S22 and S23). Previous studies have reported that stigma-anther distances are strongly correlated with outcrossing rates (Karron *et al.*, 1997; Takebayashi *et al.*, 2006), and herkogamy promotes efficient pollen dispersal by reducing stigma-anther interference (Baena-Diaz *et al.*, 2012). Furthermore, the low efficiency of *A. costatum* could be related to the visitations of large ground-dwelling insects (isopods and amphipods), which were observed only in *A. costatum* (Table 14). They were also observed in subterranean pod-like flowers of *Aspidistra elatior* (Asparagaceae) (Kato, 1995). In particular, amphipods ate pollens within the flowers and were suspected to be the main pollinators of this species (Kato, 1995; Conran & Bradbury, 2007). The flowers of *A. costatum* have wider floral entrance and larger calyx tubes (Tables S22 and S23) and are often buried underground. These characteristics could promote visitations of large ground-dwelling insects, and due to their large body sizes and low mobilities, their visitation could cause autogamy in the flowers. I considered that the differences in floral morphology and floral visitor composition are likely to be the main causes of the difference in the mating system between the two closely related species.

Transition of plant mating systems has repeatedly occurred throughout the evolutionary history of angiosperms (Charlesworth & Charlesworth, 1987; Holsinger, 2000). Although mating system evolution from outcrossing to selfing would be dominant, reverse transition has also been reported (Barrett, 2013). A previous study reported that populations with mixed mating systems often possess the genetic variation for traits promoting outcrossing (Shore & Barrett, 1990), and natural selection could cause mating system evolution to outcrossing (Fenster & Ritland, 1994; Brys *et al.*, 2014). In the two *Asarum* species, mating system evolution in the direction of increasing outcrossing would have occurred because flowers of the related species do not show herkogamy (Kishi & Irizawa, 2008). In mixed

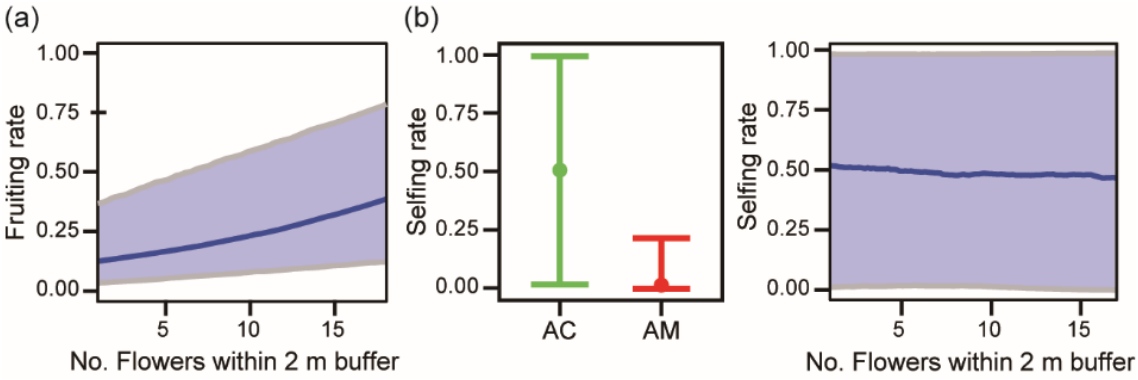

Figure 19. Marginal effects plots (mean and 95% Cis) of the number of flowers within 2 m buffer and the species (AC, *Asarum costatum* and AM, *A. minamitanianum*) for the best models of fruiting rate (a) and selfing rate (b), respectively.

mating species, outcrossing is advantageous, especially when inbreeding depression is expressed (Charlesworth *et al.*, 1990). My genetic analysis showed that the inbreeding coefficients of offspring cohorts obtained from the plot survey were higher than those of adult cohorts in three plots (Table 10), and these of seedlings used in paternity analysis were higher than those of flowering individuals in most years (Table S24). These results implied that in the two species, inbreeding depression may be expressed at the late stage after germination. Therefore, in *A. minamitanianum*, crossing with unrelated individuals would be advantageous, and the increased outcrossing rate could compensate for the costs of the elongated calyx lobes.

***Reproductive ecology of* Asarum**

Although many botanists have been interested in *Asarum* species due to their curious flowers blooming on the ground (Maekawa, 1933; Maekawa, 1953; Vogel, 1978), most aspects of their reproductive ecology have been unclear. *Asarum* species have been thought to show very limited dispersal ability (Hiura, 1978) and low frequency of pollinator visitation (Sugawara, 1988; Kakishima & Okuyama, 2018). On the other hand, as shown in this study (Table 10), *Asarum* species have relatively high genetic diversity (Matsuda & Setoguchi, 2012; Chapter 3). It has remained unclear regarding how they maintain their populations. My SGS analysis detected strong spatial autocorrelations in both cohorts of the two species (Fig. 18 and Table 10), which were also reported in other myrmecochorous plants (Nakagawa, 2010). This implies that in both species, seed dispersal would be strongly constrained. Considering the low dispersal distances of seeds and the inbreeding depression, crossing with more distant and less related individuals would be advantageous to *Asarum* species. The results of my crossing experiments (Table S30) and fruiting rates in the wild (Table 11) indicated that both species depend on pollinators to fruit. My paternity analysis detected long-distance pollen transfers in both species (Figs. 17c and S25). In shady evergreen forest understorey, which is the habitat of *Asarum* species, it has been considered that the availability of pollinator fauna is limited (Zhou *et al.*, 2007; Ssymank *et al.*, 2008). Because flies are relatively abundant in shady and moist environments, pollination by flies has been reported especially in plants growing in the forest understorey (Ssymank *et al.*, 2008; Mochizuki & Kawakita, 2018). The floral characteristics of *Asarum* species (pod-like floral structures, lacking nectar, and dark floral colours) are matched to the hypothesised fly syndromes characters (Faegri & Van Der Pijl, 2013). Thus, *Asarum* is likely to be adapted to fly pollination in order to facilitate effective crossing in the shady forest understory.

My floral visitor observations showed that visitation frequencies of flies in both species were extremely low (at most, 0.0102 individual/flower/1.5 h in *A. minamitanianum*), and that those of all visitors were also low (0.0471 in *A. costatum* and 0.0634 in *A. minamitanianum*; Table 14). In contrast, the fruiting rates varied among populations and years (0–32.4%), but in most years, more than 10% of flowers became fruits (on average, 23.5 % in *A. minamitanianum*, and 13.5 % in *A. costatum*; Table 11). These values were not extremely low, considering the expectation from the visitation rates. This tendency was reported in other *Asarum* species; in *A. tamaense*, the visitation frequencies of pollinators including flies were extremely low (25 visitors in 58 h from 120 flowers), but it showed a moderate

fruiting rate in the wild (14.0–81.3%) (Sugawara, 1988). How do *Asarum* species produce some seeds in spite of the low frequency of pollinator visitations? One possible reason could be self-compatibility (Table S30). My paternity analysis showed that both species produce selfing seeds to some extent (in *A. costatum*, 13.6–53.2% of seeds were derived from selfing, and in *A. minamitanianum*, 0–29.8%; Tables 12 and S25). Furthermore, in *Asarum* flowers, the stigma and anther appear active for more than two weeks (Takahashi et al., personal observations). I considered that the self-compatibility and longevity of flowers would enable *Asarum* species to produce fruits to some extent and to maintain the population in spite of low visitation frequencies of pollinators. Although *Asarum* species are incapable of vegetative propagation or autonomous selfing, which would be advantageous in pollinator-limited environments as reproductive assurance (Morgan & Wilson, 2005), their long life-span and longevity of flowers, combined with self-compatibility, would allow for increased opportunities for reproduction.

Conclusion

Flowers having elongated floral organs would have evolved repeatedly, and considering their ecological and energetic costs, these flowers can be expected to receive some benefits in fitness (Grace, 1993; Zhang *et al.*, 2005). However, until now, their ecological consequences have rarely been investigated, especially by comparing sister-species. My field observations and genetic analysis showed that flowers of *A. minamitanianum* were visited by flies more frequently, and conducted less selfing compared with that of *A. costatum*. Although its attraction mechanisms remain unclear, the elongated calyx lobe of *A. minamitanianum* might have evolved for effective pollen dispersal by flies. Thus, my study demonstrated that the evolution of elongated floral organs could have changed the reproductive characters and could have brought fitness advantages.

To the best of my knowledge, this study is the first to reveal multiple aspects of the reproductive ecology of perennial herbs growing in the forest understorey of warm temperate evergreen forests. *Asarum* shows long flowering time, low fruiting rate, self-compatibility with late-stage inbreeding depression, high genetic diversity, and long life-span. These characters are similar to those of long-lived tree species (Isagi *et al.*, 2007; Tamaki *et al.*, 2009; Aleksic *et al.*, 2017), which are considered to sustain populations over a long period of time. Although, compared with these tree species, the spatial scale at which individuals can reproduce is significantly small, these reproductive characters may be one of the important factors that sustain the population under the shady evergreen forests, in which pollinators are scarce.

Appendix

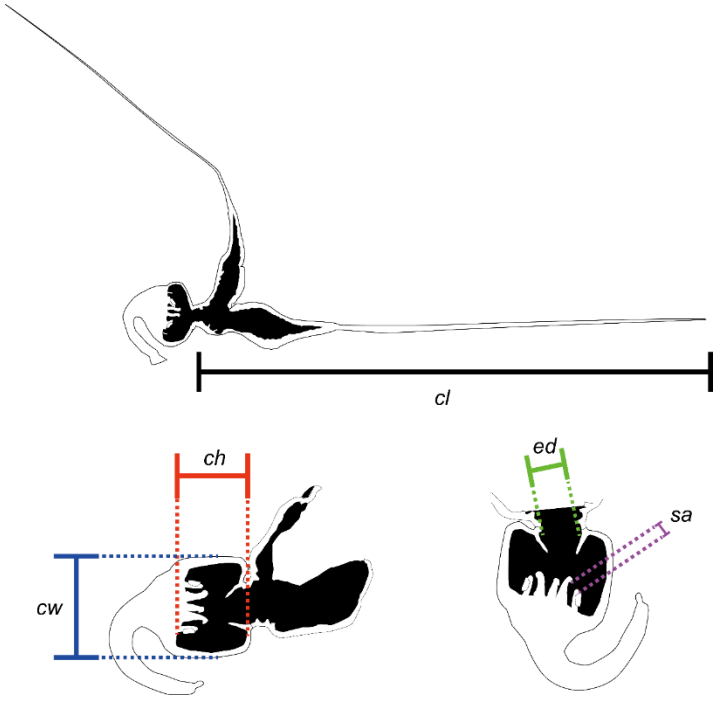

Figure S24. Five morphological characters measured in flowers of *Asarum minamitanianum* and *A. costatum*. The lines indicate measured length of floral characters: *cl* = calyx lobe length, *ch* = calyx tube height, *cw* = calyx tube width, *ed* = floral entrance diameter, and *sa* = stigma-anther distance.

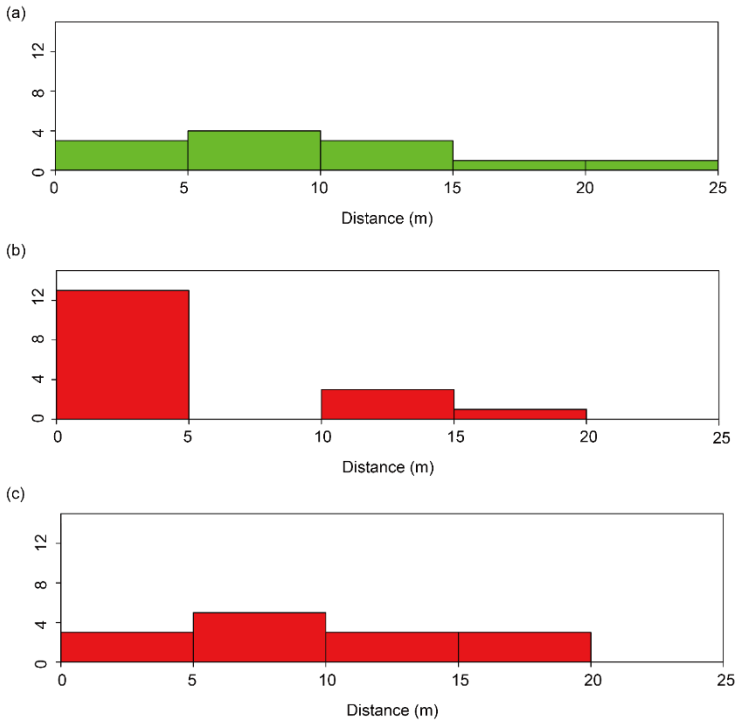

Figure S25. Histograms of pollen transfer distances of three plots, Ac1 (a), Am1 (b), and Am2 (c), estimated from the paternity analysis.

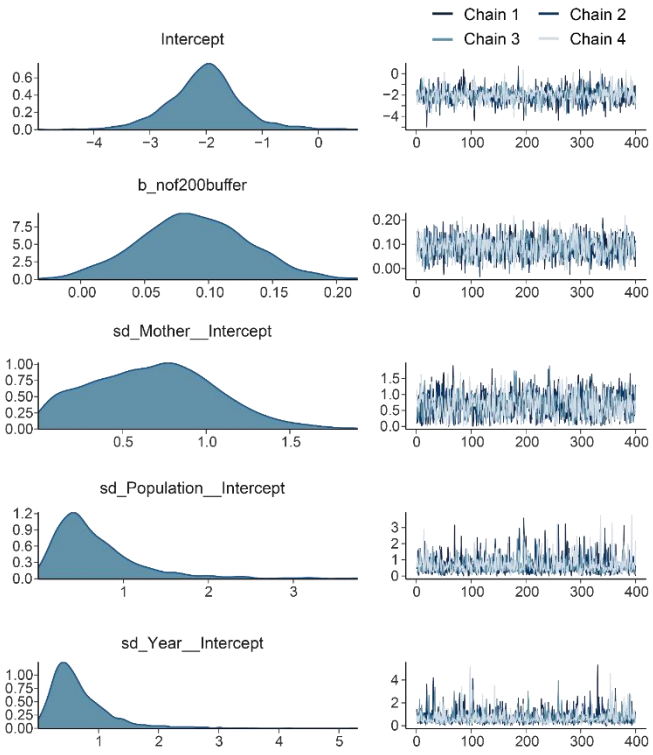

Figure S26. Distributions of posterior probability and trace plots of the main parameters (intercept and coefficient of fixed effects, and intercepts of random effects) of the best model of fruiting rate. The model description is provided in Table S20.

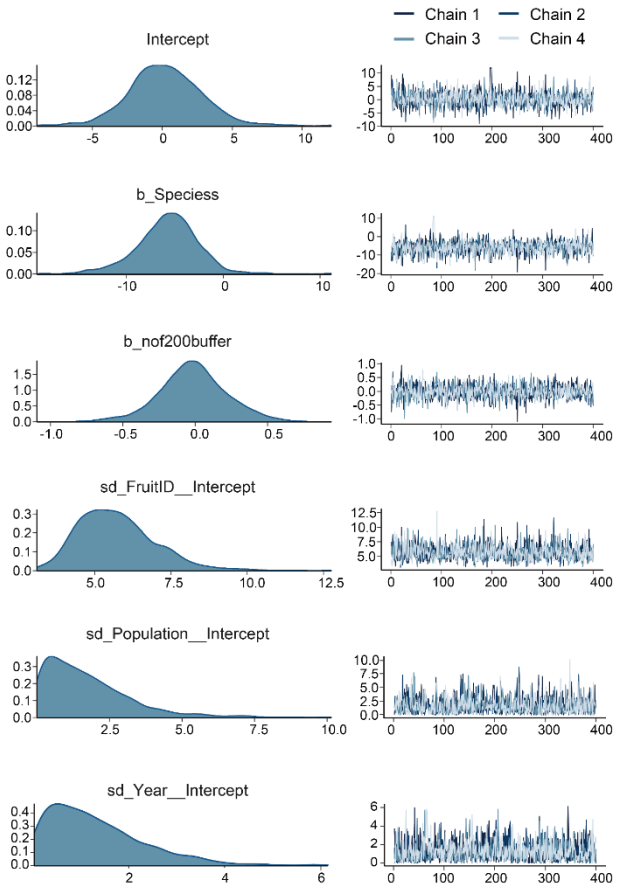

Figure S27. Distributions of posterior probability and trace plots of the main parameters (intercept and coefficient of fixed effects, and intercepts of random effects) of the best model of selfing rate. The model description is provided in Table S20.

Figure S28. Photos of collected floral visitors, Drosophilidae sp. (a), Sphaeroceridae sp. (b), and isopod (c) which visited *Asarum costatum* flowers, and of Sciaridae spp. (d), Chironomidae sp. (e), and springtail. (f) which visited *A. minamitanianum* flowers. White bars indicate 1 mm.

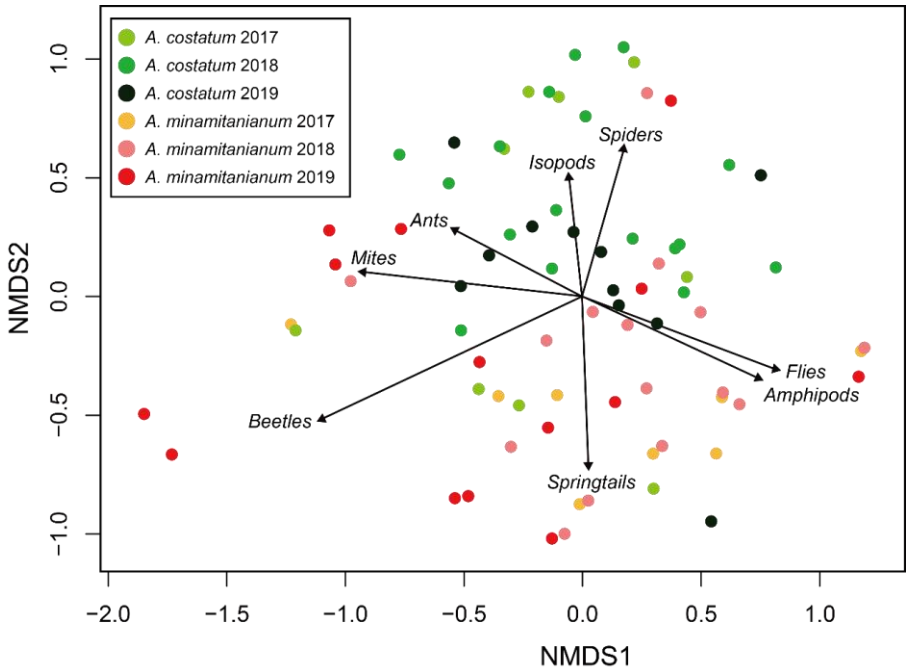

Figure S29. The two first axes of the non-metric multidimensional scaling (NDMS) analysis for compositions of the floral visitors of the two species *Asarum costatum* and *A. minamitanianum*.

Table S19. Primer information used for fine-scale spatial genetic analysis and parentage analysis.

Locus names	Primer pairs used for SGS analysis	Primer pairs used for parentage analysis†
As_2526	F: TGTGGAATTGTGAGCGGAACCGCACACAGCCTTTAC	-
	R: GTTTCTTCACACCGCCACGAAATGAG	-
As_7180	F: CTATAGGGCACGCGTGGTGAAAGTCCAGCCAAGGAGC	F: GAAAGTCCAGCCAAGGAGC
	R: GTTTCTTGTTGTGGAACCTGTCTCGG	R: GTTTCTTGTTGTGGAACCTGTCTCGG
As_59081	F: CTATAGGGCACGCGTGGTTGTTGGGATTAGCTGATGGG	F: TGTTGGGATTAGCTGATGGG
	R: GTTTCTTAGAGAAACAGGGCATCAGAAC	R: GTTTCTTAGAGAAACAGGGCATCAGAAC
As_12707	F: TGTGGAATTGTGAGCGGTTTCCCTAAGATGCTCCCAC	-
	R: GTTTCTTGTCCTCGGCAAAGCCATTC	-
As_537	F: TGTGGAATTGTGAGCGGCTGAGAAGGACAATCCACAAGC	F: TGAGAAGGACAATCCACAAGC
	R: GTTTCTTTACCGTCGTCACCGAATCC	R: GTTTCTTTACCGTCGTCACCGAATCC
As_3572	F: CTATAGGGCACGCGTGGTAGGCCAAGCAATGTGGAAAC	F: AGGCCAAGCAATGTGGAAAC
	R: GTTTCTTAGAGGAGGAGAATCTTAAAGGAATG	R: GTTTCTTAGAGGAGGAGAATCTTAAAGGAATG
As_14593	F: TGTGGAATTGTGAGCGGAGCCCTAATTCCCGCAGAC	F: AGCCCTAATTCCCGCAGAC
	R: GTTTCTTCTGCATTGTGGAGGCGTTC	R: GTTTCTTCTGCATTGTGGAGGCGTTC
As_9592	-	F: GGAATACTCGTTCTTCTTCATCTCC
	-	R: GTTTCTTAACCGGATCTGAAGGGCTC
As_24077	F: CACGACGTTGTAAAACGACCCGAGGGTGTCGGAAACAG	-
	R: GTTTCTTTGTGAATGGGAAACGAAACCC	-
As_18424	-	F: CATACGCAGTGAGCCTCAGA
	-	R: GTTTCTTCCGAAGTTTGGCGCTCTAC
As_9117	-	F: CTCGCAATGACATCGGTGG
	-	R: GTTTCTTGAGAGTGCCTACCGTCGAG
As_29176	F: CTATAGGGCACGCGTGGTTGGTTGATGAATCTTCCTCTATTACG	-
	R: GTTTCTTTCACCCAATTCGTCTCTGG	-
As_42062	F: CACGACGTTGTAAAACGACTGAGGGTGATGAGGTACCAAC	-
	R: GTTTCTTTGGCACTACTGCTTCAGGG	-
As_20984	F: CTATAGGGCACGCGTGGTAAGGGACCGCCAGAATCG	-
	R: GTTTCTTACGACTCTCCAGATCTCCAAC	-
As_21539	F: CACGACGTTGTAAAACGACCGGATCCCGAATGCGAAAC	-
	R: GTTTCTTTCAGTTCCAATCACCTCTGC	-
As_11633	F: CTATAGGGCACGCGTGGTTTTCGGGTTCCCTTCATCC	-
	R: GTTTCTTGGTGCACATCGAGTTTCCG	-
As_74749	-	F: GAGCGAGGTCCATTTACCG
	-	R: GTTTCTTCAGTAGGCTTACCCGGTGG

† All forward primers were modified with each of four kind of fluorescence (JOE, CY3.5, FAM, or CY3)

Table S20. Candidate models and model details of the GLMM analysis for each reproductive character of two species.

Model formula
Fruiting rate ~ 1 + (1|Population) + (1|Year) + (1|Mother)
Fruiting rate ~ Species + (1|Population) + (1|Year) + (1|Mother)
Fruiting rate ~ N_flower + (1|Population) + (1|Year) + (1|Mother)
Fruiting rate ~ N_flower1 + (1|Population) + (1|Year) + (1|Mother)
Fruiting rate ~ N_flower2 + (1|Population) + (1|Year) + (1|Mother)
Fruiting rate ~ N_flower3 + (1|Population) + (1|Year) + (1|Mother)
Fruiting rate ~ Species + N_flower + (1|Population) + (1|Year) + (1|Mother)
Fruiting rate ~ Species + N_flower1 + (1|Population) + (1|Year) + (1|Mother)
Fruiting rate ~ Species + N_flower2 + (1|Population) + (1|Year) + (1|Mother)
Fruiting rate ~ Species + N_flower3 + (1|Population) + (1|Year) + (1|Mother)
Selfing rate ~ 1 + (1|Population) + (1|Population:Year) + (1|Population:Year:Fruits ID)
Selfing rate ~ Species + (1|Population) + (1|Population:Year) + (1|Population:Year:Fruits ID)
Selfing rate ~ N_flower + (1|Population) + (1|Population:Year) + (1|Population:Year:Fruits ID)
Selfing rate ~ N_flower1 + (1|Population) + (1|Population:Year) + (1|Population:Year:Fruits ID)
Selfing rate ~ N_flower2 + (1|Population) + (1|Population:Year) + (1|Population:Year:Fruits ID)
Selfing rate ~ N_flower3 + (1|Population) + (1|Population:Year) + (1|Population:Year:Fruits ID)
Selfing rate ~ Species + N_flower + (1|Population) + (1|Population:Year) + (1|Population:Year:Fruits ID)
Selfing rate ~ Species + N_flower1 + (1|Population) + (1|Population:Year) + (1|Population:Year:Fruits ID)
Selfing rate ~ Species + N_flower2 + (1|Population) + (1|Population:Year) + (1|Population:Year:Fruits ID)
Selfing rate ~ Species + N_flower3 + (1|Population) + (1|Population:Year) + (1|Population:Year:Fruits ID)

N_flower; number of flowers of the individual, N_flower1; total number of flowers within 1 m buffer, N_flower2; total number of flowers within 2 m buffer, N_flower3; total number of flowers within 3 m buffer.

Table S21. Details of the conditions of floral visitor observation.

					Number of	
Species	Population	Year	Date	Time	Observed flowers	Collected visitors
Asarum costatum	Ac1	2017	5/2	14:00-15:30, 18:00-24:00	52.0	3
			5/3	0:00-1:30, 9:00-23:00	52.0	13
			5/5	9:30-23:00	52.0	16
	Ac1	2018	5/5	9:00-19:00	64.0	20
			5/6	9:00-15:30	64.0	15
			5/9	12:50-18:30	64.0	10
			5/10	10:00-17:00	104.0	28
	Ac1	2019	4/28	10:00-16:30	92.3	20
			4/29	10:00-11:30	98.0	8
			4/30	10:00-14:30	105.0	29
			5/1	9:30-14:00	126.0	31
Asarum minamitanianum	Am2	2017	4/27	18:00-24:00	17.0	0
			4/28	0:00-6:00, 18:00-24:00	17.0	0
			4/29	9:30-20:00	33.0	5
			4/30	9:00-17:00	33.0	11
			5/1	0:00-4:30	33.0	7
	Am2	2018	4/26	16:00-19:00	36.0	3
			4/27	10:00-20:00	36.0	11
			4/28	10:00-18:00, 21:00-24:00	36.0	12
			4/29	0:00-3:00, 13:00-20:00	36.0	9
			4/30	13:00-14:30	36.0	2
			5/1	10:00-16:00	36.0	15
	Am1	2019	4/18	11:30-16:00	10.7	7
			4/19	9:30-16:00	16.0	11
			4/20	11:00-16:30	21.0	3
			4/21	9:30-17:00	24.0	11

Table S22. Mean values (in mm) of five floral characters of four populations.

Species	Population	N	Calyx lobe length		Calyx tube width		Calyx tube height		Floral entrance diameter		Stigma-anther distance	
			Mean	SD	Mean	SD	Mean	SD	Mean	SD	Mean	SD
Asarum costatum	Ac1	25	17.48	2.90	11.96	1.33	6.01	1.03	3.18	0.44	1.09	0.37
	Ac2	21	17.15	3.02	11.22	1.15	5.99	1.13	2.73	0.46	0.96	0.29
	All	46	17.33	2.93	11.62	1.29	6.00	1.06	2.97	0.50	1.03	0.34
Asarum minamitanianum	Am1	26	103.10	23.83	8.85	1.47	4.70	0.75	1.79	0.49	1.77	0.47
	Am2	20	120.08	27.14	9.46	0.97	4.75	0.72	1.88	0.27	1.92	0.33
	All	46	109.31	26.10	9.12	1.30	4.72	0.73	1.83	0.41	1.84	0.42

Table S23. The effect of species term (*A. costatum* vs. *A. minamitanianum*) for each floral morphology and AIC values of full models and NULL models estimated from GLMM analysis.

Response variable	Estimate	Standard error	*t*-statistics	*p* value	AIC value	AIC value of NULL model
Calyx lobe length	93.76	8.32	11.27	0.009	744.7	761.1
Calyx tube width	-2.45	0.48	-5.15	0.036	315.8	321.9
Calyx tube height	-1.28	0.19	-6.74	< 0.001	254.3	261.9
Floral entrance diameter	-1.12	0.23	-4.88	0.039	123.1	127.4
Stigma-anther distance	0.82	0.10	8.29	0.015	98.1	103.8

Table S24. Parameters of genetic diversity across 9 microsatellite loci for seedlings and flowering individuals used for paternity analysis.

Species	Plot	Year	Cohort	N	*NA*	H_O	H_E	F_{IS}
Asarum costatum	Ac1	2016	Seedlings	22	4.7	0.718	0.677	-0.085
			Flowering individuals	23	6.0	0.633	0.662	0.032
		2018	Seedlings	47	5.0	0.541	0.648	0.164
			Flowering individuals	32	6.3	0.681	0.701	0.033
		2019	Seedlings	84	6.7	0.588	0.676	0.122
			Flowering individuals	110	8.1	0.643	0.693	0.072
	Ac2	2018	Seedlings	25	5.3	0.608	0.660	0.092
			Flowering individuals	30	7.2	0.710	0.745	0.040
		2019	Seedlings	3	2.6	0.370	0.481	0.280
			Flowering individuals	18	6.6	0.698	0.705	0.001
Asarum minamitanianum	Am1	2016	Seedlings	70	7.1	0.690	0.723	0.040
			Flowering individuals	48	7.9	0.767	0.750	-0.024
		2017	Seedlings	29	5.6	0.674	0.723	0.068
			Flowering individuals	35	7.1	0.748	0.756	0.006
		2018	Seedlings	48	6.0	0.738	0.731	-0.009
			Flowering individuals	20	7.0	0.793	0.758	-0.053
		2019	Seedlings	3	2.7	0.778	0.543	-0.426
			Flowering individuals	23	6.7	0.785	0.738	-0.067
	Am2	2016	Seedlings	44	6.1	0.673	0.721	0.071
			Flowering individuals	36	7.6	0.703	0.763	0.079
		2017	Seedlings	68	7.4	0.738	0.761	0.028
			Flowering individuals	31	7.8	0.736	0.773	0.048
		2018	Seedlings	92	6.4	0.764	0.766	0.001
			Flowering individuals	37	8.2	0.730	0.779	0.062
		2019	Seedlings	26	6.6	0.830	0.755	-0.102
			Flowering individuals	19	6.9	0.779	0.772	-0.010

N, number of individuals; *NA*, number of alleles; H_O, observed heterozygosity; H_E, expected heterozygosity; F_{IS}, fixation index.

Table S25. The results of parentage analysis and estimated selfing rates in each year.

Species	Plot	Year	Number of analysed fruits	Number of anlaysed seeds	Seed level		Fruits level		
					Selfing rate	Outcrossing rate	Selfing only	Selfing and outcrossing	Outcrossing only
Asarum costatum	Ac1	2016	4	22	0.136	0.864	0.000	0.250	0.750
		2017	0	-	-	-	-	-	-
		2018	6	47	0.532	0.468	0.333	0.500	0.167
		2019	15	81	0.259	0.741	0.200	0.467	0.333
	Ac2	2016	0	-	-	-	-	-	-
		2017	0	-	-	-	-	-	-
		2018	5	24	0.333	0.667	0.600	0.400	0.000
		2019	2	3	0.333	0.667	0.500	0.000	0.500
Asarum minamitanianum	Am1	2016	10	71	0.099	0.901	0.100	0.300	0.600
		2017	5	31	0.258	0.742	0.200	0.200	0.600
		2018	5	48	0.021	0.979	0.000	0.200	0.800
		2019	1	3	0.000	1.000	0.000	0.000	1.000
	Am2	2016	7	47	0.298	0.702	0.286	0.000	0.714
		2017	9	67	0.209	0.791	0.222	0.000	0.778
		2018	12	94	0.096	0.904	0.000	0.083	0.917
		2019	4	28	0.000	1.000	0.000	0.000	1.000

Table S26. The estimated fixed effects (mean and 95% CIs) of the best and the competitive models (delta WAIC < 2) for each reproductive character (fruiting rate and selfing rate) obtained from the Bayesian GLMM analysis.

Models	WAIC	Fixed effects	Mean	95%CI (lower)	95%CI (upper)
(Fruiting) ~ N_flower2 + (1|Population) + (1|Year) + (1|Mother)	512.5	Intercept	-2.02	-3.32	-0.65
		N_flower2	0.09	0.01	0.17
(Fruiting) ~ Species + N_flower2 + (1|Population) + (1|Year) + (1|Mother)	512.8	Intercept (*A. costatum*)	-2.50	-4.16	-0.87
		Species (*A. minamitanianum*)	0.76	-1.83	2.75
		N_flower2	0.10	0.02	0.18
(Selfing) ~ Species + N_flower + (1|Population) + (1|Population:Year) + (1|Population:Year:Fruits ID)	218.5	Intercept (*A. costatum*)	0.24	-4.69	5.60
		Species (*A. minamitanianum*)	-5.73	-12.77	0.13
		N_flower2	-0.01	-0.51	0.45
(Selfing) ~ Species + N_flower + (1|Population) + (1|Population:Year) + (1|Population:Year:Fruits ID)	219.0	Intercept (*A. costatum*)	-2.59	-7.49	2.27
		Species (*A. minamitanianum*)	-4.93	-11.19	0.94
		N_flower	1.81	0.13	3.86
(Selfing) ~ Species + N_flower1 + (1|Population) + (1|Population:Year) + (1|Population:Year:Fruits ID)	219.1	Intercept (*A. costatum*)	-0.79	-5.65	4.93
		Species (*A. minamitanianum*)	-5.40	-12.36	0.83
		N_flower1	0.35	-0.58	1.26
(Selfing) ~ Species + N_flower3 + (1|Population) + (1|Population:Year) + (1|Population:Year:Fruits ID)	219.2	Intercept (*A. costatum*)	-1.30	-6.91	4.40
		Species (*A. minamitanianum*)	-4.94	-11.71	1.22
		N_flower3	0.15	-0.18	0.54
(Selfing) ~ Species + (1|Population) + (1|Population:Year) + (1|Population:Year:Fruits ID)	219.6	Intercept (*A. costatum*)	0.05	-3.79	4.63
		Species (*A. minamitanianum*)	-5.48	-11.15	0.27

Table S27. The identified families of collected Diptera species.

Sample ID	Family name	Species	Population	Date	Collected time
17-1-1	Sphaeroceridae	*A. costatum*	Ac1	20170503	20
18-1-1	Cecidomyiidae	*A. costatum*	Ac1	20180505	9
18-1-7	Chironomidae	*A. costatum*	Ac1	20180505	12
18-1-8	Chironomidae	*A. costatum*	Ac1	20180505	12
18-1-19	Chironomidae	*A. costatum*	Ac1	20180506	10
18-1-26	Cecidomyiidae	*A. costatum*	Ac1	20180506	16
18-1-38	Sciaridae	*A. costatum*	Ac1	20180510	11
18-1-39	Sciaridae	*A. costatum*	Ac1	20180510	11
18-1-40	Sciaridae	*A. costatum*	Ac1	20180510	11
18-1-56	Sciaridae	*A. costatum*	Ac1	20180510	15
18-1-63	Sciaridae	*A. costatum*	Ac1	20180510	17
19-1-49	Dorosophilidae	*A. costatum*	Ac1	20190430	14
17-2-3	Chironomidae	*A. minamitanianum*	Am2	20170429	12
17-2-4	Sciaridae	*A. minamitanianum*	Am2	20170429	19
17-2-5	Cecidomyiidae	*A. minamitanianum*	Am2	20170429	11
17-2-6	unidentified	*A. minamitanianum*	Am2	20170430	13
17-2-7	Sciaridae	*A. minamitanianum*	Am2	20170430	13
17-2-8	Phoridae	*A. minamitanianum*	Am2	20170430	13
17-2-2	Chironomidae	*A. minamitanianum*	Am2	20170501	1
17-2-9	Sciaridae	*A. minamitanianum*	Am2	20170501	2
17-2-10	Cecidomyiidae	*A. minamitanianum*	Am2	20170501	2
18-2-5	Psychodidae	*A. minamitanianum*	Am2	20180427	11
18-2-7	Sciaridae	*A. minamitanianum*	Am2	20180427	14
18-2-17	Chironomidae	*A. minamitanianum*	Am2	20180428	14
18-2-18	Cecidomyiidae	*A. minamitanianum*	Am2	20180428	17
18-2-19	Cecidomyiidae	*A. minamitanianum*	Am2	20180428	17
18-2-37	Cecidomyiidae	*A. minamitanianum*	Am2	20180429	18
18-2-38	Phoridae	*A. minamitanianum*	Am2	20180430	14
18-2-41	Mycetophilidae	*A. minamitanianum*	Am2	20180501	11
18-2-45	Chironomidae	*A. minamitanianum*	Am2	20180501	13
18-2-52	Cecidomyiidae	*A. minamitanianum*	Am2	20180501	16
19-2-10	unidentified	*A. minamitanianum*	Am1	20190419	10
19-2-20	Chironomidae	*A. minamitanianum*	Am1	20190420	15

Table S28. PERMANOVA result for the floral visitor compositions.

Source of variation	df	SS	R^2	*F*	*P*
Species	1	3.369	0.129	12.202	0.001
Year	1	0.674	0.026	2.440	0.026

df: degrees of freedom, SS: sum of squares, *F*; *F*-value by permutation, *P*; *p* values based on 1000 simulations.

Table S29. The results of GLMM analysis and estimated species effect (*A. costatum* vs. *A. minamitanianum*) for visitation frequencies of six taxonomic groups and all visitors.

Response variable	Estimate	Standard error	*t*-statistics	*p* value	AIC value	AIC value of NULL model
Flies	1.012	0.473	2.142	0.032	170.7	172.9
Springtails	1.108	0.307	3.605	< 0.001	254.9	262.1
Mites	0.361	0.360	1.002	0.316	161.2	160.2
Spiders	-0.805	0.368	-2.187	0.029	193.5	196.7
Ants	0.186	0.637	0.292	0.770	139.0	137.2
Beetles	2.502	0.876	2.856	0.004	80.2	85.6
All visitors	0.281	0.153	1.836	0.066	416.0	416.8

Table S30. The materials and results of crossing experiments.

Individual ID	Species	Treatment	Date	Number of seeds
AC1	*Asarum costatum*	Artificial selfing	20190413	10
AC2	*Asarum costatum*	Artificial selfing	20200328	11
AC1	*Asarum costatum*	Artificial selfing	20190413	12
AC2	*Asarum costatum*	Artificial selfing	20200328	27
AC3	*Asarum costatum*	Artificial selfing	20200507	15
AM1	*Asarum minamitanianum*	Artificial selfing	20190304	18
AM2	*Asarum minamitanianum*	Artificial selfing	20190321	25
AM3	*Asarum minamitanianum*	Artificial selfing	20190327	24
AM4	*Asarum minamitanianum*	Artificial selfing	20200325	12
AM5	*Asarum minamitanianum*	Artificial selfing	20200330	12
AC4	*Asarum costatum*	Artificial outcrossing	20190413	18
AC4	*Asarum costatum*	Artificial outcrossing	20190413	19
AC4	*Asarum costatum*	Artificial outcrossing	20190413	18
AC5	*Asarum costatum*	Artificial outcrossing	20190413	12
AC5	*Asarum costatum*	Artificial outcrossing	20190413	10
AM6	*Asarum minamitanianum*	Artificial outcrossing	20190304	24
AM6	*Asarum minamitanianum*	Artificial outcrossing	20190304	16
AM7	*Asarum minamitanianum*	Artificial outcrossing	20200405	22
AM8	*Asarum minamitanianum*	Artificial outcrossing	20190304	11
AM9	*Asarum minamitanianum*	Artificial outcrossing	20190304	8
AC1	*Asarum costatum*	Only bugging	20190416	0
AC1	*Asarum costatum*	Only bugging	20190416	0
AC6	*Asarum costatum*	Only bugging	20190416	0
AC7	*Asarum costatum*	Only bugging	20190413	0
AC7	*Asarum costatum*	Only bugging	20190413	0
AM10	*Asarum minamitanianum*	Only bugging	20190304	0
AM11	*Asarum minamitanianum*	Only bugging	20190304	0
AM12	*Asarum minamitanianum*	Only bugging	20190304	0
AM12	*Asarum minamitanianum*	Only bugging	20190304	0
AM13	*Asarum minamitanianum*	Only bugging	20190304	0

General Discussion

In this study, I investigated the evolutionary history and the mechanisms for generating the floral diversity of *Heterotropa* in the SJFR. As reported by previous phylogenetic and phylogeographic studies (reviewed in Qiu et al., 2011), my results showed the range fragmentation and contractions during the Pleistocene period would have triggered diversification of *Heterotropa* especially in eastern insular systems (Chapters 1 & 2). These results basically supported the Qian & Ricklefs's (2001) hypothesis that the topographic complexities and climatic oscillations during the Pleistocene period could have generated diversity of temperate plants through allopatric speciation. Besides to geographic isolation, several studies have indicated that range shifts and formation of refugia due to climate changes could have also provided opportunities for secondary contact and subsequent hybridization (Eriksen and Topel, 2006, Medail and Diadema, 2009). Within series *Sakawanum*, my ABC analysis and ENMs implied the multiple admixture events resulted from range shifts were likely to produce hybrid taxa during the Pleistocene period (Chapter 3). This implies that secondary contacts would have also contributed to formation of the species diversity in *Heterotropa*.

In addition, speciation triggered by floral trait differentiations without geographic isolation could have also occurred in *Heterotropa* (Chapter 2). I hypothesised that flower-pollinator interactions would be concerned with the floral trait diversification in *Heterotropa*. By using series *Sakawanum*, which shows intertaxonomic clinal variation, I tested this hypothesis. Although the secondary contacts produced intermediate taxa within the series, it remained unclear whether calyx lobe length of each taxon was maintained by natural selection. My Q_{CT}-F_{ST} analysis showed that in all taxa pairs, the degrees of neutral genetic differentiations were significantly lower than the morphological differentiations, indicating that natural selection would contribute to maintaining their calyx lobe lengths (Chapter 4). The flowers with extended floral organs are also observed in other families (e.g. Annonaceae, Asparagaceae, Dioscoreaceae, and Orchidaceae), and it has been reported that such flowers were pollinated by flies (Endara et al., 2010, Lim and Raguso, 2017, Guo et al., 2019). In *A. asperum*, which is related species to series *Sakawanum* and has short calyx lobe, ground dwelling insects observed in its flowers (Okamoto and Kanoh, 1977). These considerations lead us to expect that extended calyx lobe of *A. minamitanianum* would have evolved as the results of pollinator mediated selection concerning fly pollination. To obtain the evolutionary insights into the calyx lobe extension and to infer ecological consequence of floral traits evolution, I conducted fine-scale spatial genetic analysis, multi-year floral visitor observations, paternity analysis, crossing experiments using *A. minamitanianum* and *A. costatum* (Chapter 5). The results showed that, although flies were observed in both species, visitation frequency of flies was significantly higher in *A. minamitanianum*. It has been reported that elongated filiform appendages could increase the display size, or act as landing platforms of flies (Policha et al., 2016, Katsuhara et al., 2017). Thus, there is a possibility that the extended calyx lobe of *A. minamitanianum* could be concerned with the attractions of flies, while its attraction mechanism remained unclear. In addition, *A. minamitanianum* conducted predominantly outcrossing, whereas *A. costatum* showed a wide range of selfing rate among fruits. The difference of mating system could be associated with the difference of floral visitor compositions, especially visitation frequencies of flies and large ground dwelling insects (isopods and amphipods), and the difference of floral morphology (calyx lobe length and stigma anther distance) between the two species. I considered that extended calyx lobe of *A. minamitanianum* might evolve for effective pollen dispersal by flies. Thereby, I concluded that a part of floral diversity in *Heterotropa* would be resulted from pollinator mediated selection.

My study also revealed the multiple aspects of reproductive ecology of *Heterotropa*. In the SJFR, there have been numerous studies reporting a part of reproductive ecology of temperate plants; pollinations (reviewed in Funamoto, 2019), seed dispersals (Corlett, 2011, Naoe et al., 2011, Tanaka et al., 2015), germinations (Kondo et al., 2006, Ma et al., 2012, Walck et al., 2002, Kawano et al., 2020), and seedling establishments (Kajimoto, 2002, Tokuoka et al., 2011, Han et al., 2018). However, multiple aspects of reproductive ecology have been revealed in limited species; e.g. *Magnolia stellata* (Tamaki et al., 2009, Hirayama et al., 2007, Setsuko et al., 2008), *Fagus crenata* (Yasumura et al., 2006, Hanaoka et al., 2007, Oddou-Muratorio et al., 2010, Terazawa, 1997), and *Trillium* spp. (Kawano et al., 2020, Tomimatsu and Ohara, 2003, Yamagishi et al., 2007, Kubota and Ohara, 2009). To the best of my knowledge, my study is the first comprehensive study reporting reproductive ecology of perennial herbs growing under warm-

temperate evergreen forests in this region. *Heterotropa* species showed, self-compatibility, possible pollination by ground dwelling insects and/or flies, long flowering time, low fruiting rates due to pollen limitation, strong SGS caused by the low seed dispersal distances, inbreeding depression at the late-stage, and long life-span. These reproductive characters are observed in long-lived tree species (Tamaki et al., 2009, Aleksic et al., 2017, Isagi et al., 2007), which are considered to sustain populations in a long period. During the Pleistocene period, the climatic oscillations strongly impacted the vegetation (Harrison et al., 2001) and the insect fauna (Tojo et al., 2017) of the SJFR. Population isolation and population size decline generally can lead loss of genetic diversity (Montgomery et al., 2000), and reduced genetic diversity would increase population extinction rate and reduce evolutionally potential to environmental changes (Fraser and Bernatchez, 2001). As shown in genetic researches using microsatellite markers, *Heterotropa* species have relatively high genetic diversities regardless of the distribution ranges; H_E = 0.732 - 0.781 in series *Sakawanum* taxa (Chapter 3), 0.781 and 0.782 in two species of Amami Islands (Matsuda and Setoguchi, 2012), and 0.643 in *A. takaoi* (Takahashi et al., unpublished). In contrast, although my study indicated *Heterotropa* species produced selfing seeds to some extent, the values of inbreeding coefficients are not so high; F_{IS} = 0.211 - 0.220 in series *Sakawanum*, 0.201 and 0.317 in Amami Islands, and 0.131 in *A. takaoi*. I consider that the estimated reproductive characters of *Heterotropa* would be linked with the maintenance of genetic diversity. Although the low dispersal ability promoted the population isolation of *Heterotropa*, the self-compatibility and the long flowering time would sustain populations even in environments with limited pollinators. The late-stage inbreeding depression and the longevity would mitigate loss of the genetic diversity. Thus, these reproductive characters could have also contributed to the diversification of this section in the SJFR.

Although both biotic and abiotic factors have long been recognized as fundamental drivers of diversity, many studies conducted in the SJFR have only discussed the role of abiotic drivers and their relative contributions to the diversification had been rarely investigated especially by using specious plant groups. Overall, my study revealed that geographic range shifts caused by the past climatic events would have caused isolations and secondary contacts of populations, and biotic drivers, especially the interactions of pollinators would have subsequently promoted the diversification of *Heterotropa*. My finding would contribute to the understanding of the diversification process and the mechanisms of temperate plants in the SJFR.

Acknowledgements

First of all, I'm extremely grateful to my supervisor, Prof. H. Setoguchi (Kyoto University), for giving me the opportunity to study in his laboratory, and for providing valuable comments and continued supports to my researches in the eight years. I appreciate all his enthusiasm, motivation, patience, and immense knowledge. Without his fruitful guidance and helpful feedbacks, I could not have conducted all of my researches. I'm also extremely grateful to Dr. S. Sakaguchi (Kyoto University) for supporting my researches and myself all the time, and for his constructive suggestions regarding population genetics, ecology, field works, cultivation, academia, and natural history. In addition, I'm deeply grateful to Dr. T. Teramine (Kochi Gakuen College) for his generous supports to my filed works, for giving me warm encouragements, and for providing precious comments on my researches. I'd like to express my thanks to Profs. H. Setoguchi, T. Itioka and M. Kato for reviewing my dissertation and providing fruitful comments on my research.

I gratefully thank to Profs. YX. Qiu (Zhejiang University) and Y. Isagi (Kyoto University) for giving me the opportunity to join the international projects and for supporting my field trips and molecular experiments. For their huge contributions to collecting samples in mainland China and Taiwan, I would like to thank Dr. Y. Feng (Zhejiang University), Dr. P. Li (Zhejiang University), Dr. RS. Lu (Chinese Academy of Sciences), Dr. CT. Lu (National Chiayi University), Dr. SW. Chung (Taiwan Forestry Research Institute), Mr. YS. Lin (Miaoli Distinct Agricultural Research and Extension station), Mr. YC. Chen (Miaoli Distinct Agricultural Research and Extension station). I also thank Dr. A.J. Nagano (Ryukoku University), and Dr. L. Kawaguchi (Ryukoku University) for technical and experimental supports of my RAD-seq analysis.

I deeply acknowledge Dr. H. Ikeda (Okayama University) for providing appropriate advices to my studies, Dr. M. Yamasaki (Kyoto University) for comments on the statistical analyses, Dr. J.R.P. Worth (Forestry and Forest Products Research Institute) for English proofing and profitable feedbacks to my researches, Mr. J. Nagasawa (Kyoto Prefectural University) for helpful comments about cultivation and natural history of *Asarum* species and for giving me precious samples, Dr. M. Yamamoto (Hyogo University of Teacher Education) for helps to conduct field works and beneficial discussion, Dr. S. Kameoka (Doshisha University) for always caring about me in the laboratory and for helping pollination researches, Dr. T. Ito (Tohoku University) for kindly discussing on my studies and collecting samples, Dr. K. Mochizuki (Tokyo University) for identification of Diptera species, Dr. N. Ishikawa (Osaka Prefectural University) for providing valuable insights into developmental bases of *Asarum* flowers, Dr. R. Imai (Ryukyu University) for his helpful comments on genetic analysis, Ms. Y. Umetsu for providing research assistance, and Mr. M. Tanaka (Kumamoto Prefectural Agricultural Research Center) for helps with sampling and taxonomic determination. I sincerely thank Dr. S. Gale (Hongkong University), Ms. S. Iwata (Kyoto University), Mr. S. Liao (Chinese Academy of Sciences), Mr. K. Maeda (Aichi Prefecture), Mr. R. Nakamasu (Kyoto University), Mr. S. Nemoto (Tokyo University), Mr. T. Tanada (Kyoto University), and Dr. SS. Zhou (Zhejiang University) for their helps with sampling and field works. I greatly appreciate continuous helps and warm encouragements given by all the members in Setoguchi laboratory.

This work was supported by Grants-in-Aid for Scientific Research from the Japan Society for the Promotion of Science (Nos. 24247013, 26304013 and 18J22919), the Environment Research and Technology Development Fund (grant no. 4-1702 and 4-1902), and the Environmental Research and Technology Development Fund of the Ministry of the Environment SICORP Program of the Japan Science and Technology Agency (grant no. 4-1403).

Reference list

Adams SM, Lindmeier JB, Duvernell DD. 2006. Microsatellite analysis of the phylogeography, Pleistocene history and secondary contact hypotheses for the killifish, Fundulus heteroclitus. *Molecular Ecology,* **15**: 1109-1123.

Akasawa Y. 1985. Natulae ad plantas sikkokianae XII. *Kochi Women's University. Series of Natural science.,* **33**: 11-14.

Akasawa Y, Shinma M. 1984. Study of *Asarum* in Shikoku I (In Japanese). *Botany in Kochi Prefecture* **7**: 32-89.

Aleksic JM, Piotti A, Geburek T, Vendramin GG. 2017. Exploring and conserving a "microcosm": whole-population genetic characterization within a refugial area of the endemic, relict conifer Picea omorika. *Conservation Genetics,* **18**: 777-788.

Anacker BL, Strauss SY. 2014. The geography and ecology of plant speciation: range overlap and niche divergence in sister species. *Proceedings of the Royal Society B-Biological Sciences,* **281**.

Anton KA, Ward JR, Cruzan MB. 2013. Pollinator-mediated selection on floral morphology: evidence for transgressive evolution in a derived hybrid lineage. *Journal of Evolutionary Biology,* **26**: 660-673.

Antoniazza S, Burri R, Fumagalli L, Goudet J, Roulin A. 2010. Local adaptation maintains clinal variation in melanin-based coloration of European barn owls (*Tyto alba*). *Evolution,* **64**: 1944-1954.

Antoniazza S, Kanitz R, Neuenschwander S, Burri R, Gaigher A, Roulin A, Goudet J. 2014. Natural selection in a postglacial range expansion: the case of the colour cline in the European barn owl. *Molecular Ecology,* **23**: 5508-5523.

Aoki K, Kato M, Murakami N. 2011. Phylogeography of phytophagous weevils and plant species in broadleaved evergreen forests: a congruent genetic gap between western and eastern parts of Japan. *Insects,* **2**: 128-150.

Aoki K, Suzuki T, Hsu TW, Murakami N. 2004. Phylogeography of the component species of broad-leaved evergreen forests in Japan, based on chloroplast DNA variation. *Journal of Plant Research,* **117**: 77-94.

Aoki K, Tamaki I, Nakao K, Ueno S, Kamijo T, Setoguchi H, Murakami N, Kato M, Tsumura Y. 2019. Approximate Bayesian computation analysis of EST-associated microsatellites indicates that the broadleaved evergreen tree *Castanopsis sieboldii* survived the Last Glacial Maximum in multiple refugia in Japan. *Heredity,* **122**: 326.

Aoki K, Ueno S, Kamijo T, Setoguchi H, Murakami N, Kato M, Tsumura Y. 2014. Genetic differentiation and genetic diversity of *Castanopsis* (Fagaceae), the dominant tree species in Japanese broadleaved evergreen forests, revealed by analysis of EST-associated microsatellites. *PloS one,* **9**: e87429.

Araki Y. 1937. The species of *Asarum* in the Santan District. *Acta Phytotaxonomica et Geobotanica,* **6**: 122-135.

Araki Y. 1953. Systema generis Asari. *Acta Phytotaxonomica et Geobotanica,* **15**: 33-36.

Armbruster WS. 2014. Floral specialization and angiosperm diversity: phenotypic divergence, fitness trade-offs and realized pollination accuracy. *Aob Plants,* **6**.

Baena-Diaz F, Fornoni J, Sosenski P, Molina-Freaner FE, Weller SG, Perez-Ishiwara R, Dominguez CA. 2012. Changes in reciprocal herkogamy during the tristyly-distyly transition in *Oxalis alpina* increase efficiency in pollen transfer. *Journal of Evolutionary Biology,* **25**: 574-583.

Bailey CD, Doyle JJ. 1999. Potential phylogenetic utility of the low-copy nuclear gene *pistillata* in dicotyledonous plants: Comparison to nrDNA ITS and *trnL* intron in *Sphaerocardamum* and other Brassicaceae. *Molecular Phylogenetics and Evolution,* **13**: 20-30.

Bandelt H-J, Forster P, Röhl A. 1999. Median-joining networks for inferring intraspecific phylogenies. *Molecular biology and evolution,* **16**: 37-48.

Barrett SCH, Spencer CH. 2013. The evolution of plant reproductive systems: how often are transitions irreversible? *Proceedings of the Royal Society B: Biological Sciences,* **280**: 20130913.

Barringer K, Whittemore TA. 1993. *Aristolochiaceae*: Oxford University Press, New York, NY.

Barton NH, Hewitt GM. 1985. Analysis of hybrid zones. *Annual Review of Ecology and Systematics,* **16**: 113-148.

Bates D, Machler M, Bolker BM, Walker SC. 2015. Fitting Linear Mixed-Effects Models Using lme4. *Journal of Statistical Software,* **67**: 1-48.

Beattie AJ, Culver DC. 1981. The guide of mymecochores in the herbaceous flora of west Virginia forests. *Ecology,* **62**: 107-115.

Beaumont MA, Zhang WY, Balding DJ. 2002. Approximate Bayesian computation in population genetics. *Genetics,* **162**: 2025-2035.

Bergland AO, Tobler R, Gonzalez J, Schmidt P, Petrov D. 2016. Secondary contact and local adaptation contribute to genome-wide patterns of clinal variation in *Drosophila melanogaster*. *Molecular Ecology,* **25**: 1157-1174.

Bertin RI. 1988. *Paternity in plants*: Oxford University Press on Demand.

Bertorelle G, Benazzo A, Mona S. 2010. ABC as a flexible framework to estimate demography over space and time: some cons, many pros. *Molecular Ecology,* **19**: 2609-2625.

Blomquist HL. 1957. A Revision of Hexastylis of North America. *Brittonia,* **8**: 255.

Bolger AM, Lohse M, Usadel B. 2014. Trimmomatic: a flexible trimmer for Illumina sequence data. *Bioinformatics,* **30**: 2114-2120.

Bolker B, Skaug H, Magnusson A, Nielsen A. 2012. Getting started with the glmmADMD package. *R Foundation for Statistical Computing, Vienna, Austria.*

Boucher FC, Zimmermann NE, Conti E. 2016. Allopatric speciation with little niche divergence is common among alpine Primulaceae. *Journal of Biogeography,* **43**: 591-602.

Braun ACH. 1861. Index seminum Horti Botanici Berolinensis: Appendix Plantarum Novrum et minus cognitarum quea in Horto region botanico Berolinensi coluntur.

Bremer B, Jansen RK, Oxelman B, Backlund M, Lantz H,

Kim KJ. 1999. More characters or more taxa for a robust phylogeny - Case study from the coffee family (Rubiaceae). *Systematic Biology,* **48**: 413-435.

Bridle JR, Vines TH. 2007. Limits to evolution at range margins: when and why does adaptation fail? *Trends in Ecology & Evolution,* **22**: 140-147.

Brys R, Broeck AV, Mergeay J, Jacquemyn H. 2014. The contribution of mating system variation to reproductive isolation in two closely related *Centaurium* species (Gentianaceae) with a generalized flower morphology. *Evolution,* **68**: 1281-1293.

Buehler D, Graf R, Holderegger R, Gugerli F. 2012. Contemporary gene flow and mating system of *Arabis alpina* in a Central European alpine landscape. *Annals of Botany,* **109**: 1359-1367.

Burkner PC. 2017. brms: An R Package for Bayesian Multilevel Models Using Stan. *Journal of Statistical Software,* **80**: 1-28.

Caddah MK, Mayer JLS, Bittrich V, Do Amaral MDE. 2012. Species limits in the *Kielmeyera coriacea* complex (Calophyllaceae) - a multidisciplinary approach. *Botanical Journal of the Linnean Society,* **168**: 101-115.

Campitelli BE, Stinchcombe JR. 2013. Natural selection maintains a single-locus leaf shape cline in Ivyleaf morning glory, *Ipomoea hederacea*. *Molecular Ecology,* **22**: 552-564.

Caruso CM, Eisen KE, Martin RA, Sletvold N. 2019. A meta-analysis of the agents of selection on floral traits. *Evolution,* **73**: 4-14.

Chapuis MP, Estoup A. 2007. Microsatellite null alleles and estimation of population differentiation. *Molecular Biology and Evolution,* **24**: 621-631.

Charlesworth D, Charlesworth B. 1987. Inbreeding depression and its evolutionary consequences. *Annual Review of Ecology and Systematics,* **18**: 237-268.

Chen ML. 2009. Comparative reproductive biology of *Primula merrilliana* Schltr. and *P. cicutariifolia* Pax. *Plant Systematics and Evolution,* **278**: 23-32.

Cheng CY, Yang CS. 1983. A synopsis of the chinese species of *Asarum* (Aristolochiaceae). *Journal of the Arnold Arboretum,* **64**: 565-597.

Chiang TY. 2000. Lineage sorting accounting for the disassociation between chloroplast and mitochondrial lineages in oaks of southern France. *Genome,* **43**: 1090-1094.

Chiang TY, Schaal BA. 2006. Phylogeography of plants in Taiwan and the Ryukyu archipelago. *Taxon,* **55**: 31-41.

Chiang YC, Hung KH, Schaal BA, Gest XJ, Hsu TW, Chiang TY. 2006. Contrasting phylogeographical patterns between mainland and island taxa of the *Pinus luchuensis* complex. *Molecular Ecology,* **15**: 765-779.

Chou YW, Thomas PI, Ge XJ, LePage BA, Wang CN. 2011. Refugia and phylogeography of Taiwania in East Asia. *Journal of Biogeography,* **38**: 1992-2005.

Collins WD, Bitz CM, Blackmon ML, Bonan GB, Bretherton CS, Carton JA, Chang P, Doney SC, Hack JJ, Henderson TB, Kiehl JT, Large WG, McKenna DS, Santer BD, Smith RD. 2006. The Community Climate System Model version 3 (CCSM3). *Journal of Climate,* **19**: 2122-2143.

Conran JG, Bradbury JH. 2007. Aspidistras, amphipods and Oz: Niche opportunism between strangers in a strange land. *Plant Species Biology,* **22**: 41-48.

Cornuet JM, Santos F, Beaumont MA, Robert CP, Marin JM, Balding DJ, Guillemaud T, Estoup A. 2008. Inferring population history with DIY ABC: a user-friendly approach to approximate Bayesian computation. *Bioinformatics,* **24**: 2713-2719.

Craft KJ, Ashley MV, Koenig WD. 2002. Limited hybridization between Quercus lobata and *Quercus douglasii* (Fagaceae) in a mixed stand in central coastal California. *American Journal of Botany,* **89**: 1792-1798.

Crawley SS, Hilu KW. 2012. Impact of missing data, gene choice, and taxon sampling on phylogenetic reconstruction: the *Caryophyllales* (angiosperms). *Plant Systematics and Evolution,* **298**: 297-312.

Currat M. 2012. Consequences of population expansions on European genetic diversity. *Populations Dynamics in Pre-and Early History. New Approaches by Stable Isotopes and Genetics*: 3-15.

Dakin EE, Avise JC. 2004. Microsatellite null alleles in parentage analysis. *Heredity,* **93**: 504-509.

Devaux C, Lande R. 2008. Incipient allochronic speciation due to non-selective assortative mating by flowering time, mutation and genetic drift. *Proceedings of the Royal Society B-Biological Sciences,* **275**: 2723-2732.

Doyle J, Doyle JL. 1987. Genomic plant DNA preparation from fresh tissue-CTAB method. *Phytochem Bull,* **19**: 11-15.

Drummond AJ, Rambaut A. 2007. BEAST: Bayesian evolutionary analysis by sampling trees. *Bmc Evolutionary Biology,* **7**: 8.

Drummond AJ, Suchard MA, Xie D, Rambaut A. 2012. Bayesian Phylogenetics with BEAUti and the BEAST 1.7. *Molecular Biology and Evolution,* **29**: 1969-1973.

Duchartre P. 1864. *Aristolochiaceae*. In: A. P. de Candolle and A. L. P. de Candolle, eds. 1823-1873. Prodromus Systematis Naturalis Regni Vegetabilis.... 17 vols. Paris etc. Vol. 15, pp. 421-498.

Earl DA, Vonholdt BM. 2012. STRUCTURE HARVESTER: a website and program for visualizing STRUCTURE output and implementing the Evanno method. *Conservation Genetics Resources,* **4**: 359-361.

Endara L, Grimaldi D, Roy B. 2010. Lord of the flies: pollination of *Dracula* orchids. *Lankesteriana,* **10**.

Endler JA. 1973. Gene flow and Population Differentiation Studies of clines suggest that differentiation along environmental gradients may be independent of gene flow. *Science,* **179**: 243-250.

Eriksen B, Topel MH. 2006. Molecular phylogeography and hybridization in members of the circumpolar *Potentilla* sect. *Niveae* (Rosaceae). *American Journal of Botany,* **93**: 460-469.

Etterson JR, Schneider HE, Gorden NLS, Weber JJ. 2016. Evolutionary insights from studies of geographic variation: Contemporary variation and looking to the future. *American Journal of Botany,* **103**: 5-9.

Evanno G, Regnaut S, Goudet J. 2005. Detecting the number of clusters of individuals using the software STRUCTURE: a simulation study. *Molecular*

Ecology, **14**: 2611-2620.

Excoffier L, Foll M, Petit RJ. 2009. Genetic Consequences of Range Expansions. *Annual Review of Ecology Evolution and Systematics,* **40**: 481-501.

Excoffier L, Lischer HEL. 2010. Arlequin suite ver 3.5: a new series of programs to perform population genetics analyses under Linux and Windows. *Molecular Ecology Resources,* **10**: 564-567.

Excoffier L, Smouse PE, Quattro JM. 1992. Analysis of molecular variance inferred from metric distances among DNA haplotypes: application to human mitochondrial DNA restriction data. *Genetics,* **131**: 479-491.

Faegri K, Van Der Pijl L. 2013. *Principles of pollination ecology*: Elsevier.

Felsenstein J. 1976. The theoretical population genetics of variable selection and migration. *Annual review of genetics,* **10**: 253-280.

Felsenstein J. 1985. Confidence-limits on phylogenies - An approach using the bootstrap. *Evolution,* **39**: 783-791.

Fenster CB, Armbruster WS, Wilson P, Dudash MR, Thomson JD. 2004. Pollination syndromes and floral specialization. *Annual Review of Ecology Evolution and Systematics,* **35**: 375-403.

Fenster CB, Marten-Rodriguez S. 2007. Reproductive assurance and the evolution of pollination specialization. *International Journal of Plant Sciences,* **168**: 215-228.

Fenster CB, Ritland K. 1994. Evidence for natural selection on mating system in *Mimulus* (Scrophulariaceae). *International journal of plant sciences,* **155**: 588-596.

Fielding AH, Bell JF. 1997. A review of methods for the assessment of prediction errors in conservation presence/absence models. *Environmental Conservation,* **24**: 38-49.

Fuller G. 1994. Observations on the pollination of Corybas "A". *NZNOGJ,* **52**: 18-22.

Funamoto D. 2019. Plant-pollinator interactions in east Asia: A review. *Journal of Pollination Ecology,* **25**: 46-68.

Gaddy LL. 1987. A review of the taxonomy and biogeography of *Hexastylis* (Aristolochiaceae). *Castanea,* **52**: 186-196.

Gadgil M, Bossert WH. 1970. Life historical consequences of natural selection. *American Naturalist*: 1-24.

Galen C, Stanton ML. 1989. Bumble bee pollination and floral morphology: factors influencing pollen dispersal in the alpine sky pilot, *Polemonium viscosum* (Polemoniaceae). *American Journal of Botany,* **76**: 419-426.

Gao H, Williamson S, Bustamante CD. 2007. A Markov chain Monte Carlo approach for joint inference of population structure and inbreeding rates from multilocus genotype data. *Genetics,* **176**: 1635-1651.

Gao YD, Zhang Y, Gao XF, Zhu ZM. 2015. Pleistocene glaciations, demographic expansion and subsequent isolation promoted morphological heterogeneity: A phylogeographic study of the alpine *Rosa sericea* complex (Rosaceae). *Scientific Reports,* **5**.

Garza JC, Williamson EG. 2001. Detection of reduction in population size using data from microsatellite loci. *Molecular Ecology,* **10**: 305-318.

Gaudeul M, Till-Bottraud I. 2004. Reproductive ecology of the endangered alpine species *Eryngium alpinum* L. (Apiaceae): Phenology, gene dispersal and reproductive success. *Annals of Botany,* **93**: 711-721.

Gevaert SD, Mandel JR, Burke JM, Donovan LA. 2013. High Genetic Diversity and Low Population Structure in Porter's Sunflower (*Helianthus porteri*). *Journal of Heredity,* **104**: 407-415.

Ghazoul J. 2006. Floral diversity and the facilitation of pollination. *Journal of Ecology,* **94**: 295-304.

Givnish TJ. 2010. Ecology of plant speciation. *Taxon,* **59**: 1326-1366.

Givnish TJ, Spalink D, Ames M, Lyon SP, Hunter SJ, Zuluaga A, Iles WJD, Clements MA, Arroyo MTK, Leebens-Mack J, Endara L, Kriebel R, Neubig KM, Whitten WM, Williams NH, Cameron KM. 2015. Orchid phylogenomics and multiple drivers of their extraordinary diversification. *Proceedings of the Royal Society B-Biological Sciences,* **282**: 171-180.

Goldblatt P, Bernhardt P, Vogan P, Manning JC. 2004. Pollination by fungus gnats (Diptera : Mycetophilidae) and self-recognition sites in *Tolmiea menziesii* (Saxifragaceae). *Plant Systematics and Evolution,* **244**: 55-67.

Goldstein DB, Linares AR, Cavallisforza LL, Feldman MW. 1995. Genetic absolute dating based on microsatellites and the origin of modern humans. *Proceedings of the National Academy of Sciences of the United States of America,* **92**: 6723-6727.

Gonzalez F, Rudall PJ. 2003. Structure and development of the ovule and seed in Aristolochiaceae, with particular reference to *Saruma*. *Plant Systematics and Evolution,* **241**: 223-244.

Goodwillie C, Sargent RD, Eckert CG, Elle E, Geber MA, Johnston MO, Kalisz S, Moeller DA, Ree RH, Vallejo-Marin M, Winn AA. 2010. Correlated evolution of mating system and floral display traits in flowering plants and its implications for the distribution of mating system variation. *New Phytologist,* **185**: 311-321.

Gorb SN, Gorb EV. 1995. Removal rates of seeds of five myrmecochorous plants by the ant *Formica polyctena* (Hymenoptera: Formicidae). *Oikos,* **73**: 367-374.

Gould SJ, Johnston RF. 1972. Geographic variation. *Annual Review of Ecology and Systematics,* **3**: 457-498.

Gould SJ, Lewontin RC. 1979. Spandrels of San-marco and the panglossian padigm - a critique of the adaptation program. *Proceedings of the Royal Society Series B-Biological Sciences,* **205**: 581-598.

Grace JB. 1993. The adaptive significance of clonal reproduction in angiosperms -an aquatic orespectuve. *Aquatic Botany,* **44**: 159-180.

Guindon S, Dufayard JF, Lefort V, Anisimova M, Hordijk W, Gascuel O. 2010. New Algorithms and Methods to Estimate Maximum-Likelihood Phylogenies: Assessing the Performance of PhyML 3.0. *Systematic Biology,* **59**: 307-321.

Guo X, Zhao ZT, Mar SS, Zhang DX, Saunders RMK. 2019. A symbiotic balancing act: arbuscular mycorrhizal specificity and specialist fungus gnat pollination in the mycoheterotrophic genus *Thismia* (Thismiaceae). *Annals of Botany,* **124**: 331-342.

Hahn C, Bachmann L, Chevreux B. 2013. Reconstructing mitochondrial genomes directly from genomic next-generation sequencing reads-a baiting and iterative

mapping approach. *Nucleic Acids Research,* **41**.

Haldane JBS. 1948. The theory of a cline. *Journal of Genetics,* **48**: 277-284.

Hall TA. 1999. BioEdit: a user-friendly biological sequence alignment editor and analysis program for Windows 95/98/NT. *Nucleic acids symposium series*.

Hamrick JL, Murawski DA, Nason JD. 1993. The influence of seed dispersal mechanisms on the genetic structure of tropical tree populations. *Vegetatio,* **108**: 281-297.

Hansen DM, Olesen JM, Mione T, Johnson SD, Muller CB. 2007. Coloured nectar: distribution, ecology, and evolution of an enigmatic floral trait. *Biological Reviews,* **82**: 83-111.

Haq BU, Hardenbol J, Vail PR. 1987. Chronology of fluctuating sea levels since the Triassic. *Science,* **235**: 1156-1167.

Harder LD, Barrett SCH. 1995. Mating cost of large floral displays in hermaphrodite plants. *Nature,* **373**: 512-515.

Harder LD, Johnson SD. 2009. Darwin's beautiful contrivances: evolutionary and functional evidence for floral adaptation. *New Phytologist,* **183**: 530-545.

Hardy OJ, Vekemans X. 2002. SPAGeDi: a versatile computer program to analyse spatial genetic structure at the individual or population levels. *Molecular ecology notes,* **2**: 618-620.

Harrison SP, Yu G, Takahara H, Prentice IC. 2001. Palaeovegetation - Diversity of temperate plants in east Asia. *Nature,* **413**: 129-130.

Hasumi H, Emori S. 2004. K-1 coupled model (MIROC) description. K-1 Technical Report 1. *Center for Climate System Research, University of Tokyo, Tokyo*.

Hatusima S, Yamahata E. 1988. Illegitimately published taxa of *Asarum* from Japan. *J. Phytogeogr. Taxon,* **36**: 1-8.

Hawkins JS, Ramachandran D, Henderson A, Freeman J, Carlise M, Harris A, Willison-Headley Z. 2015. Phylogenetic reconstruction using four low-copy nuclear loci strongly supports a polyphyletic origin of the genus Sorghum. *Annals of Botany,* **116**: 291-299.

Hedrick PW. 1986. Genetic polymorphism in heterogeneous environments: a decade later. *Annual Review of Ecology and Systematics,* **17**: 535-566.

Hedrick PW. 2005. A standardized genetic differentiation measure. *Evolution,* **59**: 1633-1638.

Hey J. 2010. Isolation with Migration Models for More Than Two Populations. *Molecular Biology and Evolution,* **27**: 905-920.

Hijmans RJ, Cameron SE, Parra JL, Jones PG, Jarvis A. 2005. Very high resolution interpolated climate surfaces for global land areas. *International Journal of Climatology,* **25**: 1965-1978.

Hiura I. 1978. The histories traced by the butterfly (in Japanese). Tokyo: Aoki shobou.

Hoelzer GA. 1997. Inferring phylogenies from mtDNA variation: mitochondrial-gene trees versus nuclear-gene trees revisited. *Evolution,* **51**: 622-626.

Holsinger KE. 2000. Reproductive systems and evolution in vascular plants. *Proceedings of the National Academy of Sciences of the United States of America,* **97**: 7037-7042.

Hothorn T, Bretz F, Westfall P, Heiberger R. 2008. Multcomp: simultaneous inference for general linear hypotheses. R Package Version 1.0-3.

Huang CC, Hung KH, Hwang CC, Huang JC, Lin HD, Wang WK, Wu PY, Hsu TW, Chiang TY. 2011. Genetic population structure of the alpine species *Rhododendron pseudochrysanthum* sensu lato (Ericaceae) inferred from chloroplast and nuclear DNA. *Bmc Evolutionary Biology,* **11**: 108.

Huang S, Kelly LM, Gilbert MG. 2003. *Aristolochiaceae*: Science Press.

Huang SSF, Hwang SY, Lin TP. 2002. Spatial pattern of chloroplast DNA variation of Cyclobalanopsis glauca in Taiwan and east Asia. *Molecular Ecology,* **11**: 2349-2358.

Hubisz MJ, Falush D, Stephens M, Pritchard JK. 2009. Inferring weak population structure with the assistance of sample group information. *Molecular Ecology Resources,* **9**: 1322-1332.

Hut RA, Paolucci S, Dor R, Kyriacou CP, Daan S. 2013. Latitudinal clines: an evolutionary view on biological rhythms. *Proceedings of the Royal Society B-Biological Sciences,* **280**.

Huxley JS. 1938. Clines: an auxiliary taxonomic principle. *Nature,* **142**: 219-220.

Huxley JS. 1939. Clines: an auxiliary method in taxonomy. *Bijdr. Dierk,* **27**: 491-520.

Isagi Y, Saito D, Kawaguchi H, Tateno R, Watanabe S. 2007. Effective pollen dispersal is enhanced by the genetic structure of an *Aesculus turbinata* population. *Journal of Ecology,* **95**: 983-990.

Ito M, Nagamasu H, Fujii S, Katsuyama T, Yonekura, Ebihara A, Yahara T. 2016. GreenList ver. 1.01, (http://www.rdplants.org/gl/).

Jakobsson M, Rosenberg NA. 2007. CLUMPP: a cluster matching and permutation program for dealing with label switching and multimodality in analysis of population structure. *Bioinformatics,* **23**: 1801-1806.

Jaramillo MA, Manos PS. 2001. Phylogeny and patterns of floral diversity in the genus *Piper* (Piperaceae). *American Journal of Botany,* **88**: 706-716.

Jombart T. 2008. adegenet: a R package for the multivariate analysis of genetic markers. *Bioinformatics,* **24**: 1403-1405.

Kaiser R. 2006. Flowers and fungi use scents to mimic each other. *Science,* **311**: 806-807.

Kakishima S, Okuyama Y. 2018. Floral scent profiles and flower visitors in species of *Asarum* Series Sakawanum (Aristolochiaceae). *J Bulletin of the National Museum of Nature and Science. Series B, Botany,* **44**: 41-51.

Kakishima S, Okuyama Y. 2020. Further insights into the floral biology of *Asarum tamaense* (sect. *Heterotropa*, Aristolochiaceae). *Bulletin of the National Museum of Nature and Science. Series B, Botany,* **46**: 129-143.

Kalinowski ST, Taper ML, Marshall TC. 2007. Revising how the computer program CERVUS accommodates genotyping error increases success in paternity assignment. *Molecular Ecology,* **16**: 1099-1106.

Kameoka S, Higashi H, Setoguchi H. 2015. Development of polymorphic microsatellite loci in the perennial herb *Hepatica nobilis* var. *japonica* (Ranunculaceae). *Applications in Plant Sciences,* **3**.

Karron JD, Jackson RT, Thumser NN, Schlicht SL. 1997. Outcrossing rates of individual Mimulus ringens

genets are correlated with anther-stigma separation. *Heredity,* **79**: 365-370.

Kato M. 1995. The aspodostra and the amphipod. *Nature,* **377**: 293-293.

Katsuhara K, R., Kitamura S, Ushimaru A. 2017. Functional significance of petals as landing sites in fungus-gnat pollinated flowers of *Mitella pauciflora* (Saxifragaceae). *Functional Ecology*.

Kay KM, Whittall JB, Hodges SA. 2006. A survey of nuclear ribosomal internal transcribed spacer substitution rates across angiosperms: an approximate molecular clock with life history effects. *Bmc Evolutionary Biology,* **6**: 9.

Keenan K, McGinnity P, Cross TF, Crozier WW, Prodohl PA. 2013. diveRsity: An R package for the estimation and exploration of population genetics parameters and their associated errors. *Methods in Ecology and Evolution,* **4**: 782-788.

Keller SR, Sowell DR, Neiman M, Wolfe LM, Taylor DR. 2009. Adaptation and colonization history affect the evolution of clines in two introduced species. *New Phytologist,* **183**: 678-690.

Kelly LM. 1997. A cladistic analysis of *Asarum* (Aristolochiaceae) and implications for the evolution of Herkogamy. *American Journal of Botany,* **84**: 1752-1765.

Kelly LM. 1998. Phylogenetic relationships in *Asarum* (Aristolochiaceae) based on morphology and ITS sequences. *American Journal of Botany,* **85**: 1454-1467.

Kelly LM, Gonzalez F. 2003. Phylogenetic relationships in Aristolochiaceae. *Systematic Botany,* **28**: 236-249.

Kennedy BF, Elle E. 2008. The reproductive assurance benefit of selfing: importance of flower size and population size. *Oecologia,* **155**: 469-477.

Kimura M. 1996. Quaternary paleogeography of the Ryukyu Arc. *Journal of Geography Tokyo,* **105**: 259-285.

Kinoshita S. 1973. Obituary of the Late Mr. Y. Kato. *Journal of Geobotany,* **26**: 109-111.

Kishi K, Irizawa S. 2008. *Wild ginger, Asarum (in Japanese).* Tochigi, Japan: Tochinoha-shobo.

Kizaki K, Oshiro I. 1977. Paleogeography of the Ryukyu Islands. *Marine Science Monthly,* **9**: 542-549.

Kizaki K, Oshiro I. 1980. The origin of the Ryukyu Islands. *Natural history of the Ryukyus. Tsukiji–Shokan, Tokyo*: 8-37.

Klopfstein S, Currat M, Excoffier L. 2006. The fate of mutations surfing on the wave of a range expansion. *Molecular Biology and Evolution,* **23**: 482-490.

Krak K, Caklova P, Chrtek J, Fehrer J. 2013. Reconstruction of phylogenetic relationships in a highly reticulate group with deep coalescence and recent speciation (*Hieracium*, Asteraceae). *Heredity,* **110**: 138-151.

Kume O. 1989. Growing style on the subterranean stem of two *Heterotropa* species in Kagawa prefecture. *Kagawa Seibutsu,* **15**: 81-86.

Kume O. 1993. Life style on subterranean stem of two *Heterotropa* species raised from seeds in Kagawa prefecture. *Kagawa Seibutsu,* **20**: 7-10.

Kuznetsova A, Brockhoff PB, Christensen RHB. 2017. lmerTest Package: Tests in Linear Mixed Effects Models. *Journal of Statistical Software,* **82**: 1-26.

Laaksonen T, Sirkia PM, Calhim S, Brommer JE, Leskinen PK, Primmer CR, Adamik P, Artemyev AV, Belskii E, Both C, Bures S, Burgess MD, Doligez B, Forsman JT, Grinkov V, Hoffmann U, Ivankina E, Kral M, Krams I, Lampe HM, Moreno J, Magi M, Nord A, Potti J, Ravussin PA, Sokolov L. 2015. Sympatric divergence and clinal variation in multiple coloration traits of *Ficedula flycatchers*. *Journal of Evolutionary Biology,* **28**: 779-790.

Lagomarsino LP, Condamine FL, Antonelli A, Mulch A, Davis CC. 2016. The abiotic and biotic drivers of rapid diversification in Andean bellflowers (Campanulaceae). *New Phytologist,* **210**: 1430-1442.

Lande R. 2000. Quantitative genetics and phenotypic evolution. In: Lewontin RC, Krimpas KV, eds. *Evolutionary Genetics: From Molecules to Morphology (Vol. 1)*. Cambridge, UK: Cambridge University Press.

Landrein S, Buerki S, Wang HF, Clarkson JJ. 2017. Untangling the reticulate history of species complexes and horticultural breeds in *Abelia* (Caprifoliaceae). *Annals of Botany,* **120**: 257-269.

Langella O. 2002. Population genetic software, POPULATIONS 1.2. 30. *http://bioinformatics.*

Latta RG. 1998. Differentiation of allelic frequencies at quantitative trait loci affecting locally adaptive traits. *American Naturalist,* **151**: 283-292.

Lavi R, Sapir Y. 2015. Are pollinators the agents of selection for the extreme large size and dark color in *Oncocyclus* irises? *New Phytologist,* **205**: 369-377.

Lim GS, Raguso RA. 2017. Floral visitation, pollen removal, and pollen transport of *Tacca cristata* Jack (Dioscoreaceae) by female Ceratopogonid Midges (Diptera: Ceratopogonidae). *International Journal of Plant Sciences,* **178**: 341-351.

Linder CR, Goertzen LR, Heuvel BV, Francisco-Ortega J, Jansen RK. 2000. The complete external transcribed spacer of 18S-26S rDNA: Amplification and phylogenetic utility at low taxonomic levels in Asteraceae and closely allied families. *Molecular Phylogenetics and Evolution,* **14**: 285-303.

Linder CR, Rieseberg LH. 2004. Reconstructing patterns of reticulate evolution in plants. *American journal of botany,* **91**: 1700-1708.

Lisiecki LE., Raymo ME. 2005. A Pliocene-Pleistocene stack of 57 globally distributed benthic δ18O records. *Paleoceanography*, *20*(1).

Liu BB, Abbott RJ, Lu ZQ, Tian B, Liu JQ. 2014. Diploid hybrid origin of *Ostryopsis intermedia* (Betulaceae) in the Qinghai-Tibet Plateau triggered by Quaternary climate change. *Molecular Ecology,* **23**: 3013-3027.

Liu CR, White M, Newell G. 2013a. Selecting thresholds for the prediction of species occurrence with presence-only data. *Journal of Biogeography,* **40**: 778-789.

Liu HZ, Takeichi Y, Kamiya K, Harada K. 2013b. Phylogeography of *Quercus phillyraeoides* (Fagaceae) in Japan as revealed by chloroplast DNA variation. *Journal of Forest Research,* **18**: 361-370.

Loiselle BA, Sork VL, Nason J, Graham C. 1995. Spatial genetic structure of a tropical understory shrub, *Psychotria officinalis* (Rubiaceae). *American Journal of Botany,* **82**: 1420-1425.

Lu C-T, Chiou W-L, Liu S-C, Wang J-C. 2010. *Asarum satsumense* F. Maekawa (Aristolochiaceae), a newly recorded species in Taiwan. *Taiwania,* **55**: 396-401.

Lu CT, Wang JC. 2009. Three new species of *Asarum* (section *Heterotropa*) from Taiwan. *Botanical Studies,* **50**:

229-240.

Lu CT, Wang JC. 2014. *Asarum ampulliflorum* (Aristolochiaceae), a new species from Taiwan. *Phytotaxa,* **184**: 46-52.

Lu KL. 1982. Pollination biology of *Asarum caudatum* (Aristolochiaceae) in northern California. *Systematic Botany,* **7**: 150-157.

Lu L, Fritsch PW, Matzke NJ, Wang H, Kron KA, Li DZ, Wiens JJ. 2019a. Why is fruit colour so variable? Phylogenetic analyses reveal relationships between fruit-colour evolution, biogeography and diversification. *Global Ecology and Biogeography,* **28**: 891-903.

Lu R-S, Chen Y, Tamaki I, Sakaguchi S, Ding Y-Q, Takahashi D, Li P, Isaji Y, Chen J, Qiu Y-X. 2019b. Pre-Quaternary diversification and glacial demographic expansions of *Cardiocrinum* (Liliaceae) in temperate forest biomes of Sino-Japanese Floristic Region. *Molecular phylogenetics and evolution*: 106693.

Maeda Y. 2013. Distribution and life cycle of the wild gingers (*Asarum*, Aristolochiaseae) on Amami-oshima, South Japan. Kagoshima, Japan: Kagoshima University.

Maekawa F. 1933. Species of *Asarum Journal of Japanese Botany,* **9**: 39-49, 96-103, 174-179, 241-246, 281-285, 364-370, 505-512.

Maekawa F. 1936. Aristolochiaceae. *Flora Sylvatica Koreana,* **21**: 1-28.

Maekawa F. 1953a. Geohistorical distribution of east Asiatic Asaraceae. *Proc. VII Pacific Sci. Congr.(Wellinton),* **5**: 217-219.

Maekawa F. 1953b. Relationship between geological history and the variation in plants. *Democratic Scientists Association of Japan ed., Variability of Organism*: 35-47.

Maekawa F. 1983. *Heterotropa kiusiana*. In: Ishii R, Inoue Y, eds. *Encyclopedia of horticulture*. Tokyo, Japan: Seibundo-Shinkosha.

Marriage TN, Hudman S, Mort ME, Orive ME, Shaw RG, Kelly JK. 2009. Direct estimation of the mutation rate at dinucleotide microsatellite loci in *Arabidopsis thaliana* (Brassicaceae). *Heredity,* **103**: 310.

Matsuda J, Maeda Y, Nagasawa J, Setoguchi H. 2017. Tight species cohesion among sympatric insular wild gingers (*Asarum* spp. Aristolochiaceae) on continental islands: Highly differentiated floral characteristics versus undifferentiated genotypes. *Plos One,* **12**.

Matsuda J, Setoguchi H. 2012. Isolation and characterization of microsatellite loci in *Asarum leucosepalum* (Aristolochiaceae), an endangered plant endemic to Tokunoshima Island in the Ryukyu Archipelago. *Conservation Genetics Resources,* **4**: 579-581.

Matsuoka T, Miyoshi N. 1998. Spatial shift of evergreen forests since the last glacial maximum (in Japanese). In: Yasuda Y, Miyoshi N, eds. *The illustrated vegetation history of the Japanese Archipelago*. Tokyo: Asakura-shoten.

Mayr E. 1956. Geographical character gradients and climatic adaptation. *Evolution,* **10**: 105-108.

Medail F, Diadema K. 2009. Glacial refugia influence plant diversity patterns in the Mediterranean Basin. *Journal of Biogeography,* **36**: 1333-1345.

Merila J, Crnokrak P. 2001. Comparison of genetic differentiation at marker loci and quantitative traits. *Journal of Evolutionary Biology,* **14**: 892-903.

Mesler MR, Lu KL. 1993. Pollination biology of *Asarum hartwegii* (Aristolochiaceae): an evaluation of Vogel's mushroom-fly hypothesis. *Madroño*: 117-125.

Minder A, Rothenbuehler C, Widmer A. 2007. Genetic structure of hybrid zones between *Silene latifolia* and *Silene dioica* (Caryophyllaceae): evidence for introgressive hybridization. *Molecular ecology,* **16**: 2504-2516.

Mitsui Y, Chen ST, Zhou ZK, Peng CI, Deng YF, Setoguchi H. 2008. Phylogeny and biogeography of the genus *Ainsliaea* (Asteraceae) in the Sino-Japanese region based on nuclear rDNA and plastid DNA sequence data. *Annals of Botany,* **101**: 111-124.

Mitsui Y, Nomura N, Isagi Y, Tobe H, Setoguchi H. 2011. Ecological barriers to gene flow between riparian and forest species of *Ainsliaea* (Asteraceae). *Evolution,* **65**: 335-349.

Mochizuki K, Kawakita A. 2018. Pollination by fungus gnats and associated floral characteristics in five families of the Japanese flora. *Annals of Botany,* **121**: 651-663.

Morgan MT. 1992. The evolution of traits influencing male and female fertility in outcrossing plants. *American Naturalist,* **139**: 1022-1051.

Morgan MT, Wilson WG. 2005. Self-fertilization and the escape from pollen limitation in variable pollination environments. *Evolution,* **59**: 1143-1148.

Muir G, Schlotterer C. 2005. Evidence for shared ancestral polymorphism rather than recurrent gene flow at microsatellite loci differentiating two hybridizing oaks (*Quercus* spp.). *Molecular Ecology,* **14**: 549-561.

Nakagawa M. 2010. Fine-scale genetic structure within plots of *Polygala reinii* (Polygalaceae) having an ant-dispersal seed. *Journal of Plant Research,* **123**: 355-362.

Nakamura K, Suwa R, Denda T, Yokota M. 2009. Geohistorical and current environmental influences on floristic differentiation in the Ryukyu Archipelago, Japan. *Journal of Biogeography,* **36**: 919-928.

Nei M, Tajima F, Tateno Y. 1983. Accuracy of estimated phylogenetic trees from molecular data. 2. gene frequency data. *Journal of Molecular Evolution,* **19**: 153-170.

Neinhuis C, Wanke S, Hilu KW, Muller K, Borsch T. 2005. Phylogeny of Aristolochiaceae based on parsimony, likelihood, and Bayesian analyses of *trnL-trnF* sequences. *Plant Systematics and Evolution,* **250**: 7-26.

Nomura N, Takaso T, Peng CI, Kono Y, Oginuma K, Mitsui Y, Setoguchis H. 2010. Molecular phylogeny and habitat diversification of the genus *Farfugium* (Asteraceae) based on nuclear rDNA and plastid DNA. *Annals of Botany,* **106**: 467-482.

Ohba H. 2001. Flora of Japan. *Angiospermae, Dicotyledoneae, Archichlamydeae (b), vol IIb. Koudansha, Tokyo*.

Ohi-Toma T, Sugawara T, Murata H, Wanke S, Neinhuis C, Murata J. 2006. Molecular phylogeny of *Aristolochia* sensu lato (Aristolochiaceae) based on sequences of *rbcL*, *matK*, and *phyA* genes, with

special reference to differentiation of chromosome numbers. *Systematic Botany,* **31**: 481-492.

Okamoto M, Kanoh K. 1977. The insects surrounding wild gingers. *Nature Study,* **23**: 137-139 (In Japanese.).

Okaura T, Quang ND, Ubukata M, Harada K. 2007. Phylogeographic structure and late Quaternary population history of the Japanese oak *Quercus mongolica* var. *crispula* and related species revealed by chloroplast DNA variation. *Genes & Genetic Systems,* **82**: 465-477.

Oksanen J, Kindt R, Legendre P, O'Hara B, Stevens MHH, Oksanen MJ, Suggests M. 2007. The vegan package. *Community ecology package,* **10**: 719.

Okuyama Y, Goto N, Nagano AJ, Yasugi M, Kokubugata G, Kudoh H, Qi Z, Ito T, Kakishima S, Sugawara T. 2020. Radiation history of Asian *Asarum* (sect. *Heterotropa*, Aristolochiaceae) resolved using a phylogenomic approach based on double-digested RAD-seq data. *Annals of Botany,* **126**: 245-260.

Parachnowitsch AL, Kessler A. 2010. Pollinators exert natural selection on flower size and floral display in *Penstemon digitalis*. *New Phytologist,* **188**: 393-402.

Paradis E, Claude J, Strimmer K. 2004. APE: analyses of phylogenetics and evolution in R language. *Bioinformatics,* **20**: 289-290.

Peakall R, Smouse PE. 2012. GenAlEx 6.5: genetic analysis in Excel. Population genetic software for teaching and research-an update. *Bioinformatics,* **28**: 2537-2539.

Pebesma E. 2018. Simple features for R: standardized support for spatial vector data. *The R Journal,* **10**: 439-446.

Peterson BK, Weber JN, Kay EH, Fisher HS, Hoekstra HE. 2012. Double Digest RADseq: An Inexpensive Method for De Novo SNP Discovery and Genotyping in Model and Non-Model Species. *Plos One,* **7**.

Petit RJ, Duminil J, Fineschi S, Hampe A, Salvini D, Vendramin GG. 2005. Comparative organization of chloroplast, mitochondrial and nuclear diversity in plant populations. *Molecular Ecology,* **14**: 689-701.

Petit RJ, Excoffier L. 2009. Gene flow and species delimitation. *Trends in Ecology & Evolution,* **24**: 386-393.

Phillips SJ, Dudik M. 2008. Modeling of species distributions with Maxent: new extensions and a comprehensive evaluation. *Ecography,* **31**: 161-175.

Pillon Y, Johansen JB, Sakishima T, Roalson EH, Price DK, Stacy EA. 2013. Gene discordance in phylogenomics of recent plant radiations, an example from Hawaiian *Cyrtandra* (Gesneriaceae). *Molecular Phylogenetics and Evolution,* **69**: 293-298.

Pirie MD, Humphreys AM, Galley C, Barker NP, Verboom GA, Orlovich D, Draffin SJ, Lloyd K, Baeza CM, Negritto M, Ruiz E, Sanchez JHC, Reimer E, Linder HP. 2008. A novel supermatrix approach improves resolution of phylogenetic relationships in a comprehensive sample of danthonioid grasses. *Molecular Phylogenetics and Evolution,* **48**: 1106-1119.

Policha T, Davis A, Barnadas M, Dentinger BTM, Raguso RA, Roy BA. 2016. Disentangling visual and olfactory signals in mushroom-mimicking Dracula orchids using realistic three-dimensional printed flowers. *New Phytologist,* **210**: 1058-1071.

Posada D. 2008. jModelTest: Phylogenetic model averaging. *Molecular Biology and Evolution,* **25**: 1253-1256.

Pritchard JK, Stephens M, Donnelly P. 2000. Inference of population structure using multilocus genotype data. *Genetics,* **155**: 945-959.

Proctor M, Yeo P, Lack A. 1996. *The natural history of pollination.* Portland, Oregon, USA: Timber Press.

Qi XS, Chen C, Comes HP, Sakaguchi S, Liu YH, Tanaka N, Sakio H, Qiu YX. 2012. Molecular data and ecological niche modelling reveal a highly dynamic evolutionary history of the East Asian Tertiary relict *Cercidiphyllum* (Cercidiphyllaceae). *New Phytologist,* **196**: 617-630.

Qian H, Ricklefs RE. 2000. Large-scale processes and the Asian bias in species diversity of temperate plants. *Nature,* **407**: 180-182.

Qiu YX, Fu CX, Comes HP. 2011. Plant molecular phylogeography in China and adjacent regions: Tracing the genetic imprints of Quaternary climate and environmental change in the world's most diverse temperate flora. *Molecular Phylogenetics and Evolution,* **59**: 225-244.

R Core Team. 2013. R: A language and environment for statistical computing.

Rabosky DL. 2014. Automatic Detection of Key Innovations, Rate Shifts, and Diversity-Dependence on Phylogenetic Trees. *Plos One,* **9**.

Rabosky DL, Grundler M, Anderson C, Title P, Shi JJ, Brown JW, Huang H, Larson JG. 2014. BAMMtools: an R package for the analysis of evolutionary dynamics on phylogenetic trees. *Methods in Ecology and Evolution,* **5**: 701-707.

Rambaut A. 2009. FigTree v1. 4: Tree figure drawing tool.

Rambaut A, Drummond AJ. 2013. Tracer v1. 5 Available from http://beast. bio. ed. ac. uk/Tracer. Accessed.

Raxworthy CJ, Ingram CM, Rabibisoa N, Pearson RG. 2007. Applications of ecological niche modeling for species delimitation: A review and empirical evaluation using day geckos (*Phelsuma*) from Madagascar. *Systematic Biology,* **56**: 907-923.

Ray N, Adams J. 2001. A GIS-based vegetation map of the world at the last glacial maximum (25,000-15,000 BP). *Internet archaeology,* **11**.

Raymond M, Rousset F. 1995. GENEPOP (version 1.2): population genetics software for exact tests and ecumenicism. *Journal of heredity,* **86**: 248-249.

Revell LJ. 2012. phytools: an R package for phylogenetic comparative biology (and other things). *Methods in Ecology and Evolution,* **3**: 217-223.

Rieseberg LH. 1997. Hybrid origins of plant species. *Annual Review of Ecology and Systematics,* **28**: 359-389.

Rieseberg LH, Wood TE, Baack EJ. 2006. The nature of plant species. *Nature,* **440**: 524-527.

Rosado A, Vera-Velez R, Cota-Sanchez JH. 2018. Floral morphology and reproductive biology in selected maple (*Acer* L.) species (Sapindaceae). *Brazilian Journal of Botany,* **41**: 361-374.

Rosenberg NA. 2004. DISTRUCT: a program for the graphical display of population structure. *Molecular Ecology Notes,* **4**: 137-138.

Rozas J, Ferrer-Mata A, Sánchez-DelBarrio JC, Guirao-Rico S, Librado P, Ramos-Onsins SE, Sánchez-Gracia A. 2017. DnaSP 6: DNA Sequence Polymorphism Analysis of Large Data Sets.

Molecular biology and evolution, **34**: 3299-3302.

Rundle HD, Nosil P. 2005. Ecological speciation. *Ecology Letters,* **8**: 336-352.

Rydin C, Kallersjo M. 2002. Taxon sampling and seed plant phylogeny. *Cladistics-the International Journal of the Willi Hennig Society,* **18**: 485-513.

Sakaguchi S, Sakurai S, Yamasaki M, Isagi Y. 2010. How did the exposed seafloor function in postglacial northward range expansion of *Kalopanax septemlobus*? Evidence from ecological niche modelling. *Ecological Research,* **25**: 1183-1195.

Sakaguchi S, Sugino T, Tsumura Y, Ito M, Crisp MD, Bowman D, Nagano AJ, Honjo MN, Yasugi M, Kudoh H, Matsuki Y, Suyama Y, Isagi Y. 2015. High-throughput linkage mapping of Australian white cypress pine (*Callitris glaucophylla*) and map transferability to related species. *Tree Genetics & Genomes,* **11**.

Sakaguchi S, Ueno S, Tsumura Y, Setoguchi H, Ito M, Hattori C, Nozoe S, Takahashi D, Nakamasu R, Sakagami T, Lannuzel G, Fogliani B, Wulff AS, L'Huillier L, Isagi Y. 2017. Application of simplified method of chloroplast enrichment to small amounts of tissues for chloroplast genome sequencing. *Applications in Plant Sciences,* **5**.

Salomon M. 2002. A revised cline theory that can be used for quantified analyses of evolutionary processes without parapatric speciation. *Journal of Biogeography,* **29**: 509-517.

Sant'Anna CS, Sebbenn AM, Klabunde GHF, Bittencourt R, Nodari RO, Mantovani A, dos Reis MS. 2013. Realized pollen and seed dispersal within a continuous population of the dioecious coniferous Brazilian pine *Araucaria angustifolia* (Bertol.) Kuntze. *Conservation Genetics,* **14**: 601-613.

Sapir Y, Armbruster WS. 2010. Pollinator-mediated selection and floral evolution: from pollination ecology to macroevolution. *The New phytologist,* **188**: 303-306.

Selkoe KA, Toonen RJ. 2006. Microsatellites for ecologists: a practical guide to using and evaluating microsatellite markers. *Ecology Letters,* **9**: 615-629.

Setoguchi H, Ohba H. 1995. Phylogenetic relationships in *Crossostylis* (Rhizophoraceae) inferred from restriction site variation of chloroplast DNA. *Journal of Plant Research,* **108**: 87-92.

Shi JJ, Rabosky DL. 2015. Speciation dynamics during the global radiation of extant bats. *Evolution,* **69**: 1528-1545.

Shore JS, Barrett SC. 1990. Quantitative genetics of floral characters in homostylous *Turnera ulmifolia* var. *angustifolia* Willd.(Turneraceae). *Heredity,* **64**: 105-112.

Sinn BT, Kelly LM, Freudenstein JV. 2015a. Phylogenetic relationships in *Asarum* : effect of data partitioning and a reviced classification. *American Journal of Botany,* **102**: 765-779.

Sinn BT, Kelly LM, Freudenstein JV. 2015b. Putative floral brood-site mimicry, loss of autonomous selfing, and reduced vegetative growth are significantly correlated with increased diversification in *Asarum* (Aristolochiaceae). *Molecular Phylogenetics and Evolution,* **89**: 194-204.

Slatkin M. 1973. Gene flow and selection in a cline. *Genetics,* **75**: 733-756.

Sokal oR, Sneath PHA. 1963. *Principles of numerical taxonomy*: WH Freeman.

Spitze K. 1993. Population structure in *Daphnia obtusa*: quantitative genetic and allozymic variation. *Genetics,* **135**: 367-374.

Ssymank A, Kearns CA, Pape T, Thompson FC. 2008. Pollinating flies (Diptera): a major contribution to plant diversity and agricultural production. *Biodiversity,* **9**: 86-89.

Stebbins GL. 1970. Adaptive radiation of reproductive characteristics in angiosperms, I: pollination mechanisms. *Annual review of ecology and systematics,* **1**: 307-326.

Strauss SY, Irwin RE. 2004. Ecological and evolutionary consequences of multispecies plant-animal interactions. *Annual Review of Ecology Evolution and Systematics,* **35**: 435-466.

Strauss SY, Whittall JB. 2006. Non-pollinator agents of selection on floral traits. *Ecology and evolution of flowers*: 120-138.

Sugawara T. 1987. Taxonomic studies of *Asarum* sensu lato III. comparative floral anatomy. *Botanical Magazine-Tokyo,* **100**: 335-348.

Sugawara T. 1988. Floral biology of *Heterotropa tamaensis* (Aristolochiaceae) in Japan. *Plant Species Biology,* **3**: 7-12.

Sugawara T. 2006. Aristorochiaceae. In: Iwatsuki K, Boufford DE, Ohba H, eds. *Flora of Japan*. Tokyo: Kodansha.

Sugawara T. 2012. A Taxonomic Study of *Asarum celsum* and Its Allies (Aristolochiaceae) on Amami-oshima, Southwestern Kyushu, Japan. *APG: Acta phytotaxonomica et geobotanica,* **62**: 61-68.

Sugawara T, Ogisu M. 1992. Karyomorphology of 11 species of *Asarum* (Aristolochiaceae) from Taiwan and mainland China. *Acta Phytotaxonomica et Geobotanica,* **43**: 89-96.

Tajima F. 1989. Statistical-method for testing the neutral mutation hyopothesis by DNA polymorphism. *Genetics,* **123**: 585-595.

Takahashi D, Sakaguchi S, Isagi Y, Setoguchi H. 2018. Comparative chloroplast genomics of series *Sakawanum* in genus *Asarum* (Aristolochiaceae) to develop single nucleotide polymorphisms (SNPs) and simple sequence repeat (SSR) markers. *Journal of Forest Research,* **23**: 387-392.

Takahashi D, Sakaguchi S, Setoguchi H. 2017. Development and characterization of EST-SSR markers in *Asarum sakawanum* var. *stellatum* and cross-amplification in related species. *Plant Species Biology,* **32**: 256-260.

Takahashi Y. 2015. Mechanisms and tests for geographic clines in genetic polymorphisms. *Population Ecology,* **57**: 355-362.

Takebayashi N, Wolf DE, Delph LF. 2006. Effect of variation in herkogamy on outcrossing within a population of *Gilia achilleifolia*. *Heredity,* **96**: 159-165.

Takhtajan AL. 1980. Outline of the classification of flowering plants (Magnoliophyta). *The botanical review,* **46**: 225-359.

Tamaki I, Ishida K, Setsuko S, Tomaru N. 2009. Interpopulation variation in mating system and late-stage inbreeding depression in *Magnolia stellata*. *Molecular Ecology,* **18**: 2365-2374.

Teramine T. 1981. *Asarum* of Kochi prefecture. *Plants of Kochi,* **4**: 79-134.

Thompson JD, Higgins DG, Gibson TJ. 1994. CLUSTAL-W - improving the sensitivity of progressive multiple

sequence alignment through sequence weighting, position-specific gap penalties and weight matrix choice. *Nucleic Acids Research,* **22**: 4673-4680.

Tillich M, Lehwark P, Pellizzer T, Ulbricht-Jones ES, Fischer A, Bock R, Greiner S. 2017. GeSeq - versatile and accurate annotation of organelle genomes. *Nucleic Acids Research,* **45**: W6-W11.

Tsuda Y, Nakao K, Ide Y, Tsumura Y. 2015. The population demography of *Betula maximowicziana*, a cool-temperate tree species in Japan, in relation to the last glacial period: its admixture-like genetic structure is the result of simple population splitting not admixing. *Molecular Ecology,* **24**: 1403-1418.

Tsukada M. 1984. A vegetation map in the Japanese Archipelago approximately 20, 000 years B. P. *Japanese Journal of Ecology,* **34**: 203-208.

Ujiie H. 1990. Geological history of the Ryukyu Island arc. *Nature of Okinawa; geomorphology and geology. Hirugisha, Naha*: 251-255.

Vasemagi A. 2006. The adaptive hypothesis of clinal variation revisited: Single-locus clines as a result of spatially restricted gene flow. *Genetics,* **173**: 2411-2414.

Vekemans X, Hardy OJ. 2004. New insights from fine-scale spatial genetic structure analyses in plant populations. *Molecular Ecology,* **13**: 921-935.

Vogel S. 1978. Pilzmiickenblumen als Pilzmimenten I.[fungus-gnat flowers mimicking fungi] Flora 167. 329-66. *Asarum, Aristolochia. Pollination by fungus-gnats. Floral morphology, Aristolochiaceae, Incompatibility Pollination (PMBD, 185610740)*.

Wahlund S. 1928. Zusammensetzung von Populationen und Korrelationserscheinungen vom Standpunkt der Vererbungslehre aus betrachtet. **11**: 65-106.

Wallberg A, Thollesson M, Farris JS, Jondelius U. 2004. The phylogenetic position of the comb jellies (Ctenophora) and the importance of taxonomic sampling. *Cladistics,* **20**: 558-578.

Wang Y, Wang QF, Gituru WR, Guo YH. 2004. A new species of *Asarum* (Aristolochiaceae) from China. *Novon,* **14**: 239-241.

Wang YH, Jiang WM, Comes HP, Hu FS, Qiu YX, Fu CX. 2015. Molecular phylogeography and ecological niche modelling of a widespread herbaceous climber, *Tetrastigma hemsleyanum* (Vitaceae): insights into Plio–Pleistocene range dynamics of evergreen forest in subtropical China. *New Phytologist,* **206**: 852-867.

Waser NM. 1983. The adaptive nature of floral traits: ideas and evidence. *Pollination biology,* **1**: 241-285.

Watanabe S. 2010. Asymptotic Equivalence of Bayes Cross Validation and Widely Applicable Information Criterion in Singular Learning Theory. *Journal of Machine Learning Research,* **11**: 3571-3594.

Watt C, Mitchell S, Salewski V. 2010. Bergmann's rule; a concept cluster? *Oikos,* **119**: 89-100.

Weber MG, Strauss SY. 2016. Coexistence in Close Relatives: Beyond Competition and Reproductive Isolation in Sister Taxa. *Annual Review of Ecology, Evolution, and Systematics, Vol 47,* **47**: 359-381.

Weir BS, Cockerham CC. 1984. Estimating F-statistics for the analysis of population structure. *evolution*: 1358-1370.

White TJ, Bruns T, Lee S, Taylor J. 1990. Amplification and direct sequencing of fungal ribosomal RNA genes for phylogenetics. *PCR protocols: a guide to methods and applications,* **18**: 315-322.

Whitlock MC. 2008. Evolutionary inference from QST. *Molecular ecology,* **17**: 1885-1896.

Wildman HE. 1950. Pollination of *Asarum canadense* L. *Science (New York, NY),* **111**: 551.

Willmer P. 2011. *Pollination and floral ecology*: Princeton University Press.

Wolfe KH, Li W-H, Sharp PM. 1987. Rates of nucleotide substitution vary greatly among plant mitochondrial, chloroplast, and nuclear DNAs. *Proceedings of the National Academy of Sciences,* **84**: 9054-9058.

Worth JR, Larcombe MJ, Sakaguchi S, Marthick JR, Bowman DM, Ito M, Jordan GJ. 2016. Transient hybridization, not homoploid hybrid speciation, between ancient and deeply divergent conifers. *American journal of botany,* **103**: 246-259.

Wright S. 1943. Isolation by distance. *Genetics,* **28**: 114.

Wu Z, Wu S. 1996. A proposal for a new floristic kingdom (realm)-the E. Asiatic kingdom, its delineation and characteristics. Beijing, China/Berlin, Heidelberg, Germany: Beijing: China Higher Education Press/Springer-Verlag.

Xing FQ, Mao JF, Meng JX, Dai JF, Zhao W, Liu H, Xing Z, Zhang H, Wang XR, Li Y. 2014. Needle morphological evidence of the homoploid hybrid origin of Pinus densata based on analysis of artificial hybrids and the putative parents, Pinus tabuliformis and *Pinus yunnanensis*. *Ecology and Evolution,* **4**: 1890-1902.

Xu CY, Julien MH, Fatemi M, Girod C, Van Klinken RD, Gross CL, Novak SJ. 2010. Phenotypic divergence during the invasion of Phyla canescens in Australia and France: evidence for selection-driven evolution. *Ecology Letters,* **13**: 32-44.

Yakimowski SB, Rieseberg LH. 2014. The role of homoploid hybridization in evolution: a century of studies synthesizing genetics and ecology. *American Journal of Botany,* **101**: 1247-1258.

Yamagishi H, Tomimatsu H, Ohara M. 2007. Fine-scale spatial genetic structure within continuous and fragmented Populations of Trillium camschatcense. *Journal of Heredity,* **98**: 367-372.

Yamaji H, Fukuda T, Yokoyama J, Pak JH, Zhou CZ, Yang CS, Kondo K, Morota T, Takeda S, Sasaki H, Maki M. 2007. Reticulate evolution and phylogeography in *Asarum* sect. *Asiasarum* (Aristolochiaceae) documented in internal transcribed spacer sequences (ITS) of nuclear ribosomal DNA. *Molecular Phylogenetics and Evolution,* **44**: 863-884.

Yang LQ, Hu HY, Xie C, Lai SP, Yang M, He XJ, Zhou SD. 2017. Molecular phylogeny, biogeography and ecological niche modelling of *Cardiocrinum* (Liliaceae): insights into the evolutionary history of endemic genera distributed across the Sino-Japanese floristic region. *Annals of Botany,* **119**: 59-72.

Yoichi W, Jin XF, Peng CI, Tamaki I, Tomaru N. 2017. Contrasting diversification history between insular and continental species of three-leaved azaleas (*Rhododendron* sect. *Brachycalyx*) in East Asia. *Journal of Biogeography,* **44**: 1065-1076.

Yokoyama Y, Lambeck K, De Deckker P, Johnston P, Fifield LK. 2000. Timing of the Last Glacial Maximum from observed sea-level minima. *Nature,* **406**: 713-716.

Yu Y, Harris AJ, He XJ. 2010. S-DIVA (Statistical Dispersal-

Vicariance Analysis): A tool for inferring biogeographic histories. *Molecular Phylogenetics and Evolution,* **56**: 848-850.

Zeng LP, Zhang Q, Sun RR, Kong HZ, Zhang N, Ma H. 2014. Resolution of deep angiosperm phylogeny using conserved nuclear genes and estimates of early divergence times. *Nature Communications,* **5**.

Zhang L, Barrett SCH, Gao JY, Chen J, Cole WW, Liu Y, Bai ZL, Li QJ. 2005. Predicting mating patterns from pollination syndromes: The case of "sapromyiophily" in *Tacca chantrieri* (Taccaceae). *American Journal of Botany,* **92**: 517-524.

Zhang ZQ, Kress WJ, Xie WJ, Ren PY, Gao JY, Li QJ. 2011. Reproductive biology of two Himalayan alpine gingers (*Roscoea* spp., Zingiberaceae) in China: pollination syndrome and compensatory floral mechanisms. *Plant Biology,* **13**: 582-589.

Zhou HP, Chen J, Chen F. 2007. Ant-mediated seed dispersal contributes to the local spatial pattern and genetic structure of *Globba lanciangensis* (Zingiberaceae). *Journal of Heredity,* **98**: 317-324.

Zink RM, Remsen JVJ. 1986. Evolutionary processes and patterns of geographic variation in birds. NY: Plenum Press.